Promotoren : dr. G.J. Fleer, hoogleraar in de fysische en kolloidchemie
dr. J. Lyklema, hoogleraar in de fysische en kolloidchemie

MACROMOLECULES AT INTERFACES

A flexible theory for hard systems

9. Het verdient aanbeveling de treinreiziger die alleen via een omweg zijn bestemming kan bereiken een vergoeding voor het ongemak aan te bieden, in plaats van de extra railkilometers in rekening te brengen.

10. Naarmate men met meer decimalen werkt, loopt men een groter risico de komma verkeerd te plaatsen.

11. Onderzoek dat gericht is op het als eerste publiceren van een doorbraak die binnen korte tijd op meerdere plaatsen verwacht wordt, is nauwelijks van wetenschappelijke waarde.

12. Praktikumuitrusting dient van minstens zodanige kwaliteit te zijn dat de student niet met twee linkerhanden leert te werken.

13. Het verschil tussen een voordracht en een lezing staat op papier.

14. Het eind is zoek als men alleen naar treinen, bruggen en lussen staart.

    Dit proefschrift, hoofdstukken 2,3,4 en 5.

15. Bij het itereren is het zaak niet in herhaling te vervallen.

Jan M.H.M. Scheutjens
MACROMOLECULES AT INTERFACES
A flexible theory for hard systems
Wageningen, 11 januari 1985.

STELLINGEN

1. De parametrische modellen van het Centraal Planbureau berekenen een vraag bij een gegeven antwoord.

2. Aan veel polymeeradsorptiemodellen zit kop noch staart.

   Dit proefschrift, hoofdstukken 2,3,4,5, en paragraaf 6.5.

3. Destabilisatie van kolloiden door adsorberend polymeer is mogelijk in elk oplosmiddel.

   Dit proefschrift, hoofdstuk 5.

4. De grensvlakeigenschappen van een enorme diversiteit van polymeersystemen kan met één theorie beschreven worden.

   Dit proefschrift, hoofdstuk 6.

5. De Gennes' verlies van vertrouwen in "mean field"-theorieën is eerder het gevolg van een vrome wens dan van een vaderlijke gedachte.

   De Gennes, P.G., Macromolecules, 15 (1982) 492.

6. Het negeren van de afkoelcurve bij het meten van warmtegeleiding door middel van een niet-stationaire meetmethode betekent verlies van gratis informatie en een lagere meetnauwkeurigheid.

   I.A. van Haneghem, proefschrift, Landbouwhogeschool, Wageningen (1981).

7. Ten onrechte wordt een wetenschappelijke publicatie vaak gezien als een eindprodukt. In werkelijkheid is het een (vaak kostbare) investering die zijn rendement nog moet opbrengen.

8. Het frequentiespectrum van geluidsboxen wordt niet optimaal benut. Via elektronische weg kan de bandbreedte toenemen met afnemend geluidsniveau.

Jan M.H.M. Scheutjens

MACROMOLECULES AT INTERFACES

A flexible theory for hard systems

Proefschrift
ter verkrijging van de graad van
doctor in de landbouwwetenschappen,
op gezag van de rector magnificus,
dr. C.C. Oosterlee,
in het openbaar te verdedigen
op vrijdag 11 januari 1985
des namiddags te vier uur in de aula
van de Landbouwhogeschool te Wageningen

ISBN = 90 6754 851-03

ABSTRACT

Scheutjens, Jan M.H.M., Laboratory for Physical and Colloid Chemistry, Agricultural University, Wageningen, The Netherlands.
MACROMOLECULES AT INTERFACES; a flexible theory for hard systems.
Ph.D. Thesis, Agricultural University, Wageningen, (1985).
168 + 8 pages, 61 figures, 4 tables. English and Dutch summaries.

A statistical theory for flexible macromolecules at interfaces has been developed. The theory is based on a lattice model in which the equilibrium set of molecular conformations in a concentration profile is evaluated, using a self-consistent procedure. In this way, the Flory-Huggins theory for polymer solutions is extended to inhomogeneous solutions of macromolecules without any additional assumption. Apart from the Flory-Huggins polymer-solvent interaction parameter χ, a similar parameter χ_s is used to describe the interaction of polymer segments with a solid interface. The average number of molecules in each particular conformation can be computed, so that a very detailed picture of the interfacial structure is obtained. Thus also the train, loop, and tail size distributions of adsorbed polymer can be calculated. In principle, there are no adjustable parameters in the theory. Moreover, there are no restrictions on the system parameters such as polymer concentration, chain length, number of species in a mixture or solvent quality, although in some cases numerical problems may occur. Results are given for adsorption of homopolymers, polydisperse polymer, polyelectrolytes, and star-branched polymer, for the structure of lipid bilayers and of the amorphous phase of semicrystalline polymer, and for the interaction between surfaces due to the presence of adsorbing or nonadsorbing polymer. Available experimental data on adsorption isotherms, bound fraction, layer thickness, surface fractionation, steric stabilization, and polymer bridging agree very well with the theoretical predictions.

Free descriptors: polymer adsorption theory, lattice model, polymer chain statistics, step weighted walk, adsorbed chain conformation, macromolecular interfacial structure, segment density distribution, polymer concentration profile, polymer adsorption isotherm, surface tension, steric stabilization, flocculation, polymer bridging, surface fractionation.

CONTENTS

Chapters 2 and 3 are reprinted with permission from the Journal of Physical Chemistry.
Chapter 4 is reprinted with permission from "The Effect of Polymers on Dispersion Properties", Tadros, T.F., Ed., Academic Press, London, (1982).
Chapter 5 is submitted for publication in Macromolecules.

1 INTRODUCTION

1.1 GENERAL

The subject of this study is the behaviour of linear, flexible polymer molecules at interfaces. A new statistical theory has been developed, which gives a very detailed picture of the equilibrium state of the interfacial region. The basic concept of this theory is applicable to all systems involving concentrated inhomogeneous distributions of polymer molecules in thermodynamic equilibrium.

Polymer adsorption from solution is a very universal phenomenon. Many applications are based on the repulsive or attractive forces between two polymer layers[1].

In food technology and pharmacy the utilization of natural polymers like polysaccharides and proteins as stabilizers for emulsions is widespread. Other examples where the stabilization of colloids plays a major role are pesticides, cosmetics, paints and inks.

Destabilization of dispersions occurs often at low concentrations of polymer and is important in mineral processing and water purification. This phenomenon is called flocculation, since one of the essential steps is the forming of large flocs with a loose but stable structure. The capability of inducing floc formation makes polymer very helpful for the improvement of soil structure.

Polymer adsorption and adhesion are operative in biological systems and interfere with many processes used in polymer technology. It is crucial in the production of magnetic tapes, rubber coatings for tires, and for the operation of gum erasers.

Most applications have been developed without insight into the underlying mechanisms. Some 30 years ago the knowledge about polymer adsorption was very poor, but it has increased steadily over the last decades[2]. In view of the diversity of materials, the lack of suitable experimental techniques and the complexity of polymer adsorption, it is not surprising that in most cases a comparison between theoretical and experimental results show only

qualitative agreement. A detailed description of polymers at interfaces is therefore of extreme importance for all applications mentioned above. A quantitative prediction of the forces between two polymer covered colloidal particles hinges on the knowledge of the exact shape of the polymer layers in interaction. Due to the thermal motion of the flexible polymer molecules, this shape is statistically determined and hence, a theory for polymer adsorption is necessarily based on statistical methods.

1.2 POLYMER STATISTICS

1.2.1 Polymers

A flexible, linear polymer molecule consists of a chain of monomer units. A variety of polymers exists[3]. The number of units in a chain may be as large as 10^5, but is usually between 10^2 and 10^4. Molecules with less than around 100 units are called oligomers.

For homopolymers the repeating units are all identical, whereas copolymers have two or more different types of monomer units in sequences that are either systematically (synthetic alternate and block copolymers, but also natural macromolecules like DNA, RNA, and proteins) or statistically (random and blocky copolymers) arranged. Polyelectrolytes contain units that are electrically charged. According to the nature of the charges the polyelectrolyte is either weak or strong.

The primary structure of flexible polymers is not always strictly linear. Some polymers are branched (irregular, star- or comb-like) and a special class is formed by the ring polymers.

In a homodisperse polymer sample all chains have the same number and type of monomer units. Most synthetic and many biological polymers are polydisperse: they have a statistically determined chain length distribution. The term heterodisperse is used to refer to a distribution in monomer sequences in random and blocky copolymers.

Solution and adsorption properties of polymers depend largely on the characteristics of the chains and a general theory for macromolecules at interfaces must be able to incorporate the main features of each polymer type in order to predict its behaviour in real systems.

1.2.2 Polymers in solution

The solubility of macromolecules is low, due to their high molecular weights. A polymer chain in solution interacts simultaneously with a very large number of solvent molecules. Because of the rotational freedom of the chemical bonds between the monomer units the chain can assume a large number of different spatial arrangements and its shape is continually changing by thermal motion. For sterical reasons each bond has a small number of preferred rotational angles which determine the main permissible distributions, called conformations, of the chain. The number of conformations is extremely large. For example, if for a chain of x monomer units each bond has on the average three preferred angles, the number of conformations is 3^{x-1}, which is approximately $10^{x/2}$. Even for polymers with only 100 monomer units per molecule this number is already as high as 2.10^{47}. Since it is impossible to consider every permissible conformation individually, a statistical approach must be adopted.

The shape of the macromolecules is a weighted average of the shape of their conformations. Energetically favourable conformations have a relatively high probability. Specific interactions between monomer units, such as in proteins, have a strong influence and reduce the number of significant conformations considerably. Therefore, proteins are relatively rigid, whereas most homopolymers are flexible.

Much theoretical work has been done on the average shape of homopolymers[4]. To some extent, they can be described as a sequence of identical and rigid segments with bond angles that can assume any value. The length of a segment and the number of segments per chain are adjusted such as to mimic the length and flexibility of a real chain. Thus, with increasing flexibility of the real chain, the number of segments increase and their length decreases. Typically, each segment represents 2 to 5 monomer units.

If the segments are infinitely thin, there is no excluded volume for the segments and the conformations of the chain can be simulated by random walks. The average shape of such a chain is that of a random coil. The radius of gyration of such a coil, for a chain of r segments, is proportional to $r^{0.5}$. However, a real polymer chain has a finite thickness and it is clear that two monomer units will never occupy the same volume. Hence, self-avoiding walks are more appropriate. Computer simulations indicate[5] that a chain of r spherical segments has a radius of gyration proportional to $r^{0.6}$.

For finite chains the exponent depends on the ratio between length and thickness of a segment and, for various geometries, it has a value between 0.5 and 0.6. The volume of the chain acts as a repulsive force between the segments which causes the coil to expand.

Although locally the chains are always self-avoiding, the overall conformation of the chain depends also on the solvent quality. There are two cases in which a polymer coil has the dimensions of a random walk: in pure liquid polymer and in an ideally poor or Θ-solvent at low concentrations of polymer[5]. In liquid polymer the repulsive force between segments of the same chain equals that between segments of different chains. Coil expansion does not decrease the total repulsion, but merely the number of conformations. Only the entropy determines the average conformation. At low concentrations in a Θ-solvent the hard core repulsion between the segments is compensated by a mutual attraction, or equivalently, by a repulsion between segments and solvent. Obviously, this latter repulsion decreases with decreasing solvent concentration, hence, with increasing polymer concentration. Consequently, in a Θ-solvent, the coil expansion as a function of polymer concentration exhibits a maximum and it is zero in very dilute solutions and in pure liquid polymer.

The solvent quality is determined by the net interaction between segments and solvent. The free energy of mixing of polymer and solvent has been extensively examined by Flory and Huggins, who approximated the solution by a semicrystalline lattice. They introduced the parameter χ, which gives the interaction energy difference (in kT units) when a solvent molecule is transferred from pure solvent to liquid polymer[4]. For an athermal solvent $\chi = 0$ and it increases with decreasing solvent quality. The entropy of mixing was calculated by evaluating the number of distinguishable ways in which a given number of solvent molecules and sequences of segments can be placed in the lattice. It appeared that $\chi = 0.5$ for a Θ-solvent. In a worse than Θ-solvent ($\chi > 0.5$) the polymer is not soluble at all concentrations leading to phase separation domains. For $\chi < 0.5$ the solution is thermodynamically stable at all concentrations.

A lattice model is especially suitable for quantitative comparisons between free energies under different conditions. The set of possible configurations on a lattice comprises a representative sample of the infinite number of spatial distributions in a real system.

1.2.3 Polymer adsorption

Flexible polymer molecules are able to adjust their conformation in the presence of an interface such as to maximize short range interactions between polymer segments and the surface. The attraction between segment and surface is multiplied by the large number of adsorbed segments per polymer chain so that a strong attractive force per molecule is present, even when the contribution per segment is only small. If enough surface area is available, each single chain in the system will be adsorbed. In this case the adsorbed macromolecules are so far apart that they do not affect each other (isolated chains). The spherical shape of the polymer coils in solution changes drastically upon adsorption[6,7].

A very elegant model for the description of the adsorption of isolated chains is that of DiMarzio and Rubin[6,7], who developed a matrix method for the generation of all conformations, with their appropriate probabilities, of a chain near a wall. As in the Flory-Huggins model, they represent the conformations of the chain by random walks on a lattice. Each step in or towards a lattice layer adjoining the wall simulates a segment in contact with the surface and hence, is assigned a weighting factor $\exp(\chi_s)$, where $-\chi_s$ is the adsorption energy per segment (in kT units).

This and other models predict that most of the segments of isolated adsorbed homopolymers form long sequences, 'trains', in contact with the surface. The trains are interconnected by short 'loops' of segments sticking into the solution. The chain ends are either adsorbed or form dangling 'tails'. The average conformation of an adsorbed chain depends on the adsorption energy. If χ_s is below a critical value χ_{sc}, the polymer does not adsorb, whereas a value slightly above χ_{sc} causes the chain to adsorb in a very flat conformation with long trains, short loops, and hardly any tail. The critical adsorption energy χ_{sc} is the energy per segment that just compensates the conformational entropy loss of the chain when its shape changes from a 3-dimensional coil to a 2-dimensional conformation parallel to the surface.

If the surface is saturated with polymer, the segments have to compete for surface sites. With increasing polymer concentration, the fraction of segments in loops and tails will increase[1]. The first theories on polymer adsorption at high concentrations calculate the number and lengths of loops by minimizing the free energy of an adsorbed polymer layer with a predeter-

mined shape of the segment density profile in the loop region. For instance, Silberberg[8] used a constant loop density and Hoeve[9] an exponential decay. For computational reasons, tails were not taken into account.

A few lattice models allow for the computation of segment density profiles at high concentration: that of Mackor and Van der Waals[10] for adsorption of rigid rods, of Ash et al.[11] for adsorption of very short flexible oligomers, and that of Roe[12] for flexible homopolymers. The most advanced theory is that of Ash et al., but it suffers from severe computational problems. Only results for chains not longer than tetramers have been obtained. The Roe theory applies for relatively thin adsorbed polymer layers, with most of the segments in trains. This theory is not adaptable to copolymers or special chain structures like branches and it gives no information on the average conformation of the adsorbed polymer in terms of train, loop, and tail distributions.

1.2.4 Reversibility of polymer adsorption

Theories that are based on equilibrium thermodynamics are not very useful for systems in which the establishment of equilibrium is very slow. A rather common opinion is that adsorption and desorption of polymer are very slow processes. Evidence that seems to support this view is amply available: the adsorbed amount often increases slowly in time, even on a time scale of weeks and once adsorbed, polymers are difficult to desorb by dilution. Another problem is that the amount adsorbed per surface area often increases with increasing volume of the equilibrium solution. Because of these 'artefacts' many experimental data were not very reproducible and polymer adsorption was considered to be irreversible.

Fortunately, it has been shown recently that many of the apparent irreversibility effects are now quantitatively explainable using simple arguments[13]. The most important parameter which has often been overlooked is the polydispersity of the polymer. From dilute and semidilute solutions of a polydisperse sample, long chains adsorb preferentially over shorter ones. When the surface is saturated with polymer, the chains are competing for surface sites and small differences in chain length will discriminate between 'winners' (long chains) and 'loosers' (short chains). The resulting fractionation process may take a long time, because the diffusion of a small

fraction of very long chains towards the surface through a high concentration of lower molecular weight polymer is slow. Thus, the average molecular weight of the adsorbate increases slowly with time, due to the displacement process. The variation in adsorbed amount reflects the molecular weight dependence of the adsorption. If the latter is weak, displacement still occurs, but it does not lead to a higher adsorption.

Adding more polymer, either by increasing the solution concentration at constant volume or increasing the solution volume at constant concentration, is tantamount to introducing new winners and the composition of the adsorbate will change again. On the other hand, removing polymer from the solution, which contains only loosers, does not affect the interface. Hence, the hysteresis after addition and removal of the same amount of polymer is caused by a difference in composition of these polymer fractions and consequently, this hysteresis does not detract from the reversibility of polymer adsorption.

Strong evidence that polymer adsorption is reversible is also available. Apart from the quantitative prediction of polydispersity effects while assuming complete equilibrium, polymer adsorption is usually reversible with respect to changes in solvent type, pH, and salt concentration. Hence, theories on equilibrium thermodynamics are in most cases appropriate and polydispersity effects should be taken into account when the polymer is not homodisperse.

1.2.5 Steric stabilization and flocculation

Polymer adsorption has a very pronounced effect on the stability of colloidal systems[1]. A strong interaction between polymer covered particles arises as soon as adsorbed polymer layers overlap each other. In a better than Θ-solvent this interaction is repulsive and increases the stability of the dispersion, whereas in a worse than Θ-solvent the force is attractive and flocculation ensues.

Loops and tails protuding from one particle may form bridges by adsorbing on free surface of another particle, inducing an attraction between these surfaces. For flocculation to be effective the net interaction between the particles must be attractive. If the particles are stabilized by electrostatic forces, the loops and tails must protude beyond the double layer

in order to reach the opposite surface. A thick polymer layer is not consistent with free surface on the particles, hence flocculation occurs only over a limited range of surface coverages. Bridging works most efficiently when fully covered particles are mixed with an equal portion of uncovered particles[14].

For a quantitative evaluation of the interaction between two adsorbed polymer layers, the segment density profiles and the conformations of the polymer must be known as a function of the particle separation.

DiMarzio and Rubin[15] have adopted their matrix model for one chain between two plates and showed that the interaction between the surfaces is repulsive for non-adsorbing polymer ($\chi_s < \chi_{sc}$) and attractive for adsorbing polymer ($\chi_s > \chi_{sc}$), independent of the interplate distance.

For real systems one expects a repulsive force at small surface separations if the amount of polymer between the surfaces remains constant, since polymer occupies a certain volume. Hence, a single chain model is not able to predict essential characteristics of a many chain system. A quantitative model should give information for high surface coverages.

1.3 PURPOSE AND BASIC CONCEPTS OF THIS STUDY

The aim of the present study is to develop a theory that gives a detailed description of the behaviour of macromolecules at interfaces. For polymer between two surfaces, the model must be able to predict steric stabilization and flocculation quantitatively.

The lattice model of DiMarzio and Rubin[15] is chosen as a starting point, since it allows to obtain all relevant information about the chain conformations, is not restricted to homopolymers, and the generation of conformations is much simpler than in the theory of Ash et al.[11].

The most important problem is to incorporate the volume of the segments so that each lattice site is not occupied by more than one segment at a time. In the model of DiMarzio and Rubin, this volume exclusion is neglected. Consequently, all steps have the same probability, except steps in or towards a surface layer where the adsorption energy is operating. In a sophisticated model, all steps into a lattice site already occupied by a segment have to be prohibited. An exact solution of this problem is not yet feasible. An approximate solution is possible by using a mean field ap-

proach. Then the assumption is made that the probability that a site on distance i from a surface is occupied is equal to the average volume fraction ϕ_i of segments at distance i. This leads to a weighting factor $1 - \phi_i$ for each step in or towards layer i. In this way a step into a region of high segment density becomes less probable and the generation of conformations via random walks is shifted, to some extent, towards that via self-avoiding walks. The volume fraction ϕ_i is to be obtained by the matrix method, where the matrix is now a function of all ϕ_i's. A self-consistent solution can be found numerically.

When two surfaces approach each other and the polymer remains adsorbed, the volume fractions ϕ_i increase and eventually the step probabilities decrease rapidly. The result is that the force between the surfaces is always repulsive at short separations. At the minimum possible distance there is only polymer in the gap ($\phi_i \to 1$), the step probabilities are essentially zero and the force is infinite.

Physically, the relation between step probability and volume fraction simulates segments competing for surface sites. An interesting consequence is that adsorption of many chains on one plate can be studied using the same model. For example, adsorption isotherms can be computed over the entire concentration range, from zero up to liquid polymer, and for any chain length.

The model as given above, applies to athermal solvents, i.e., when the energy of a segment does not depend on the local concentration of other segments. For other solvents the net interaction energy between segments gives rise to another Boltzmann factor in the step probabilities, similar to the factor $\exp(\chi_s)$ for the adsorption energy. According to the theory of Flory and Huggins[4] the interaction energy of a segment at i equals $-\chi\langle\phi_i\rangle$ kT, where χ is the polymer-solvent interaction parameter and $\langle\phi_i\rangle$ is the average volume fraction of segments around a site at i. In fact, a segment competes with a solvent molecule for a lattice site. Since a step corresponds to the replacement of a solvent molecule by a segment the total energy change is $-2\chi\langle\phi_i\rangle$ kT and hence, the Boltzmann factor becomes $\exp(2\chi\langle\phi_i\rangle)$. As discussed in section 1.2.2, in a Θ-solvent the interaction energy compensates the repulsive volume forces between the segments at low concentrations. In such a solvent $\chi = 0.5$ and if the step probabilities for steps not touching the surface are set equal to $(1-\phi_i)\exp(2\chi\langle\phi_i\rangle)$ the exponent indeed compensates the decrease of the factor $1-\phi_i$ at low concentra-

tions in a Θ-solvent. In this way the solvent quality as expressed by the χ-parameter is incorporated in the theory.

In order to give the theory a sound thermodynamic basis, a partition function has been derived from which the step probabilities can be found directly, using a statistical thermodynamic procedure (see chapter 2).

1.4 COMPUTATIONAL PROBLEMS

The first computer program that solved the implicit equations was based on a primitive iteration scheme and performed several hundreds of iterations for polymer chains up to 40 segments long. For a chain of r segments, a series of $r^2/2$ matrix-vector multiplications was necessary for each iteration. Fortunately, a considerable simplification of the DiMarzio-Rubin equations was possible (see the appendix of chapter 2) that reduced the number of matrix-vector multiplications to r per iteration.

The number of iterations could be decreased by using the Newton-Ralphson method, for which a good initial starting point is necessary. Such a starting point can be obtained from the polymer adsorption theory of Roe[12]. With increasing chain length r, a number of problems occur.

i) For adsorption on one plate the number of iteration variables increases, because the thickness of the adsorbed layer and hence, the distance for which the segment density is higher than the solution concentration increases proportional to $\sqrt{r}$. On the average, a total of $3\sqrt{r}$ variables is required.

ii) A total of $3r\sqrt{r}$ quantities is to be stored during the matrix multiplications. As this is currently impossible on most computers for $r \gtrsim 1000$ an overlay structure, using a disk as backing store, or repeatedly recomputing of data is unavoidable.

iii) The sequence of r matrix multiplications may induce floating point overflows or underflows. A careful renormalisation of vectors solves this problem.

iv) The Roe theory is not valid for long chains and provides in that case a poor starting point, leading to a large number of iterations.

Calculations have been performed for $r \leq 10^4$, which covers almost the whole molecular weight range of available polymers.

The exchangeability of computer programs between different computers is

still poor. The software crisis forces one to rediscover most of the computational tricks and to develop a new program for almost each desired variation of a model. A suitable programming language for the type of calculations in this study would have facilities for structured programming, dynamic memory allocation, vector processing, on-line debugging, and access to a mathematical library, including optimization routines. Currently, widely used programming languages in science are Fortran, Basic, Algol60, and Pascal. Of these, only Algol has the dynamic array facility which is very suitable for this study. Unfortunately, it is impossible to write portable Algol programs, since the input and output statements are not standardized.

The first program of this study has been written in Algol60 and all subsequent programs in Simula67. Simula is based on Algol60 with the addition of many facilities such as pointer structures. It is available on many computers and is well standardized, but the number of users is not large. Some simplified versions of our programs have been translated into Fortran.

1.5 OUTLINE OF THIS STUDY

In chapter 2 the new theory is introduced and its derivation is given starting from the partition function. The theory requires only 5 parameters, all having a clear physical meaning. In principle, they are experimentally accessible. A number of numerical results for adsorption of homopolymers is shown and, where appropriate, compared with predictions from other theories. It is demonstrated that the tail fraction of adsorbed polymer is much larger than has been expected before. The assumption in other theories that end effects can be ignored is not warranted at finite solution concentrations.

In chapter 3 the principles of the theory are explained in a more physical way and it is shown how to obtain more information about the structure of the adsorbed polymer, such as the train, loop, and tail size distributions. In addition, the thickness of the adsorbed layer is shown to be proportional to the quare root of the chain length in all solvents.

Comparison with experimental results in chapter 4 shows excellent agreement for adsorption of homodisperse polymers. Preferential adsorption from a solution of polydisperse polymer is examined theoretically and a transition from preferential adsorption of long chains to preferential adsorption of short chains is predicted when the concentration of polymer in the solution

increases beyond a volume fraction of the order of 10%.

In chapter 5 the interaction between adsorbed polymer layers is studied in detail. It is predicted that the force is always attractive for systems where polymer is allowed to desorb when two particles come close (full thermodynamic equilibrium). When the amount of polymer between the surfaces is constant, the force is repulsive at high concentrations of polymer and attractive at low concentrations, even in good solvents. This prediction agrees with experimental evidence. The attraction originates from bridging of polymer between two particles.

The principles of the new theory are applicable to many other systems involving flexible polymers. In chapter 6 a number of examples are given: adsorption of polydisperse polymer, of star-branched polymer, and of polyelectrolytes; the structure of lipid bilayers and of the amorphous phase of semi-crystalline polymer; and depletion flocculation in the presence of non-adsorbing polymer.

The advantage of the new concept is that it can handle the entire molecular weight range, from monomers up to very long polymers, the whole concentration range, all types of solvent, all sequences of different segments within the polymer chain, all types of branches along the chain and all mixtures of different (chain) molecules. Recent interest from technical and industrial laboratories indicates that this study is not only of theoretical importance.

1.6 REFERENCES

1. Vincent, B., Adv. Colloid Interface Sci., **4** (1974) 193.
2. Fleer, G.J.; and Lyklema, J., in: "Adsorption from Solution at the Solid/Liquid Interface". Parfitt, G.D.; and Rochester, C.H., Eds., Acad. Press, London, (1983) 153.
3. "Macromolecules", Bovey, F.A.; and Winslow, F.H., Eds.; Acad. Press, London, (1979).
4. Flory, P.J., "Principles of Polymer Chemistry", Cornell University Press, Ithaca, N.Y., (1953).
5. De Gennes, P.G., "Scaling Concepts in Polymer Physics", Cornell University Press, Ithaca, N.Y., (1979).
6. DiMarzio, E.A., J. Chem. Phys., **42** (1965) 2101.
7. Rubin, R.J., J. Chem. Phys., **43** (1965) 2392.
8. Silberberg, A., J. Chem. Phys., **48** (1968) 2835.
9. Hoeve, C.A.J., J. Chem. Phys., **44** (1966) 1505.
10. Mackor, E.L.; and Van der Waals, J.H., J. Coll. Sci., **7** (1952) 535.
11. Ash, S.G.; Everett, D.H.; and Findenegg, G.H., Trans. Faraday Soc., **66** (1970) 708; ibid., **67** (1971) 2122.
12. Roe, R.J., J. Chem. Phys., **60** (1974) 4192.
13. Cohen Stuart, M.A.; Scheutjens, J.M.H.M.; and Fleer, G.J., J. Polym. Sci., Polym. Phys. Ed., **18** (1980) 559.
14. Fleer, G.J.; and Lyklema, J., J. Colloid Interface Sci., **46** (1974) 1.
15. DiMarzio E.A.; and Rubin, R.J., J. Chem. Phys., **55** (1971) 4318.

Chapter 2

[Reprinted from the Journal of Physical Chemistry, 83, 1619 (1979).]

Statistical Theory of the Adsorption of Interacting Chain Molecules. 1. Partition Function, Segment Density Distribution, and Adsorption Isotherms

J. M. H. M. Scheutjens* and G. J. Fleer

Laboratory for Physical and Colloid Chemistry, De Dreijen 6, Wageningen, The Netherlands *(Received July 17, 1978; Revised Manuscript Received December 29, 1978)*

We present a general theory for polymer adsorption using a quasi-crystalline lattice model. The partition function for a mixture of polymer chains and solvent molecules near an interface is evaluated by adopting the Bragg–Williams approximation of random mixing within each layer parallel to the surface. The interaction between segments and solvent molecules is taken into account by use of the Flory–Huggins parameter χ; that between segments and the interface is described in terms of the differential adsorption energy parameter χ_s. No approximation was made about an equal contribution of all the segments of a chain to the segment density in each layer. By differentiating the partition function with respect to the number of chains having a particular conformation an expression is obtained that gives the numbers of chains in each conformation in equilibrium. Thus also the train, loop, and tail size distribution can be computed. Calculations are carried out numerically by a modified matrix procedure as introduced by DiMarzio and Rubin. Computations for chains containing up to 1000 segments are possible. Data for the adsorbed amount Γ, the surface coverage θ, and the bound fraction $p = \theta/\Gamma$ are given as a function of χ_s, the bulk solution volume fraction ϕ_*, and the chain length r for two χ values. The results are in broad agreement with earlier theories, although typical differences occur. Close to the surface the segment density decays roughly exponentially with increasing distance from the surface, but at larger distances the decay is much slower. This is related to the fact that a considerable fraction of the adsorbed segments is present in the form of long dangling tails, even for chains as long as $r = 1000$. In previous theories the effect of tails was usually neglected. Yet the occurrence of tails is important for many practical applications. Our theory can be easily extended to polymer in a gap between two plates (relevant for colloidal stability) and to copolymers.

I. Introduction

The adsorption of polymers at interfaces is an important phenomenon, both from a theoretical point of view and for numerous practical applications. One of the areas where polymer adsorption plays a role is in colloid science, since many colloidal systems are stabilized or destabilized by polymeric additives. In these cases, not only the adsorbed amount is an important parameter, but also the way in which the polymer segments are distributed in the vicinity of a surface. An adsorbed polymer molecule generally exists of *trains* (sequences in actual contact with the surface), *loops* (stretches of segments in the solution of which both ends are on the surface), and *tails* (at the ends of the chain with only one side fixed on the surface). If two surfaces are present at relatively short separations, *bridges* (of which the ends are adsorbed on different surfaces) may also occur. The properties of systems in which polymer is present depend strongly on the length and distribution of trains, loops, tails, and bridges.

Many of the older theories[1-6] on polymer adsorption treat the case of an isolated chain on a surface. These treatments neglect the interaction between the segments and have, therefore, little relevance for practical systems, since even in very dilute solutions the segment concentration near the surface may be very high. Other theories[7,8] account for the interaction between chain segments but make specific assumptions about the segment distribution near the surface which are not completely warranted, such as the presence of a surface phase with only adsorbed molecules[7] or the neglect of tails.[8] For oligomers up to four segments a sophisticated theory has been presented[9] but its application to real polymer molecules is impossible due to the tremendous computational difficulties involved. The most comprehensive theory for polymer adsorption as yet has been given by Roe,[10] although here also a simplifying assumption is made, namely, that each of the segments of a chain gives the same contribution to the segment density at any distance from the surface. Roe arrives at the segment density profile near the surface, but does not calculate loop, train, and tail size distributions. Recently, Helfand[11] has shown that Roe's theory is also incorrect on another point, since the inversion symmetry for chain conformations is not properly taken into account. Helfand corrects this by introducing the so-called flux constraint, but his calculations apply only to infinite chain lengths.

Less work has been done on the problem of polymer between two plates. DiMarzio and Rubin[12] give an elegant

matrix procedure for this case, but are not able to incorporate the polymer–solvent interaction. In two other recent theories[13,14] this was done for terminally adsorbing polymers. The paper by Levine et al.[14] can be considered as a combination of the matrix method of DiMarzio and Rubin and the self-consistent field theory.[15] However, here also the loop, train, and tail size distributions were not calculated.

In this series of articles, we describe how the probability of any chain conformation in a lattice adjoining one or two interfaces is found from the partition function for the mixture of polymer chains and solvent molecules in the lattice. The crucial difference with the theories of Roe and Helfand is that the partition function is not written in terms of concentrations of individual segments, but in terms of concentrations of chain conformations; throughout the derivation the chains are treated as connected sequences of segments. The interaction between segments and solvent molecules is taken into account by using the Bragg–Williams approximation of random mixing within each layer parallel to the surface, in a way similar to the well-known Flory–Huggins theory for moderately concentrated polymer solutions. The segment density near the interface is found from a modification of DiMarzio and Rubin's matrix formalism.[12] Since the probability of each conformation can be calculated, the distribution of trains, loops, and tails (and for the two-plate problem also bridges) can be found.

In this first paper we derive the adsorption isotherms and the segment density distribution for polymer adsorbing on one plate. In a second article, the loop, train, and tail size distribution will be treated in more detail. The general trends are in agreement with earlier theories,[7-10] but an important difference occurs concerning the segment density at relatively large distances from the surface. In this region, the main contribution to the segment concentration appears to be due to the presence of long dangling tails. This outcome was not found by former theories and may be considered as one of the most interesting results of the present treatment. It is certainly very important in the stabilization and flocculation of colloidal particles by polymers.

In a subsequent publication we shall treat the problem of polymer between two plates which is, among other applications, relevant for flocculation. Our method can easily be extended to (block and random) copolymers, to heterogeneous surfaces, etc. In later contributions these aspects will be dealt with.

II. Theory

A. Formulation of the Model. We consider a mixture of n polymer molecules, each consisting of r segments, and n^0 solvent molecules distributed over a lattice such that each solvent molecule occupies one lattice site. In the present paper, we consider only homopolymers of which each segment has the same size as a solvent molecule and also occupies one lattice site. The lattice adjoins an adsorbing surface and is divided into M layers of sites parallel to the surface, numbered $i = 1, 2, ..., M$. Each layer contains L lattice sites. Therefore

$$n^0 + rn = ML \tag{1}$$

The volume fractions of solvent in layer i are indicated by ϕ_i^0 and ϕ_i, respectively, and are given by

$$\phi_i^0 = n_i^0/L \qquad \phi_i = n_i/L \tag{2}$$

where n_i^0 and n_i are the numbers of solvent molecules and polymer segments in layer i. Far from the surface these volume fractions approach the equilibrium bulk volume fractions ϕ_*^0 and ϕ_*, respectively.

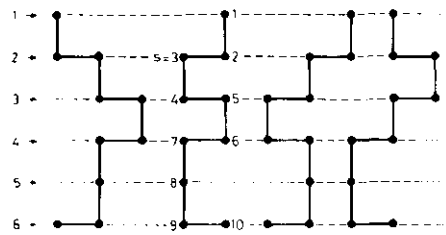

Figure 1. Some examples of different arrangements for a chain of 10 segments ($r = 10$). All the indicated arrangements belong to the conformation (1,1)(2,2)(3,2)(4,3)(5,3)(6,4)(7,4)(8,5)(9,6)(10,6). This example applies to a simple square two-dimensional lattice ($z = 4$, $\lambda_1 = 1/4$, $\lambda_0 = 1/2$). The number of different arrangements in the given conformation is $z^9\lambda_1^5\lambda_0^4 = 16$. Only four of them are indicated.

If z is the coordination number of the lattice, a lattice site in layer i has z nearest neighbors, of which a fraction λ_{j-i} is in layer j. Thus, $\lambda_{j-i} = \lambda_0$ if $j = i$ and $\lambda_{j-i} = \lambda_1 = \lambda_{-1}$ if $j = i \pm 1$. As there are no nearest neighbors in nonadjacent layers, $\lambda_{j-i} = 0$ if $|j - i| \geq 2$, and we may write

$$\sum_{j=1}^{M} \lambda_{j-i} = 1 \qquad 1 < i < M \tag{3}$$

For the two boundary layers ($i = 1$ and $i = M$), a correction has to be applied since there is only one adjacent layer, and a segment has only $z(\lambda_0 + \lambda_1) = z(1 - \lambda_1)$ nearest neighbors. Thus

$$\sum_{j=1}^{M} \lambda_{j-i} = 1 - \lambda_1 \qquad i = 1, M \tag{4}$$

The segments of a polymer chain are labeled $s = 1, 2, ..., r$. Each chain can assume a large number of possible conformations in the lattice. We characterize a *conformation* by defining the layer numbers in which each of the successive chain segments find themselves. We denote such a conformation by

$$(1,i)(2,j)(3,k)...(r-1,l)(r,m)$$

indicating that the first segment is in i, the second in j, the third in k, etc.

We have to realize that a conformation defined in this way is actually a set of many different arrangements. If segment s is placed in i and segment $s + 1$ in j, the number of different positions of segment $s + 1$ with respect to segment s is $z\lambda_0$ if $j = i$ and $z\lambda_1$ if $j = i \pm 1$. A dimer with conformation $(1,i)(2,j)$ can assume $Lz\lambda_{j-i}$ different positions; a trimer with conformation $(1,i)(2,j)(3,k)$ can be arranged in $Lz^2\lambda_{j-i}\lambda_{k-j}$ different ways, at least if backfolding of the chain is allowed. For example, in a simple cubic lattice ($z\lambda_1 = 1$) backfolding occurs in the conformation (1,2)(2,3)(3,2). In section II.D, we shall correct partly for this backfolding effect. Figure 1 illustrates for a simple case some different arrangements in a conformation.

We label the different conformations by c, d, ... If conformation c for an r-mer is characterized by the sequence given above, the number of different arrangements in this conformation is given by $Lz^{r-1}\lambda_{j-i}\lambda_{k-j}...\lambda_{m-l}$. More generally, we can write for the number of arrangements $L\omega_c z^{r-1}$ where ω_c is given by

$$\omega_c = \prod_{s=1}^{r-1} (\lambda_{s,s+1})_c \tag{5}$$

Here $(\lambda_{s,s+1})_c = \lambda_0$ if, in conformation c, segments s and $s + 1$ are in the same layer, and $(\lambda_{s,s+1})_c = \lambda_1$ if these two segments are in neighboring layers. Since z^{r-1} is the

number of arrangements for a chain in bulk polymer, of which one of the segments is fixed, ω_c may be considered as the ratio between the number of arrangements of conformation c and that in bulk polymer.

If the number of polymer molecules in conformation c is n_c, we have

$$n = \sum_c n_c \tag{6}$$

where the summation extends over all possible conformations c. Obviously, the number of terms in the summation of eq 6 increases sharply with r. In a few cases we will consider all the possible arrangements of only a part of the chain. Then, we will use the symbol $\omega_c(s,t)$ to indicate the relative number of arrangements of the chain part from segment s up to and including segment t. Similarly, a summation $\sum_{c(s,t)}$ specifies that all the possible conformations of that part of the chain have to be taken into account. In this terminology, ω_c in (5) could be written as $\omega_c(1,r)$ and $\sum_c$ in (6) as $\sum_{c(1,r)}$.

For the further elaboration it is expedient to introduce the symbol $r_{i,c}$ for the number of segments that conformation c has in layer i. Then the number of segments in layer i is given by

$$n_i = \sum_c r_{i,c} n_c \tag{7}$$

In the following sections we need a symbol to indicate the layer number in which segment s of conformation c finds itself. For this we use $k(s,c)$. Here, k is one of the layer numbers 1, 2, ..., M and is completely determined if conformation c is specified.

One remark on the use of conformations as defined above is in order. This definition corresponds to one particular way of grouping the possible arrangements of individual chains in a set. Other ways of grouping are, in principle, possible. Also, a procedure could be used in which the individual chain arrangements are not combined in sets but are all treated separately. It is easily proven that, although the partition function to be derived below is slightly changed, the equations obtained after maximization of the partition function are identical. Therefore, the grouping of chain arrangements in conformations as defined above is only a matter of convenience.

B. Partition Function. Roe[10] gives an approximate expression for the canonical partition function $Q(M,L,T,\{n_i^0\})$ for a given concentration profile $\{n_i^0\}$ of solvent molecules in a lattice of M layers with L lattice sites each. From this partition function, the equilibrium distribution of solvent molecules and thus also the overall distribution of polymer segments can be derived. Roe made no attempt to calculate the distribution of trains, loops, and tails.

Roe's approach involves the assumption that the distribution of a polymer segment does not depend on its ranking number s. The contribution of *each* of the r chain segments to the segment concentration ϕ_i in each layer is considered to be equal to ϕ_i/r. This is correct in bulk but not near an interface, because the interface imposes restrictions which are not necessarily the same for end and inner segments. As Helfand[11] has shown, Roe's derivation contains another error because the inversion symmetry is not obeyed. This is the requirement that conformation c, defined as $(1,i)(2,j)...(s,k)...(r,l)$, should have the same probability as the inverted conformation c', characterized by the sequence $(1,l)...(r-s+1,k)...(r-1,j)(r,i)$. Helfand maintains this symmetry by introducing an extra constraint, the flux constraint. His results apply only to infinitely high chain lengths. The flux constraint is only necessary if the partition function is written in terms of, and maximized with respect to, *the concentrations of individual segments in each layer*. It may be considered as a correction which is necessary to account fully for the connected nature of the segments in a chain.

An alternative derivation is possible if the partition function is maximized with respect to the numbers of polymer chains in each conformation, i.e., with respect to *concentrations of chains in each conformation*. This has the additional advantage of giving immediately the probability of every chain conformation in the equilibrium situation, so that the train, loop, and tail size distribution can be easily evaluated. Moreover, as will be shown below, the inversion symmetry is an automatic result of this approach. Thus, we want the canonical partition function $Q(M,L,T,\{n_c\})$ for an arbitrary but specified set of conformations $\{n_c\}$. We have to realize that a given overall segment distribution can be the result of a great number of different combinations of trains, loops, and tails.

We now give a derivation of $Q(M,L,T,\{n_c\})$. Since the numbers of chains in each conformation and thus the numbers of solvent molecules in each layer are specified, the energy U of the system for each of the possible ways of arrangement is the same, at least if we adopt the Bragg–Williams approximation. Therefore, the partition function can be written as the product of a combinatory factor (representing the configurational entropy) and $\exp(-U/kT)$. In accordance with Flory[16] and Roe[10] we take as the reference state disoriented bulk polymer and pure solvent. Then

$$Q(M,L,T,\{n_c\}) = \frac{\Omega}{\Omega^+} e^{-U/kT} \tag{8}$$

Here Ω is the number of ways of arranging n_c, n_d, n_e, ... polymer molecules in specified conformations, and n_1^0, ...n_i^0, ...n_M^0 solvent molecules over M distinguishable layers of L lattice sites each. Ω^+ is the number of ways of arranging n polymer chains over nr lattice sites in amorphous bulk polymer.

The combinatory factor Ω has to be evaluated according to the assigned distribution of conformations $\{n_c\}$. Naturally, if this set of conformations $\{n_c\}$ is specified, the concentration profile $\{n_i\}$ is completely determined.

We use the Bragg–Williams approximation of random mixing within each layer. This implies that the polymer segments in each layer are considered to be randomly distributed over the L lattice sites. The number of ways of placing a chain in conformation c in the empty lattice is $L\omega_c z^{r-1}$ (see eq 5). If part of the lattice sites is already occupied, a chain can only be placed if all the appropriate sites are vacant. Then we have to apply r correction factors, one for each of the chain segments. The correction factor for each segment is the vacancy probability of the site to be occupied. According to the Bragg–Williams approximation, we assume that all sites in layer i have the same vacancy probability, equal to $1 - \nu_i/L$, where ν_i is the number of previously occupied lattice sites in layer i. Obviously, $\nu_i = 0$ for an empty layer. The number of possibilities of placing one chain in conformation c can now be written as $L\omega_c z^{r-1}\prod_{s=1}^{r}(1 - \nu_{k(s,c)}/L) = \omega_c(z/L)^{r-1}\prod_{s=1}^{r}(L - \nu_{k(s,c)})$, where $\nu_{k(s,c)}$ is the number of previously occupied sites in the layer where segment s of conformation c is placed. For example, if conformation c of a hexamer is given by $(1,i)(2,j)(3,i)(4,j)(5,k)(6,j)$, $\omega_c = \lambda_1^5$ and the number of possibilities of placing this conformation in a lattice where a_i, a_j, and a_k lattice sites in the layers i, j, and k are already occupied is $(\lambda_1 z/L)^5(L - a_i)(L - a_j)(L - a_i - 1)(L - a_j - 1)(L - a_k)(L - a_j - 2)$. Generally, since $r_{i,c}$ segments are placed in layer i, this layer contributes $r_{i,c}$ factors, namely, $(L - a_i)(L - a_i - 1)(L - a_i - 2)...(L - a_i - r_{i,c} + 1)$, to the multiple product $\prod_{s=1}^{r}(L - \nu_{k(s,c)})$. The product over

the segment numbers can thus be replaced by a product over the layer numbers. The number of arrangements ω of placing the first chain (in conformation c) in the empty lattice ($a_i = 0$ for all i) becomes

$$\omega = \omega_c (z/L)^{r-1} \prod_{i=1}^{M} \prod_{\nu_i=0}^{r_{i,c}-1} (L - \nu_i) \tag{9}$$

where layers in which conformation c has no segments (thus for which $r_{i,c} = 0$) do not contribute to ω.

Placing all the n_c chains of conformation c gives a factor $\omega_c^{n_c}(z/L)^{(r-1)n_c}$ in (9) while the multiplication extends up to $\nu_i = n_c r_{i,c} - 1$. Similarly, the number of arrangements for $n = \sum_c n_c$ chains is

$$\omega(n) = (z/L)^{(r-1)n} \prod_c \omega_c^{n_c} \prod_{i=1}^{M} \prod_{\nu_i=0}^{n_i-1} (L - \nu_i) \tag{10}$$

because $n_i = \sum_c r_{i,c} n_c$ segments are placed in each layer. Next, solvent molecules have to be arranged over the $L - n_i$ remaining lattice sites, giving for each layer $\prod_{n_i=n_i}^{L-1}(L - \nu_i)$ possibilities. Thus, we find for Ω the simple expression

$$\Omega = (L!)^M (z/L)^{(r-1)n} \prod_c \frac{\omega_c^{n_c}}{n_c!} \prod_{i=1}^{M} \frac{1}{n_i^0!} \tag{11}$$

since $\prod_{i=1}^{M} L! = (L!)^M$. The factorials $n_c!$ and $n_i^0!$ in (11) correct for the indistinguishability of the n_c chains in each conformation c and of solvent molecules within each layer.

It may be noted that the order of placing chains and solvent molecules is irrelevant for the final result. Similarly, it does not matter which of the r chain segments of a chain is placed first.

The combinatory factor Ω^* has been derived by Flory[16] and can be written as

$$\Omega^* = \frac{(rn)!}{n!}(z/rn)^{(r-1)n} \tag{12}$$

This combinatory factor can also be found by a procedure similar to the derivation of our eq 11. In the bulk all the layers i are identical, so that the distinction in lattice layers is irrelevant. Since rn is the total number of (equivalent) lattice sites in bulk polymer, the factor $(L!)^M$ in (11) has to be replaced by $(rn)!$ and the factor $L^{(r-1)n}$ by $(rn)^{(r-1)n}$. Moreover, all possible conformations are equally probable, and we can group them together in only one conformation. Substitution of $n_c = n$, $\omega_c = 1$, and $n_i^0 = 0$ in (11) gives the Flory expression (eq 12), demonstrating that our eq 11 is in complete agreement with earlier theories.

Combination of (11) and (12) gives for the entropy part of ln Q:

$$\ln \Omega/\Omega^* = ML \ln L - \sum_c n_c \ln n_c/\omega_c - \sum_i n_i^0 \ln n_i^0 - n \ln r - (r-1)n \ln L \tag{13}$$

if Stirling's approximation for the factorials is applied.

The energy of the system contains a contribution due to the adsorption energy and a mixing term originating from the polymer–solvent interaction. We assume that in both cases only nearest-neighbor interactions are involved. The mixing term depends on the number of contacts between segments and solvent molecules. Each solvent molecule in layer i has $z\lambda_{j-i}$ contacts in layer j, a fraction ϕ_j of which are with polymer segments, according to the Bragg–Williams approximation. Since a site in i has neighbors in the layers $j = i-1, i, i+1$ the number of unlike contacts per solvent molecule in i is $z\sum_{j=1}^{M}\lambda_{j-i}\phi_j$. The total number of contacts is found by multiplying with n_i^0 and summing over all layers i. Thus, the total number of contacts of solvent molecules with segments is $z\sum_{i=1}^{M} n_i^0 \langle\phi_i\rangle$ and the (equal) number of segment–solvent molecule contacts is $z\sum_{i=1}^{M} n_i \langle\phi_i^0\rangle$, where the *site volume fractions* $\langle\phi_i\rangle$ for segments and $\langle\phi_i^0\rangle$ for solvent molecules are defined as

$$\langle\phi_i\rangle = \sum_{j=1}^{M} \lambda_{j-i}\phi_j \qquad \langle\phi_i^0\rangle = \sum_{j=1}^{M} \lambda_{j-i}\phi_j^0 \tag{14}$$

In the bulk solution $\langle\phi_*\rangle = \phi_*$ and $\langle\phi_*^0\rangle = \phi_*^0$. For $1 < i < M$, $\langle\phi_i\rangle + \langle\phi_i^0\rangle = 1$; for $i = 1$ and $i = M$, $\langle\phi_i\rangle + \langle\phi_i^0\rangle = 1 - \lambda_1$ (compare eq 4).

Using the familiar Flory–Huggins polymer solvent interaction parameter,[16] we can write for the energy part of ln Q:

$$U = n_1 u_s + n_1^0 u_s^0 + kT\chi \sum_{i=1}^{M} n_i^0 \langle\phi_i\rangle \tag{15}$$

In this equation, u_s and u_s^0 are the adsorption energies of a segment and a solvent molecule, respectively. They represent the energy change corresponding to the transfer of a segment (or solvent molecule) from bulk polymer (or solvent) to the surface. Equation 15 has also been given by Roe.[10]

It may be noted here that the energy terms in eq 15 also contain the thermal entropy, i.e., the additive part of the entropy proportional to the number of segments or solvent molecules. This thermal entropy includes vibrational and rotational contributions; the adsorption energy u_s may contain entropy terms due to orientation of solvent molecules near the surface (hydrophobic bonding). In this sense, the energy terms u_s, u_s^0, and $kT\chi$ may be considered as free energies. Obviously, the configurational part of the entropy is accounted for in ln Ω/Ω^*.

C. Conformation Probability. Equations 13 and 15 give the logarithm of the partition function at a given distribution of conformations $\{n_c\}$, which in general does not correspond to the equilibrium distribution. In order to find this equilibrium distribution, i.e., the number of chains n_d in a particular conformation d in the equilibrium situation, we have to find the derivative of ln Q with respect to n_d. The free energy of mixing is given by $F/kT = -\ln Q$. At constant temperature and volume the variation in F is given by $dF = \sum_c \mu_c\, dn_c + \sum_{i=1}^{M} \mu_i^0\, dn_i^0$. In equilibrium the chemical potentials $\mu_c = \mu_d = \ldots \mu_{chain}$ of a chain with respect to that in bulk polymer, and $\mu_i^0 = \mu_j^0 = \ldots \mu^0$ of a solvent molecule with respect to that in pure solvent are constant throughout the system. Adding one chain in conformation d (and removing r solvent molecules to maintain constant volume) changes F by an amount $(\partial F/\partial n_d)_{M,L,T,n_{c\neq n_d}}$, so that

$$-kT\left(\frac{\partial \ln Q}{\partial n_d}\right)_{M,L,T,n_{c\neq n_d}} = \mu_{chain} + \mu^0 \sum_{i=1}^{M}\left(\frac{\partial n_i^0}{\partial n_d}\right)_{M,L,T,n_{c\neq n_d}} = \mu_{chain} - r\mu^0 \tag{16}$$

Roe[10] derived an analogous expression using the grand canonical partition function. In eq 16 $\mu_{chain} - r\mu^0$ is a constant at given temperature and overall composition. The derivative $\partial n_i^0/\partial n_d$ in (16) is obtained by realizing that the differentiation has to be performed at constant volume. This implies that on addition of one chain in conformation d, r solvent molecules are removed from the system, of which the spatial distribution is given by

$$r_{i,d} = -(\partial n_i^0/\partial n_d)_{M,L,T,n_{c\neq n_d}} \tag{17}$$

because in each layer $r_{i,d}$ solvent molecules are displaced by the $r_{i,d}$ segments that conformation d has in layer i. Obviously

$$\sum_{i=1}^{M} r_{i,d} = r \tag{18}$$

The logarithm of the partition function is given by eq 13 and 15. The derivative of eq 13 is easily found with the help of (17), (18), and $\partial n/\partial n_d = \partial(\sum_c n_c)/\partial n_d = 1$. The result is

$$\frac{\partial \ln (\Omega/\Omega^+)}{\partial n_d} = -\ln \frac{n_d}{L} + \ln \omega_d - \ln r + r - 1 + \sum_{i=1}^{M} r_{i,d} \ln \phi_i^0 \tag{19}$$

For the differentiation of (15) we use also relation 17. We obtain

$$\frac{\partial(-U/kT)}{\partial n_d} = \sum_{i=1}^{M} r_{i,d}\{\chi_s\delta_{1,i} + \chi(\langle\phi_i\rangle - \langle\phi_i^0\rangle)\} \tag{20}$$

Here χ_s is the adsorption energy parameter, defined as

$$\chi_s = -(u_s - u_s^0)/kT \tag{21}$$

χ_s corresponds to the difference between the free energy of the transfer of a segment from bulk polymer to the surface and that of the transition of a solvent molecule from pure solvent to the surface. χ_s is positive if a segment is adsorbed preferentially to a solvent molecule. It is identical with the χ_s parameter used by Silberberg[7] and Roe.[10]

Combining eq 16, 19, and 20, we obtain

$$\ln n_d/L = \ln C + \ln \omega_d + \sum_{i=1}^{M} r_{i,d} \ln P_i \tag{22}$$

or

$$n_d/L = C\omega_d \prod_{i=1}^{M} P_i^{r_{i,d}} \tag{23}$$

where the constant C is given by $C = (1/r)\exp(\mu_{chain} - r\mu^0)/kT$ and the quantity P_i is defined as

$$\ln P_i = \chi_s\delta_{1,i} + \chi(\langle\phi_i\rangle - \langle\phi_i^0\rangle) + \ln \phi_i^0 \tag{24}$$

P_i is a very important parameter determining the probability of finding a free segment (monomer) in layer i. This can be concluded from (23). For $r = 1$, this equation reads $\phi_i = n_i/L = P_i \exp(\mu - \mu^0)/kT$. As for monomers P_i is proportional to ϕ_i, we may call P_i the *free segment probability*. According to eq 24, P_i may be written as $\phi_i^0 e^{-\Delta f_i'/kT}$, where $\Delta f_i'$ is the difference in free energy (excluding the configurational entropy) between a free segment and a solvent molecule in layer i. $\Delta f_i'$ contains an adsorption energy contribution $-kT\chi_s$ for the first layer and a mixing term $kT\chi(\langle\phi_i^0\rangle - \langle\phi_i\rangle)$ arising from the segment–solvent interaction. The Boltzmann factor $\exp(-\Delta f_i'/kT)$ has to be corrected by a factor ϕ_i^0, the fraction of the volume in layer i not occupied by segments. This factor $\phi_i^0 = 1 - \phi_i$ originates from the configurational entropy term of $\ln Q$; ϕ_i represents the volume fraction which is excluded due to the presence of other segments. This effect is partly analogous to the well-known excluded volume effect for polymer chains in solution. If $\phi_i^0 \simeq 1$, this "exclusion factor" is not important. That ϕ_i^0 is an entropy contribution may also be seen by writing P_i as $\exp(-\Delta f_i/kT)$ where $\Delta f_i = \Delta f_i' - kT \ln \phi_i^0$ now also includes the configurational entropy term $k \ln \phi_i^0$.

The starting point for further analysis is eq 23. It gives the relation between the number of chains in each conformation (of which the number of segments in each layer $r_{i,d}$ is known) and the free segment probability P_i in each of the layers. Equation 23 tells us that the probability of a conformation d is proportional to the quantity $\omega_d \prod_{i=1}^{M} P_i^{r_{i,d}}$, which we will call the *conformation probability*. From this probability, all information on the segment density distribution and other equilibrium properties (such as the train, loop, and tail size distribution) may be obtained.

Equation 23 leads immediately to the conclusion that any conformation has the same probability as its inverted conformation (in which the segments are placed in reverse order), since all $r_{i,d}$ values are the same for both conformations. Thus the inversion symmetry discussed in section II.B is an automatic result of our derivation and need not be introduced as an extra constraint, as was done by Helfand.[11] As discussed before, this is due to the fact that the partition function is maximized with respect to the number of chains in every conformation, which accounts completely for the connected nature of the chain segments.

D. Segment Density Distribution. In this section we calculate the equilibrium segment density distribution from the conformation probability $P(r)_c$, which according the the previous section can be defined as

$$P(r)_c = \omega_c \prod_{i=1}^{M} P_i^{r_{i,c}} = \omega_c \prod_{s=1}^{r} P_{k(s,c)} \tag{25}$$

Here we have used the fact that a product of P_i over the consecutive layer numbers i may be replaced by a product over the consecutive segment ranking numbers s. In both products the free segment probabilities corresponding to each chain segment are taken once, and only the order in which the P_i's occur is different. $P_{k(s,c)}$ is the free segment probability for a segment in the layer where segment s of a chain in conformation c finds itself. This layer number is completely specified if c is given.

We define the *chain probability* as the summation of $P(r)_c$ over all possible conformations:

$$P(r) = \sum_c P(r)_c \tag{26}$$

$P(r)$ will be needed as a normalization factor.

It is useful to consider the probability $P(s,i;r)$ that the sth segment of any chain of r segments finds itself in i. The probability $P(s,i;r)_c$ of a conformation c of which the sth segment is in i is equal to $P(r)_c$ with the additional condition that $P_{k(s,c)} = P_i$:

$$P(s,i;r)_c = \omega_c \prod_{t=1}^{s-1} P_{k(t,c)} P_i \prod_{t=s+1}^{r} P_{k(t,c)} = \frac{\omega_c}{P_i} \prod_{t=1}^{s} P_{k(t,c)} \prod_{t=s}^{r} P_{k(t,c)} \tag{27}$$

The last part of eq 27 is obtained by including $P_{k(s,c)} = P_i$ in both multiple products and is written in this way for later convenience. Note that $P(s,i;r)_c$ equals $P(r)_c$ if segment s in conformation c is in layer i, and zero if s is not in i. Obviously, the probability of finding the sth segment of any chain in layer i, $P(s,i;r)$, is obtained by summing over all possible conformations:

$$P(s,i;r) = \sum_c P(s,i;r)_c \tag{28}$$

Summation of $P(s,i;r)$ over all layers gives just the chain probability $P(r)$:

$$\sum_{i=1}^{M} P(s,i;r) = \sum_c \sum_{i=1}^{M} P(s,i;r)_c = \sum_c P(r)_c = P(r) \tag{29}$$

As mentioned above, the summation of $P(s,i;r)_c$ over all layers gives only one nonzero term $P(r)_c$.

A special case of $P(s,i;r)$ is the probability $P(r,i;r)$ that the end segment of any chain of r segments is in layer i. We use an abbreviated notation for this quantity: $P(i,r) \equiv P(r,i;r)$. We can write $P(i,r)$ as $\sum_c P(r)_c$ with the addi-

tional condition that $P_{k(r,c)} = P_i$. According to (25):

$$P(i,r) = P_i \sum_c \omega_c \prod_{s=1}^{r-1} P_{k(s,c)} \tag{30}$$

From (29) it follows:

$$\sum_{i=1}^{M} P(i,r) = P(r) \tag{31}$$

We designate $P(i,r)$ as the *end segment probability*.

The segment density in layer i is proportional to the summation of $P(s,i;r)$ over all the r chain segments:

$$\frac{\phi_i}{\sum_{i=1}^{M} \phi_i} = \frac{\sum_{s=1}^{r} P(s,i;r)}{\sum_{i=1}^{M} \sum_{s=1}^{r} P(s,i;r)} = \frac{1}{rP(r)} \sum_{s=1}^{r} P(s,i;r) \tag{32}$$

Thus, if we are able to evaluate the probabilities $P(s,i;r)$ we can calculate the segment volume fraction ϕ_i in each layer. This we accomplish in two steps. First we show that $P(s,i;r)$ for any s can be expressed in the end segment probabilities $P(i,s)$ and $P(i,r-s+1)$, and next we use a well-known matrix procedure[12] to obtain the end segment probabilities $P(i,s)$.

The first step starts from eq 28 in which the summation over all the possible conformations of the entire chain, $\sum_{c(1,r)}$, is replaced by a summation over all the possible conformations of the first part of the chain, $\sum_{c(1,s)}$, and one for the second part, $\sum_{c(s,r)}$. If segment s is in layer i, the possible conformations $c(1,s)$ are independent of the conformations $c(s,r)$ because for any conformation of the first s segments all conformations for the last $r - s + 1$ segments are possible. Thus, we may use the relation $\sum_i \sum_j a_i b_j = (\sum_i a_i)(\sum_j b_j)$. Substituting (27) for $P(s,i;r)_c$ and splitting the multiple product $\omega_c = \omega_c(1,r) = \prod_{t=1}^{r-1} (\lambda_{t,t+1})_c$ in the factors $\omega_c(1,s)$ and $\omega_c(s,r)$ (compare eq 5), we may write:

$$P(s,i;r) = \sum_{c(1,s)} \sum_{c(s,r)} P(s,i;r)_c = \frac{1}{P_i} \Big(\sum_{c(1,s)} \omega_c(1,s) \prod_{t=1}^{s} P_{k(t,c)} \Big) \Big(\sum_{c(s,r)} \omega_c(s,r) \prod_{t=s}^{r} P_{k(t,c)} \Big)$$

Since $P_{k(s,c)} = P_i$, the first factor between brackets equals $P(i,s)$, according to (30); the second factor is equal to $P(i,r-s+1)$ because the number of conformations of the last $r - s + 1$ segments should be equal to that of the first $r - s + 1$ segments. Therefore we have

$$P(s,i;r) = P(i,s)P(i,r-s+1)/P_i \tag{33}$$

Thus, through eq 32 and 33 ϕ_i for r-mers can be expressed as a function of end segment probabilities of shorter chains.

The second step for the calculation of ϕ_i is to find a procedure to evaluate $P(i,s)$. If the end segment of an r-mer is in layer i, the $(r-1)$th segment can be in layer j $(1 \le j \le M)$, with a nonzero probability only if $j = i - 1$, i, $i + 1$. The probability $P(i,r)$ that the end segment of an r-mer is in i can then be expressed in the probabilities $P(j,r-1)$ that the end segment of an $(r-1)$-mer is in layer j. Using eq 30, we can again split the summation in two parts: $\sum_{c(1,r)} = \sum_{c(1,r-1)} \sum_{c(r-1,r)}$. As the rth segment is fixed in layer i, the summation $\sum_{c(r-1,r)}$ includes only the possible positions of the $(r-1)$th segment and may be replaced by a summation over j if $\omega_c(r-1,r)$ is replaced by $\lambda_{j,i}$ and $P_{k(r-1,c)}$ by P_j. Thus

$$P(i,r) = \sum_j \lambda_{j-i} P_i P_j \sum_{c(1,r-1)} \omega_c(1,r-1) \prod_{s=1}^{r-2} P_{k(s,c)}$$

In this expression we recognize $P(j,r-1)$, so that we can write

$$P(i,r) = \sum_j \lambda_{j-i} P_i P(j,r-1) \tag{34}$$

It may be noted here that in this derivation it was assumed that the free segment probabilities P_i for the last segment, P_j $(j = i, i \pm 1)$ for the penultimate $((r-1)$th) segment and P_k $(k = j, j \pm 1)$ for the antepenultimate segment are independent of each other. P_i, P_j, and P_k include a factor for the *average* solvent volume fractions in the layers i, j, and k. This assumption implies that backfolding of the chain (i.e., $k = i$ in the example given) is allowed under the constraint of the average excluded volume in each layer. In other words, if segment $r - 2$ is placed in i and segment $r - 1$ in $i + 1$, segment r may fold back to i with a probability P_i in which the presence of the $(r-2)$th segment is accounted for in the same way as the presence of all other segments in i. Segment $r - 2$ is, like all the previously placed segments, considered to be "smeared out" over all the lattice sites L in i. A similar approximation is made in the familiar Flory–Huggins lattice theory.[16]

Equation 34 can be expressed as a matrix multiplication by defining a vector $\mathbf{P}(r)$ with M components $P(i,r)$, whose sum according to (31) equals $P(r)$, and a matrix $\boldsymbol{W}$ of which the elements W_{ij} are equal to $\lambda_{j-i}P_i$. Therefore

$$\mathbf{P}(r) = \boldsymbol{W}\mathbf{P}(r-1) = \boldsymbol{W}^{r-1}\mathbf{P}(1) \tag{35}$$

where the components of the vector $\mathbf{P}(1)$ are the "end" segment probabilities of a monomer and are thus simply equal to P_i as defined by (24). The matrix $\boldsymbol{W}$ is, apart from a different interpretation of P_i (in which the polymer–solvent interactions are included), identical with that used by DiMarzio and Rubin.[12]

Thus we can calculate all the end segment probabilities $P(i,s)$ for $s = 1, 2, \ldots, r$. Substituting (33) into (32) and realizing that $\sum_{i=1}^{M} \phi_i = nr/L$, we obtain

$$\phi_i = \frac{n}{LP(r)} \frac{1}{P_i} \sum_{s=1}^{r} P(i,s)P(i,r-s+1) \tag{36}$$

From these M implicit equations the M ϕ_i's and the equilibrium values for P_i can be solved by an iteration procedure (see section III). We can arrange all the necessary information in the array shown in eq 37, where the

$$\boldsymbol{P} = \begin{bmatrix} P(1,1) & \ldots & P(1,s) & \ldots & P(1,r) \\ \vdots & & \vdots & & \vdots \\ P(i,1) & \ldots & P(i,s) & \ldots & P(i,r) \\ \vdots & & \vdots & & \vdots \\ P(M,1) & \ldots & P(M,s) & \ldots & P(M,r) \end{bmatrix} \tag{37}$$

components of the first column are equal to $P_1 \ldots P_i \ldots P_M$ and the components of the sth column $P(i,s)$ are found from the first after $s - 1$ matrix multiplications. The sum of the components of the last column is equal to $P(r)$ according to (31). For the calculation of ϕ_i we need the ith row of array $\boldsymbol{P}$, and we have to add the r products of the first and the last, the second and the penultimate, the third and the antepenultimate element, etc.

All the probabilities $P(i,s;r)$, $P(i,r)$, and $P(r)$ used in this section depend on the lattice size M and on the average segment concentration rn/ML. We shall need these quantities in a following paper where we shall discuss the case of a polymer between two plates at relatively short separation and a constant amount of polymer. For the adsorption on a single plate we relate the concentration of polymer to the bulk volume fraction ϕ_b. It appears advantageous in this case to use probabilities related to those in the bulk solution.

E. Adsorption Isotherms. In calculating adsorption isotherms and related properties, the state of a chain or a segment near the interface has to be compared to that in the bulk of the solution. Consequently, it is useful to define the probabilities of any configuration near the interface with respect to those in bulk. We shall denote bulk properties by an asterisk.

The free segment probability P_* for a segment in the bulk solution is analogously to eq 24 given by

$$\ln P_* = \chi(\phi_* - \phi_*^0) + \ln \phi_* \tag{38}$$

We now define the free segment probability p_i with respect to the bulk solution as

$$p_i = P_i/P_* \tag{39}$$

It is easily verified that p_i can be written as $(\phi_i^0/\phi_*^0)\cdot \exp(-\Delta f_i^*/kT)$, where Δf_i^* is the free energy difference (excluding the configurational entropy) for the exchange of a solvent molecule in layer i and a free segment in the bulk. The entropy factor ϕ_i^0/ϕ_*^0 accounts for the difference in the "volume exclusion" effect for a segment in layer i and a segment in bulk. It is obvious that p_* equals unity.

With eq 39 we define the vectors $\mathbf{p}(r)$ and the matrix $\boldsymbol{w}$ as

$$\mathbf{p}(r) = \mathbf{P}(r)/P_*^r \qquad p(i,1) = p_i \tag{40}$$

$$\boldsymbol{w} = \boldsymbol{W}/P_* \qquad w_{ij} = \lambda_{j-i}p_i \tag{41}$$

It may be noted here that the error introduced by allowing backfolding (accounting for the average volume fraction) is eliminated here to a large extent if this effect is equally important in the bulk and in layer i, because probabilities in layer i are now compared with those in bulk. Now eq 35 becomes

$$\mathbf{p}(r) = \boldsymbol{w}\mathbf{p}(r-1) = \boldsymbol{w}^{r-1}\mathbf{p}(1) \tag{42}$$

In a more explicit form, (42) can be given as shown in eq 43. Equation 36 can be written in a simpler way by re-

$$\begin{bmatrix} p(1,r) \\ \vdots \\ p(i,r) \\ \vdots \\ p(M,r) \end{bmatrix} = \begin{bmatrix} \lambda_0\rho_1 & \lambda_1\rho_1 & 0 & \cdots & 0 \\ \lambda_1\rho_2 & & & & \vdots \\ 0 & \ddots & \lambda_1\rho_i & \lambda_0\rho_i & \lambda_1\rho_i \\ & & & & 0 \\ 0 & \cdots & 0 & \lambda_1\rho_M & \lambda_0\rho_M \end{bmatrix}^{r-1} \begin{bmatrix} \rho_1 \\ \vdots \\ \rho_i \\ \vdots \\ \rho_M \end{bmatrix} \tag{43}$$

alizing that from (34), which remains valid if P_i and $P(i,r)$ are replaced by p_i and $p(i,r)$, follows that $p(*,r) = p(*,r-1) = p(*,1) = p_* = 1$. Equation 36 applied for bulk solution gives

$$\phi_* = nr/Lp(r) \tag{44}$$

This can be substituted in (36), giving the result

$$\phi_i = \frac{\phi_*}{r}\frac{1}{p_i}\sum_{s=1}^{r} p(i,s)p(i,r-s+1) \tag{45}$$

Also the components $p(i,s)$ can be arranged in an array $\boldsymbol{p}$ (eq 46). The sum of the components of the last vector

$$\boldsymbol{p} = \begin{bmatrix} p(1,1) & \cdots & p(1,s) & \cdots & p(1,r) \\ \vdots & & \vdots & & \vdots \\ p(i,1) & \cdots & p(i,s) & \cdots & p(i,r) \\ \vdots & & \vdots & & \vdots \\ p(M,1) & \cdots & p(M,s) & \cdots & p(M,r) \end{bmatrix} \tag{46}$$

of $\boldsymbol{p}$ is indicated by $p(r)$, analogously to eq 31.

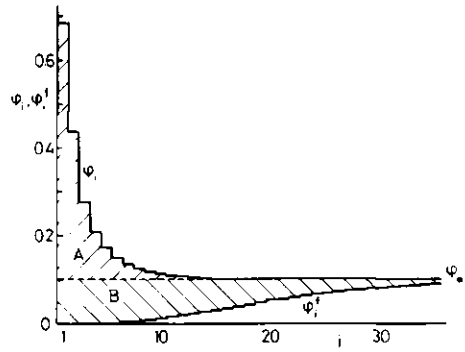

Figure 2. Illustration of the definition of the excess adsorbed amount Γ_{exc} and the adsorbed amount Γ. Γ_{exc} is equal to area A, while Γ equals the sum of A and B. In order to show the difference between Γ and Γ_{exc} more clearly, a rather high bulk volume fraction ($\phi_* = 0.1$) was chosen in this example. The concentration profiles have been calculated for $r = 1000$, $\chi_s = 1$, $\chi = 0.5$, and $\lambda_0 = 0.5$ (hexagonal lattice).

The simplest way of defining the adsorbed amount is to consider only the excess concentration of segments in each layer with respect to the bulk concentration. Then the excess adsorbed amount per surface site is

$$\Gamma_{exc} = \sum_{i=1}^{M} (\phi_i - \phi_*) \tag{47}$$

This definition was used by Roe. However, another definition is sometimes useful. If we want to know the number of chain segments belonging to adsorbed chains, subtracting ϕ_* from ϕ_i for all layers is not the correct procedure, since the volume fraction ϕ_i in the layers close to the surface is predominantly (or completely, for $i = 1$) due to adsorbed chains. In order to find the number of adsorbed molecules, we have to correct only for the volume fraction ϕ_i^f of free (i.e., nonadsorbed) chains that have not a single segment in the first layer (see Figure 2). In the surface layer ($i = 1$), $\phi_i^f = \phi_1^f = 0$, for the other layers $\phi_i^f \leq \phi_*$, so that eq 47 gives an underestimation of the adsorbed amount. Therefore we define the adsorbed amount Γ as

$$\Gamma = \sum_{i=1}^{M} (\phi_i - \phi_i^f) \tag{48}$$

Γ thus gives the number of segments of adsorbed chains per surface site; if $\Gamma = 1$, one equivalent monolayer is adsorbed. This definition of Γ was also used by Silberberg.[7] Note that the summation of (48) contains only nonzero terms for $i \leq r$.

The problem now is to find ϕ_i^f. A free chain has only one extra restriction: no segment of the chain may be in the first layer. This is equivalent to the statement that for the segments of free polymer molecules the free segment probability p_1 in the first layer equals zero (equivalent to $\chi_s = -\infty$), while in the other layers the free segment probability p_i is the same for segments of adsorbed and nonadsorbed chains. Naturally, the value of p_i for $i > 1$ is based on the total segment density ϕ_i. We may therefore define a vector $\mathbf{p}_f(1)$ with components $p_f(i,1) = (1 - \delta_{1,i})p(i,1)$ and a matrix $\boldsymbol{w}_f$ with elements $w_{fij} = (1 - \delta_{1,i})\lambda_{j-i}p_i$. The end segment probability vector for free chains is then given by

$$\mathbf{p}_f(r) = \boldsymbol{w}_f\mathbf{p}_f(r-1) = \boldsymbol{w}_f^{r-1}\mathbf{p}_f(1) \tag{49}$$

As before, we can write these vectors $\mathbf{p}_t(r)$ in an array where the sum of the components of the last vector is denoted as $p_t(r)$ (eq 50).

$$p_t = \begin{bmatrix} 0 & 0 \ldots\ldots\ldots 0 \ldots\ldots\ldots 0 \\ p_2 & p_t(2,2) \ldots\ldots p_t(2,s) \ldots\ldots p_t(2,r) \\ \vdots & \vdots \\ p_i & p_t(i,2) \ldots\ldots p_t(i,s) \ldots\ldots p_t(i,r) \\ \vdots & \vdots \\ p_M & p(M,2) \ldots\ldots p_t(M,s) \ldots\ldots p_t(M,r) \end{bmatrix} \quad (50)$$

Comparing (50) with (46), we note that $p_t(i,s) = p(i,s)$ for $i > s$, $p_t(i,s) < p(i,s)$ for $2 \le i \le s$, while $p_t(1,s) = 0$. For each i, the value of ϕ_i^t can now be found from (45), substituting $p_t(i,s)$ for $p(i,s)$. For the calculation of Γ we need $\sum_{i=1}^{M} \phi_i^t$ which can be derived directly from $p_t(r)$. To that end, we realize that according to (44) $nr/L = \sum_{i=1}^{M} \phi_i = p(r)\phi_*$. Analogously, $\sum_{i=1}^{M} \phi_i^t = p_t(r)\phi_*$, so that (48) may be written as

$$\Gamma = [p(r) - p_t(r)]\phi_* = p_a(r)\phi_* \quad (51)$$

where $p_a(r) \equiv p(r) - p_t(r)$ is the adsorbed chain probability which we shall need as a normalization constant for the adsorbed chains. It may be noted that, unlike $P(r)$ as used in the previous section, the adsorbed chain probability $p_a(r) = \Gamma/\phi_*$ is independent of M, at least for large M.

Thus, for the calculation of Γ at given ϕ_* we need the normalization constant $p(r)$, which is found by the iteration procedure to be described in section III, and $p_t(r)$. Once the iteration process has given the free segment probabilities $p_i = p(i,1)$, $p_t(r)$ and thus $p_a(r)$ are simply the result of $r - 1$ matrix multiplications according to (49).

F. Interfacial Free Energy. Using the Gibbs convention (see, e.g., ref 17), we assign to the Gibbs dividing plane a surface excess free energy F^σ, a surface excess n^σ of polymer molecules, and a surface excess $n^{0\sigma}$ of solvent molecules. The relation between these surface excesses is given by[17]

$$F^\sigma = \gamma A + n^\sigma \mu_{\text{chain}} + n^{0\sigma}\mu^0 \quad (52)$$

where μ_{chain} and μ^0 are the chemical potentials of a polymer molecule and a solvent molecule with respect to the reference state, γ is the interfacial free energy, and A is the interfacial area. The free energy $F - F^\sigma$ of the bulk phase is then

$$F - F^\sigma = (n - n^\sigma)\mu_{\text{chain}} + (n^0 - n^{0\sigma})\mu^0 \quad (53)$$

Combining (52) and (53), and introducing $a = A/L$ as the area per surface site, we find

$$\frac{\gamma a}{kT} = -\frac{1}{L}\ln Q - \frac{n}{L}\frac{\mu_{\text{chain}}}{kT} - \frac{n^0}{L}\frac{\mu^0}{kT} \quad (54)$$

The term $\ln Q$ is given by eq 13 and 15. Expressions for μ_{chain} and μ^0 have been derived by Flory:[16]

$$\mu_{\text{chain}}/kT = 1 - \phi_* - r\phi_*^0 + \ln \phi_* + r\chi\phi_*^0(1 - \phi_*) \quad (55)$$

$$\mu^0/kT = 1 - \phi_*^0 - \phi_*/r + \ln \phi_*^0 + \chi\phi_*(1 - \phi_*^0) \quad (56)$$

Equation 55 can also be derived by differentiating $\ln Q$ with respect to n_c at constant T, n_i^0, and n_d ($d \neq c$); similarly, eq 56 follows from the derivative of $\ln Q$ with respect to n_i^0 at constant T, n_c, and n_j^0 ($j \neq i$).

Before substituting (55) and (56) into (54), we rewrite n_c in eq 13. With the equilibrium condition (25) and the normalization condition (26), we obtain $n_c/n = \omega_c(\prod_{i=1}^{M} P_i^{r_{i\infty}})/P(r)$. Using $P(r) = P_*^r p(r)$ (eq 40) and eq 44, we find

$$\frac{n_c}{L} = \frac{\omega_c \phi_*}{r}\prod_i p_i^{r_{i\infty}} \quad (57)$$

which can be substituted into (13), giving after some rearrangement

$$-\ln Q = n \ln \phi_* + \sum_i n_i^0 \ln \phi_i^0 + \sum_i n_i \ln p_i + U/kT \quad (58)$$

Thus the $n_c \ln n_c$ term in $\ln Q$ is replaced by a term containing the free segment probability p_i. The energy term of (58) is given by (15). Combining eq 54, 55, 56, and 58, we derive the following expression for γ:

$$\frac{\gamma a}{kT} = \frac{\phi_1 u_s + \phi_1^0 u_s^0}{kT} + \sum_{i=1}^{M}\left\{\phi_i^0 \ln \frac{\phi_i^0}{\phi_*^0} + \phi_i \ln p_i - (\phi_i^0 - \phi_*^0) - (\phi_i - \phi_*)/r\right\} + \chi \sum_{i=1}^{M} |\phi_i^0((\phi_i) - \phi_*) - \phi_*^0(\phi_i - \phi_*)| \quad (59)$$

This equation can easily be extended for systems with more than two components. For a binary system ($\phi_i + \phi_i^0 = 1$) the term $-\sum_{i=1}^{M}\{(\phi_i^0 - \phi_*^0) + (\phi_i - \phi_*)/r\}$ reduces to $[1 - (1/r)]\Gamma_{\text{exc}}$. Apart from the $\phi_i \ln p_i$ term, all the terms of eq 59 also appear in Roe's equation (eq 36 of ref 10). In section V we give a more detailed comparison between Roe's and our theories.

III. Method of Computation

Equation 45 comprises M implicit simultaneous equations from which the M unknown ϕ_1, ϕ_2, ..., ϕ_M can be solved by an iterative procedure. If for a given ϕ_* an initial estimate for the concentration profile $\{\phi_i\}$ is used, the vector $\mathbf{p}(1)$ follows from (40) in combination with (38) and (24) and the matrix $\boldsymbol{w}$ from (41). In principle, a new value for $\{\phi_i\}$ could then be calculated using (45), and the procedure could be repeated by finding new values for the components $p(i,1)$, for $\boldsymbol{w}$ and again $\{\phi_i\}$. It turned out, however, that in this way the iteration usually does not converge. Therefore, a slightly more complicated method was applied, in which $X_i = \ln\{\phi_i/(1 - \phi_i)\}$ instead of ϕ_i was chosen as the iteration variable and Newton's method (see, e.g., ref 18) was used to improve the convergence of the iteration. This method is easier to apply if the variables are unconstrained, and therefore the variable X_i was preferred to the variable ϕ_i, which is constrained within 0 and 1.

The procedure was as follows. We indicate the initial estimate by $\{\phi_i\}^{(1)}$ and the kth solution by $\{\phi_i\}^{(k)}$. From $\{\phi_i\}^{(k)}$ the vector $\mathbf{p}(1)^{(k)}$ and the matrix $\boldsymbol{w}^{(k)}$ were calculated using (41). Then a new set $\{\phi_i\}^{(k')}$ was found from (45). The $(k + 1)$th solution follows from

$$\mathbf{X}^{(k+1)} = \mathbf{X}^{(k)} - [\boldsymbol{G}^{(k)}]^{-1}\mathbf{g}^{(k)}$$

where $\mathbf{X}^{(k)}$ is a vector whose ith component $X_i^{(k)} = \ln\{\phi_i^{(k)}/(1 - \phi_i^{(k)})\}$, $\mathbf{g}^{(k)}$ is a vector with components $g_i^{(k)} = \ln(\phi_i^{(k')}/\phi_i^{(k)})$, and the matrix $\boldsymbol{G}^{(k)}$ is the Hessian,[18] with elements $G_{ij}^{(k)} = \partial g_i^{(k)}/\partial X_j$. In order to avoid the complex differentiation which is necessary to find $G_{ij}^{(k)}$ differences where used for the derivatives: $G_{ij}^{(k)} \simeq \Delta g_i^{(k)}/\Delta X_j$. The initial estimate $\{\phi_i\}^{(1)}$ was found from Roe's approximate expression[10] and is itself the result of a short iteration.

If we want to calculate the segment density distribution and the adsorbed amount for an r-mer, it is in principle necessary to use a lattice with more than r layers, i.e., $M > r$, since then all the possible conformations, including the completely perpendicular ones, can be taken into account. This would require a large amount of computing time and an enormous storage capacity in the computer.

TABLE I: Numerical Example of the Free Segment Probability p_i, the Polymer Volume Fraction ϕ_i, and the Volume Fraction due to Segments of Adsorbed Chains $\phi_i - \phi_i^f$, as a Function of the Layer Number i[a]

i	p_i	ϕ_i	$\phi_i - \phi_i^f$	ϕ_i^R
		$\chi = 0$		
1	1.6251	4.0815×10^{-1}	4.0815×10^{-1}	4.1979×10^{-1}
2	0.8343	1.7409×10^{-1}	1.7409×10^{-1}	1.8029×10^{-1}
3	0.9400	6.9353×10^{-2}	6.9342×10^{-2}	6.6164×10^{-2}
4	0.9697	3.9993×10^{-2}	3.9958×10^{-2}	2.8415×10^{-2}
5	0.9823	2.7510×10^{-2}	2.7428×10^{-2}	1.5078×10^{-2}
6	0.9888	2.1089×10^{-2}	2.0931×10^{-2}	1.0068×10^{-2}
7	0.9925	1.7388×10^{-2}	1.7117×10^{-2}	8.3540×10^{-3}
8	0.9949	1.5084×10^{-2}	1.4661×10^{-2}	8.0960×10^{-3}
9	0.9964	1.3569×10^{-2}	1.2950×10^{-2}	8.4583×10^{-3}
10	0.9974	1.2531×10^{-2}	1.1672×10^{-2}	8.9942×10^{-3}
11	0.9982	1.1798×10^{-2}	1.0656×10^{-2}	9.4711×10^{-3}
12	0.9987	1.1267×10^{-2}	9.8037×10^{-3}	9.8014×10^{-3}
13	0.9991	1.0878×10^{-2}	9.0560×10^{-3}	9.9854×10^{-3}
14	0.9994	1.0589×10^{-2}	8.3785×10^{-3}	1.0062×10^{-2}
15	0.9996	1.0374×10^{-2}	7.7506×10^{-3}	1.0076×10^{-2}
16	0.9998	1.0214×10^{-2}	7.1603×10^{-3}	1.0061×10^{-2}
17	0.9999	1.0096×10^{-2}	6.6009×10^{-3}	1.0039×10^{-2}
18	1.0000	1.0010×10^{-2}	6.0964×10^{-3}	1.0020×10^{-2}
19	1.0001	9.9499×10^{-3}	5.5645×10^{-3}	1.0007×10^{-2}
20	1.0001	9.9087×10^{-3}	5.0858×10^{-3}	1.0000×10^{-2}
		$\chi = 0.5$		
1	1.5412	6.7976×10^{-1}	6.7976×10^{-1}	6.8544×10^{-1}
2	0.8982	4.2532×10^{-1}	4.2531×10^{-1}	4.3667×10^{-1}
3	0.9843	2.5583×10^{-1}	2.5579×10^{-1}	2.4809×10^{-1}
4	0.9889	1.8157×10^{-1}	1.8146×10^{-1}	1.4778×10^{-1}
5	0.9935	1.3752×10^{-1}	1.3731×10^{-1}	9.2992×10^{-2}
6	0.9958	1.0880×10^{-1}	1.0845×10^{-1}	6.1294×10^{-2}
7	0.9972	8.8726×10^{-2}	8.8197×10^{-2}	4.2082×10^{-2}
8	0.9981	7.4009×10^{-2}	7.3261×10^{-2}	3.0050×10^{-2}
9	0.9986	6.2835×10^{-2}	6.1831×10^{-2}	2.2351×10^{-2}
10	0.9990	5.4120×10^{-2}	5.2828×10^{-2}	1.7363×10^{-2}
11	0.9992	4.7177×10^{-2}	4.5569×10^{-2}	1.4123×10^{-2}
12	0.9994	4.1550×10^{-2}	3.9603×10^{-2}	1.2034×10^{-2}
13	0.9995	3.6925×10^{-2}	3.4619×10^{-2}	1.0719×10^{-2}
14	0.9996	3.3078×10^{-2}	3.0400×10^{-2}	9.9288×10^{-3}
15	0.9997	2.9846×10^{-2}	2.6786×10^{-2}	9.4943×10^{-3}
16	0.9998	2.7109×10^{-2}	2.3662×10^{-2}	9.2974×10^{-3}
17	0.9998	2.4776×10^{-2}	2.0940×10^{-2}	9.2534×10^{-3}
18	0.9999	2.2775×10^{-2}	1.8554×10^{-2}	9.3013×10^{-3}
19	0.9999	2.1053×10^{-2}	1.6451×10^{-2}	9.3978×10^{-3}
20	0.9999	1.9565×10^{-2}	1.4592×10^{-2}	9.5133×10^{-3}

[a] In the last column the volume fraction as calculated from Roe's theory,[10] ϕ_i^R, is shown. Data are given for an athermal solvent ($\chi = 0$) and a Θ solvent ($\chi = 0.5$). Hexagonal lattice ($\lambda_1 = 0.5$), $\chi_s = 1$, $r = 1000$, $\phi_* = 0.01$.

Fortunately, a faster computation with much less storage requirements is possible. With increasing i the elements $p(i,s)$, the end segment probabilities, converge to unity since far from the surface the probability of finding an end segment is equal to that in bulk. This convergence is rather slow for high s. However, it turned out that the free segment probabilities $p_i = p(i,1)$ approach unity at much smaller i (see also Table I). Therefore, the complete calculations were only carried out for the first m layers, where m is defined as the number of the last layer where p_i differs more than a predetermined value (e.g., 10^{-4}) from unity. Then all the components p_i for $i > m$ may be set equal to 1. According to eq 34:

$$p(i,s) = p_i[\lambda_1 p(i-1,s-1) + \lambda_0 p(i,s-1) + \lambda_1 p(i+1,s-1)] \quad (60)$$

The ith component of the sth vector follows from the $(i-1)$th, ith, and $(i+1)$th component of the $(s-1)$th vector. As $p_i = 1$ for $i > m$, all the elements in the lower left corner ($i \geq m + s$) of the array $\boldsymbol{p}$ are equal to 1 (see Figure 3).

In order to get the complete segment density distribution for the first m layers, the elements $p(i,s)$ for $i \leq m$ are required. By inspection of eq 60 it appears that the elements of groups I, IIA, and IIB (see Figure 3) are needed to calculate these elements. Thus in the computation routine for $s \leq r/2$ the first $m + s - 1$ components of the sth vector were calculated from the first $m + s$ components of the $(s-1)$th vector, after which the elements $p(i,s-1)$ with $i > m$ were discarded by the computer and only the first m elements were stored. Similarly, for $s > r/2$ the first $m + r - s$ components of $\mathbf{p}(s)$ were calculated from the first $m + r - s + 1$ components of $\mathbf{p}(s-1)$; again only the first m components were stored.

In this way all the elements of the first m layers and thus the complete segment distribution for these layers could be calculated within a reasonable computing time, without the need of excessive storage capacity.

For the calculation of the adsorbed amount we rewrite eq 47 as $\Gamma_{exc} = \phi^*(p(r) - M) = \phi^* \sum_{i=1}^{M} \delta_{i,r}$ where $\delta_{i,r}$ is defined as $p(i,r) - 1$. The problem now is to find the sum $S(r)$ of $\delta_{i,r}$ for $i > m$: $S(r) = \sum_{i=m+1}^{m+r} \delta_{i,r}$ (see Figure 3). It can be shown that this sum can be expressed as a function of the elements of the mth and $(m+1)$th row only: $S(r) = \lambda_1 \sum_{s=1}^{r-1} |p(m,s) - p(m+1,s)|$. To prove this relation we realize that $\delta_{i,s} = 0$ for $i \geq m + s$, i.e., for the elements of group III in Figure 3. Next we apply (60) for $i > m$ (thus $p_i = 1$). Since $\lambda_0 + 2\lambda_1 = 1$ we have

$$\delta_{i,s} = \lambda_1 \delta_{i-1,s-1} + \lambda_0 \delta_{i,s-1} + \lambda_1 \delta_{i+1,s-1} \qquad (i > m) \quad (61)$$

Starting with $\delta_{m+1,r}$ we find $\delta_{m+1,r} = \lambda_1 \delta_{m,r-1} + \lambda_0 \delta_{m+1,r-1} +$

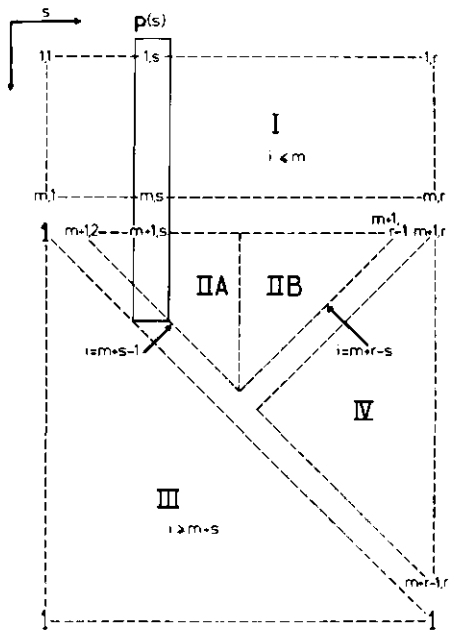

Figure 3. Schematic representation of the array p. In the layers beyond m the components p_i ($i > m$) of the first vector $p(1)$ may be set equal to 1. We can distinguish four groups of elements in the array. The elements of group I ($i \leq m$) are calculated and stored in the computer memory. Those of group II ($m < i < m + s$ for II.A, $m < i \leq m + r - s$ for II.B) are needed for the calculation of $p(m,s)$; once $p(m,s)$ has been obtained the elements of the ($s - 1$)th vector for which $i > m$ can be discarded. All the elements of group III ($i \geq m + s$) are equal to 1. The elements of group IV ($m + r - s < i < m + s$; $r/2 < s \leq r$) are not required in the computation. The sum $p(r)$ of the components of the last vector $p(r)$ is needed for the calculation of the adsorbed amount Γ. It turns out that $\sum_{i=m+1}^{m+r} p(i,r)$ can be obtained from the two sets of elements $p(m,s)$ and $p(m+1,s)$ of the mth and $(m + 1)$th row of the array.

$\lambda_1\delta_{m+2,r-1} = \lambda_1(\delta_{m,r-1} - \delta_{m+1,r-1}) + (\lambda_1 + \lambda_0)\delta_{m+1,r-1} + \lambda_1\delta_{m+2,r-1}$. Applying (61) for $\delta_{m+2,r}$ it follows that $\delta_{m+1,r} + \delta_{m+2,r} = \lambda_1(\delta_{m,r-1} - \delta_{m+1,r-1}) + \delta_{m+1,r-1} + (\lambda_1 + \lambda_0)\delta_{m+2,r-1} + \lambda_1\delta_{m+3,r-1}$. Repeating this procedure, and using $\delta_{m+r,r-1} = 0$ we find $S(r) = \lambda_1(\delta_{m,r-1} - \delta_{m+1,r-1}) + S(r-1)$. In the same way this last sum can be expressed in the components of the $(r-2)$th vector, giving $S(r) = \lambda_1(\delta_{m,r-1} - \delta_{m+1,r-1} + \delta_{m,r-2} - \delta_{m+1,r-2}) + S(r-2)$. Proceeding to the left in Figure 3 we finally end up with the relation

$$S(r) = \lambda_1 \sum_{s=1}^{r-1} (\delta_{m,s} - \delta_{m+1,s}) = \lambda_1 \sum_{s=1}^{r-1} |p(m,s) - p(m+1,s)| \tag{62}$$

Here we made use of the fact that $S(1) = 0$.

Thus an accurate value for $p(r)$ and Γ_{exc} is found, using only the elements $p(i,s)$ for $i \leq m + 1$. The same procedure can be applied for $p_1(r)$, from which Γ is found according to eq 51.

It may be noted that this procedure of setting $p_i = 1$ for $i > m$ is not the same as a step function approach. The procedure enables us to find the sums $\sum_{i=m+1}^{r+m}\phi_i$ and $\sum_{i=m+1}^{r+m}\phi_i^f$ over the layers beyond m to a good approximation, although the individual ϕ_i's for $i > m$ are not calculated. This is equivalent to the evaluation of the part of the areas A and B (Figure 2) that is beyond m. The accuracy of this extrapolation was shown for $r = 1000$, $\phi_* = 10^{-2}$, $\chi_s = 1$ (see also Table I). Using $m = 20$, calculated adsorbed amounts are $\Gamma = 0.91498$ and $\Gamma = 2.4455$ for $\chi = 0$ and $\chi = 0.5$, respectively. Extending m to 35 (the limit for $r = 1000$ on our computer) gave $\Gamma = 0.91565$ and $\Gamma = 2.4442$ for the same conditions. The differences are below 0.1% so that, in order to save computing time, in most cases $m = 20$ was chosen.

All the calculations were carried out with a DEC system-10 Model 1060 computer using a program written in Algol. The iteration procedure according to Newtons method was usually completed in five cycles with an accuracy of better than 0.01% in ϕ. The computing time increases roughly quadratic with increasing r. Calculations were possible for chains up to 1000 segments, in which case about 0.5 h of computation time is required.

On request the computer program will be made available by the authors.

IV. Results and Discussion

In this section we present a selection of numerical results which show the dependence of some characteristics of the adsorbed layer on parameters related to the polymer–solvent–surface system. For the latter parameters we choose the chain length r, the polymer–solvent interaction parameter χ, the adsorption energy parameter χ_s, and the equilibrium bulk volume fraction ϕ_*. For the adsorbed layer characteristics we take properties which in principle can be measured, as, e.g., described in the following references. Thus, we give results for the adsorbed amount[19] Γ, the fraction θ of the surface covered by segments[20] ($\theta = \phi_1$), and the fraction p of segments of adsorbed chains which is on the surface[21] ($p = \theta/\Gamma$). Results for another experimental variable, the layer thickness, will be discussed in another paper.

First we have to choose the type of the lattice as expressed in the fraction λ_0 of neighbors in the same layer. As has been shown by Roe,[10] theoretical results are qualitatively independent of the lattice type, while only minor quantitative differences occur. Unless otherwise stated, we confine ourselves to a close-packed hexagonal lattice: $\lambda_0 = 0.5$, $\lambda_1 = 0.25$. In a few cases a comparison will be made with a simple cubic lattice: $\lambda_0 = 2/3$, $\lambda_1 = 1/6$. More results for a cubic lattice have been published elsewhere.[22] Most of the data presented are for $\chi_s = 1$ or 3, and for two values of χ: $\chi = 0$, corresponding to an athermal solvent, and $\chi = 0.5$, equivalent to a Θ solvent. The value for ϕ_* is usually taken in the (semi-) dilute solution region, since in that region most experimental data are available; only when a comparison with other theories is desirable, we give results for composite adsorption isotherms extending over the whole range of ϕ_*. Although a more detailed comparison with other theories will not be made until the next chapter, we refer occasionally to results of other authors in the discussion of the following figures.

Table I gives a typical example of the free segment probability p_i and the concentration profile ϕ_i for $r = 1000$, $\phi_* = 10^{-2}$, $\chi_s = 1$, and $\chi = 0$ and 0.5. Also the volume fraction due to adsorbed chains, $\phi_i - \phi_i^f$, is shown. To facilitate comparison with Roe's theory, the concentration profile as calculated from his eq 29 is given. Data for $\chi = 0.5$ are plotted in Figure 4.

The dependence of p_i on ϕ_i is given in eq 24 and 39. Using the relation $\langle\phi_i\rangle + \langle\phi_i^0\rangle = 1 - \lambda_1\delta_{1,i}$ (see text following eq 14), we can write

$$\ln p_i = (\chi_s + \lambda_1\chi)\delta_{1,i} + 2\chi(\langle\phi_i\rangle - \phi_*) + \ln(\phi_i^0/\phi_*^0) \tag{63}$$

In the first layer the adsorption energy dominates p_i and

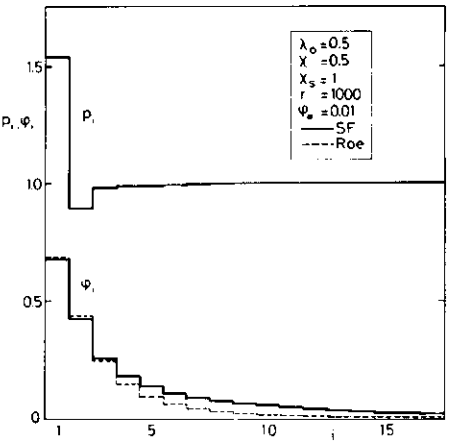

Figure 4. Segment density profile ϕ_i and free segment probability p_i as a function of the distance from the surface. Hexagonal lattice ($\lambda_0 = 0.5$), $\chi_s = 1$, $\chi = 0.5$, $r = 1000$, and $\phi_b = 0.01$. The dotted line is the concentration profile calculated from the theory of Roe.[10]

the free segment probability is higher than 1. In the other layers the factor ϕ_i^0/ϕ_b^0 is the most important one and causes p_i to be smaller than 1 and to increase with increasing i. (In other cases, e.g., at very low ϕ_b, the interaction term in (63) may be dominant, so that p_i then decreases continuously with increasing i.) A very important feature of Table I and Figure 4 is that p_i approaches unity much faster than ϕ_i approaches the bulk value ϕ_b; this is the basis for the procedure described in section III for the evaluation of the amount of adsorbed polymer present in the layers beyond $i = 20$. In some cases (e.g., $\chi = 0$, i around 20 in Table I), ϕ_i is slightly lower than ϕ_b (and thus p_i slightly higher than 1), an effect which is related to the buildup of the adsorbed layer in terms of loops and tails. This will be discussed more extensively in the next paper.[23]

The segment density ϕ_i decreases continuously with increasing distance from the surface (except when ϕ_i approaches ϕ_b from below, as mentioned in the previous paragraph). In the layers close to the surface ϕ_i is slightly lower than predicted by Roe's approximate theory,[10] while further from the surface the latter theory gives a serious underestimation for the segment density. As will be shown in the next paper, the segment density at larger distances is mainly due to the presence of long dangling tails, which have been neglected in previous polymer adsorption theories.[8,24] These theories predict an exponential decay of ϕ_i with distance for homopolymers. Table I and Figure 4 show that this is approximately correct for the layers close to the surface, but not at larger distances where tails become important. The presence of tails and the concomitant occurrence of segments at relatively large distances could be very important in the application of polymers for the stabilization or destabilization of colloidal particles.

Figure 5a shows adsorption isotherms, Figure 5b the occupancy of the surface layer (θ), and Figure 5c the bound fraction $p = \theta/\Gamma$ as a function of ϕ_b. The adsorption isotherms have a Langmuir character for low values of r (for $r = 1$ and $\chi = 0$, our equations reduce to the Langmuir equation), while those for high chain length are of the high affinity type often found in experiments. These features show up more clearly if the adsorbed amount Γ is plotted

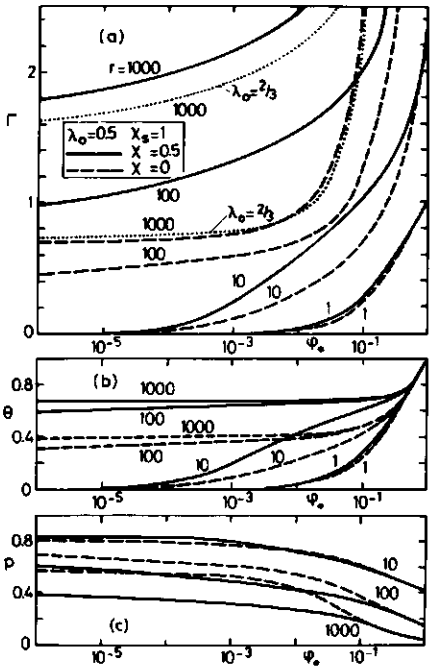

Figure 5. The adsorbed amount Γ (a), the surface coverage θ (b), and the bound fraction $p = \theta/\Gamma$ (c) as a function of the bulk volume fraction ϕ_b. The data apply to a hexagonal lattice ($\lambda_0 = 0.5$) and an adsorption energy parameter $\chi_s = 1$. The chain length r is indicated. Full lines are for a Θ solvent ($\chi = 0.5$), broken lines for an athermal solvent ($\chi = 0$). The two dotted lines in Figure 5a apply for $r = 1000$ in a simple cubic lattice ($\lambda_0 = 2/3$) and $\chi = 0$ and 0.5, respectively.

against a linear scale for ϕ_b. The overall shape of the isotherms is similar to that of the curves given by, e.g., Silberberg[7] and Hoeve[8,25] and similar trends with respect to the effects of solvent quality and molecular weight occur: the adsorption increases with decreasing solvent power and increasing chain length.

To illustrate the influence of the lattice type, two (dotted) curves for $\lambda_0 = 2/3$ (simple cubic lattice) and $r = 1000$ are shown in Figure 5a. The differences are small. For $\chi = 0.5$, Γ is slighly higher for the hexagonal lattice ($\lambda_1 = 1/4$) as compared to the cubic one ($\lambda_1 = 1/6$). For $\chi = 0$ the adsorption is slightly lower for the hexagonal lattice for low ϕ_b, but higher for high ϕ_b. The effect at $\chi = 0$ can be explained by realizing that if λ_1 increases there are more possibilities for a segment to "cross over" to a neighboring layer, giving rise to a slightly flatter concentration profile, a lower bound fraction, and thus to a lower adsorption energy per chain. For low ϕ_b this implies a lower adsorbed amount, while for high ϕ_b there are more possibilities for loop and tail formation due to the lower volume fraction in the outer layers. For $\chi = 0.5$, an extra effect occurs in that the "effective" adsorption energy parameter $\chi_s + \lambda_1\chi$ (see, e.g., (63)) increases with increasing λ_1; hence the adsorbed amount is higher for the hexagonal lattice.

Figure 5b demonstrates that the fraction θ of the surface which is covered by segments increases with ϕ_b for short chains but is hardly dependent on ϕ_b for higher chain lengths. As expected, θ is higher in poorer solvents, since

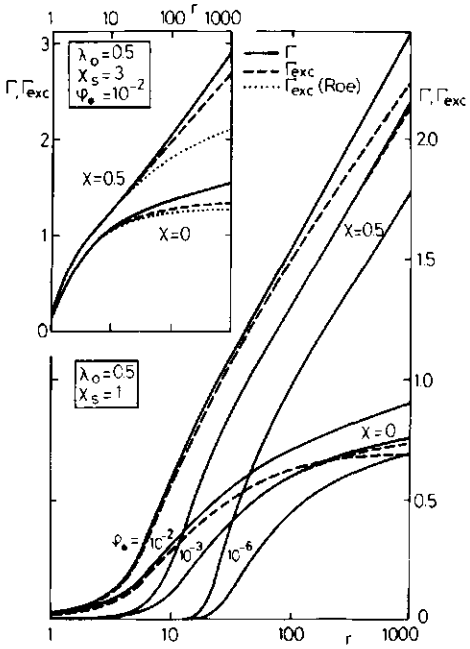

Figure 6. The adsorbed amount Γ (full lines) and the excess adsorbed amount Γ_{exc} (broken lines) as a function of the chain length r, for three values of the bulk volume fraction ϕ_b and for a Θ solvent ($\chi = 0.5$) and an athermal solvent ($\chi = 0$). Hexagonal lattice, $\chi_s = 1$. The inset applies to $\chi_s = 3$ and $\phi_b = 0.01$. The dotted lines give Γ_{exc} as calculated from the theory of Roe.[10]

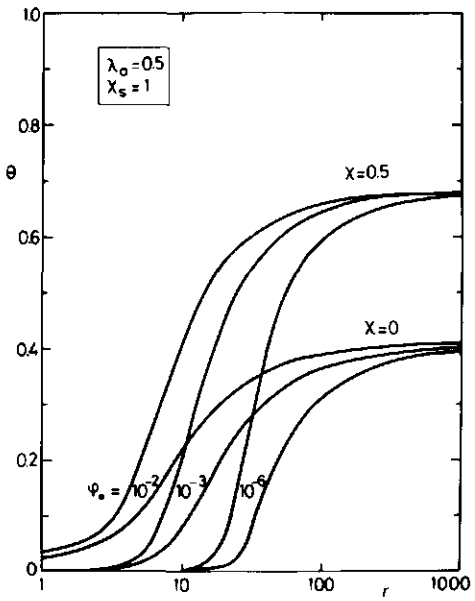

Figure 7. The surface coverage $\theta = \phi_1$ as a function of chain length r, for three values of the bulk volume fraction ϕ_b and $\chi = 0.5$ and 0. Hexagonal lattice, $\chi_s = 1$.

the segments prefer other segments to solvent molecules as immediate neighbors. The dependence of θ on r will be discussed further in connection with Figure 7.

Figure 5c gives the dependency of the bound fraction p (i.e., the fraction of segments of adsorbed chains in contact with the surface) on the bulk volume fraction ϕ_b. The bound fraction decreases slightly with increasing ϕ_b and decreases with increasing molecular weight. Both these trends have been found experimentally.[20,21] For short chains the effect of solvent power on p is only of minor importance (for $r = 1$, $p = 1$ under all conditions), for higher chain lengths p increases with decreasing χ. This is because in good solvents the extension of the adsorbed layer is smaller than in poor solvents (at the same ϕ_b).

In Figure 6 the adsorbed amount Γ is plotted as a function of chain length at $\phi_b = 10^{-2}$, 10^{-3}, and 10^{-6}, and for $\chi = 0$ and 0.5. The dashed curves give the excess adsorbed amount Γ_{exc} (see eq 47 and Figure 2). At low ϕ_b and low r there is hardly any difference between Γ and Γ_{exc}, but as ϕ_b and r increase, Γ_{exc} becomes progressively smaller than Γ, as is to be expected. The most conspicuous feature of Figure 6 is that, at $\chi = 0$, Γ levels off at high chain lengths, while, at $\chi = 0.5$, Γ (but not Γ_{exc}) increases linearly with log r. Both Silberberg[7] and Hoeve[8,25] predict that in athermal solvents the adsorbed amount reaches a limiting value at high chain lengths, in accordance with our results. For Θ solvents, Silberberg finds again a leveling off while Hoeve predicts an increase without bounds. Although we are as yet only able to make computations up to $r = 1000$, our results seem to support Hoeve's view. However, we find for high chain lengths an important contribution of long dangling tails, and these are neglected in Hoeve's treatment.

A more quantitative comparison is possible with Roe's results.[10] This is shown in the inset of Figure 6 for $\chi_s = 3$ and $\phi_b = 10^{-2}$. Roe presents only data for Γ_{exc}. It is obvious that both for $\chi = 0$ and $\chi = 0.5$ Roe's theory underestimates Γ_{exc} at high r, the difference increasing to about 25% for $r = 1000$ (in Θ solvents) and probably much more for higher chain lengths. Thus, the sharp leveling off which Roe shows in his Figure 16 is too pronounced, and is probably due to the approximations used in his theory.

If plotted on the same scale, the curves for $\chi_s = 1$ and $\chi_s = 3$ in Figure 6 run nearly parallel. Apparently the slope of the lines depends on χ, not on χ_s. This is related to the fact that upon increase of the chain length the additionally adsorbed amount is accomodated not in trains, but in loops and tails, and is thus determined mainly by the polymer–solvent interaction.

Figure 7 shows θ as a function of chain length, at constant ϕ_b. At low r the adsorbed amount and the surface coverage are small, and there is only little effect of the solvent quality. With increasing r the surface coverage increases until a plateau is reached where θ is independent of chain length and ϕ_b. In that region, the adsorbed amount Γ still increases, but the extra segments are accomodated in layers further from the surface. The plateau of θ at high r is higher in Θ solvents, since the segments attract each other, and this attraction balances the unfavorable entropic situation at a higher θ than in good solvents.

From experiments, the surface coverage θ and the bound fraction p are often obtained not as a function of ϕ_b (see Figure 5b and 5c), but as a function of Γ. In Figure 8a and 8b the dependence of θ on Γ is given for $\chi = 0$ and $\chi = 0.5$, respectively, and in Figure 8c and 8d the corresponding

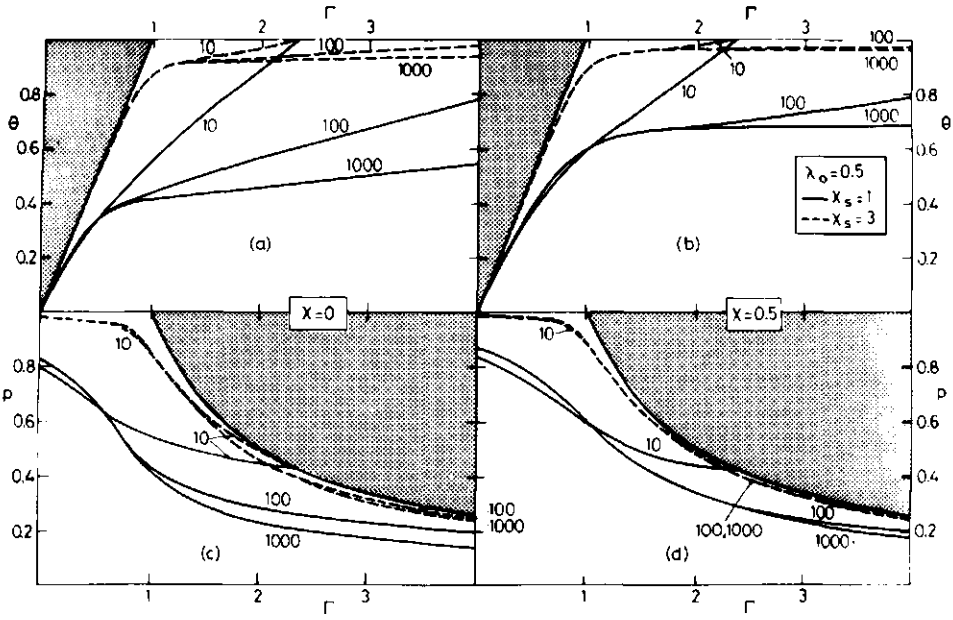

Figure 8. The surface coverage θ (a, b) and the bound fraction p (c, d) as a function of the adsorbed amount Γ, for $\chi = 0$ (a, c) and $\chi = 0.5$ (b, d). The chain length r is indicated. Hexagonal lattice, $\chi_s = 1$ (full lines) and $\chi_s = 3$ (broken lines). The shaded areas are inaccessible regions ($\theta > \Gamma$ or $\theta > 1$). Note that there exists a maximum adsorbed amount Γ^{max} (when $\phi_* = 1$) which is independent of χ or χ_s. For $r = 1$, $\Gamma^{max} = 1$; for $r = 10$, $\Gamma^{max} = 2.36$; for $r = 100$, $\Gamma^{max} = 6.25$ (not indicated in the figure); and for $r = 1000$, Γ^{max} is greater than 18.

curves for $p = \theta/\Gamma$ are shown. There are several interesting features in these graphs. For monomers, $\theta = \Gamma$ (corresponding to the straight lines in Figure 8a and 8b) and $p = 1$. The shaded areas in Figure 8 are inaccessible regions, since there θ would be higher than Γ or greater than 1. For chain molecules ($r > 1$) only part of the segments is adsorbed, and θ increases more slowly than Γ so that p decreases. As expected, the shape of the adsorbed molecules becomes less flat as the adsorbed amount increases.

At relatively low Γ the curves for different chain lengths nearly coincide. One has to realize, however, that greatly different equilibrium bulk volume fractions are involved. At high Γ (and thus high ϕ_*) the lines diverge and reach $\theta = 1$ (full surface coverage) at $\phi_* = 1$ (i.e., bulk polymer). At that point the adsorbed amount reaches its maximum value Γ^{max} which depends on r (and slightly on λ_0), but not on χ or χ_s. Clearly, Γ^{max} should lie in between 1 (completely flat chains) and r (only one end segment adsorbed). For $r = 10$, $\Gamma^{max} = 2.36$; for $r = 100$, Γ^{max} is 6.25 (not indicated in the figure) and for $r = 1000$, the maximum adsorbed amount could not yet be calculated precisely due to convergence problems of the iteration, but it is around 19. That Γ^{max} is independent of χ or χ_s is due to the fact that in bulk polymer the configuration of the chains is only determined by entropic factors, since the energy of all the segments on the surface is the same, and all segments in the other layers are in an identical environment. As is well known,[26,27] chain molecules assume unperturbed dimensions in bulk polymer.

At intermediate values for Γ, the surface coverage θ is nearly independent of Γ and r. At $\chi_s = 1$ this applies only for longer chains, but for higher adsorption energies ($\chi_s = 3$) this is true for chains as short as ten segments and up. In this region p decreases steadily with increasing Γ. These effects are related to the accommodation of segments in the outer regions of the adsorbed layer, without altering the segment concentration in the surface layer. Again it has to be realized that for different chain lengths this region of constant θ occurs at different ϕ_*.

It can be seen from Figure 8 that θ and p increase if χ_s becomes higher. This is easily understood. Similarly, θ and p increase with increasing χ, an effect which is more pronounced at low χ_s and for high molecular weights. Naturally, the influence of the parameters χ and χ_s is strongest in the intermediate range of Γ since, for given r, all $\theta(\Gamma)$ curves converge to the same starting point (at $\Gamma = 0$) and end point (at $\Gamma = \Gamma^{max}$). It is interesting to note that *at a given adsorbed amount* the occupancy of the first layer is smaller in good solvents, so that the amount in loops and tails and the average layer thickness is greater than in poor solvents. However, in order to get the same Γ in a good solvent, much higher polymer concentrations are needed than in a poor solvent (see Figure 5a).

Koopal et al.[20] obtained experimental curves of θ and p as a function of Γ which are similar to those of Figure 8. They found that θ increases with Γ and then reaches a plateau, and is independent of molecular weight. Other experiments[21] gave also results corroborating the picture given in Figure 8.

Figure 9 shows the effect of the adsorption energy parameter χ_s on Γ (Figure 9a) and θ (Figure 9b). For infinitely long chains, adsorption occurs only if χ_s exceeds the "critical adsorption energy"[10,12] $\chi_{sc} = -\ln(1 - \lambda_1)$ which for a hexagonal lattice equals 0.288. For finite chain lengths the critical adsorption energy is smaller. With increasing χ_s the adsorbed amount and the surface coverage increase until, around $\chi_s = 3$, a semiplateau is found. The overall shape of the curves in Figure 9a strongly

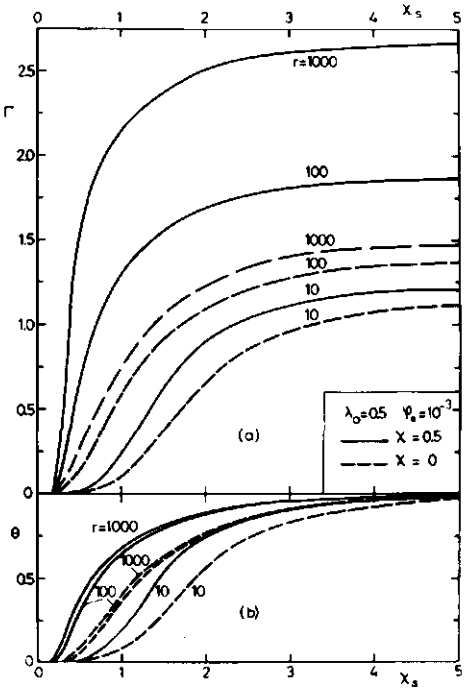

Figure 9. The adsorbed amount Γ (a) and the surface coverage θ (b) as a function of the adsorption energy parameter χ_s, for $\chi = 0.5$ (full lines) and $\chi = 0$ (broken lines). Hexagonal lattice, $\phi_b = 0.001$. The chain length r is indicated.

resembles that of Roe's Figure 15[10] (where Γ_{exc}, not Γ, is plotted), although some quantitative differences occur: at higher chain lengths the adsorbed amount is significantly higher than that according to Roe's results, and the molecular weight dependence, both for $\chi = 0$ and $\chi = 0.5$, is stronger than that predicted by Roe. As discussed above, these differences may be due to the fact that Roe's theory underestimates the contribution of tails. From Figure 9b it may be concluded that for longer chains θ is very close to unity if $\chi_s \geq 3$. The effects of solvent power and chain length on θ have been considered already in connection with Figure 7.

Other results on the structure of the adsorbed layer, such as the root-mean-square thickness of the layer, the fraction of segments present in tails and loops, and the train, tail, and loop size distribution, have been obtained. These aspects will be dealt with more extensively in a forthcoming publication.[23] At the present moment we just mention two significant results. First, the root-mean-square thickness appears to increase proportionally to the square root of the chain length. Secondly, the contribution of tails is dominant over that of the loops in the outer regions of the adsorbed layer. In dilute solutions ($\phi_b \approx 10^{-3}$) up to 15% of the segments may be present in (on average) one tail per adsorbed molecule. These effects are very important in systems where polymer is used to stabilize or destabilize colloidal suspensions.

V. Comparison with Other Theories

Many of the earlier theories[1-6] on polymer adsorption treat the case of an isolated macromolecule on a surface. These theories are only valid for very good solvents and in systems so dilute that no measurements are possible. Their relevance for practical systems is therefore small. In these treatments the interaction between the segments is neglected, which in our terminology is equivalent to writing eq 63 simply as $\ln p_i = \chi_s \delta_{1,i}$. Indeed our model reduces completely to that of DiMarzio and Rubin[12] if we make this simplification (for a proof of this see Appendix I). All "isolated chain" theories predict that, for reasonable adsorption energies, polymers adsorb on a surface in a very flat conformation, such that the bound fraction p is close to unity. However, even if the bulk volume fraction ϕ_b is quite small the segment density in the surface region may be quite high. Therefore, the polymer–solvent interaction has to be taken into account.

The first attempts to incorporate this interaction are due to Hoeve[6,25] and Silberberg.[7] Hoeve's theory involves drastic approximations, but the general trends seem to be predicted reasonably well as shown in the previous chapter. An apparent drawback of his treatment is the neglect of tails. A quantitative comparison of his results with the present theory is difficult. Silberbergs starting point is the assumption of an "adsorbed phase" in which only segments of *adsorbed* chains are present, and the segment concentration profile is considered to be a step function. In this way no distinction between loops and tails can be made. Nevertheless his results, showing the same general trends as Hoeve's theory, are in broad agreement with ours. Also in this case a more detailed comparison is not easy.

There are two recent treatments which can be compared with the present theory in more detail. One is due to Levine et al.,[14] the other is that of Roe[10] and has already been mentioned several times.

We became aware of the theory by Levine et al. while preparing this manuscript. As discussed more extensively elsewhere[22] the basic idea of these authors is nearly the same as ours: both treatments extend DiMarzio and Rubin's[12] matrix procedure by incorporating the interaction between segments and solvent. However, Levine et al. apply their model only to the concentration profile of terminally adsorbing polymer in a cubic lattice between two plates; the authors do not attempt to use it for adsorption on a single plate or to derive the loop, train, and tail size distribution, and they do not consider a different lattice type. Apart from that there is a fundamental difference with our theory in the underlying equations. While in the present treatment the free segment probability p_i is derived from the partition function (see section II.C), Levine et al. adapt a method due to Whittington[28] to find p_i (denoted by them as the weighting factor $g(\xi)$). The result is eq 63, in which $\langle \phi_i \rangle$ is simply replaced by ϕ_i. From a physical point of view this seems to be not warranted, since a segment in layer i interacts not only with segments and solvent molecules in i but also with those in adjoining layers. In a forthcoming publication on the two plate problem we shall make a more detailed comparison with the results of Levine et al.

Roe[10] treats the adsorption of polymers in a way similar to our theory by setting up the partition function of the mixture of chains and solvent molecules near an interface. He uses the approximation that the distribution of a segment is the same for all the r segments of a chain. In the further elaboration he can then avoid the rather cumbersome matrix procedure necessary in our (and Levine's) theory. Helfand[11] has shown that Roe's treatment contains another error, because the inversion symmetry is not properly taken into account. As discussed in section II.B, Helfand corrects this by introducing a flux

TABLE II: Comparison of Numerical Results for Γ_{exc} for Oligomers (r = 1,2, 4) around the Maximum in the Composite Adsorption Isotherm,[a] as Obtained from the Theories of Ash et al. (AEF),[b] Roe (R),[c] and the Present Theory (SF)

	$r = 1$		$r = 2$			$r = 4$		
ϕ_*	AEF	R/SF	AEF	R	SF	AEF	R	SF
0.1	0.64	0.6341	0.94	0.9508	0.9553	1.27	1.3123	1.3333
0.2	0.71	0.7108	0.95	0.9591	0.9681	1.28	1.3027	1.3396
0.4	0.61	0.6119	0.76	0.7587	0.7639	0.94	0.9166	0.9337

[a] Hexagonal lattice ($\lambda_0 = 0.5$), $\chi_s = 2.3$, $\chi = 0.92$. [b] Data read from Figure 13 of ref 9. [c] Results obtained by our own computer program.

constraint which can be expressed as the condition that the number of bonds from layer i to layer j should be equal to that in opposite direction. Since Helfand formulates this flux constraint only for infinite chain lengths, his results apply only for $r \to \infty$ and cannot be compared directly with ours.

Below, we describe in some detail the differences between the results of Roe (R),[10] Ash, Everett, and Findenegg (AEF),[9] and the present treatment (SF). The AEF theory is an extension to oligomers of the theory for monomer adsorption from regular solutions[29,30] and considers the statistical mechanics of oligomers in all possible orientations. Our theory differs from that of AEF in two respects: (1) backfolding is allowed, enabling us to use the matrix method; (2) any segment pair has a contact energy described by the χ parameter, even if two neighboring segments belong to the same molecule. The AEF theory is thus more exact than ours, but due to computational difficulties it has only been used up to $r = 4$.

For monomers ($r = 1$), our eq 45 is identical with Roe's eq 29 and to the equations given by Ono and Kondo[29] and Lane[30] for monomer adsorption from a regular solution. Our numerical results are identical with those of AEF. Roe's own calculations are slightly but consistently higher, but this is due to numerical errors, as Roe suspects already; when we programmed Roe's equations (using also here Newton's method for the iteration) we obtained identical results. This is shown in Table II. The data in this table apply to χ_s and χ values as given in Figure 13 of ref 9 ($\chi_s = 2.3$ corresponds to $\log K = 1$, $\chi = 0.92$ to $w = 0.92kT$ in AEF's terminology).

For dimers ($r = 2$), the numerical results of Roe's equations deviate slightly from ours. This is probably due to the lack of inversion symmetry in Roe's theory since the approximation that all chain segments are equally distributed should not be relevant for dimers. If this equal distribution of segments were the only assumption in Roe's treatment, his equations should reduce to ours for $r = 1$ *and* $r = 2$. For dimers, this is not the case.

Comparing our results for dimers and tetramers with those of AEF (see Table II), we see that there is a small difference. For dimers, this can only be caused by the overestimation of the interaction energy in our treatment, as discussed above. This effect is apparently not very important, considering that the data of Table II apply for a high value of χ. For tetramers, the backfolding effect may also play a role, and differences of the order of 5% in Γ_{exc} occur. It is possible that for high r the errors are less.

For longer chain lengths we can compare our results only with those of Roe. Figure 10 shows a few results. For short chains the differences in Γ_{exc} are very small but for longer chains the differences increase, especially in poor solvents. For $r = 1000$, $\chi = 0.5$ and in the range $\phi_* = 0$ to $\phi_* = 10^{-1}$, Γ_{exc} is about 30% higher than according to Roe. The higher adsorbed amount is mainly caused by the higher segment concentration in the outer regions of the adsorbed layer, stemming partly from loops but mainly from long

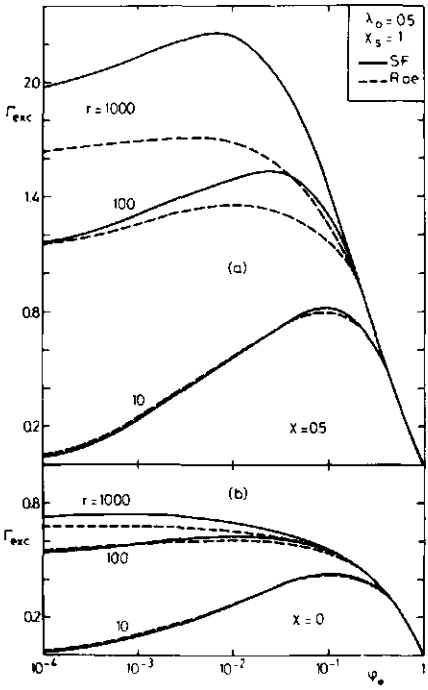

Figure 10. Comparison of composite adsorption isotherms calculated with the present theory (SF, full lines) and with the theory of Roe[10] (broken lines) for $\chi = 0.5$ (a) and $\chi = 0$ (b). Hexagonal lattice, $\chi_s = 1$. The chain length r is indicated.

dangling tails. This point will be worked out in our next paper.[23] It is in this outer region that Roe's treatment underestimates the segment density, and it is just that region which contributes most strongly to the interaction of polymer covered particles. Thus, although Roe's approximation works surprisingly well for the adsorbed amount of not too long chains, it is likely to predict far too low forces of interaction between colloidal particles in the presence of polymers. For problems in the area of colloid stability the action of relatively long tails has to be taken into account, even for adsorbed homopolymers.

We conclude with some final remarks on the dependence of the results on the type of lattice. One of the obvious drawbacks of a lattice theory is that it is not easy to relate the results to real continuous systems. One just hopes that the general trends will be described with sufficient accuracy. Fortunately these general features do not depend strongly on the lattice type chosen. This was demonstrated for a few cases in the previous section, and has been shown more extensively by Roe. In recent years there have been

a few attempts[13,15,31] to derive a continuum theory for polymer adsorption. To our knowledge, only one paper has been published[13] in which results for polymer adsorption accounting for the polymer–solvent interaction were obtained. These results are for terminally adsorbing polymers between two plates, and may be compared to the work of Levine et al.[14] (using essentially the same procedure as ours). It turns out that the calculated concentration profiles and the effect of the interaction on them are very similar, the differences being of the same order of magnitude as what is typical when different lattices are used. Thus, it seems that the continuum and lattice theories give, generally speaking, similar results. In a future paper on the interaction of two plates in the presence of polymer, we shall discuss these points in more detail.

Acknowledgment. The authors thank Professor Dr. A. Silberberg for useful discussions and valuable comments.

Appendix I

Relation between Our Procedure and the Model of DiMarzio and Rubin. In our terminology, the combination of eq 2.5 and 2.11 of the paper of DiMarzio and Rubin[12] can be written as

$$\nu_i(r) = \frac{1}{rp(r)}\{p_i \mathbf{u}^T \mathbf{p}_i(r-1) + \sum_{s=1}^{r-1} \mathbf{u}^T \mathbf{p}_i(s-1)p(i,r-s+1)\} \tag{A.1}$$

Here $\mathbf{u}^T$ is the row vector (1, 1, ..., 1) and $\mathbf{p}_i(s) = \mathbf{w}^s\Delta_i$, with Δ_i a column vector with the ith component equal to 1 and all the other components zero. According to our notation, the symbols $N + 1$ and θ_i of DiMarzio and Rubin have to be replaced by r and $\ln p_i = \chi_s\delta_{1,i}$, respectively. Equation A.1 can be simplified by writing the matrix $\mathbf{w}$ as a product of two symmetrical matrices $\mathbf{x}$ and $\mathbf{y}$, of which the elements are $x_{ij} = p_i\delta_{i,j}$ (only nonzero elements along the diagonal) and $y_{ij} = \lambda_{j-i}$. Then $\mathbf{w} = \mathbf{xy}$ and the transpose of $\mathbf{w}$ equals $\mathbf{w}^T = \mathbf{yx}$. Using elementary matrix algebra

$$\mathbf{u}^T\mathbf{p}_i(s-1) = \mathbf{u}^T\mathbf{w}^{s-1}\Delta_i = (\mathbf{u}^T\mathbf{w}^{s-1}\Delta_i)^T = \Delta_i^T(\mathbf{yx})^{s-1}\mathbf{u} = \Delta_i^T(\mathbf{x}/p_i)(\mathbf{yx})^{s-1}\mathbf{u} = p_i^{-1}\Delta_i^T(\mathbf{xy})^{s-1}\mathbf{xu} = p_i^{-1}\Delta_i^T\mathbf{w}^{s-1}\mathbf{p}(1) = p(i,s)/p_i$$

Thus eq A.1 can be simplified much more simply as

$$\nu_i(r) = \frac{1}{rp(r)} \sum_{s=1}^{r} p(i,s)p(i,r-s+1)/p_i \tag{A.2}$$

Since $\nu_i = n_i/\sum_i n_i = L\phi_i/nr$ this equation is identical with our eq 44 and 45 combined.

Appendix II

List of Symbols. In the following list the most important or most frequently used symbols have been collected.

A	area
a	A/L, area per lattice site
c, d, ...	specification number for chain conformation
F, F^σ	free energy of the system with respect to the reference state, surface excess free energy
i, j, ...	layer number
k	Boltzmann's constant
$k(s,c)$	number of the layer in which the sth segment of a chain in conformation c finds itself
L	number of lattice sites per layer
M	number of lattice layers
m	number of layers for which complete calculations have been performed
n, n^0	number of polymer molecules, number of solvent molecules, in the system
n_c	number of polymer molecules in conformation c
n_i, n_i^0	number of polymer segments, number of solvent molecules, in layer i
n^σ, $n^{0\sigma}$	surface excess of polymer molecules, surface excess of solvent molecules
P_i, P_*, $P_{k(s,c)}$	free segment probability in layer i, in bulk solution, and in the layer where the sth segment of a chain in conformation c is present (eq 24)
$P(i,s)$	end segment probability, i.e., the probability that the end segment of an s-mer is in layer i
$\mathbf{P}(s)$	column vector with M components $P(i,s)$
$P(r)$	chain probability, i.e., sum of the components of $\mathbf{P}(r)$ (eq 26 and 31)
$\boldsymbol{P}$	array of all the r vectors $\mathbf{P}(s)$
$P(r)_c$	conformation probability (eq 25)
$P(s,i;r)$	probability that the sth segment of an r-mer is in layer i
$P(s,i;r)_c$	probability of conformation c of an r-mer of which the sth segment is in i
p	bound fraction θ/Γ
p_i	P_i/P_*, free segment probability in layer i with respect to the bulk solution
$p(i,s)$	$P(i,s)/P_*^s$, end segment probability of an s-mer with respect to the bulk solution
$\mathbf{p}(s)$	column vector with M components $p(i,s)$
$p(r)$	chain probability with respect to the bulk solution, i.e., sum of the components of $\mathbf{p}(r)$
$\boldsymbol{p}$	array of all the r vectors $\mathbf{p}(s)$
$p(s,i;r)$	probability (with respect to bulk solution) that the sth segment of an r-mer is in i
$p_f(i,s)$	end segment probability (with respect to bulk) for free, nonadsorbed s-mers
$\mathbf{p}_f(s)$	column vector with M components $p_f(i,s)$
$p_f(r)$	chain probability (with respect to bulk) of free chains, i.e., sum of the components of $\mathbf{p}_f(r)$
$\boldsymbol{p}_f$	array of all the r vectors $\mathbf{p}_f(r)$
$p_a(r)$	$p(r) - p_f(r)$, chain probability (with respect to bulk) of adsorbed chains
$Q(M, L, T, \{n_c\})$	partition function at given distribution of conformations
r	number of segments per chain
$r_{i,c}$	number of segments that a chain in conformation c has in layer i
s,t, ...	segment ranking number
T	absolute temperature
U	energy of the system with respect to the reference state
u_s, u_s^0	adsorption energy of a segment, and of a solvent molecule
$\boldsymbol{W}$	matrix with elements $W_{ij} = \lambda_{j-i}P_i$
$\mathbf{w}$	matrix with elements $w_{ij} = \lambda_{j-i}p_i$
$\mathbf{w}_f$	matrix with elements $w_{f,ij} = \lambda_{j-i}p_i(1 - \delta_{1,j})$
z	coordination number of the lattice
Γ, Γ_{exc}	adsorbed amount, and excess adsorbed amount (eq 47 and 48)
γ	surface tension
$\delta_{i,j}$	Kronecker delta; if $i = j$, $\delta_{i,j} = 1$; if $i \neq j$, $\delta_{i,j} = 0$
λ_{j-i}	fraction of nearest neighbors in layer j around a site in i; $\lambda_{j-i} = 0$ if $\lvert j - i\rvert \geq 2$
λ_0, λ_1	fraction of nearest neighbors in the same layer, and in an adjacent layer
$(\lambda_{s,s+1})_c$	fraction of nearest neighbors that a site in the layer, where the sth segment of conformation

c is found, has in the layer where the $(s + 1)$th segment is; thus $(\lambda_{s,s+1})_c$ equals λ_0 if s and $s + 1$ are in the same layer, and λ_1 if s and $s + 1$ are in adjacent layers

θ ϕ_1, surface coverage or segment volume fraction in the first layer

μ_{chain}, μ^0 chemical potential of a chain, and a solvent molecule with respect to the reference state

ν_i number of previously occupied sites in layer i (eq 9)

ϕ_i, ϕ_* segment volume fraction in layer i, and in the bulk solution

ϕ_i^r volume fraction due to nonadsorbed chains

ϕ_i^0, ϕ_*^0 solvent volume fraction in layer i, and in the bulk solution

$\langle\phi_i\rangle$, $\langle\phi_i^0\rangle$ site volume fraction of segments, and solvent, in layer i (defined in eq 14)

χ Flory–Huggins polymer–solvent interaction parameter

χ_s differential adsorption energy parameter (eq 21)

Ω, Ω^* combinatory factor for the mixture of polymer and solvent, and for amorphous bulk polymer

ω, $\omega(n)$ number of ways of placing the first chain, and the first n chains, in an empty lattice (eq 9 and 10)

ω_c ratio between the number of arrangements of a chain in conformation c and that of a chain in bulk polymer (eq 5)

References and Notes

(1) R. Simha, H. L. Frisch, and F. R. Eirich, *J. Phys. Chem.*, **57**, 584 (1953); H. L. Frisch and R. Simha, *J. Chem. Phys.*, **24**, 652 (1956); **27**, 702 (1957).
(2) A. Silberberg, *J. Phys. Chem.*, **66**, 1872, 1884 (1962); *J. Chem. Phys.*, **46**, 1105 (1967).
(3) E. A. DiMarzio, *J. Chem. Phys.*, **42**, 2101 (1965); E. A. DiMarzio and F. L. McCrackin, *ibid.*, **43**, 539 (1965); C. A. J. Hoeve, E. A. DiMarzio, and P. Peyser, *ibid.*, **42**, 2558 (1965).
(4) R. J. Rubin, *J. Chem. Phys.*, **43**, 2392 (1965); *J. Res. Natl. Bur. Stand., Sect. B*, **70**, 237 (1966).
(5) R. J. Roe, *J. Chem. Phys.*, **43**, 1591 (1965); **44**, 4264 (1966).
(6) K. Motomura and R. Matuura, *J. Chem. Phys.*, **50**, 1281 (1969); K. Motomura, K. Sekita, and R. Matuura, *Bull. Chem. Soc. Jpn.*, **44**, 1243 (1971); K. Motumura, Y. Morol, and R. Matuura, *ibid.*, **44**, 1248 (1971).
(7) A. Silberberg, *J. Chem. Phys.*, **48**, 2835 (1968).
(8) C. A. J. Hoeve, *J. Polym. Sci. C*, **30**, 361 (1970); *ibid.*, **34**, 1 (1971).
(9) S. G. Ash, D. H. Everett, and G. H. Findenegg, *Trans. Faraday Soc.*, **66**, 708 (1970).
(10) R. J. Roe, *J. Chem. Phys.*, **60**, 4192 (1974).
(11) E. Helfand, *J. Chem. Phys.*, **63**, 2192 (1975); *Macromolecules*, **9**, 307 (1976).
(12) E. A. DiMarzio and R. J. Rubin, *J. Chem. Phys.*, **55**, 4318 (1971).
(13) A. K. Dolan and S. F. Edwards, *Proc. R. Soc. London, Ser. A*, **343**, 427 (1975).
(14) S. Levine, M. M. Thomlinson, and K. Robinson, *Discuss. Faraday Soc.*, **65**, in press.
(15) S. F. Edwards, *Proc. Phys. Soc.*, **85**, 613 (1965); *J. Phys. A*, **2**, 145 (1969); P. G. de Gennes, *Rep. Prog. Phys.*, **32**, 187 (1969).
(16) P. J. Flory, "Principles of Polymer Chemistry", Cornell University Press, Ithaca, NY, 1953.
(17) IUPAC, "Definitions, Terminology and Symbols in Colloid and Surface Chemistry", prepared for publication by D. H. Everett, *Pure Appl. Chem.*, **31**, 579 (1972).
(18) D. A. H. Jacobs, "The State of the Art in Numerical Analysis", Academic Press, London, 1977.
(19) For reviews see: A. Silberberg, *J. Phys. Chem.*, **68**, 1884 (1962); F. Patat, E. Killmann, and C. Schliebener, *Fortschr. Hochpolym. Forsch.*, **3**, 332 (1964); J. J. Kipling, "Adsorption from Solutions of Non-electrolytes", Academic Press, New York, 1965, Chapter 5; R. R. Stromberg in "Treatise on Adhesion and Adhesives", Vol. I, R. L. Patrick, Ed., Marcel Dekker, New York, 1967, Chapter 3; B. Vincent, *Adv. Colloid Interface Sci.*, **4**, 193 (1974).
(20) L. K. Koopal and J. Lyklema, *J. Chem. Soc., Faraday Discuss.*, **59**, 230 (1975); J. Lyklema, *Pure Appl. Chem.*, **46**, 149 (1976); L. K. Koopal, *Commun. Agric. Univ. Wageningen*, 78-12 (1978).
(21) G. R. Joppien, *Makromol. Chem.*, **175**, 1931 (1974); **176**, 1129 (1975); E. Dietz, *ibid.*, **177**, 2113 (1976); E. Killmann; *Croata Chim. Acta*, **48**, 463 (1976); *Polymer*, **17**, 864 (1976); I. D. Robb and R. Smith, *ibid.*, **18**, 500 (1977).
(22) J. M. H. M. Scheutjens and G. J. Fleer, *Discuss. Faraday Soc.*, **65**, in press.
(23) J. M. H. M. Scheutjens and G. J. Fleer, to be published.
(24) F. Th. Hesselink, *J. Phys. Chem.*, **75**, 65 (1971).
(25) C. A. J. Hoeve, *J. Chem. Phys.*, **44**, 1505 (1966).
(26) H. Benoit, *J. Macromol. Sci. B*, **12**, 27 (1976).
(27) R. DeSantis and H. G. Zachmann, *Colloid Polym. Sci.*, **255**, 729 (1977).
(28) S. G. Whittington, *J. Phys. A*, **3**, 28 (1970).
(29) S. Ono and S. Kondo in "Handbuch der Physik", Vol. 10, S. Flügge, Ed., Springer, Berlin, 1960, p 134.
(30) J. E. Lane, *Aust. J. Chem.*, **21**, 827 (1968).
(31) I. S. Jones and P. Richmond, *J. Chem. Soc., Faraday Trans. 2*, **73**, 1062 (1977).

Chapter 3

J. Phys. Chem. 1980, 84, 178-190

Statistical Theory of the Adsorption of Interacting Chain Molecules. 2. Train, Loop, and Tail Size Distribution

J. M. H. M. Scheutjens* and G. J. Fleer

Laboratory for Physical and Colloid Chemistry, Agricultural University, De Dreijen 6, 6703 BC Wageningen, The Netherlands

(Received May 31, 1979)

On the basis of an improved matrix model for polymer adsorption, in which the volume of the segments and the segment–solvent interaction is taken into account, the conformation of adsorbed chains is calculated. Results are obtained for the distribution of individual chain segments, the concentration profile due to loops and tails, the root-mean-square layer thickness, the numbers and average length of trains, loops, and tails, and the train, loop, and tail size distribution. The distribution of end segments is quite different from that of middle segments. Ignoring this difference, which is done in older theories, is equivalent to the assumption that end effects are negligible, and is mostly incorrect. The concentration profile due to loop segments decays exponentially with increasing distance from the surface, in agreement with previous theories. However, except for the layers close to the surface, the contribution of tails is dominant over that of the loops. Also in the root-mean-square layer thickness the main contribution is due to tail segments; the layer thickness in all cases is proportional to the square root of the chain length. At reasonable adsorption energies, the conformation of isolated chains is very flat, with most segments in trains, a small fraction in loops, and a negligible fraction in tails. In even very dilute solutions the length of tails becomes significant, while that of loops increases and that of trains decreases. At semidilute concentrations, more than 20% of the segments may be in tails, with an average tail size of about 15% of the chain length. In bulk polymer, a chain in contact with the surface consists, on the average, of two tails of roughly 1/3 chain length each, while in the middle section short trains and longer loops alternate. As far as possible, our results will be compared with other theoretical predictions and with experiment. One result is that the spread of the train size around its average value is identical with the train size distribution as derived by Hoeve et al.

I. Introduction

In a variety of practical applications, such as colloid stability, adhesion, biology, polymer technology, etc., the conformation of polymer chains in the vicinity of an interface is of considerable interest. Adsorbed polymer molecules have only part of their segments on the surface while a substantial fraction of the segments are protruding into the solution. The segments on the surface are present in *trains* of variable length, the others are in *loops* (with both ends in contact with the surface), and in one or two *tails* at the end of the adsorbed molecule. The way in which the polymer segments are distributed over trains, loops, and tails largely determines the physical properties of the system.

In the first article[1] of this series, it was shown that a well-known matrix formalism[2,3] for a random walk near a surface can be adapted to include the competition between the segments and the segment–solvent interaction. Each segment of a chain can be assigned a weighting factor, the *free segment probability*, which must be introduced into the matrix. This weighting factor depends, within the limits of the Bragg–Williams approximation for random mixing in each layer parallel to the surface, on the local concentration, on the local concentration gradient, and on the energy parameters χ_s and χ. The two latter parameters describe the interaction of segments with the surface and the solvent, respectively. From the matrix the number of chains in any given conformation can then be found. In this paper we calculate the fraction of the segments in trains, loops, and tails, the average train, loop, and tail size, and the train, loop, and tail size distribution. Moreover, the concentration profile and the root-mean-square extension due to loops and tails are obtained.

Unlike previous theories,[4-6] our model considers the chains as connected sequences of segments throughout the derivation. In this way it is possible to avoid the usual approximation[4-8] that any chain segment, whether it is in the middle part of the chain or near one of the chain ends, gives the same contribution to the segment density at any distance from the surface. In this article it is shown that this approximation, which is closely related to the neglect of end effects, is often not valid in practical systems. On the contrary, even at very dilute bulk concentrations tails play a very important role and largely determine the segment distribution in the outer regions of the adsorbed layers. In this respect there is a fundamental difference with isolated molecules near a surface[9-12] where end effects can be safely neglected.

From recent experiments on polymer stabilized free liquid films[13] it was concluded that the interaction in the film extends over such large distances that long dangling tails are probably present in the adsorbed polymer layer. This article confirms that, even for homopolymers, a considerable fraction of the segments may be present in tails, especially if the system is relatively concentrated. This is certainly important in the stabilization and flocculation of colloidal systems by polymers.

II. Theory

A. The Matrix Formalism. In the preceding article[1] it has been shown how the segment density distribution and the adsorbed amount for polymer chains in a lattice adjoining an adsorbing surface can be calculated. The lattice consists of M layers of lattice sites parallel to the surface, labeled $i = 1, 2, ..., M$, where $i = 1$ is the layer adjacent to the surface and $i = M$ is a layer in the bulk solution. A lattice site has z nearest neighbors, a fraction λ_0 of which are in the same layer and a fraction λ_1 in each of the adjoining layers. In a simple cubic lattice $z = 6$, $\lambda_0 = 2/3$, and $\lambda_1 = 1/6$; in a hexagonal lattice $z = 12$, $\lambda_0 = 1/2$, and $\lambda_1 = 1/4$. Obviously $\lambda_0 + 2\lambda_1 = 1$.

A central quantity in the theory is the *free segment probability* p_i, expressing the preference of a free segment (monomer) for a site in layer i over a site in the bulk

solution. More accurately, p_i is the equilibrium constant for the exchange of a segment in the bulk solution with a solvent molecule in layer i, or $-kT \ln p_i$ is the free energy associated with this exchange. In the case of noninteracting segments and a nonadsorbing surface, $p_i = 1$ for any layer i. In the first layer adjacent to an adsorbing surface $p_i = p_1 > 1$ since the adsorption energy difference between segments and solvent molecules favors the presence of a segment in this layer. If the segments interact with each other and with the solvent, p_i contains (for any layer i) an entropy factor accounting for the fact that a fraction of sites in layer i is occupied by segments and an energy factor originating from the segment–solvent interaction.

For polymer chains, the quantity p_i has to be used as a weighting factor for each of the chain segments that is in layer i. In other words, the probability that a chain of r segments has a given conformation (specified by indicating the layer number where each of the chain segments is situated) is proportional to the multiple product of r weighting factors p_i, p_j, p_k, ...; the number of times that the weighting factor p_i occurs in this multiple product is equal to the number of segments of this conformation in layer i.

DiMarzio and Rubin[2,3] have shown that for the calculation of the statistics of polymer chains in a lattice a matrix method is very useful. A chain of r segments is considered as a random walk of $r - 1$ steps, in which a weighting factor may be assigned to each segment. Through the matrix the *end segment probability* $p(i,r)$, i.e., the probability that the end segment of a chain of r segments is in layer i, can be easily evaluated. Let us first consider the end segment probability $p(i,2)$ of a dimer. If the end segment, in this case the second segment, is in layer i, the first segment can be in layers $i - 1$, i, or $i + 1$. The probability that the first segment is in $i - 1$ *and* the end segment in i is equal to $p_{i-1}\lambda_1 p_i$. Similarly, the probability that both segments of the dimer are in layer i is $p_i\lambda_0 p_i$, that of the first being in $i + 1$ *and* the second in i is $p_{i+1}\lambda_1 p_i$. Therefore, we find that $p(i,2) = p_i(\lambda_1 p_{i-1} + \lambda_0 p_i + \lambda_1 p_{i+1})$. In the same way, the end segment probability for an $r$mer can be written in terms of end segment probabilities for an $(r-1)$mer:

$$p(i,r) = p_i\{\lambda_1 p(i-1,r-1) + \lambda_0 p(i,r-1) + \lambda_1 p(i+1,r-1)\} \quad (1)$$

Any term $p(i,r)$ in (1) is zero for $i \leq 0$ since then $p_i = 0$. Equation 1 applies for each of the M layers, so that we have M simultaneous equations which can be expressed conveniently in a matrix formalism:

$$\mathbf{p}(r) = \mathbf{w}\mathbf{p}(r-1) = \mathbf{w}^{r-1}\mathbf{p}(1) \quad (2)$$

where the column vector $\mathbf{p}(r)$ has M components $p(i,r)$, the column vector $\mathbf{p}(1)$ has M components $p(i,1) = p_i$, and $\mathbf{w}$ is an $M \times M$ matrix with elements

$$w_{ij} = \lambda_{j-i} p_i \quad (3)$$

with $\lambda_{j-i} = \lambda_1$ if $|j - i| = 1$ and $\lambda_{j-i} = \lambda_0$ if $j = i$. For $|j - i| \geq 2$, $\lambda_{j-i} = 0$. More explicitly, eq 2 and 3 may be written as shown in eq 4. Equation 1 is part of one matrix multiplication and $\mathbf{p}(r)$ follows from $\mathbf{p}(1)$ through $r - 1$ matrix multiplications.

Equation 4, as written, suggests that a second surface is present just beyond layer M. If M is large enough, this is irrelevant. As shown previously,[1] only a limited number of layers has to be taken into account in order to obtain an accurate description of a polymer solution in equilibrium with one surface.

B. The Free Segment Probability. Before we show how the segment density distribution can be derived from the end segment probabilities we consider the free segment

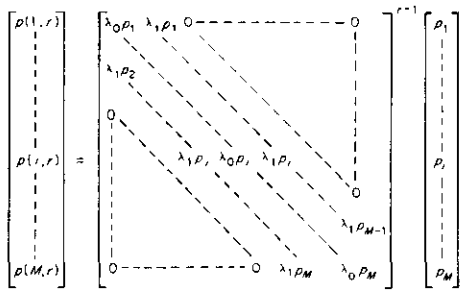

(4)

probability p_i somewhat more closely. If $p_i = 1$ for each i we have a purely random walk between nonadsorbing surfaces. If the surface has a higher affinity for segments than for solvent molecules we can define a differential adsorption energy[4,8] χ_s which is the difference in adsorption energy (in units of kT) of a segment and a solvent molecule. The preference of a segment over a solvent molecule in the surface layer can then be expressed by a Boltzmann factor e^{χ_s}. Polymer chains of which the segments do not interact with each other or with solvent may then be described as a random walk in which a segmental weighting factor e^{χ_s} is assigned to each visit to the surface layer: $p_1 = e^{\chi_s}$, $p_i = 1$ for $i > 1$. This case has been described in detail by DiMarzio and Rubin[3] for polymer chains between two surfaces.

For interacting chains the polymer–solvent interaction and the occupation of part of the lattice sites in each layer by other segments have to be incorporated in p_i. Both effects depend on the volume fractions ϕ_i and $\phi_i^0 = 1 - \phi_i$ of segments and solvent molecules, respectively, in layer i, and on the corresponding volume fractions ϕ_* and ϕ_*^0 in the bulk solution. The derivation of p_i from the partition function of the system has been given before.[1] For an adsorbing surface in equilibrium with a bulk solution the free segment probability may be written as

$$p_i = \frac{\phi_i^0}{\phi_*^0} e^{2\chi(\langle\phi_i\rangle - \phi_*)} e^{(\chi_s + \lambda_1\chi)\delta_{1,i}} \quad (5)$$

where χ is the well-known Flory–Huggins polymer–solvent interaction parameter,[14] and the Kronecker delta $\delta_{1,i}$ equals unity for $i = 1$ and zero for $i > 1$.

The factor ϕ_i^0/ϕ_*^0 originates from the difference in the configurational entropy of a segment in layer i and that of a segment in the bulk solution, since the number of ways in which an extra segment can be placed in a layer in which a fraction ϕ_i^0 of the sites is not occupied by segments is proportional to ϕ_i^0. For the layers close to the surface, the factor ϕ_i^0/ϕ_*^0 is smaller than unity.

The first Boltzmann factor in (5), $e^{2\chi\langle\phi_i\rangle}/e^{2\chi\phi_*}$, represents the interaction between a segment and its nearest neighbors. The site volume fraction $\langle\phi_i\rangle$ is defined as

$$\langle\phi_i\rangle = \lambda_1\phi_{i-1} + \lambda_0\phi_i + \lambda_1\phi_{i+1} \quad (6)$$

and has to be used because a segment has a fraction λ_0 of its contacts in the same layer and a fraction λ_1 in each of the adjoining layers. Since the bulk solution is homogeneous, $\langle\phi_*\rangle = \phi_*$. For athermal solvents $\chi = 0$ and this Boltzmann factor reduces to 1. In poor solvents the exponent is positive for layers where the segment concentration (averaged over the layers $i - 1$, i, and $i + 1$) is higher than in the bulk solution, expressing the net attraction between segments.

The last factor in (5) is due to the adsorption energy and differs from unity only for $i = 1$. The term $\lambda_1\chi$ in the exponent stems from the fact that for a segment in the first layer $\lambda_1 z$ contacts in the solution have been exchanged against $\lambda_1 z$ surface contacts. Even if $\chi_s = 0$ (e.g., for a liquid–air interface) there is a remaining energy contribution in the first layer due to the segment–solvent interaction.

C. The Overall Segment Density Distribution. For monomers the segment density profile can be easily evaluated. From the definition of p_i it follows that in this case $p_i = \phi_i/\phi_*$, or

$$\phi_i = p_i\phi_* \tag{7}$$

This gives with eq 5 a set of M implicit equations in M unknown ϕ_i's. For $\chi = 0$ the Langmuir equation[15] results; for nonathermal solutions the equations are identical with those given by Ono and Kondo[16] and by Lane[17] for adsorption of monomers from a regular solution.

For polymers the situation is more complex because the r chain segments are not independent of each other. The segment density depends on the number of chains in each conformation, and is the result of contributions of all the r chain segments. First, we consider the volume fraction $\phi_i(s)$ due to the segments with ranking number s ($s = 1, 2, ..., r$). In the bulk solution each of the r chain segments gives the same contribution to ϕ_*: $\phi_*(s) = \phi_*/r$. Near the surface not all the conformations are equally probable, resulting in a different spatial distribution for end and inner segments. If we define $p(s,i;r)$ as the probability (with respect to the bulk solution) that the sth segment of an $r$mer is in layer i we may write $p(s,i;r) = \phi_i(s)/\phi_*(s)$ or

$$\phi_i(s) = (\phi_*/r)p(s,i;r) \tag{8}$$

The quantity $p(s,i;r)$ can be expressed in end segment probabilities of shorter chains ending in i. Any conformation of an $r$mer with the sth segment in i can be described as the result of two walks ending in i, starting at the chain ends, and having $s - 1$ and $r - s$ steps, respectively. The corresponding end segment probabilities are $p(i,s)$ and $p(i,r-s+1)$, where the appropriate weighting factors p_j ($j = 1, 2, ..., M$) for the first s segments are included in $p(i,s)$ and those for the last $r - s + 1$ segments in $p(i, r - s+1)$. Thus, the weighting factor p_i for the sth segment occurs in both end segment probabilities. The probability that the sth segment of an $r$mer is in i is then equal to the joint probability that both chain parts end in i, divided by p_i:

$$p(s,i;r) = p(i,s)\ p(i,r-s+1)/p_i \tag{9}$$

This is a very important relation, which we shall use several times.

Note that in this derivation the inversion symmetry is automatically accounted for, since a segment situated s segments away from one chain end has the same probability of being in layer i as one that is s segments away from the other end (i.e., with ranking number $r + s - 1$). Helfand[5] has shown that this symmetry is not always obeyed in other theories.

Substituting (9) into (8) we obtain

$$\phi_i(s) = \frac{\phi_*}{rp_i}p(i,s)\ p(i,r-s+1) \tag{10}$$

$$\phi_i = \frac{\phi_*}{rp_i}\sum_{s=1}^{r}p(i,s)\ p(i,r-s+1) \tag{11}$$

This procedure of deriving the segment density due to each individual chain segment from two end segment probabilities, and the subsequent summation over all the chain segments to obtain ϕ_i, has been used previously, e.g., by Hoeve,[18] Helfand and Tagami,[19] and Levine et al.[20]

It is easily shown that in the bulk solution $p(*,s) = p_*^s = 1$ so that eq 10 reduces to $\phi_*(s) = \phi_*/r$; near a surface $p(i,s)$ differs from unity and the volume fraction $\phi_i(s)$ depends on the ranking number s. Equation 11 is a generalization of (7). The combination of eq 4, 5, and 11 constitutes a set of M implicit equations in the M unknown ϕ_i's, from which the concentration profile and the M p_i's may be solved numerically by an interative procedure as described previously.[1] Equation 11 for M layers contains $M \times r$ end segment probabilities $p(i,s)$, which may be arranged in an array $\boldsymbol{p}$:

$$\boldsymbol{p} = \begin{bmatrix} p_1 & \cdots & p(1,s) & \cdots & p(1,r) \\ \vdots & & \vdots & & \vdots \\ p_i & \cdots & p(i,s) & \cdots & p(i,r) \\ \vdots & & \vdots & & \vdots \\ p_M & \cdots & p(M,s) & \cdots & p(M,r) \end{bmatrix} \tag{12}$$

The sth column of $\boldsymbol{p}$ is the end segment probability vector $\mathbf{p}(s)$; it is found from the first vector $\mathbf{p}(1)$ after $s - 1$ matrix multiplications, according to (4). The array $\boldsymbol{p}$ contains all the end segment probabilities and, hence, all the information on the distribution of polymer molecules in the system. For example, according to eq 11 the overall segment distribution ϕ_i is found from the elements $p(i,s)$ of the ith row of the array by summing the products of the first and the last elements, of the second and penultimate elements, etc. In order to calculate properties of adsorbed chains (such as the distribution of segments of adsorbed polymer molecules, the distribution of segments over trains, loops, and tails, and the train, loop, and tail size distribution) it is necessary to differentiate between free and adsorbed polymer chains.

D. Free and Adsorbed Chains. Free chains do not have a single segment in the first layer. If we assign a segmental weighting factor p_i^f to each segment of a free chain which is in layer i, we have for the surface layer $p_1^f = 0$, while for the other layers ($i > 1$) $p_i^f = p_i$. The end segment probabilities $p_f(i,r)$ for free chains can then be calculated from eq 2 and 3 which now read

$$\mathbf{p}_f(r) = \mathbf{w}_f\mathbf{p}_f(r-1) = \mathbf{w}_f^{r-1}\mathbf{p}_f(1) \tag{13}$$

where the elements of the matrix $\mathbf{w}_f$ are given by

$$w_{f,ij} = \lambda_{j-i}p_i(1 - \delta_{1,i}) \tag{14}$$

and the components of the vector $\mathbf{p}_f(1)$ are

$$p_f(1,i) = p_i^f = p_i(1 - \delta_{1,i}) \tag{15}$$

For $i = 1$, the elements of $\mathbf{w}_f$ and $\mathbf{p}_f(1)$ are zero, while for $i > 1$ they are identical with those of $\mathbf{w}$ and $\mathbf{p}(1)$, respectively.

Analogously to eq 12 the vectors $\mathbf{p}_f(s)$ may be arranged in an array $\boldsymbol{p}_f$. If only the first r components of each vector are indicated, $\boldsymbol{p}_f$ can be represented as shown in eq 16

$$\boldsymbol{p}_f = \begin{bmatrix} 0 & \cdots & 0 & \cdots & 0 \\ p_2 & \cdots & p_f(2,s) & \cdots & p_f(2,r) \\ \vdots & \diagdown & \vdots & & \vdots \\ p_i & \cdots & p(i,i-1) & \cdots & p_f(i,r) \\ & \diagdown & \vdots & \diagdown & \\ & & p(s+1,s) & & \\ & \diagdown & & \diagdown & \\ p_r & \cdots & p(r,s) & \cdots & p_f(r,r) \end{bmatrix} \tag{16}$$

where $p_f(1,s) = 0$, $p_f(i,s) = p(i,s)$ if $i > s$ (lower left corner

of $\mathbf{p}_f$) and $p_f(i,s) < p(i,s)$ for $2 \leq i \leq s$. The sth vector of the array is found from the first after $s - 1$ matrix multiplications. The segment distribution of free chains may be found in the same way as in eq 10 and 11.

Next, we consider the end segment probabilities $p_a(i,s)$ and the array $\mathbf{p}_a$ for adsorbed chains. Since a chain is either adsorbed or free, we may write

$$p(i,s) = p_a(i,s) + p_f(i,s) \tag{17a}$$

$$\mathbf{p}(s) = \mathbf{p}_a(s) + \mathbf{p}_f(s) \tag{17b}$$

$$\mathbf{p} = \mathbf{p}_a + \mathbf{p}_f \tag{17c}$$

$p_a(i,s)$ is the probability that the end segment of an adsorbed $s$mer is in i. The array $\mathbf{p}_a$ can be represented as shown in eq 18 where $p_a(1,s) = p(1,s)$, $p_a(i,s) = 0$ if $i > s$

$$\mathbf{p}_a = \begin{bmatrix} p_1 & \cdots & p(1,s) & \cdots & p(1,r) \\ 0 & \ddots & & & \\ & & p_a(s,s) & & \\ 0 & & & & p_a(r,r) \end{bmatrix} \tag{18}$$

(end segments of adsorbed $s$mers cannot be outside the first s layers) and $p_a(i,s) < p(i,s)$ for $2 \leq i \leq s$.

The sum of the components of the last vector $\mathbf{p}_a(r)$, denoted as $p_a(r)$, gives the probability that the end segments of adsorbed $r$mers are somewhere in the system:

$$p_a(r) = \sum_{i=1}^{r} p_a(i,r) \tag{19}$$

Thus $p_a(r)$ gives the probability that a chain is adsorbed. The quantity $p_a(r)$ will be needed as a normalization factor. For example, the fraction of adsorbed chains that have their end segment in layer i is given by $p_a(i,r)/p_a(r)$.

For the calculation of the properties of adsorbed chains the array $\mathbf{p}_a$ plays a central role, and it is necessary to have accurate values for its elements $p_a(i,s)$. They can be calculated from eq 17, but the accuracy of the numbers obtained for relatively large i is low since in the outer regions of the adsorbed layer the difference between $p(i,s)$ and $p_f(i,s)$ is very small. More accurate values for $p_a(i,s)$ may be obtained by a different procedure, which is given in Appendix I.

E. The Segment Density Distribution in Trains, Loops, and Tails. The overall volume fraction ϕ_i is the sum of the contributions of free chains ϕ_i^f and that of adsorbed chains ϕ_i^a. In turn, the latter is the sum of the contributions due to trains (ϕ_i^{tr}), loops (ϕ_i^l), and tails (ϕ_i^t). All the segments in the first layer belong to trains. Therefore

$$(i = 1) \qquad \phi_1 = \phi_1^{tr} \tag{20}$$

$$(i > 1) \qquad \phi_i = \phi_i^l + \phi_i^t + \phi_i^f \tag{21}$$

As shown in section IIC, the segment density is the result of the contributions of all individual chain segments. Substituting (17a) into (10) we find

$$\phi_i(s) = \frac{\phi_*}{rp_i}\{p_a(i,s)p_a(i,r-s+1) + p_a(i,s)\ p_f(i,r-s+1) + p_a(i,r-s+1)\ p_f(i,s) + p_f(i,s)\ p_f(i,r-s+1)\} \tag{22}$$

Since segments in the surface layer cannot belong to free chains, $p_f(1,s) = 0$ and $p_a(1,s) = p(1,s)$. Thus for $i = 1$ the last three terms of (22) vanish and the equation reduces to (20), after summation over s.

Segments in the other layers ($i > 1$) may belong to loops or tails of adsorbed chains or to nonadsorbed free molecules. The first term of (22) gives the contribution of a segment belonging to a loop, the two middle terms that of a segment in one of the two tails of an adsorbed chain, and the last term represents the contribution of a segment of a free chain. The quantity $p_a(i,s)$ gives the probability that the end segment of an adsorbed $s$mer is in i; it contains all the conformations for which at least one of the previous segments is in the first layer. Analogously to eq 9, the product $p_i^{-1}\, p_a(i,s)\, p_a(i,r-s+1)$ is the probability that the sth segment is in layer i while at least one of the first $s - 1$ segments and at least one of the last $r - s$ segments are adsorbed. In other words, the first term of eq 22 gives the contribution of the segments with ranking number s which are in a loop. The volume fraction ϕ_i^l due to the loops is obtained after a summation over s

$$(i > 1) \qquad \phi_i^l = \frac{\phi_*}{rp_i}\sum_{s=1}^{r} p_a(i,s)\ p_a(i,r-s+1) \tag{23}$$

Segments for which $s < i$ cannot belong to loops; this is automatically accounted for in (23) since $p_a(i,s) = 0$ for $i > s$.

By similar reasoning the product $p_i^{-1}p_a(i,s)\ p_f(i,r-s+1)$ is the probability that segment s is in i while at least one of the first $s - 1$ segments and none of the last $r - s$ segments is adsorbed. Thus the second term of (22) gives the contribution of a segment s in a tail at the end of an adsorbed chain, and the third term that of a segment in a tail at the beginning of the chain. Since the summation over all s for these two terms gives the same result, we have

$$\phi_i^t = \frac{2\phi_*}{rp_i}\sum_{s=1}^{r} p_a(i,s)\ p_f(i,r-s+1) \tag{24}$$

Analogously, the volume fraction due to free chains is given by

$$\phi_i^f = \frac{\phi_*}{rp_i}\sum_{s=1}^{r} p_f(i,s)\ p_f(i,r-s+1) \tag{25}$$

In this way the volume fractions ϕ_1^{tr}, ϕ_i^l, ϕ_i^t, and ϕ_i^f can be calculated from the elements of the ith row of the arrays $\mathbf{p}_a$ and $\mathbf{p}_f$.

From the concentration profile the root-mean-square layer thickness t follows immediately:

$$t^2 = \frac{1}{\Gamma}\sum_{i=1}^{M} i^2\phi_i^a \tag{26}$$

Here $\Gamma = \sum_{i=1}^{M}\phi_i^a$ is the adsorbed amount expressed as the number of segments belonging to adsorbed chains per surface site. Γ is proportional to the probability $p_a(r)$ that a chain is adsorbed[1]

$$\Gamma = \phi_* p_a(r) \tag{27}$$

This relation follows from $\Gamma = \sum_{s=1}^{r}\sum_{i=1}^{M}\phi_i^a(s)$, where $\phi_i^a(s)$ is the volume fraction in layer i due to segments of adsorbed chains with ranking number s. Analogously to eq 8, $\phi_i^a(s)$ may be written as $r^{-1}\phi_* p_a(s,i;r)$ in which $p_a(s,i;r)$ is the probability that the sth segment of an adsorbed $r$mer is in layer i. Since $\sum_{i=1}^{M} p_a(s,i;r) = \sum_{i=1}^{M} p_a(i,r)$ (the probability that the sth segment is somewhere in the system, is equal to the probability that the end segment is somewhere in the system), eq 27 follows.

In the same way we can define the root-mean-square thickness due to the loops t_l and that due to the tails t_t

$$t_l^2 = \sum_{i=1}^{M} i^2\phi_i^l / \sum_{i=1}^{M}\phi_i^l \tag{28}$$

$$t_t^2 = \sum_{i=1}^{M} i^2\phi_i^t / \sum_{i=1}^{M}\phi_i^t \tag{29}$$

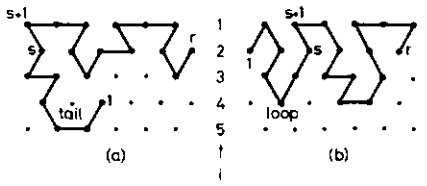

Figure 1. Schematic representation of chain conformations where the sth segment is the last of a tail (a) or a loop (b).

Obviously, the rms thickness t_{tr} due to trains equals 1.

F. Average Train, Loop, and Tail Size. Tail Size Distribution. For the calculation of the average train, loop, and tail size we need the number of trains (n_{tr}), loops (n_l), and tails (n_t) per adsorbed molecule. We can obtain these numbers by counting the number of transitions from layers 2 to 1. At each of these transitions a loop or a tail ends and a new train is formed. If the sth segment of a chain is in layer 2 and the $(s + 1)$th in layer 1, s is the last segment of a loop if at least one of the previous segments is adsorbed (see Figure 1b), while s is the last segment of a tail if none of the first s chain segments are adsorbed (see Figure 1a). The probability of the conformations in which the bond between two consecutive segments s and $s + 1$ is from the second to the first layer is equal to λ_1, multiplied by the probabilities that the first chain part of s segments ends in the second layer and that the last chain part of $r - s$ segments starts (or ends) in the first layer.

Let us begin with the calculation of the number of loops. We consider a chain of which the sth segment is the last of a loop and is in layer 2, while the $(s + 1)$th segment is the first of a train and is in the surface layer (Figure 1b). The probability that the first chain part of s segments is adsorbed and ends in the second layer is $p_s(2,s)$, the probability that the bond between s and $s + 1$ is from the second to the first layer is λ_1, and the probability that the second chain part of $r - s$ segments starts (or ends) on the surface equals $p(1,r-s)$, which is identical with $p_s(1,r-s)$. Thus the probability that the sth segment is the last of a loop is $p_s(2,s)\lambda_1 p_s(1,r-s)$. The number of loops per chain ending at the sth chain segment is found after dividing by $p_s(r)$. Summation over s gives

$$n_l = \frac{\lambda_1}{p_s(r)} \sum_{s=1}^{r-1} p_s(2,s) p_s(1,r-s) \tag{30}$$

The first term in (30) gives no contribution, since $p_s(2,1) = 0$; a loop cannot end at $s = 1$.

The number of trains is easily found from

$$n_{tr} = n_l + 1 \tag{31}$$

because a loop is always situated between two trains.

Analogously, the probability that the first s segments of a chain form a tail of s segments, with the sth segment in layer 2 and the $(s + 1)$th chain segment in the surface layer, is given by $p_t(2,s)\lambda_1 p_s(1,r-s)$. Normalization with $p_s(r)$ gives the number of tails per chain with length s

$$n_t(s) = \frac{2\lambda_1}{p_s(r)} p_t(2,s)\ p_s(1,r-s) \tag{32}$$

where the factor 2 accounts for the fact that a tail of s segments may be formed at both ends of the chain. Equation 32 represents the tail size distribution. After summation over s we obtain the total number of tails per chain:

$$n_t = \frac{2\lambda_1}{p_s(r)} \sum_{s=1}^{r-1} p_t(2,s)\ p_s(1,r-s) \tag{33}$$

An equivalent expression for n_t is found by realizing that any chain has two tails, unless an end segment is on the surface. The latter probability is $2p_s(1,r)/p_s(r)$ per adsorbed chain, so that we may write immediately

$$n_t = 2 - 2p_s(1,r)/p_s(r) \tag{34}$$

Equations 33 and 34 give identical results.

Having obtained n_{tr}, n_t, and n_l, we can calculate the fraction of segments in trains (ν_{tr}), tails (ν_t), and loops (ν_l). For the fraction in trains we have

$$\nu_{tr} = \phi_1/\Gamma = \phi_1/\phi_* p_s(r) \tag{35}$$

For the fraction of segments in tails we use the result for $n_t(s)$ as given in (32)

$$\nu_t = \frac{1}{r} \sum_{s=1}^{r-1} s n_t(s) \tag{36}$$

Finally, for the fraction in loops we have

$$\nu_l = 1 - \nu_{tr} - \nu_t \tag{37}$$

The average length of trains, tails, and loops is now easily obtained. The average train length l_{tr} is given by the number of segments in trains divided by the number of trains:

$$l_{tr} = r\nu_{tr}/n_{tr} \tag{38}$$

Similarly, we may write for the average tail length l_t and for the average loop length l_l

$$l_t = r\nu_t/n_t \tag{39}$$

$$l_l = r\nu_l/n_l \tag{40}$$

G. Train and Loop Size Distribution. In eq 32 we have obtained the tail size distribution $n_t(s)$, i.e., the number of tails with length s. The derivation of the analogous train and loop size distribution is slightly more complicated. We start with the trains.

We consider an adsorbed rmer of which the tth segment is in the second layer and the $(t + 1)$th is in the surface layer and is the first segment of a train of s segments long. Then the $(t + s)$th segment is the last segment of this train and the $(t + s + 1)$th segment is again in the second layer. The probability that the end segment of the first chain part of t segments is in the second layer is $p(2,t)$, the probability of s consecutive train segments is $\lambda_0^{s-1}\ p_1^s$, and the probability that the first segment of the last $r - s - t$ chain segments is in layer 2 is $p(2,r-s-t)$. Including the transition probabilities from the first to the second layer at the bonds t, $t + 1$ and $t + s$, $t + s + 1$ we find for the probability of this chain conformation

$$p(2,t)\lambda_1\lambda_0^{s-1}p_1^s\lambda_1 p(2,r-s-t)$$

This expression applies for $t = 1$ up to and including $t = r - s - 1$. A train starting at the first segment would correspond to $t = 0$, but then the factor $p(2,t)\lambda_1$ should be equal to unity. We may include this situation in the above expression by defining formally $p(2,0) = 1/\lambda_1$. (Note, however, that $p(2,0)$ may not be identified with the second component of a vector $\mathbf{p}(0)$ for which the relation $\mathbf{p}(1) = \boldsymbol{w}\mathbf{p}(0)$ holds.) Similarly, a train at the end of the chain may be included if we allow for t the (maximum) value $r - s$. The number of trains of length s per chain is now found by summation over t and normalization with $p_s(r)$

$$n_{tr}(s) = \frac{\lambda_1^2\lambda_0^{s-1}p_1^s}{p_s(r)} \sum_{t=0}^{r-s} p(2,t)\ p(2,r-s-t) \tag{41}$$

where $p(2,0) = 1/\lambda_1$. Thus the train size distribution can be calculated from the elements of the second row of the array $\boldsymbol{p}$, given in (12).

For the loop size distribution we consider a chain of which the tth segment is the last of a train and the $(t + 1)$th segment is the first of a loop of s segments. Thus the $(t + 1)$th and the $(t + s)$th segments are both in the second layer, the tth and $(t + s + 1)$th are on the surface. The probability of this chain conformation can be written as

$$p_a(1,t)\lambda_1 p_t(2,s)\lambda_1 p_a(1,r-s-t) \tag{42}$$

where $p_t(2,s)$ is the probability that a tail of s segments ends in the second layer. Here a loop is considered as a special case of a tail (of which not a single segment is on the surface), i.e., as a tail ending in the second layer. The quantity $p_t(2,s)$ may be identified with the second component of a tail end segment probability vector $\mathbf{p}_t(s)$. For $s = 1$, the tail is only one segment long and the tail end segment is necessarily in the second layer: $p_t(2,1) = p_2$, $p_t(i,1) = 0$ if $i \neq 2$. Hence, we have for the components of the vector $\mathbf{p}_t(1)$

$$p_t(i,1) = p_2\delta_{2,i} \tag{43}$$

Analogously to eq 13 we find the components $p_t(i,s)$ for longer tails after $s - 1$ matrix multiplications

$$\mathbf{p}_t(s) = \mathbf{w}_f^{s-1}\mathbf{p}_t(1) \tag{44}$$

where the matrix $\mathbf{w}_f$ has to be used because no tail segment can be in the first layer. The tail end segment probabilities may again be arranged in an array $\mathbf{p}_t$ as in eq 45 where

$$\mathbf{p}_t = \begin{bmatrix} 0 & \cdots & 0 & \cdots & 0 \\ p_2 & \cdots & p_t(2,s) & \cdots & p_t(2,r-1) \\ 0 & & & & \\ 1 & \cdots & p_t(t,r-1) & \cdots & p_t(t,r-1) \\ & & p_t(t+1,s) & & \\ 0 & \cdots & 0 & & p_t(r,r-1) \end{bmatrix} \tag{45}$$

$p_t(1,s) = 0$ and $p_t(i,s) = 0$ if $i > s + 1$, since a tail of s segments starting in the second layer can maximally extend up to layer $s + 1$. Note that this array contains only $r - 1$ vectors; at least one segment of the chain should be on the surface.

The factor $p_t(2,s)$ in (42) can now be taken from the second row of $\mathbf{p}_t$. The loop size distribution is obtained after summation over t

$$n_l(s) = \frac{\lambda_1^2 p_t(2,s)}{p_a(r)} \sum_{t=1}^{r-s-1} p_a(1,t)\, p_a(1,r-s-t) \tag{46}$$

Since the loop is preceded by a train segment (ranking number t) and the $(t + s + 1)$th segment should again be on the surface, the summation extends up to $t = r - s - 1$.

From (41) and (46), the numbers of trains and loops and the average train and loop length could be obtained in a way similar to the derivation for tails, as given in eq 32, 33, 36, and 39. However, in the previous section an easier method was given for these quantities. The results are identical, as should be expected.

III. Results and Discussion

In the previous paper[1] several examples were given of the dependence of the adsorbed amount Γ, the surface occupancy θ $(=\phi_1)$, and the bound fraction p $(=p_{1r})$ on the bulk solution volume fraction ϕ_* and the chain length r, for different values of the interaction parameters χ and χ_s. Here we concentrate on the structural aspects of the adsorbed layer, such as the distribution of individual segments and the buildup of the layer in terms of trains, loops, and tails. All of the results apply to a hexagonal lattice ($\lambda_0 = 0.5$) and an adsorption energy parameter $\chi_s = 1$. For the polymer–solvent interaction parameter χ we use the values 0.5 (Θ solvent) and 0 (athermal solvent). While the previously reported calculations were for maximally 35 lattice layers, most of the present data are for 80 layers. This high number is necessary if accurate values for the root-mean-square layer thickness are to be obtained.

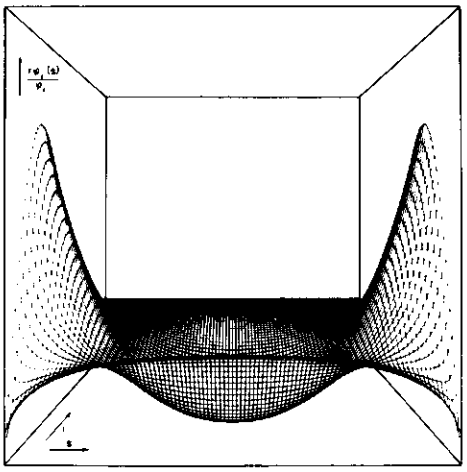

Figure 2. The relative contribution of segments with ranking number s to the volume fraction ϕ_i in layer i, $r\phi_i(s)/\phi_i$, as a function of layer number i (from front to back) and ranking number s (from left to right). One looks from the surface (front plane) toward the solution. Eighty layers are indicated, corresponding to 80 lines parallel to the surface. The relative contribution of every 10th segment is plotted ($s = 1, 11, 21, \ldots, 501, 510, 520, \ldots, 1000$) so that 101 lines run perpendicular to the surface. See also Figure 3.

A. Distribution of Individual Segments. We begin with the distribution of individual chain segments. In Roe's theory[4] the approximation was made that any chain segment (ranking number $s = 1, 2, \ldots, r$) would give the same contribution $\phi_i(s)$ to the volume fraction ϕ_i in any layer i. This is equivalent to the assumption $\phi_i(s) = \phi_i/r$ for any s. The extent to which the ratio $r\phi_i(s)/\phi_i$ deviates from unity gives a measure of the validity of this assumption. Figure 2 shows a computer drawing of the dependence of $r\phi_i(s)/\phi_i$ on s and i, in perspective view, for $r = 1000$, $\phi_* = 10^{-3}$, and $\chi = 0.5$. The segment ranking number s is plotted from left to right, and the layer number i from front to back. Thus one looks from the surface toward the bulk solution. Eighty layers ($i = 1, 2, \ldots, 80$) are indicated, corresponding to 80 lines parallel to the surface. Every 10th segment is taken ($s = 1, 11, 21, \ldots, 501, 510, 520, \ldots, 1000$) so that 101 lines run in the direction perpendicular to the surface.

This figure shows that, for $i = 1$, $r\phi_i(s)/\phi_i$ is smaller than 1 for end segments (left and right in the figure) and higher for middle segments. Further away from the surface the relative contribution of end segments increases and that of middle segments decreases; around $i = 20$ the relative probability of finding end segments is maximal and that for middle segments minimal. At still greater distances $\phi_i(s)$ becomes more weakly dependent on s, until about $i = 60$, when all of the segments contribute equally to the overall volume fraction ϕ_i. This last result is to be expected for polymer chains in bulk solution.

More quantitative detail is seen in a projection of Figure 2 in the $r\phi_i(s)/\phi_i$–s plane. This is shown in Figure 3 for

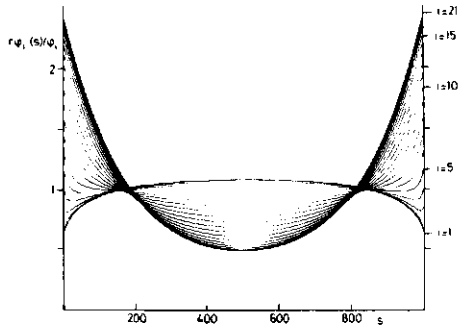

Figure 3. Projection of Figure 2 for the first 21 layers in a plane parallel to the surface. In this case the relative contribution $r\phi_i(1)/\phi_i$ for end segments has its maximum value 2.42 in layer 21. Hexagonal lattice. $\chi_s = 1$, $\chi = 0.5$, $r = 1000$, $\phi_* = 0.001$.

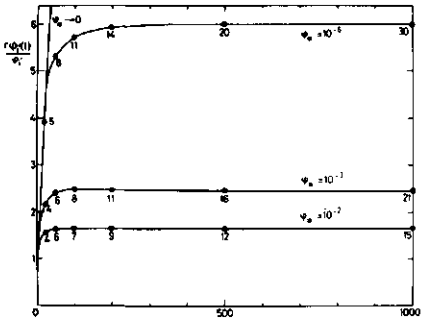

Figure 4. Maximum values for $r\phi_i(1)/\phi_i$ (see Figure 2) as a function of chain length r for four bulk volume fractions ϕ_*. For several volume fractions the layer i', where the maximum occurs, is indicated. Hexagonal lattice, $\chi_s = 1$, $\chi = 0.5$.

the first 21 layers. In this example $i = 21$ is the layer where the ratio $r\phi_i(1)/\phi_i$ for end segments has its maximum value 2.42; for the layers further away this ratio decreases again. In the first layer the ratio of volume fractions due to end and middle segments, $\phi_i(1)/\phi_i(500)$, is 0.600; for layer 21 it is 5.01.

We have obtained graphs like Figure 3 for other chain lengths and other bulk volume fractions. They all look similar, exhibiting a minimum value for $r\phi_i(1)/\phi_i$ in the first layer and a maximum value in a layer $i = i'$ some distance away from the surface. In order to give an idea of the trends, we have plotted in Figure 4 the maximum value $r\phi_{i'}(1)/\phi_{i'}$ as a function of r for some values of ϕ_*. The layer i' where the maximum occurs is indicated for various combinations of r and ϕ_*.

The above results allow an evaluation of the validity of the assumption of an equal distribution of all chain segments, as made by Roe. Roe[4] states that (1) the conformational constraint imposed by the presence of a surface is less severe to end than to inner segments, and (2) the assumption of an equal contribution ϕ_i/r for all segments, independent of the segment ranking number, is better for smaller chain lengths. The first point seems to be incorrect, as shown in the Figures 2–4; except for very high ϕ_*, the probability of finding end segments close to the surface is *lower* than that for middle segments, implying that the conformational restrictions are higher for end segments. (However, we found for $\phi_* \rightarrow 1$ a small preference for end segments in the surface layer, of the order of 18% for $r = 1000$.) The second point is correct for chains up to $r \simeq 100$, as indicated by the rising portions of $r\phi_{i'}(1)/\phi_{i'}$ in Figure 4. For longer chains the maximum deviation from a uniform segment distribution becomes nearly independent of chain length (although the layer number i' where this maximum occurs increases with r).

The fact that end segments occur more frequently than middle segments, at some distance from the surface, points clearly to the importance of tails, since only segments that are close to the chain ends can be in tails. Thus end effects may probably not be neglected, as was done in previous theories[4-8]. This conclusion will be corroborated by the results discussed below.

One special feature of Figure 3 deserves attention. Segments with ranking number around $s = 0.18r$ (or $0.82r$) have a distribution which is in all layers nearly equal to the average value ϕ_i/r, as indicated by the fact that all the lines for different i intersect around this ranking number. This (approximately) common intersection point at $s = 0.18r$ is also found for other chain lengths and concentrations. Thus it seems that, regardless of chain length, about 36% of the segments (at both chain ends) show an "end segment behavior". We have no indication that this fraction decreases drastically for chains longer than $r = 1000$. Also, from the nearly constant value of $r\phi_{i'}(1)/\phi_{i'}$ for $r > 100$ (see Figure 4) it seems that end segments in the layers further away from the surface are dominant, independent of r. Therefore, even for long chains ($r > 1000$) tails probably play an important role in the adsorbed layer.

Figure 4 shows that the plateau value of $r\phi_{i'}(1)/\phi_{i'}$ at high chain lengths increases if the bulk solution becomes more dilute. This may *not* be interpreted as an increase of the tail fraction, but says merely that at $i = i'$ the contribution $\phi_{i'}(1)$ due to end segments is much higher than the average segment contribution $\phi_{i'}/r$, but $\phi_{i'}$ can be quite low in dilute solutions. Actually, it will be shown below that for isolated chains the effect of tails becomes negligible, in accordance with previous theories.[9,10] A high ratio $r\phi_{i'}/\phi_{i'}$ means only that the (few) segments occurring in layer i' are nearly exclusively tail segments. Similarly, the effect that the layer i' (where end segments have their maximum relative contribution to ϕ_i) shifts further away from the surface for lower bulk concentrations may not be interpreted as an increase of the layer thickness with decreasing ϕ_*. The high values for i' at low ϕ_* are related to the fact that the (few) segments at distance i' belong predominantly to *adsorbed* chains. For higher ϕ_* the free, nonadsorbed chains contribute significantly to the segment concentration at large distance, thereby decreasing the value for $r\phi_{i'}(1)/\phi_{i'}$ since this ratio is an average over adsorbed and free chains.

B. Concentration Profile and Layer Thickness. Figure 5 shows the overall concentration profile and those due to loop and tail segments, for $r = 1000$, $\phi_* = 10^{-6}$, and $\chi = 0.5$. The volume fractions, ϕ_i, ϕ_i^l and ϕ_i^t are plotted on a logarithmic scale. In this example, 38% of the segments are in trains, 55.5% in loops, and 6.5% in tails (see Figures 10 and 11). Previous theories[7] predict an exponential concentration profile. Figure 5 shows that this is not true for the adsorbed layer as a whole (i.e., ϕ_i), but very nearly so for the loop segment contribution: $\log \phi_i^l$ vs. i is practically a straight line. Thus, Hoeve's theory[7] would describe the concentration profile correctly if end effects were to be negligible. From Figure 5 it is clear that this is not the case, even if the tail fraction is as low as 6.5%; in the region from $i = 20$ to $i = 40$, ϕ_i is nearly completely

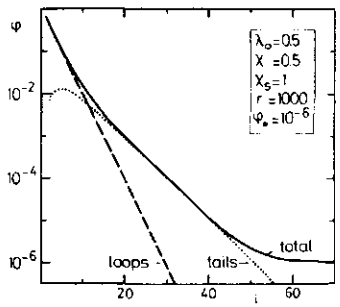

Figure 5. The volume fraction ϕ_i (full line) and its components ϕ_i^l due to loops (broken line) and ϕ_i^t due to tails (dotted line) on a logarithmic scale as a function of the distance from the surface. The loop contribution ϕ_i^l decreases essentially exponentially with i.

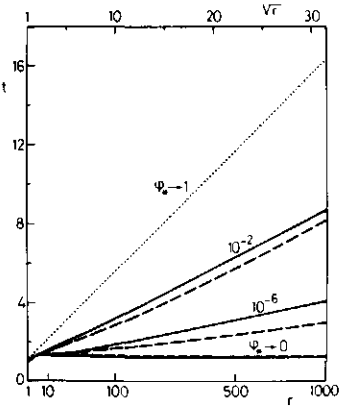

Figure 6. The root-mean-square layer thickness t as a function of the square root of the chain length r, for four values of the bulk volume fraction ϕ_*. Hexagonal lattice, $\chi_s = 1$. Full lines, $\chi = 0.5$; broken lines, $\chi = 0$; dotted line, bulk polymer.

determined by the tails. Only at very small distances (below $i = 5$) do the loops dominate over the tails. In the outer regions of the adsorbed layer (beyond $i = 50$) the contribution ϕ_i^f due to free chains (not indicated in the figure) is the most important; beyond $i = 60$ $\phi_i \simeq \phi_*$.

The tail contribution ϕ_i^t shows a maximum around layer 5. Around the 10th layer the concentration due to tail segments is equal to that due to loop segments. These features are approximately the same under conditions that the tail fraction is considerably higher (e.g., if $\phi_* = 10^{-2}$).

The fact that loops are not found at some distance from the surface is of considerable practical importance. It implies that the interaction between colloidal particles in the presence of polymers (e.g., in flocculation or protection experiments) is to a large extent determined by long dangling tails.

Hoeve[7] calculated that for Θ solvents the root-mean-square layer thickness should be proportional to the square root of molecular weight. In Figure 6 the rms layer thickness t is plotted as a function of $r^{1/2}$ for isolated chains ($\phi_* \to 0$), for a dilute and a semidilute concentration ($\phi_* = 10^{-6}$ and 10^{-2}), and for (practically) pure bulk polymer ($\phi_* \to 1$). In the case of isolated chains t is small and nearly independent of chain length. However, for finite concentrations and $\chi = 0.5$, t increases linearly with $r^{1/2}$ (apart from some irregularities for very short chains, $r \lesssim 20$); the slope of the line increases with increasing ϕ_*. For $\chi = 0$, the line for $\phi_* = 10^{-2}$ is not completely straight and lies somewhat below that for $\chi = 0.5$. In bulk polymer ($\phi_* \to 1$) the conformation of the adsorbed chains is independent of χ and χ_s, as discussed previously.[1]

TABLE I: Root-Mean-Square Layer Thickness Due to Loops t_l and Tails t_t, and the Overall rms Thickness t Due to All Segments of Adsorbed Chains for $r = 1000$: Hexagonal Lattice, $\chi_s = 1$

	$\chi = 0$			$\chi = 0.5$		
ϕ_*	t_l	t_t	t	t_l	t_t	t
$\to 0$	4.36	6.38	1.24	4.25	5.82	1.20
10^{-6}	3.37	9.92	2.94	4.18	9.58	4.01
10^{-2}	4.64	18.44	8.27	5.56	16.64	8.68
$\to 1$	8.22	19.70	16.43	8.22	19.70	16.43

The similarity between our results and Hoeve's prediction for $\chi = 0.5$ is at first sight surprising, since Hoeve's theory considers only loops and, as we have seen above, tail segments are dominant in the outer regions of the adsorbed layer. However, if we calculate the rms thicknesses due to loop and tail segments separately, we find that *both* t_l and t_t are practically proportional to $r^{1/2}$. Values of t, t_l, and t_t for $r = 1000$ are given in Table I. The overall thickness t is some average of t_l, t_t, and the contribution t_{tr} due to trains ($t_{tr} = 1$), weighted according to the fraction of segments in loops, tails, and trains. For $\phi_* \to 0$ t is only slightly above t_{tr}, in dilute solutions $t \simeq t_l$, while for higher ϕ_* t is mainly determined by the tails. The linear relationship between t_l and $r^{1/2}$ is in agreement with Hoeve's theory for $\chi = 0.5$, but that between t_t and $r^{1/2}$ has not been found before, at least for interacting chains. In this context it is worthwhile noting that Roe[12] derived, for isolated chains with χ_s close to the critical adsorption energy, also a proportionality of t_t with $r^{1/2}$.

It is interesting to compare the adsorbed layer thickness with the dimensions of a chain in solution. For chains in a z-choice lattice it has been found[21] that the radius of gyration R_G, expressed in the length of a step in the lattice, can be written as

$$R_G^2 = (r/6)(1 + z^{-1})(1 - z^{-1}) \qquad (47)$$

If this relation holds for a hexagonal lattice where backfolding is allowed ($z = 12$) we obtain, for $r = 1000$, $R_G = 14.03$. From Table I we see that in bulk polymer the rms thickness t is somewhat higher than R_G, while in dilute solutions it is a factor 2–3 lower. Naturally, these numbers depend on χ and χ_s (except if $\phi_* \to 1$). Layer thicknesses of the order of magnitude of R_G have often been reported in the literature, but in most cases the measured layer thickness is not easily converted to the rms thickness. Recent ellipsometric data of Killmann et al.[22] and Smith et al.[23] for polystyrene adsorbed on metal surfaces from different solvents show that in all cases the square root dependency holds; for a concentration of 5×10^{-3} (w/w) these authors find that $t/R_G \simeq 0.6$–1 (depending on the metal used as substrate) for a Θ solvent and $t/R_G \simeq 0.3$–0.6 for a better solvent. These trends are in satisfactory agreement with our theoretical results, considering that the conversion of ellipsometric thicknesses to rms thicknesses was based on an exponential concentration profile, which is not valid if tails are present. Moreover, the χ_s values that apply to the metal surfaces used in the experiments are not known.

A conspicuous feature of the results shown in Figure 6 is that with increasing ϕ_* the rms thickness increases much more strongly than the adsorbed amount Γ, as a consequence of the increasing tail fraction at high ϕ_* (see also

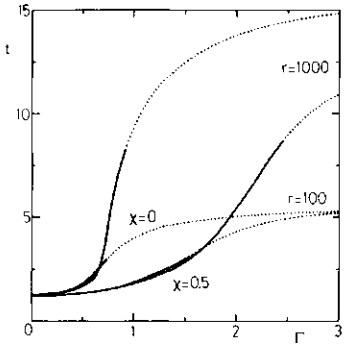

Figure 7. The root-mean-square layer thickness t as a function of the amount adsorbed Γ, for two values of the chain length r, at $\chi = 0$ and 0.5. Hexagonal lattice, $\chi_s = 1$. The lines are dotted for $\phi_* > 0.01$.

Figures 10 and 11). For example, for $r = 1000$ and $\chi = 0.5$, Γ increases by 37% and t by 120% in the range $\phi_* = 10^{-6}$–10^{-2}; for $\chi = 0$ these differences are even more pronounced, namely, 32 and 182%. Similar trends have been found experimentally.[22,24,25] It is clear that the explanation is found in the progressively increasing fraction of segments in tails with increasing bulk concentration, at least for homodisperse polymers. For heterodisperse samples, often used in experiments, the preferential adsorption of long chains over shorter ones should also be taken into account. We have reported recently on the consequences of polydispersity in practical systems.[26]

In the preceding article,[1] we have shown that, at given χ and χ_s, the conformation parameters p ($=\nu_{tr}$) and θ ($=\phi_1$) are a function of only the adsorbed amount Γ, at least in the usual measuring range for ϕ_* and Γ. In other words, in this range p and θ depend on Γ, but not on the chain length r provided the concentration is adapted such that Γ remains constant. If the adsorbed amount is the same, short chains, at high ϕ_*, have the same conformation as longer chains at lower ϕ_* (if the conformation is characterized by p and θ). Another measure for the conformation is the layer thickness t, and one may wonder if also in this respect the conformation is a function of Γ only. Figure 7 gives a plot of t against Γ for $\chi = 0$ and 0.5, and $r = 100$ and 1000. In order to show the usual experimental range more clearly, the curves are dotted for bulk volume fractions $\phi_* > 10^{-2}$.

We can distinguish three regions in each curve: at low Γ the layer thickness is small and nearly constant (flat conformation), at intermediate values of Γ the layer thickness increases with increasing Γ (formation of longer loops and tails), while at high Γ the layer thickness levels off, slowly approaching the thickness corresponding to bulk polymer (compare Table I). In this latter region the molecules penetrate each other (thereby increasing Γ) without changing their conformation drastically. The interesting part of Figure 7 is in the region below $\phi_* = 10^{-2}$ where the layer thickness is indeed a function of Γ only, and does not depend on chain length. Thus it is reasonable to conclude that, at given χ and χ_s, the conformation is only determined by Γ, independent of ϕ_* and r.

For intermediate values of Γ, the layer thickness increases more strongly with Γ (and is higher) in good solvents than in poor solvents. Naturally, in good solvents a much higher ϕ_* is necessary to attain the same Γ as in poor solvents. This higher thickness and steeper rise of $t(\Gamma)$ in good solvents are due to the stronger mutual repulsion of the segments, as compared to the situation in poorer solvents.

C. Number and Length of Trains, Loops, and Tails. In Figures 8–11 we consider the contributions of trains, loops, and tails to the composition of the adsorbed layer, as a function of chain length. In all cases $\chi_s = 1$ and $\chi = 0.5$ (solid lines) or 0 (broken lines). As in Figure 6, four bulk volume fractions are chosen: $\phi_* \to 0$, corresponding to a purely random walk as treated in the model of DiMarzio and Rubin,[2,3] two (semi)dilute concentrations $\phi_* = 10^{-6}$ and 10^{-2}, and (nearly) pure bulk polymer near a surface ($\phi_* \to 1$). Figure 8 gives the average number of loops n_l and tails n_t per chain (note that $n_{tr} = n_l + 1$), Figure 9 the average length of trains l_{tr}, of loops l_l, and of tails l_t, and Figure 10 the fraction of segments in trains ν_{tr}, in loops ν_l, and in tails ν_t. In all these figures a linear scale for r is used. In order to show some interesting details for short chains, Figure 11 gives ν_{tr} and ν_t against r on a logarithmic scale.

For isolated chains of not too short a length, the number of loops (and trains) is proportional to chain length, and the number of tails is independent of r. The loop size is

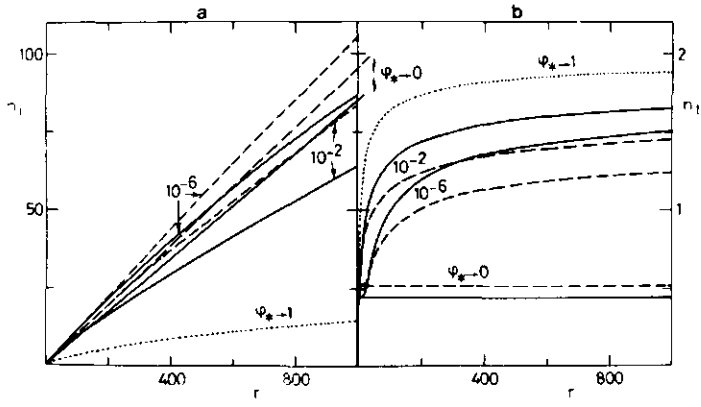

Figure 8. The average number of (a) loops per chain n_l, and (b) tails per chain n_t, as a function of chain length r. The bulk solution volume fraction ϕ_* is indicated. Hexagonal lattice, $\chi_s = 1$. Full lines, $\chi = 0.5$; broken lines, $\chi = 0$; dotted line, bulk polymer.

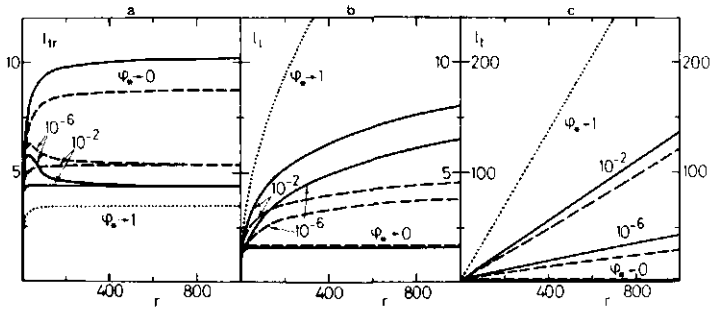

Figure 9. The average length of (a) trains l_{tr}, (b) loops l_l, and (c) tails l_t, as a function of the chain length r. The bulk solution volume fraction ϕ_s is indicated. Hexagonal lattice, $\chi_s = 1$. Full lines, $\chi = 0.5$; broken lines, $\chi = 0$; dotted line, bulk polymer.

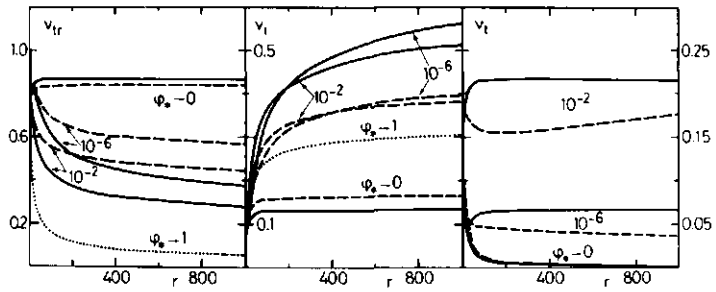

Figure 10. The fraction of segments in (a) trains ν_{tr} (often denoted as p), (b) loops ν_l, and (c) tails ν_t, as a function of the chain length r. The bulk solution volume fraction ϕ_s is indicated. Hexagonal lattice, $\chi_s = 1$. Full lines, $\chi = 0.5$; broken lines, $\chi = 0$; dotted line, bulk polymer. The fraction of segments in tails ν_t for bulk polymer is shown in Figure 11b.

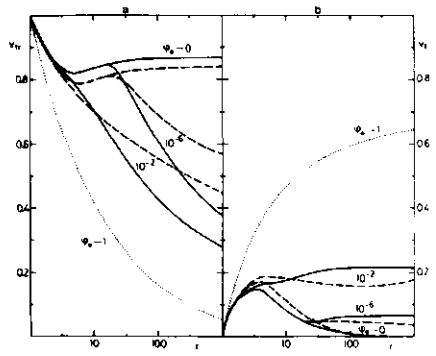

Figure 11. The fraction of segments in (a) trains ν_{tr} ($= p$), and (b) in tails ν_t against the chain length r on a logarithmic scale. The bulk solution volume fraction ϕ_s is indicated. Hexagonal lattice, $\chi_s = 1$. Full lines, $\chi = 0.5$; broken lines, $\chi = 0$; dotted line, bulk polymer. See also Figure 10, where the same data are plotted against r on a linear scale.

small (only 1.50 for $\chi = 0.5$), the train size is relatively large (about 10 for $\chi = 0.5$) and the tails are very short ($l_t = 2$). Train, loop, and tail sizes are practically independent of chain length for $r \gtrsim 50$. Thus the adsorbed molecules assume a very flat conformation. More than 85% of the segments are in trains and less than 15% in loops; tails play hardly any role. The only effect of an increase in chain length is an increase in the numbers of trains and loops of constant size. All these trends have been predicted by previous theories;[9-12] unless the difference between χ_s and the critical adsorption energy is quite small, isolated polymer chains lay practically flat on the surface.

The situation changes drastically if only a very small equilibrium concentration (e.g., $\phi_s = 10^{-6}$) is present in the solution. Then competition between the adsorbed molecules takes place and the adsorbed layer becomes more extended. Let us first consider the effects at relatively high chain lengths ($r \gtrsim 50$) and compare, for a Θ solvent, $\phi_s = 10^{-6}$ with extremely dilute solutions ($\phi_s \to 0$).

The numbers of trains and loops are slightly higher than for isolated molecules, but the increase with r is less (the line for $\phi_s = 10^{-6}$ in Figure 8a comes below that for $\phi_s \to 0$ above $r = 1000$). The number of tails per chain increases up to about 1.5. The train size is about 4.3 and independent of r, the loop length exceeds the train length and increases with r, and the tail size is nearly (but not completely) proportional to r and reaches a value of 43 for $r = 1000$. The fraction of segments in trains decreases with r and is only 0.38 for $r = 1000$, that in loops increases up to 0.55, and the tail fraction is about 0.07 for any r. The shape of adsorbed molecules is dramatically changed, compared to isolated coils at a surface, even for $\phi_s = 10^{-6}$.

For higher bulk volume fractions these trends are more pronounced: there are fewer trains (of about the same length as for $\phi_s = 10^{-6}$), longer loops, and more tails of considerably greater size. For example, for a chain of $r = 1000$ at $\phi_s = 10^{-2}$ and $\chi = 0.5$ the average tail length is 131, and 21% of the segments are in the tails. In athermal solvents adsorbed chains are flatter than in Θ solvents, at the same bulk volume fraction. However, the contribution of tails is only slightly smaller.

In pure bulk polymer ($\phi_s \to 1$) the average shape of chains in contact with the surface is only determined by

entropic factors, since the transfer of a chain segment from one lattice site to another does not change the energy; the results do not depend on χ or χ_s. The conformation of the adsorbed chains is very extended; the number of trains and loops is small, the trains are short (about 3.4 segments) and the loops long (21 segments for $r = 1000$), and there are nearly two tails per molecule of a length which increases (practically) proportionally to chain length; for $r = 1000$ the average tail size is 344. For a chain of 1000 segments only 5% of the segments are present in the trains, 30% are in loops, and 65% in tails. This conformation resembles closely that described by Roe[12] for *isolated molecules* with χ_s equal to the critical adsorption energy. For this case Roe concluded that on average an adsorbed chain is divided up into three roughly equal sections, i.e., two long tails and a middle part in which trains of length 3 (hexagonal lattice) and loops of length $(r/3)^{1/2}$ (18.3 for $r = 1000$) alternate. The reason for this similarity is probably that both in bulk polymer and in a random walk near a surface at the critical adsorption energy the conformation is only determined by the entropy.

It is interesting to note one other peculiar feature of the results for $\phi_* \to 1$. In Figure 6 it was shown that t increases linearly with the square root of chain length, for all ϕ_*. We find that for bulk polymer Γ, the number of monolayers that can be filled with segments belonging to adsorbed chains, also shows this dependency on $r^{1/2}$: for $r \gtrsim 5$ we obtain $\Gamma(\phi_* \to 1) = 0.64 + 0.562r^{1/2}$, while the tail contribution can be written as $\Gamma_{\text{tails}}(\phi_* \to 1) = 0.374r^{1/2}$. This $\Gamma - r^{1/2}$ dependence is surprising in view of the fact that, at low ϕ_*, Γ is linear in log r, which implies a much weaker dependency on chain length. We can only give a qualitative explanation. At $\phi_* = 1$ *all the lattice sites are occupied* by polymer. The volume fraction ϕ_1^f due to chains with undisturbed bulk conformations increases from zero at the surface to 1 at a distance from the surface that is proportional to $r^{1/2}$. The remaining lattice sites, the number of which is proportional to $r^{1/2}$, are occupied by segments of disturbed (i.e., adsorbed) chains, so that Γ is expected to increase linearly with the square root of the chain length.

So far we have restricted the discussion about train, loop, and tail sizes to relatively long chains. For oligomers ($r \lesssim 20$) a few typical effects occur as may be seen in the Figures 9a and 11. Figure 9a exhibits a maximum in the train size (around $r = 20$) for low concentrations ($\phi_* = 10^{-6}$). For chains shorter than about 15 segments the train size is the same as for isolated chains ($\phi_* \to 0$); for chains longer than 30 segments the train size decreases and becomes independent of chain length for high r. The maximum in l_{tr} corresponds to the point where the surface occupancy θ is about 0.1; below that value trains can be easily formed and have about the same size as in isolated chains, but as the surface becomes more occupied it is increasingly difficult to form long trains so that l_{tr} decreases. In principle, this effect occurs also at higher ϕ_* (e.g., 10^{-2}) but since then a surface occupancy of 0.1 is attained at lower r the maximum is suppressed.

Figure 11a shows an S-shaped curve for ν_{tr} as a function of r at low ϕ_*. The minimum of ν_{tr} at $r = 5$ is due to the fact that around this chain length loop formation has become possible so that more than one train can be formed and hence ν_{tr} can increase again. The maximum around $r = 20$ is due to the difficulty of forming long trains on a surface which becomes more occupied, as discussed above.

Figure 11b shows that a maximum in ν_t occurs around $r = 4$ at low concentrations ($\phi_* = 10^{-6}$). For shorter chains only tails may be formed and no loops; for longer chains

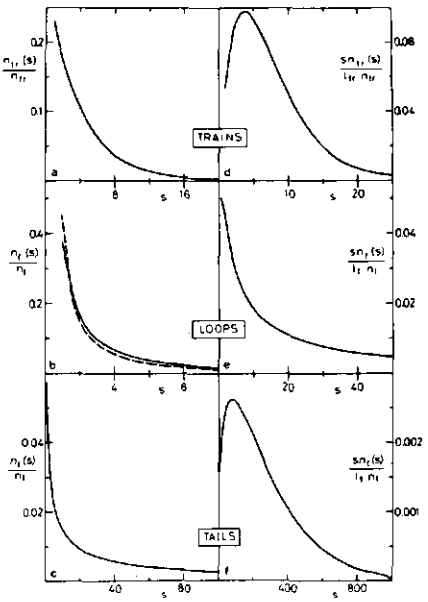

Figure 12. (a) The train size distribution $n_{tr}(s)/n_{tr}$, (b) loop size distribution $n_l(s)/n_l$, and (c) tail size distribution $n_t(s)/n_t$. On the right-hand side figures the fraction of (d) train segments $sn_{tr}(s)/l_{tr}n_{tr}$ in trains of lengths s, that of (e) loop segments $sn_l(s)/l_ln_l$, and of (f) tail segments $sn_t(s)/l_tn_t$ are given. Hexagonal lattice, $\chi_s = 1$, $\chi = 0.5$, $r = 1000$, $\phi_* = 0.001$. The broken line in Figure 12b gives the loop size distribution according to Hoeve's theory (see text).

the increasing number of loops makes the tail fraction decrease. At higher r ($\simeq 20$) the surface becomes more crowded and the tail fraction again increases. For higher volume fractions ($\phi_* = 10^{-2}$) a relatively high surface occupancy is already attained for $r = 5$, so that the maximum is not pronounced ($\chi = 0$) or disappears altogether ($\chi = 0.5$).

D. Train, Loop, and Tail Distribution. In the previous section we have considered the average values for the train, loop, and tail sizes. In this section we discuss the way in which the train, loop, and tail sizes are distributed around their averages. Figure 12a gives the fraction of trains of length s, $n_{tr}(s)/n_{tr}$, Figure 12b the analogous fraction $n_l(s)/n_l$ for loops, and Figure 12c $n_t(s)/n_t$ for trains. In parts d–f of Figure 12 the fraction of segments $sn_{tr}(s)/l_{tr}n_{tr}$ in trains of length s, the corresponding fraction $sn_l(s)/l_ln_l$ for loops, and $sn_t(s)/l_tn_t$ for tails are given. The data of Figure 12 apply to $r = 1000$, $\phi_* = 10^{-3}$, and $\chi = 0.5$. The average values for the train, loop, and tail sizes are $l_{tr} = 4.315$, $l_l = 7.531$, and $l_t = 89.001$.

Short trains are the most abundant, and the number of trains decreases strongly with increasing train length (Figure 12a). The train segment distribution curve displays a maximum at $s \approx 4$, which is close to the average train length 4.3 (Figure 12d). Trains longer than 25 segments hardly contribute to the number of trains or to the number of segments in trains.

The loop size distribution (Figure 12b) is, for small loop sizes, steeper than the train size distribution, so that no maximum occurs in the loop segment distribution (Figure 12e) and only a faint shoulder is observed. However, for larger loop sizes the decay is much slower; long loops (s

= 50 or more) contribute significantly to the number of loop segments.

Also in the tail size distribution (Figure 12c) the smaller tails occur most frequently, and the initial decay is slow enough to give a maximum in the segment distribution curve (Figure 12f) around $s = 80$ (close to the average tail length 89). For long tail sizes, the number of tails decays very slowly with increasing s, and tails up to 800 segments still give a significant contribution to the number of tail segments. Note the truncation of the tail segment distribution curve just below $s = 1000$; obviously tail sizes above the chain length are impossible. Parts c and f of Figure 12 show that the tail size distribution is very broad.

E. Comparison with the Hoeve Theory. Hoeve[7,10] has given approximate expressions for the average train and loop size, and for the train and loop size distribution. His expressions apply to long chains in which the loops have Gaussian distribution and where end effects are negligible. Although our theory does not use these approximations, it is instructive to compare a few results. As discussed in section III.B, both models predict an exponential loop segment concentration profile and a layer thickness which is linearly dependent on the square root of chain length.

Hoeve's results are expressed in terms of a parameter λ defined such that λr is the difference in free energy (in units of kT) between an adsorbed chain and a chain in the bulk solution. The parameter λ, which has negative value for adsorbing chains, occurs in the final equations through the Truesdell functions[27] $f_{-1/2}(\lambda)$ and $f_{3/2}(\lambda)$, where $f_m(\lambda) = \sum_{n=1}^{\infty} n^m e^{n\lambda}$. For λ approaching zero, these functions approach the limits $f_{-1/2} = (\pi/-\lambda)^{1/2}$ and $f_{-3/2} = 2.612$. According to Hoeve's theory, the average train and loop sizes are given by

$$l_{tr}^{(H)} = 1 + 1/cf_{-3/2}(\lambda) \tag{48}$$

$$l_l^{(H)} = f_{-1/2}(\lambda)/f_{3/2}(\lambda) \tag{49}$$

where c is a flexibility parameter which for flexible chains in a five-choice cubic lattice is equal to $16/(75\pi^{1/2}) = 0.120$.[18] In a recent paper,[28] Hoeve gives for an exact model (in which the Gaussian approximation for loops is avoided) a value $c = 0.102$ for the same system.

From eq 48 and 49 it follows that for long chains ($\lambda \to 0$) $l_{tr}^{(H)}$ is nearly insensitive to λ, in contradistinction to $l_l^{(H)}$. Since $-\lambda$ decreases with increasing chain length and solution concentration, the loops become longer when r and ϕ_s increase, while the train size is practically independent of r and ϕ_s. Our theory predicts the same trends (see Figure 9), showing qualitative agreement between both models.

The absolute numbers for the loop and train size are more difficult to compare. Since the precise value to be used for λ is unknown, a direct comparison between l_l and $l_l^{(H)}$ is impossible to make. For the train size we can use its limit for long chains. For $\lambda \to 0$, $l_{tr}^{(H)}$ depends only on the flexibility parameter c (thus on the lattice type). For the two c values given above, $l_{tr}^{(H)}$ equals 4.2 and 4.8, respectively. We find $l_{tr} = 4.3$ for a hexagonal lattice and 7.5 for a six-choice cubic lattice. Considering the different approaches in both models, the agreement is satisfactory.

Another comparison is possible for the train size and loop size distribution. In this case we do not consider the average train and loop size, but the spread around the average values. By rearranging Hoeve's equations[7,10] we obtain for the train size distribution

$$\frac{n_{tr}(s)}{n_{tr}} = \frac{1}{l_{tr}}\left(\frac{l_{tr} - 1}{l_{tr}}\right)^{s-1} \tag{50}$$

showing that $n_{tr}(s)$ can be given as a function of s and its average value $\langle s \rangle = l_{tr}$ only. For the loop size distribution Hoeve obtains

$$n_l(s)/n_l = s^{-3/2}e^{\lambda s}/f_{-3/2}(\lambda) \tag{51}$$

where λ follows from l_l through eq 49.

It turns out that, if we use the value obtained with our model for l_{tr}, eq 50 gives results for $r \gtrsim 100$ that are numerically identical with the train size distribution as calculated by our method, both for a hexagonal and a simple cubic lattice. This surprising result, which is apparently independent of the lattice type, is probably related to the fact that a train may be considered as a two-dimensional random walk in which each step has the same weighting factor p_1. Factors like the surface occupancy, the adsorption energy, the segment–solvent interaction, and the lattice type obviously affect the average train length l_{tr}, but not the distribution of chain lengths around this average value.

For the loop size distribution we have calculated λ, using (49), from our value for l_l, and substituted this in (51); the results are plotted in Figure 12b (dashed line). The agreement is less good than that for trains, but the differences are still not very great. Complete agreement cannot be expected since in the derivation of (51) even the small loops are supposed to have Gaussian distribution. Moreover, in our model each step in or toward layer i is weighted with a weighting factor p_i which is not the same for different layers, in contradistinction to Hoeve's random walk treatment. Nevertheless, it is gratifying that similar results are obtained.

IV. Conclusions

We have obtained a detailed picture for the structure of the adsorbed layer for interacting polymers.

In the limit of extremely dilute solutions, our theory reduces to earlier models for isolated chains near an adsorbing surface. In this case, the conformation is very flat, at least if χ_s is not too low; most of the segments are in trains, loops are short, and tails are negligible.

Even for very small equilibrium concentrations the competition between the adsorbed molecules becomes so strong that only a small fraction of the segments can find a place on the surface and a substantial part has to be accommodated in loops and tails. As a consequence, the train size decreases, the loops become longer, and, most importantly, the length of the tails is considerable. Even in dilute solutions around 20% of the segments may be present in one or two dangling tails. The segment concentration in the outer regions of the adsorbed layer is largely due to these tails. Thus the tails determine to a large extent the average layer thickness and the interaction between polymer covered colloidal particles. It was found that the root-mean-square layer thickness is proportional to the square root of the chain length, also if tails are present.

In bulk polymer near a surface the tails become so long that they contain about two thirds of the segments belonging to adsorbed chains. Molecules in contact with the surface consist of three parts of roughly equal size: two long tails and a middle part in which very short trains and longer loops alternate. This type of conformation was also found by Roe,[12] not for bulk polymer, but for isolated molecules with an adsorption energy which is close to the critical value. In both cases the chain conformation is only determined by entropic factors.

In our model computations for chain lengths up to slightly more than 1000 segments are possible. One may wonder whether long tails occur also for longer chains. We cannot rule out the possibility that for infinite chain length

the (relative) contribution of tails is small, as assumed in previous theories. However, our results give no indications that for chains up to, e.g., 10^4 segments tails may be neglected. This conclusion is based on the nearly linear relationship between tail size and chain length, and on the fact that the fraction of segments in tails hardly decreases with increasing molecular weight. Moreover, the similarity of our results for bulk polymer with those for isolated chains under conditions close to the critical adsorption energy suggests strongly that tails should also be taken into account for very long chains. Also the essentially linear relationship between the root-mean-square layer thickness due to tail segments and the square root of the chain length points in the same direction. Hence, we are led to believe that in all systems of practical importance tails do play an important role. This conclusion seems to be in agreement with recent experimental data.[13]

Appendix I. Accurate Calculation of the End Segment Probabilities for Adsorbed Chains

From eq 17 follows

$$\mathbf{p}_a(s) = \mathbf{p}(s) - \mathbf{p}_t(s) = \mathbf{w}\mathbf{p}(s-1) - \mathbf{w}_t\mathbf{p}_t(s-1) \quad \text{(A1)}$$

Since $\boldsymbol{w}_t$ differs from $\boldsymbol{w}$ only in that the elements of the first row of $\boldsymbol{w}_t$ are zero, the components of the vectors $\boldsymbol{w}\mathbf{p}(s-1)$ and $\boldsymbol{w}_t\mathbf{p}(s-1)$ are identical, except for $i = 1$:

$$\boldsymbol{w}\boldsymbol{p}(s-1) = \boldsymbol{w}_t\mathbf{p}(s-1) + p(1,s)\Delta_1 \quad \text{(A2)}$$

where Δ_1 is a column vector of which the first component is 1 and all the other components zero. Substituting this into (A1), we have

$$\mathbf{p}_a(s) = \boldsymbol{w}_t\mathbf{p}_a(s-1) + p(1,s)\Delta_1 \quad \text{(A3)}$$

The value for $p(1,s)$ is taken from the array $\boldsymbol{p}$ and the first vector $\mathbf{p}_a(1)$ equals $p_1\Delta_1$, with components:

$$p_a(i,1) = p_1\delta_{1,i} \quad \text{(A4)}$$

From eq A3 and A4 the elements $p_a(i,s)$ can be calculated with much greater accuracy than from eq 17.

References and Notes

(1) Scheutjens, J. M. H. M.; Fleer, G. J. *J. Chem. Phys.* **1979**, *83*, 1619.
(2) DiMarzio, E. A. *J. Chem. Phys.* **1965**, *42*, 2101.
(3) DiMarzio, E. A.; Rubin, R. J. *J. Chem. Phys.* **1971**, *55*, 4318.
(4) Roe, R. J. *J. Chem. Phys.* **1974**, *60*, 4192.
(5) Helfand, E. *J. Chem. Phys.* **1975**, *63*, 2192.
(6) Helfand, E. *Macromolecules*, **1976**, *9*, 307.
(7) Hoeve, C. A. J. *J. Chem. Phys.* **1966**, *44*, 1505; *J. Polym. Sci.* **1970**, *C30*, 361; **1971**, *C34*, 1.
(8) Silberberg, A. *J. Chem. Phys.* **1968**, *48*, 2835.
(9) Silberberg, A. *J. Phys. Chem.* **1962**, *66*, 1872; *J. Chem. Phys.* **1967**, *46*, 1105.
(10) DiMarzio, E. A.; McCrackin, F. L. *J. Chem. Phys.* **1965**, *43*, 539; Hoeve, C. A. J.; DiMarzio, E. A.; Peyser, P. *J. Chem. Phys.* **1965**, *42*, 2558.
(11) Rubin, R. J. *J. Chem. Phys.* **1965**, *43*, 2392; *J. Res. Natl. Bur. Stand., Sect. B* **1966**, *No. 70*, 237.
(12) Roe, R. J. *J. Chem. Phys.* **1965**, *43*, 1591; **1966**, *44*, 4264.
(13) Lyklema, J.; Vliet, T. van. *Faraday Discuss. Chem. Soc.* **1978**, *65*, 25.
(14) Flory, P. J. "Principles of Polymer Chemistry"; Cornell University Press: Ithaca, N. Y., 1953.
(15) See, e.g., Everett, D. H. *Trans. Faraday Soc.* **1964**, *60*, 1803.
(16) Ono, S.; Kondo, S. in "Handbuch der Physik"; Flügge, S., Ed.; Springer: Berlin, 1960; Vol. 10, p 134.
(17) Lane, J. E. *Aust. J. Chem.* **1968**, *21*, 827.
(18) Hoeve, C. A. J. *J. Chem. Phys.* **1965**, *43*, 3007.
(19) Helfand, E.; Tagami, Y. *J. Chem. Phys.* **1972**, *56*, 3592.
(20) Levine, S.; Thomlinson, M. M.; Robinson, K. *Discuss. Faraday Soc.* **1975**, *65*, 202.
(21) Yamakawa, T. "Modern Theory of Polymer Solutions"; Harper & Row: New York, 1971; p 124.
(22) Killmann, E.; Eisenlauer, J.; Korn, M. *J. Polym. Sci.: Polym. Symp.* **1977**, *61*, 413.
(23) Smith, L. E.; Stromberg, R. R. Conference on Polymers at the Liquid–Liquid Interface, Loughborough, 1975.
(24) Killmann, E.; Wiegand, H.-G. *Makromol. Chem.* **1970**, *132*, 239.
(25) Killmann, E.; Kuzenko, M. V. *Angew. Makromol. Chem.* **1974**, *35*, 39.
(26) Cohen Stuart, M. A.; Scheutjens, J. M. H. M.; Fleer, G. J. *J. Polym. Sci.* In press.
(27) Truesdell, C. *Ann. Math.* **1945**, *46*, 144.
(28) Hoeve, C. A. J. *J. Polym. Sci.; Polym. Symp.* **1977**, *61*, 389.

Chapter 4

SOME IMPLICATIONS OF RECENT POLYMER ADSORPTION THEORY

J.M.H.M. Scheutjens and G.J. Fleer

Laboratory for Physical and Colloid Chemistry, Agricultural University, De Dreijen 6, 6703 BC Wageningen, The Netherlands

SUMMARY

The basic ideas of a recently developed polymer adsorption theory are briefly outlined and some implications of this theory are discussed.

For chains in a theta-solvent which are not too short, the amount adsorbed from dilute solutions, as expressed by the total surface coverage θ, increases linearly with the logarithm of the chain length r, whereas in a better solvent the chain length dependence is smaller. Both these trends are in excellent quantitative agreement with recent experimental results for homodisperse polymers. Also bound fraction data, previously published, agree very well with the theoretical predictions.

The total surface coverage, θ, is the sum of an excess contribution θ_{ex} and a depletion part θ_d. Whereas θ_{ex} increases approximately linearly with log r, θ_d is proportional to $\sqrt{r}$. For infinitely long chains or in highly concentrated systems, θ_d is larger than θ_{ex}, so that under these conditions a square root dependence of the adsorbed amount on chain length is expected.

Results are given for the concentration dependence of θ, over a very wide range of concentrations, from extremely dilute solutions where the adsorbed molecules behave as isolated chains ($\phi_* \to 0$) up to bulk polymer ($\phi_* \to 1$). From such θ-ϕ_* plots a transition concentration ϕ_*^c can be derived, which characterises the transition from the linear initial part of the isotherm to the pseudoplateau region. ϕ_*^c is a quantitative measure for the high affinity character of the adsorption.

Tails, which have been neglected in previous theories, play an important role for all chain lengths encountered in practice. The results for the r.m.s. layer thickness, and the contribution of tails to it, are presented as a function of

[Reprinted with permission from "The Effect of Polymers on Dispersion Properties", Tadros, T.F., Ed., Academic Press, London, (1982).]

the solution concentration and compared with recent experimental data.

Finally, some consequences of the theory for the adsorption of a mixture of polymer chains having different chain lengths are pointed out. In dilute solutions long chains adsorb preferentially over short ones, whereas in concentrated systems the reverse is true. A simple equation is derived which allows the computation of the relative contribution of each component in the adsorbed layer from the total adsorbed amount and the solution concentration.

INTRODUCTION

During the last few decades, considerable progress has been made in the development of theories for polymer adsorption at an interface. The first theories (Silberberg, 1962, 1967; DiMarzio, 1965; DiMarzio and McCrackin, 1965; Hoeve *et al.*, 1965; Rubin, 1965, 1966; Motomura and Matuura, 1969; Motomura *et al.*, 1971a, 1971b) treat the relatively simple case of an isolated chain on a surface. Although these theories provide a suitable starting point for more realistic models, they have little relevance for practical systems since the interaction between the segments is neglected. Even in very dilute solutions the segment volume fraction near the interface is usually of the order of 0.5, so that the interaction between the segments plays a very important role. Later theories (Hoeve, 1966, 1970, 1971; Silberberg, 1968; Roe, 1974) account for this segment-solvent interaction but use serious approximations in order to obtain manageable equations: Hoeve (1966, 1970, 1971) and Silberberg (1968) neglect the occurrence of tails and make an *a priori* assumption about the segment concentration profile in the loop region (Silberberg (1968) uses a step function and Hoeve (1966, 1970, 1971) an exponential decay), whereas Roe (1974) assumes that the spatial distribution of each of the chain segments, whether in the middle part of the chain or near one of the chain ends, is the same. In effect, as we have shown before (Scheutjens and Fleer, 1980), this latter assumption is more or less equivalent to the neglect of tails.

Recently, we have presented a new theory which avoids these approximations (Scheutjens and Fleer, 1979, 1980). In our model all the possible chain conformations, including those encompassing tails, are completely taken into account with their proper statistical weight, and no *a priori* assumptions are made about the segment concentration profile. Chain conformations are described as step-weighted random walks in a lattice. The lattice is divided into layers parallel to the surface which are numbered i = 1,2,3 ... , where i = 1 corr-

esponds to the layer adjacent to the surface. The weighting factor p_i for each step in or into layer i depends on the solvent volume fraction ϕ_i^o in this layer and on that in the two neighbouring layers, ϕ_{i-1}^o and ϕ_{i+1}^o. For all layers except the first we may write:

$$(i \geq 2) \qquad p_i = \frac{\phi_i^o}{\phi_*^o} \frac{e^{-2\chi<\phi_i^o>}}{e^{-2\chi\phi_*^o}} \tag{1}$$

where ϕ_*^o is the solvent volume fraction in the equilibrium solution, χ is the well-known Flory-Huggins polymer-solvent interaction parameter, and $<\phi_i^o>$ is the weighted average of the volume fractions in the layers i-1, i and i+1:

$$<\phi_i^o> = \lambda_1\phi_{i-1}^o + \lambda_o\phi_i^o + \lambda_1\phi_{i+1}^o \tag{2}$$

The parameters λ_o and λ_1 are determined by the geometry of the lattice: λ_o is the fraction of neighbouring sites which are in the same layer, and λ_1 that for each of the two neighbouring layers ($2\lambda_1 + \lambda_o = 1$). In a hexagonal lattice $\lambda_o = \frac{1}{2}$ and $\lambda_1 = \frac{1}{4}$.

The two factors in equation (1) are both due to the interaction of segments with each other and with the solvent. The entropy factor ϕ_i^o/ϕ_*^o accounts for the lower probability of a step in or towards layer i as compared to a step in the bulk solution if $\phi_i^o<\phi_*^o$. The factor $e^{-2\chi<\phi_i^o>}/e^{-2\chi\phi_*^o}$ originates from the segment-solvent interaction: in a solvent which is poorer than athermal ($\chi>0$) the repulsion between segments and solvent molecules favours a step into a layer with low ϕ_i^o.

These two factors play also a role in the surface layer (i = 1) but, in addition, the adsorption energy difference between a segment and a solvent molecule (expressed by the adsorption energy parameter χ_s) makes a step in or towards this layer more probable:

$$(i = 1) \qquad p_1 = \frac{\phi_1^o}{\phi_*^o} \frac{e^{-2\chi<\phi_1^o>}}{e^{-2\chi\phi_*^o}} e^{\chi_s - \lambda_1\chi} \tag{3}$$

With the help of equations (1) and (3) the statistical weight for any chain conformation can be easily evaluated: the conformation probability for a chain of r segments is proportional to the product of r weighting factors $p_i, p_j, p_k \ldots$. In this product the weighting factor p_i for layer i occurs as

many times as the number of segments that the given conformation has in layer i.

In this way the statistical weight for any chain conformation can be calculated for a given solvent concentration profile ϕ_1^o, ϕ_2^o, ϕ_3^o ... , ϕ_*^o. Using a matrix formalism first introduced by Rubin and DiMarzio (Rubin, 1965; DiMarzio and Rubin, 1971), these statistical weights can be used to calculate the overall segment concentration profile ϕ_1, ϕ_2, ϕ_3 ... , ϕ_* in the adsorbed layer (which is the result of the contribution of all possible chain conformations). With the boundary constraints $\phi_i^o+\phi_i = 1$ (for any i), a set of implicit equations in all ϕ_i^o's is thus obtained which can be solved numerically. A derivation of equations (1) and (3) from maximizing the partition function and a full account of the matrix formalism and the numerical evaluation has been given before (Scheutjens and Fleer, 1979, 1980). In this paper we show a few typical results and discuss some implications which are relevant from a theoretical as well as an experimental point of view. All the numerical results in this paper are for a hexagonal lattice ($\lambda_o = 0.5$).

MOLAR MASS DEPENDENCE OF THE ADSORBED AMOUNT AND THE BOUND FRACTION

All the available theories for the adsorption of the interacting polymer chains predict that the adsorbed amount is an increasing function of the chain length, at least for not too long chains. In poor solvents this dependence is stronger than in good solvents. Although in this respect there is qualitative agreement between the various theories, the quantitative aspects are fairly different. Silberberg's theory (1968) predicts that at very high chain length the amount adsorbed from a Θ-solvent levels off, whereas Hoeve's theory (1966) gives a square root dependence on molar mass, even for very long chains. According to our theory (Scheutjens and Fleer, 1979), for a Θ-solvent, the adsorbed amount increases linearly with log r, at least for not too short chains. Until recently, there was hardly accurate experimental data on well-defined systems for which a comparison with theory was feasible. Fortunately, in the last few years two experimental studies (Vander Linden and Van Leemput, 1978a, 1978b; Kawaguchi *et al.*, 1980) became available which enable such a comparison. They deal with the adsorption of nearly homodisperse polystyrene (PS) samples from a Θ-solvent (cyclohexane at 35°C) onto silica, covering a very wide range of relative molar mass (M = 600 up to 2 x 10^6, corresponding to r = 6 - 20,000). Figure 1 gives the experimental points (filled symbols) for the adsorbed amount Γ (in $mg \cdot m^{-2}$) as a function of

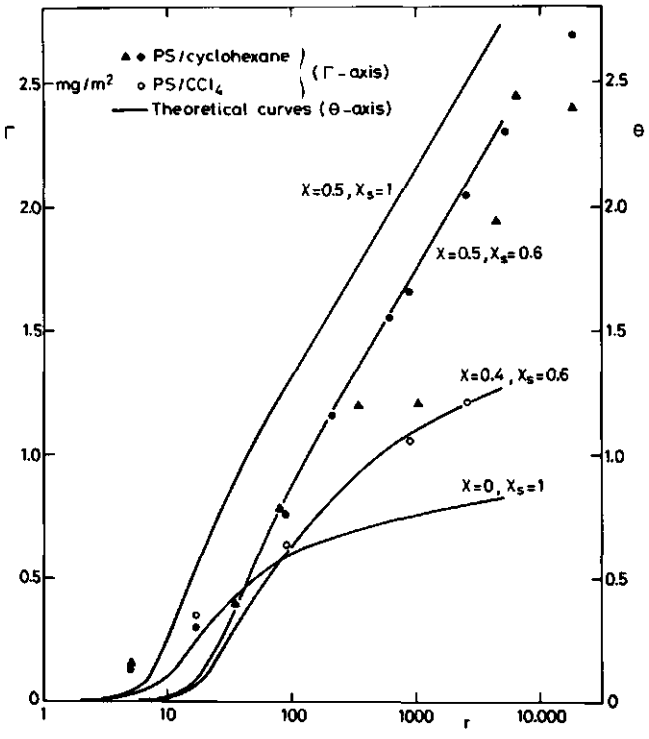

Fig. 1. Comparison of experimental data for the adsorbed amount Γ (in mg·m^{-2}, left hand scale) as a function of chain length with our theoretical predictions for the total surface coverage θ (in numbers of equivalent monolayers, right hand scale). The experimental points are for nearly homodisperse polystyrene from cyclohexane (θ-solvent) and carbon tetrachloride on silica as reported by Vander Linden and Van Leemput (1978a) (circles), and Kawaguchi et al. *(1980) (triangles), at a solution concentration around 1 g·dm^{-3}. The theoretical curves are for a hexagonal lattice (λ_o = 0.5), ϕ_* = 10^{-3} and for χ and χ_s values as indicated.*

log r. The curves in this figure represent theoretical results according to our theory, adopting the specified values of χ_s and assuming that a theoretical segment corresponds to a monomer unit; the amount of polymer is expressed as the total surface coverage θ (i.e., the number of equivalent monolayers, or $\theta = \Gamma/\Gamma^{mon}$). The open circles in Fig. 1 are experimental adsorption results (Vander Linden and Van Leemput, 1978a) from $CC\ell_4$ at 35°C. For this system χ = 0.396 at

25°C (Bristow and Watson, 1958). We used 0.4 at 35°C.

Qualitatively, the agreement between the results of Vander Linden and Van Leemput (1978a) and our theory is excellent. The data of Kawaguchi *et al.* (1980) show more scatter, but still the trend is the same. The Γ - log r dependency for $\chi = 0.5$ is strongly corroborated by these experiments. Quantitative agreement between theory and experiment would be obtained if the monolayer capacity of polystyrene on silica would be 1 $mg \cdot m^{-2}$, if the adsorption energy parameter χ_s would be 0.6 (both for cyclohexane and CCl_4), and if one monomer unit of PS would correspond to one theoretical segment in the lattice. Although Vander Linden and Van Leemput assumed a monolayer capacity of 0.52 $mg \cdot m^{-2}$, a value of 1 $mg \cdot m^{-2}$ agrees very well with calculations from molecular models. The same value for χ_s in both solvents would be fortuitous, since the energy associated with the exchange of one segment of PS with one solvent molecule depends, in general, on the solvent used. As to the third point, one would expect that one theoretical segment would comprise more than one monomer unit. Despite these uncertainties and the incomplete agreement for very short chains in Fig.1, the overall agreement between theory and experiment is gratifying. Moreover, a different

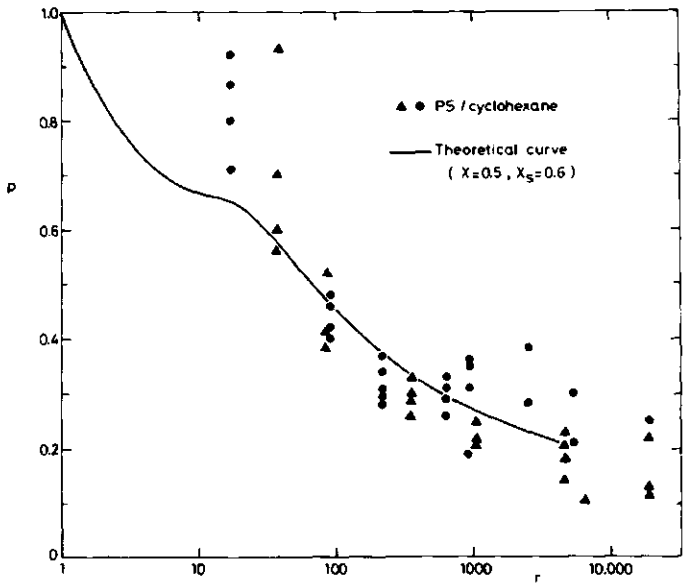

Fig.2. Comparison of experimental bound fraction data as a function of chain length with theoretical predictions. The experimental points are from the same references as in Fig.1, and the symbols have the same meaning.

choice for the number of monomer units per segment would not affect the linear dependency on log r; the theoretical curve could be easily made to fit the experimental points by simultaneously adjusting the value of χ_s.

Figure 2 gives experimental results for the bound fraction p, i.e., the fraction of segments in contact with the surface, as a function of log r, for PS from cyclohexane as measured by the same authors using IR-spectroscopy. Although considerable scatter is present in the experimental points, there is again a very good agreement between theory (solid curve) and experiment for $r \gtrsim 50$. For very short chains some discrepancy occurs, as in Fig.1. This might be related to a poorer degree of monodispersity for short chains (leading to some adsorption fractionation), to the presence of end groups in the polymer (that are relatively important in short chains), or to the heterogeneity of the silica surface (which would tend to increase the adsorption, especially at low adsorbed amounts).

Vander Linden and Van Leemput (1978a) also gave a few results for p as measured in CCl_4 as the solvent. We have not included these in Fig. 2, since these few data show more scatter than those for cyclohexane. Contrary to the predictions of all theories (assuming not too different χ_s-values), the bound fraction in this better solvent seems to be lower than in cyclohexane.

LIMITING BEHAVIOUR OF THE ADSORBED AMOUNT FOR VERY LONG CHAINS

As stated in the previous section, for long chains adsorbed from a θ-solvent the theories of Hoeve (1966, 1970, 1971) and Silberberg (1968) contradict each other as to the chain length dependence of Γ. Silberberg finds a plateau for Γ at high r ($\theta \approx 3.9$ monolayers for high χ_s and $r \gtrsim 10^4$), whereas Hoeve predicts that $\Gamma \sim \sqrt{r}$. It is interesting to note that for solvents only slightly better than θ-solvents, Hoeve's treatment also leads to a levelling-off for long chain lengths (e.g., for $\chi = 0.495$ Hoeve's theory gives $\theta \approx 4.4$ monolayers for high χ_s and $r \gtrsim 10^5$).

One might wonder whether there is any physical background from which the limiting behaviour of long chains can be predicted. From polymer solution theory it is known that, for infinitely long chains, θ-conditions lead to phase separation. It seems reasonable that this phase separation is promoted near a surface because the extra free energy gained upon adsorption increases the tendency of the polymer to accumulate near the surface; this would be the first step in the phase separation process. On this basis a limit for θ at χ =

0.5 is not to be expected. In a later publication, Silberberg (1972) discussed the possibility of multilayer formation around $\chi = 0.5$.

Due to computational problems, we cannot apply our theory to very long chains. As yet, calculations for $r \lesssim 5000$ have been made. Nevertheless, the results obtained so far suggest that an extrapolation to longer chains is possible.

According to our definition, the adsorbed amount θ is made up from two contributions, the excess adsorbed amount θ_{ex} and the depletion adsorbed amount θ_d (see Fig. 2 of Scheutjens and Fleer (1979) and the inset of Fig. 3). For not too long chains in dilute solutions, θ_d is negligible with respect to θ_{ex}. The excess adsorbed amount increases strongly at low ϕ_*, passes through a maximum at intermediate ϕ_*, and decreases at still higher ϕ_* until at $\phi_* = 1$ (bulk polymer) $\theta_{ex} = 0$. We find the following approximate equations for the chain length dependence of θ_{ex} and θ_d:

$$\theta_{ex} \approx (1 - \phi_*)\ (a + b \log r) \quad (\chi = 0.5) \tag{4}$$

$$\theta_d \approx \phi_*(0.64 + 0.562\ \sqrt{r}) \tag{5}$$

These equations are valid for not too short chains. The parameter b in equation (4) depends essentially only on χ, whereas a is a function of ϕ_* and χ_s. The numerical coefficients in equation (5) are nearly independent of ϕ_*, χ and χ_s. For $\phi_* \to 1$ (where $\theta = \theta_d$), the adsorbed amount for long chains is proportional to $\sqrt{r}$. This suggests that under these conditions polymers also have a Gaussian distribution near the interface, in accordance with published data (Benoit, 1976; De Santis and Zachmann, 1977) which show that chains in bulk polymer behave as undisturbed Gaussian coils. This is to be expected since under these conditions only entropy factors play a role; for $\phi_* \to 1$ the adsorption energy parameter χ_s loses its significance.

The fact that equations (4) and (5) are very accurately obeyed, in the whole accessible range of chain lengths above $r \approx 50$, suggests that an extrapolation to longer chain lengths is allowed. Results for $\phi_* = 10^{-3}$ and $\phi_* = 1$ are given in Fig. 3. As discussed above, $\theta_{ex} = 0$ and $\theta = \theta_d$ for $\phi_* = 1$ (note that a θ-$\sqrt{r}$ dependence becomes an exponential curve if θ is plotted as a function of log r). For $\phi_* = 10^{-3}$, θ_{ex} is the dominating term up to $r \approx 10^5$, while for longer chains the relative weight of θ_d is increasing rapidly. For $\phi_* > 10^{-3}$, θ_d is already important for shorter chains; for lower volume fractions the curve for θ_d shifts to higher chain lengths.

If this extrapolation procedure is valid, the conclusion

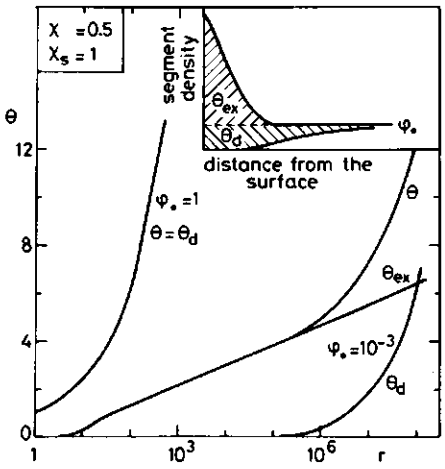

Fig. 3. The total surface coverage θ and its components θ_{ex} and θ_d as a function of chain length, for $\phi_* = 1$ (bulk polymer) and $\phi_* = 10^{-3}$. Hexagonal lattice ($\lambda_o = 0.5$), $\chi_s = 1$, $\chi = 0.5$. The inset gives a qualitative picture of the segment concentration profile in the adsorbed layer. The hatched areas correspond to the excess surface coverage θ_{ex} and the depletion surface coverage θ_d, respectively.

is that for very high chain lengths there is no limit for the adsorbed amount. The higher the polymer solution concentration, the more θ will tend to become proportional to $\sqrt{r}$. Note, however, that the apparent agreement with Hoeve's model is not real, since his theory applies only to dilute solutions, in which the contribution of θ_d is negligible.

CONCENTRATION DEPENDENCE OF THE ADSORBED AMOUNT

Experimental adsorption isotherms for homodisperse polymers are usually of the so-called high-affinity type, i.e., for very low concentrations ($\phi_* < 10^{-6}$) the isotherm coincides with the ordinate axis whereas the adsorbed amount levels off rapidly once the concentration in solution becomes measurable. At very high concentrations experimental determination of the adsorbed amount is very difficult, since then the relative difference between the initial and the equilibrium concentration is small. Therefore, the accessible experimental concentration range is rather limited.

Our theory is, in principle, applicable to the whole con-

entration range, from extremely dilute solutions (where the adsorbed molecules behave as isolated chains) up to $\phi_* = 1$ (bulk polymer). It is illustrative to show some typical results over a very wide range of concentrations. Figure 4 gives

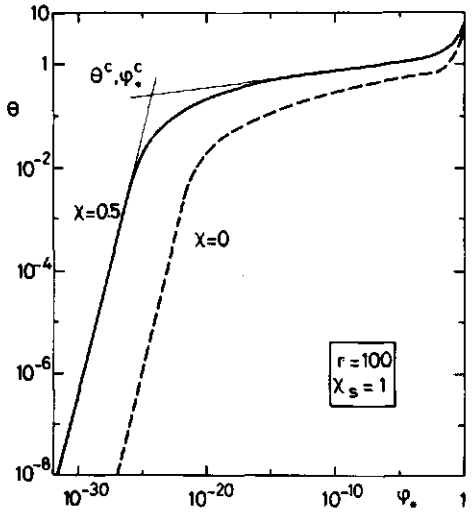

Fig. 4. Adsorption isotherms over a very wide range of concentrations, for chains of 100 segments from an athermal and a θ-solvent. Both the total surface coverage θ and the solution volume fraction ϕ_* are plotted on a logarithmic scale. The values θ^c and ϕ_*^c at the intersection of the two straight lines are a measure for the transition between the isolated chain region (left below) and the region where the surface becomes covered to a considerable extent. Hexagonal lattice ($\lambda_o = 0.5$), $\chi_s = 1$.

the total surface coverage θ as a function of ϕ_* with both quantities plotted on a logarithmic scale, for a relatively short polymer (r = 100) adsorbing from an athermal and from a θ-solvent.

In extremely dilute solutions the curves are linear with a slope equal to 1 : in that region θ is just proportional to ϕ_*. This is the domain where theories for isolated chains (Silberberg, 1962, 1967; DiMarzio, 1965; DiMarzio and McCrackin, 1965; Hoeve *et al.*, 1965; Rubin, 1965, 1966; Roe, 1965; Motomura and Matuura, 1969; Motomura *et al.*, 1971a, 1971b) are valid, but which is not interesting from an experimental point of view. As soon as the surface becomes covered to an extent of more than a few per cent, excluded volume effects start to play a role and the increase in θ with increasing ϕ_*

becomes much smaller. In the intermediate region the curves are again approximately linear with an increase in θ of a few per cent per decade of ϕ_* (for $r = 100$, $\chi_s = 1$ and $\chi = 0.5$, θ is proportional to $\phi_*^{0.03}$ in the range $10^{-15} \lesssim \phi_* \lesssim 10^{-5}$; for longer chains or higher χ_s this range is much wider towards more dilute solutions). At still higher volume fractions θ gradually increases more strongly with ϕ_* until at $\phi_* = 1$ the value given by equation (5) is reached. For volume fractions higher than a few tenths the adsorbed amount is found to increase linearly with ϕ_*.

In the region applying to isolated chains the molecules lie rather flat, with p values typically around 0.8. The difference between the curves for $\chi = 0$ and $\chi = 0.5$, in this region, is due to the term $\lambda_1\chi$ in the exponent of equation (3). If the chains would lie completely flat, the segmental weighting factors p_1 (with respect to the bulk of the solution) for all segments of adsorbed chains are the same, so that $\theta = \phi_1 \sim \phi_* p_1^r$. In extremely dilute solutions $\phi_*^o \approx 1$, $\phi_1^o \approx 1$ and $\langle\phi_1^o\rangle \approx 1-\lambda_1$. Therefore, $p_1 \approx e^{\chi_s+\lambda_1\chi}$ and $\theta \sim \phi_* e^{r(\chi_s+\lambda_1\chi)}$, showing clearly that the differences in Fig. 5 between $\chi = 0$ and $\chi = 0.5$ are due to a difference in the "effective" adsorption energy parameter $\chi_s + \lambda_1\chi$.

An indication for the transition region between isolated adsorbed molecules and chains that are competing for adsorption sites is obtained by extrapolating the two linear regions in Fig. 4 and determining the coordinates ϕ_*^c and θ^c of the intersection point. The magnitudes of θ^c and ϕ_*^c have some relevance for experimentalists. For $\theta > \theta^c$, $\phi_* > \phi_*^c$ the adsorbed amount depends only slightly on the solution concentration. If one tries to measure desorption, one has to dilute the solution to concentrations of the order of ϕ_*^c, which corresponds to an extremely low concentration even for relatively short chains. This is probably the reason for the widely held belief that polymer adsorption is an irreversible phenomenon: only if the solution is diluted to an extremely large extent, appreciable desorption may be expected. This analysis shows that such an experimental finding is not contradictory to the criterium for a real thermodynamic equilibrium; it merely demonstrates that in dilute polymer solutions the adsorption equilibrium is situated nearly completely on the side of the surface, on account of the high number of segments per chain. Some consequences of this idea for the adsorption of heterodisperse polymers have been pointed out in a previous paper (Cohen Stuart *et al.*, 1980).

In Fig. 5 the dependence of ϕ_*^c on chain length is shown for two values of χ and χ_s. The value of ϕ_*^c decreases exponentially with increasing chain length and depends strongly on

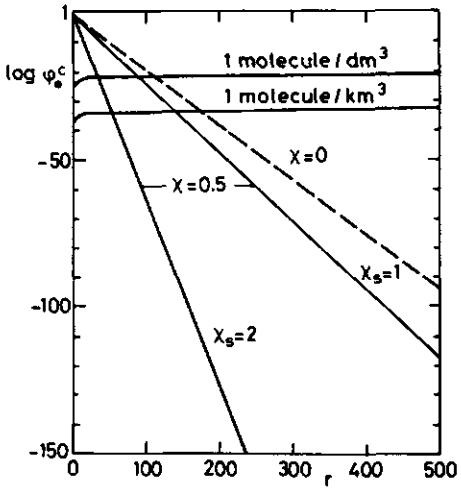

Fig. 5. Dependence of the transition concentration ϕ_*^c on the chain length, for χ_s = 1, χ = 0 and 0.5, and for χ_s = 2, χ = 0.5. The nearly horizontal curves correspond to the low concentrations 1 molecule/dm^3 and 1 molecule/km^3 . Hexagonal lattice (λ_o = 0.5).

χ_s. In order to emphasize how low the values of ϕ_*^c usually are, the concentrations corresponding to "1 molecule per m^3" and "1 molecule per km^3" are indicated in Fig. 5 as (on this scale) nearly horizontal lines.

LAYER THICKNESS AND TAILS

In a previous contribution (Scheutjens and Fleer, 1980) we have reported some results for the root-mean-square layer thickness t as a function of chain length, for a constant solution concentration. The most conspicuous feature turned out to be the linear dependence of t on the square root of chain length, even if a considerable fraction of the segments are present in long dangling tails. This square root dependence has also been found experimentally several times, most recently by Takahashi *et al.* (1980), for a very wide range of chain lengths of polystyrene adsorbed from cyclohexane onto chrome. In this section we consider the layer thickness as a function of the solution concentration and the contribution of tails and loops to this thickness.

The root-mean-square (r.m.s.) layer thicknesses due to tail segments t_t, due to loop segments t_l, and due to all segments of adsorbed chains (including trains) t, are calcul-

ated from the following equations:

$$t_t^2 = \frac{\sum_i i^2 \phi_i^t}{\sum_i \phi_i^t} \qquad t_\ell^2 = \frac{\sum_i i^2 \phi_i^\ell}{\sum_i \phi_i^\ell} \qquad t^2 = \frac{\sum_i i^2 \phi_i^a}{\sum_i \phi_i^a} \tag{6}$$

where ϕ_i^t and ϕ_i^ℓ are the contributions of tails and loops, to the segment volume fraction ϕ_i^a due to adsorbed chains in layer i. According to these definitions, the thicknesses are expressed with the length of a step in the lattice as the unit.

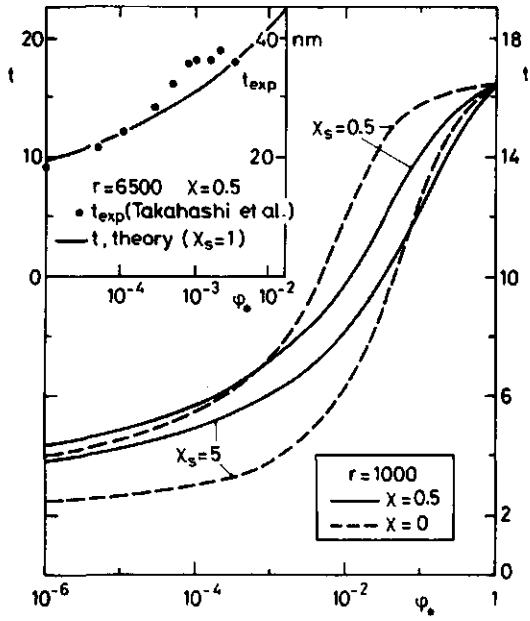

Fig.6. The root-mean-square layer thickness t as a function of the solution concentration, for chains of 1000 segments with χ_s = 0.5 and 5, and χ = 0 (dashed curves) and 0.5 (solid curves). Hexagonal lattice (λ_o = 0.5). In the inset a comparison is given between experimental and theoretical layer thicknesses as a function of concentration for chains of 6500 segments. The values for t_{exp} (in nm, right hand scale) were reported by Takahashi et al., *(1980), and apply to polystyrene from cyclohexane (Θ-solvent) on chrome, the theoretical curve for t (in units of a lattice step length, left hand scale) was computed for a hexagonal lattice (λ_o = 0.5), with χ_s = 1 and χ = 0.5.*

Figure 6 shows the overall r.m.s. layer thickness t as a function of ϕ_* (on a logarithmic scale) for a low ($\chi_s = 0.5$) and high ($\chi_s = 5$) value of the adsorption energy parameter and for $\chi = 0$ and 0.5. In dilute solutions t is rather low (approaching $t \tilde{\propto} 1$ for $\phi_* \tilde{\propto} \phi_*^c$); it increases rather steeply in the region $10^{-3} \lesssim \phi_* \lesssim 10^{-1}$, whereas above $\phi_* = 0.1$ it flattens to attain finally the value for bulk polymer which is independent of χ and χ_s.

A very interesting aspect of Fig. 6 is that the layer thickness depends only weakly on χ or χ_s, despite the fact that the adsorbed amount is a rather strongly varying function of these parameters. Moreover, the trends in t and θ do not run in parallel. With a change of χ_s from 0.5 to 5 the adsorbed amount increases (for $\phi_* = 10^{-3}$ and $\chi = 0.5$ by a factor of 2, for $\phi_* = 10^{-3}$ and $\chi = 0$ by a factor of 5), but the layer thickness *decreases*. Apparently the increasing number of segments of adsorbed chains is accommodated in the layers close to the surface, without extending the adsorbed layer. Similarly, for $\chi_s = 0.5$ the adsorbed amount from a Θ-solvent is higher than from an athermal solvent by a factor of about 6 (around $\phi_* = 10^{-3}$), yet the layer thickness is hardly different from the two solvents. Only for $\chi_s = 5$, at not too high concentrations, the trends in t and θ coincide.

Very little experimental data are available for the concentration dependence of t. Only in a very recent article (Takahashi, 1980) did we find some measurements over a wide concentration range. The inset of Fig. 6 shows that there is quite reasonable agreement between theory and experiment as to the general trend, for polystyrene consisting of 6500 monomer units. The theoretical curve for this chain length was obtained by extrapolating the calculated results for lower r according to the square root dependence mentioned above. It is very difficult to compare the absolute values of the measured thickness with the calculated ones: quantitative agreement would exist if the thickness of a lattice layer would correspond to 2 nm, but we have, as yet, no solid arguments for such a conversion factor. Apart from that, there is considerable doubt whether the ellipsometric r.m.s. thickness, obtained by assuming an exponential segment distribution, gives the correct results if tails are present, in which case the concentration profile is more diffuse.

In Fig. 7 we have plotted the r.m.s. thickness due to tails and loops separately. The general trends are the same as in Fig. 6, with t_t considerably higher than t_ℓ, as expected. A theory neglecting tails underestimates the layer thickness seriously. Comparison of the effect of tails on the layer thickness with the fraction of segments in tails (see inset in Fig. 7) demonstrates that in all cases, even if ν_t is

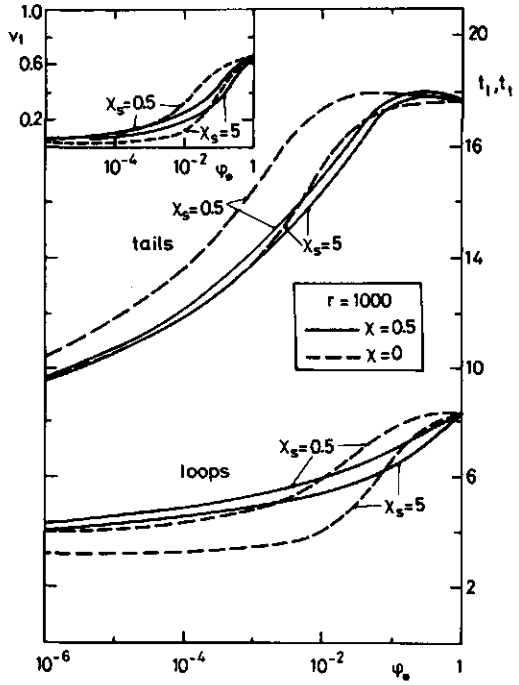

Fig. 7. The contribution of loops (t_l) and tails (t_t) to the overall layer thickness t, for the same conditions as in Fig. 6 (where t was given). The inset shows the variation in the fraction ν_t of segments of adsorbed chains that belong to tails, as a function of ϕ_*.

low, tails give the dominant contribution to the extension of an adsorbed layer. Moreover, also here the thickness is rather invariant for a change in χ or χ_s, whereas the *fraction* (ν_t) and even more strongly the *number* of tail segments ($\nu_t\theta$) are considerably influenced by these parameters.

PREFERENTIAL ADSORPTION

It is generally accepted that high molar mass polymer adsorbs preferentially over lower molar mass material. Several studies have given experimental evidence for such a preference (Felter *et al.*, 1969; Felter and Ray, 1970; Howard and Woods, 1972; Sadakne and White, 1973; Vander Linden and Van Leemput, 1978b; Cohen Stuart *et al.*, 1980). In a paper about the effect of polydispersity on polymer adsorption (Cohen Stuart *et al.*, 1980) we did already present a few calculations based upon the theory of Roe (1974). In a recent article, Roe (1980)

gave some more results of this type.

Here we shall discuss the physical background and the underlying principles in a semiquantitative way. The equilibrium for polymers adsorbing from solution is governed by the balance between energy and entropy. The energy terms arise from the adsorption energy ($\chi_s kT$ per adsorbing segment) and the mixing energy (as expressed by the χ-parameter). For the sake of simplicity, we will neglect this latter term (i.e., we consider an athermal solvent). Including the mixing energy in the equations below is straightforward, but not necessary for the illustration of the principal points.

Entropy contributions stem from the entropy of mixing and from the loss of conformational entropy upon adsorption. The entropy of mixing is just the configurational part of the Flory-Huggins expression. If ϕ_1 is the polymer volume fraction in the first layer, this term can be approximated as $k\ell n(\phi_1/\phi_*)$ per molecule, regardless of the chain length, because only the possible positions of the centre of gravity of the chain have to be considered. Therefore, the entropy of mixing is relatively important for short chains. For solvent molecules desorbing from the surface the entropy of mixing is $-k\ \ell n\ (\phi_1^o/\phi_*^o)$ per molecule.

For polymer chains adsorbing at the interface, the entropy loss of the first segment is accounted for in the entropy of mixing. All the other chain segments attaching to the surface lose a fraction λ_1 of their possible positions. Hence the ratio between the number of possible positions in the free and adsorbed state is $1/(1-\lambda_1)$, corresponding to a conformational entropy loss of $-k \ln (1-\lambda_1)$ per adsorbed segment.

If a monomer is exchanged against a solvent molecule on the surface, the resulting free energy change per monomer can be written as:

$$\Delta f_m/kT = -\chi_s + \ln(\phi_{1,m}/\phi_{*,m}) - \ln\ (\phi_1^o/\phi_*^o) \qquad (7)$$

where the second and third terms represent the entropy of mixing of the monomer and the solvent molecule, respectively. Putting $\Delta f_m = 0$ leads immediately to a Langmuir type equation.

For the adsorption of a polymer molecule of which pr segments are in contact with the surface, the analogous free energy change per chain is

$$\Delta f_p/kT = -\ pr\chi_s\ -\ (pr-1)\ \ln\ (1-\lambda_1) + \ln(\phi_{1,p}/\phi_{*,p}) - pr \ln\ (\phi_1^o/\phi_*^o) \qquad (8)$$

Note that the factor pr occurs in the entropy of mixing for the solvent, but not in that for the polymer. From this equation it follows directly that long polymer chains will only adsorb if χ_s exceeds a critical value χ_{sc}. In dilute solutions of weakly adsorbing polymer the last term of equation (8) vanishes, the ratio $\phi_{1,p}/\phi_{*,p}$ is of order unity, and Δf_p can only become zero if the adsorption energy compensates the loss of conformational entropy. This occurs if $\chi_s > \chi_{sc} = -\ell n(1-\lambda_1)$. At equilibrium, $\phi_{1,p}/\phi_{*,p} = 1/(1-\lambda_1)$ at $\chi = \chi_{sc}$, in agreement with previous results (DiMarzio and Rubin, 1971).

For a discussion of preferential adsorption we have to consider the adsorption free energy difference between a polymer chain and pr monomers. From equations (7) and (8) we obtain:

$$(\Delta f_p - pr\Delta f_m)/kT = -(pr-1)\ \ln\ (1-\lambda_1)$$

$$+\ \ln(\phi_{1,p}/\phi_{*,p})\ -\ pr\ \ln\ (\phi_{1,m}/\phi_{*,m}) \qquad (9)$$

Since the adsorption energy is the same for a monomer and one polymer segment, only the conformational and mixing entropies determine whether the polymer adsorbs preferentially. Preferential adsorption of polymer occurs when at equilibrium ($\Delta f_p = pr\Delta f_m$) $\phi_{1,p}/\phi_{*,p} > \phi_{1,m}/\phi_{*,m}$. We will now analyse this situation.

The first term of equation (9) represents the conformational entropy and is always positive. For $\chi_s > \chi_{sc}$, both $\phi_{1,p}/\phi_{*,p}$ and $\phi_{1,m}/\phi_{*,m}$ are greater than unity, so that the second term is positive and the last one negative. The configurational entropy loss for the monomers (last term) is larger than the conformational entropy loss for the polymer (first term) because $\phi_{1,m}/\phi_{*,m} > e^{\chi_{sc}} = 1/(1-\lambda_1)$. The sum of the first and last terms of equation (9), which is negative, has to be compensated by a positive second term. As this term does not contain the large factor pr, $\phi_{1,p}/\phi_{*,p} \gg \phi_{1,m}/\phi_{*,m}$. Hence, in dilute solutions polymers adsorb preferentially with respect to shorter ones, the reason being that the configurational (or translational) entropy loss of the short chains is the largest contribution to the free energy.

With increasing bulk concentrations of monomer and polymer, the ratios $\phi_{1,p}/\phi_{*,p}$ and $\phi_{1,m}/\phi_{*,m}$ both decrease. Then the first term in equation (9) becomes relatively important, even though p decreases slightly. This term has to be compensated by the sum of the second and last terms. As the logarithm in the last term is multiplied by pr, $\phi_{1,p}/\phi_{*,p}$ must decrease much more strongly than $\phi_{1,m}/\phi_{*,m}$, indicating a less

pronounced preference for polymer. As soon as $\phi_{1,m}/\phi_{*,m}$ becomes smaller than $1/(1-\lambda_1)$, the second term becomes even negative ($\phi_{1,p} < \phi_{*,p}$). Hence, in concentrated solutions monomers adsorb preferentially with respect to polymers, and short chains with respect to longer ones. In this concentration region the conformational entropy dominates the free energy, disfavouring the adsorption of long chains.

At some intermediate concentration both species must have the same affinity for the surface. If we take the same bulk solution concentration for polymer and monomer ($\phi_{*,m} = \phi_{*,p} = \frac{1}{2}\phi_*$) we find from (9) that, at the transition point where $\phi_{1,m} = \phi_{1,p}$, the ratio $\phi_{1,p}/\frac{1}{2}\phi_*$ equals $1/(1-\lambda_1) = e^{\chi^{sc}}$. As $\phi_{1,p} + \phi_{1,m}$ is only slightly below 1 (for not too low χ_s) we conclude that the transition point is situated around $\phi_* \approx 0.7$.

A more quantitative relation between the adsorbed amounts θ_a and θ_b of two polymers **a** and **b**, adsorbing from a solution with concentrations $\phi_{*,a}$ and $\phi_{*,b}$, can be found in the following way. As a simple model, we consider the mixed adsorbate layer as a region where the average weighting factor per segment is $\bar{p}$ times as high as in the bulk of the solution. Obviously, $\bar{p}$ is an average over the layers close to the surface of the factors p_i as given in equations (1) and (3). It depends on the solvent profile in the adsorbed layer which is determined by the parameters χ and χ_s and on the total solution concentration $\phi_* = \phi_{*,a} + \phi_{*,b}$, but is independent of the individual volume fractions $\phi_{*,a}$ and $\phi_{*,b}$. The ratio $\theta_a/\phi_{*,a}$ is proportional to $\bar{p}^{r_a}$ so that

$$\theta_a = A\phi_{*,a}\bar{p}^{r_a} \qquad \theta_b = A\phi_{*,b}\bar{p}^{r_b} \tag{10}$$

where A is a proportionality constant. A mathematical proof by means of the matrix formalism shows that equation (10) is rigorously valid provided that r_a and r_b are high enough (see Appendix I). By elimination of $\bar{p}$ from the two equations above we find a relation between $\theta_a/\phi_{*,a}$ and $\theta_b/\phi_{*,b}$,

$$\frac{\theta_a}{\phi_{*,a}} = \frac{\theta_b}{\phi_{*,b}} \left(\frac{\theta_b}{A\phi_{*,b}}\right)^{r_a/r_b - 1} \tag{11}$$

Experimentally, one usually measures the total adsorbed amount Γ which is proportional to the total surface coverage $\theta = \theta_a + \theta_b$. The contribution of component **a** to the total adsorbed amount can be found by substituting $\theta_b = \theta - \theta_a$ so that an implicit equation in θ_a is obtained. We tested this equation for previously published data (Cohen Stuart *et al.*, 1980) based upon the theory of multicomponent systems by Roe (1974). (Our own theory can also be extended to more than two

components, but as yet we have not made computations). Figure 8 shows the relative contribution θ_a/θ of component **a** as a function of the chain length ratio r_a/r_b, both for r_b = 100

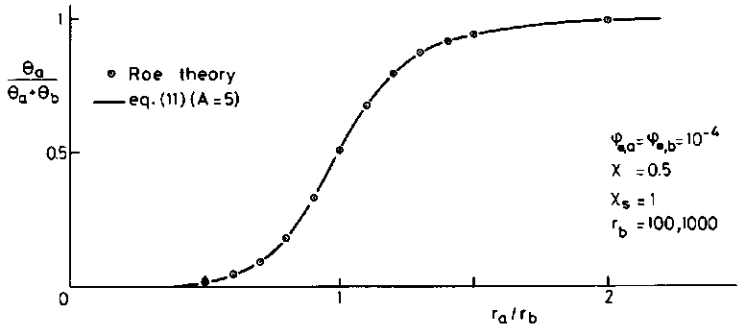

*Fig. 8. The fractionation effect occurring upon adsorption of a mixture of two polymer chains **a** and **b**, with different chain lengths r_a and r_b. The figure gives the fraction θ_a/θ of component **a** in the adsorbed layer as a function of the chain length ratio r_a/r_b, at an equal volume fraction (10^{-4}) in the solution for both components. The points were calculated with the theory of Roe (1974), the solid line with our equation (11) using A = 5. In both theories the values for θ_a/θ as a function of r_a/r_b are independent of r_b. Hexagonal lattice (λ_o = 0.5), χ_s = 1, χ = 0.5.*

and r_b = 1000, at an equal solution concentration for each polymer. For r_b = 100, the total surface coverage θ varied from 1.151 monolayers at r_a = 50 to 1.338 at r_a = 200; for r_b = 1000 the values for θ ranged from 1.636 at r_a = 500 to 1.725 at r_a = 2000. Although the total surface coverage depends on chain length, the relative contribution of each component to θ turns out to be independent of this parameter: one single curve applies to both values of r_b. The points in Fig. 8 were computed using Roe's theory, the solid line was calculated from θ according to equation (11) after substituting $\theta_b = \theta - \theta_a$, using A = 5. The results are rather insensitive to the value taken for the adjustable parameter A: variation of A in the range 4-6 hardly affects the results.

From the excellent agreement between the points and the solid line in Fig. 8 we may conclude that equation (11) gives a very good description of the adsorption fractionation. It allows the evaluation of the contribution of each component in the mixture if the total adsorbed amount is known. We note that equations (10) and (11) apply to the total surface coverage $\theta = \theta_{ex} + \theta_d$. In the comparison with Roe's theory (Fig. 8) only θ_{ex} could be used since θ_d (and θ) cannot be obtained

from this model. For dilute solutions and not too low θ, the differences between θ_{ex} and θ are small but for low θ_a or θ_b (left and right in Fig. 8) θ_d is not completely negligible with respect to θ. For relatively high ϕ_*, equation (11) can only be applied if the contribution of θ_d is taken into account.

Equation (11) has one other interesting consequence. Consider a system at low ϕ_* where $r_b/r_a > 2$, so that the adsorbed layer consists mainly of long chains (component **b**). If one adds to this system some of the short chain component **a**, $\theta_b/\phi_{*,b}$ will remain essentially constant. Then also $\theta_a/\phi_{*,a}$ is constant, or $\theta_a \sim \phi_{*,a}$, as for isolated chains (see Figure 4). Thus the minor component on the surface behaves as isolated chain "islands" in the "sea" of long chains, exhibiting low affinity for the surface.

Concluding this section on preferential adsorption, we observe that a clear picture is emerging as to the physical background of this phenomenon, with long chains predominantly on the surface at low and moderate solution concentrations, whereas in very concentrated solutions the short chains have a preference for the surface. In the first case, the driving force is the translational entropy of the short chains in solution, in the latter situation the conformational entropy loss for the long chains is the main factor. A simple formula (equation (11)) gives an accurate quantitative description of the relative adsorption in mixtures of not too short polymer chains.

APPENDIX I

According to the matrix formalism, the step-weighted random walk can be mathematically described as:

$$\underset{\sim}{p}_a(r) = \underset{\approx}{w}_a \underset{\sim}{p}_a(r-1) = \underset{\approx}{w}_a^{r-1} \underset{\sim}{p}_a(1) \qquad \text{(A1)}$$

The end segment probability vector $\underset{\sim}{p}_a(r)$ contains the unnormalized statistical weights for adsorbed chains (see equation (8) of Scheutjens and Fleer (1980)) and the operator $\underset{\approx}{w}_a$ is defined in equation (A3) of the same paper. For long chains (A1) can be written as

$$\underset{\sim}{p}_a(r) = \Lambda^{r-1} \underset{\sim}{p}_e \qquad \text{(A2)}$$

where $\underset{\sim}{p}_e$ is the eigenvector belonging to the largest eigenvalue Λ of $\underset{\approx}{w}_a$. The total surface coverage is found from a summation of $\underset{\sim}{p}_a(r)$ over all layers (Scheutjens and Fleer, 1979):

$$\theta = \phi_* \sum_i p_a(i,r) = \phi_* \Lambda^{r-1} \sum_i p_e(i) \qquad \text{(A3)}$$

This equation is identical to equation (10), with $\bar{p} = \Lambda$ and $A = \Lambda^{-1} \sum_i p_e(i)$.

REFERENCES

Benoit, H. (1976). *J. Macromol. Sci. B.* 12, 27-40.

Bristow, G.M. and Watson, W.F. (1958). *Trans. Farad. Soc.* 54, 1742-1747.

Cohen Stuart, M.A., Scheutjens, J.M.H.M. and Fleer, G.J. (1980). *J. Polym. Sci. Polym. Phys. Ed.* 18, 559-573.

De Santis, R. and Zachmann, H.G. (1977). *Colloid Polym. Sci.* 255, 729-734.

DiMarzio, E.A. (1965). *J. Chem. Phys.* 42, 2101-2106.

DiMarzio, E.A. and McCrackin, F.L. (1965). *J. Chem. Phys.* 43, 539-547.

DiMarzio, E.A. and Rubin, R.J. (1971). *J. Chem. Phys.* 55, 4318-4336.

Felter, R.E., Moyer, E.S. and Ray, L.M. (1969). *J. Polymer. Sci.* B7, 529-533.

Felter, R.E. and Ray, L.N. (1970). *J. Colloid Interface Sci.* 32, 349-360.

Hoeve, C.A.J., DiMarzio, E.A., and Peyser, P. (1965). *J. Chem. Phys.* 42, 2558-2563.

Hoeve, C.A.J. (1966). *J. Chem. Phys.* 44, 1505-1509.

Hoeve, C.A.J. (1970). *J. Polym. Sci.* C30, 361-367.

Hoeve, C.A.J. (1971). *J. Polym. Sci.* C34, 1-10.

Howard, G.J. and Woods, S.J. (1972), *J. Polym. Sci., A-2,* 10, 1023-1028.

Kawaguchi, M., Hayakawa, K., and Takahashi, A. (1980). *Polym J.* 12, 265-270.

Motomura, K., and Matuura, R. (1969). *J. Chem. Phys.* 50, 1281-1287.

Motomura, K., Sekita, K. and Matuura, R. (1971a). *Bull. Chem. Soc. Jpn.* 44, 1243-1248.

Motomura, K., Moroi, Y., and Matuura, R. (1971b). *Bull. Chem. Soc. Jpn.* 44, 1248-1252.

Roe, R.J. (1965). *J. Chem. Phys.* 43, 1591-1598.

Roe, R.J. (1966). *J. Chem. Phys.* 44, 4264-4272.

Roe, R.J. (1974). *J. Chem. Phys.* 60, 4192-4207.

Roe, R.J. (1980). *Polym. Sci. Techn.* 12B, B, 629-641.

Rubin, R.J. (1965). *J. Chem. Phys.* 43, 2392-2407.

Rubin, R.J. (1966). *J. Res. Natl. Bur. Stand.* B70, 237-247.

Sadakne, G.S., and White, J.L. (1973). *J. Appl. Polym. Sci.* 17, 453-469.
Scheutjens, J.M.H.M., and Fleer, G.J. (1979). *J. Phys. Chem.* 83, 1619-1635.
Scheutjens, J.M.H.M., and Fleer, G.J. (1980). *J. Phys. Chem.* 84, 178-190.
Silberberg, A. (1962). *J. Phys. Chem.* 66, 1872-1883.
Silberberg, A. (1967). *J. Chem. Phys.* 46, 1105-1114.
Silberberg, A. (1968). *J. Chem. Phys.* 48, 2835-2851.
Silberberg, A. (1972). *J. Colloid Interface Sci.* 38, 217-226.
Takahashi, A., Kawaguchi, M., Hirota, H., and Kato, T. (1980). *Macromolecules* 13, 884-889.
Vander Linden, C., and Van Leemput, R. (1978a). *J. Colloid Interface Sci.* 67, 48-62.
Vander Linden, C., and Van Leemput, R. (1978b). *J. Colloid Interface Sci.* 67, 63-69.

DISCUSSION

Killmann: We found a square root dependence of the ellipsometric thickness on molecular weight at the chromium - gold and platinum surfaces out of different solvents. The values of the thicknesses are lower with lower net adsorption energy. Have you an explanation from your theory?

Scheutjens and Fleer: Our results show that the root-mean-square thickness of adsorbed polymer increases linearly with the square root of the chain length, both for θ-solvents and for athermal solvents. The effect of the adsorption energy is, except for $\chi_s \lesssim 0.5$, rather small (see also our Fig. 6). However, in all cases studied as yet we find that the r.m.s. thickness increases with decreasing net adsorption energy, in contradistinction to your experimental results for the ellipsometric thickness. A possible reason for this discrepancy could be that the proportionality constant between the ellipsometric thickness, which is a function of the *excess* concentration profile, and the r.m.s. thickness, calculated from the segment density profile due to adsorbed chains (compare the difference between the excess coverage θ_{ex} and the total coverage θ), depends on the adsorption energy χ_s. We intend to check this conjecture in future work by including the ellipsometric thickness, which is easily computed from a given concentration profile, in our numerical results.

Silberberg: In defense of earlier theories I would like to point out that they are lattice theories much as your calculations are. In fact what was done in those earlier theories was

to approximate the surface layer by zones not however by a large number, as in your case, but by three zones. The layer of contacting segments, a layer defined by the loops and the bulk solution. The contribution moreover of tails was written into the equations but finally ignored for computational reasons. This made the results of intrinsic validity only in the case of extreme molecular weight, molecular weights much in excess of the ones used in your computations. Yet most of the features which you point out are (rather unsurprisingly) also predicted by the earlier work. Of course, it cannot be expected that the detailed effects of chain tails can be compared since these were not considered. I think the most important input of your beautiful work is the discussion of finite bulk concentrations. This was (again for reasons of computational convenience) ignored in earlier work, but the contribution of the unadsorbed polymer coils becomes very significant as soon as there is mean coil overlap in solution.

For practical separations by adsorption, kinetic effects are important. Some of the earliest results on polymer/surface interactions erroneously suggested that low molecular weight fractions are preferably adsorbed simply because over a limited period of contact the faster diffusing species gets there first.

Scheutjens and Fleer: It is definitely not our intention to blame those earlier theories that take into account the interaction between polymer molecules. We consider them still very useful, especially for their computational convenience. We only warn against extrapolation of results obtained with *isolated chain theories* to real systems where high concentrations at the surface occur. For instance, a very persistent but incorrect idea is that strong adsorption implies a flat conformation, even in the (semi)plateau of the adsorption isotherm. This idea is refuted not only by our theory, but also by earlier *many-chain theories*.

We agree that many of the features predicted by our theory are also found by previous theories for mutually interacting polymer chains. For many purposes those earlier theories are appropriate. However, for the calculation of the segment density profile and the layer thickness they break down if end effects are ignored.

Your statement that in the case of extremely high molecular weight the tails can be neglected is, for finite solution concentrations, not yet proven. Our computations indicate that tails are still very important for any chain length encountered in practice. Therefore, your point is only of theoretical interest: even if for extremely long chains tails

were to be negligible, this cannot be measured experimentally since such extreme molecular weights do not exist.

We agree with your comment on the kinetic effects of adsorption fractionation. A commercial fractionation method based on adsorption is hard to imagine. However, if one needs a small very homodisperse fraction of a particular polymer for experimental work, fractionation by adsorption might be worthwhile to consider. After equilibrium (≃ 24 hours?) the polymer in solution is free of high molecular weight species. Adsorbed polymer of high M may be desorbed by adding a suitable low molecular weight compound with a high affinity for the surface.

Cohen-Stuart: Foam fractionation (R. Lemlich (ed.) (1972). "Adsorptive Bubble Separation Techniques", Academic Press, New York.) is a technique where preferential adsorption at a gas/liquid interface is the fractionating mechanism. Since the gas/liquid interface is very mobile, exchange rates are in this case probably fast enough to establish the expected preferential adsorption of the larger molecules over the smaller ones.

5 INTERACTION BETWEEN TWO ADSORBED POLYMER LAYERS*

SUMMARY

The effect of adsorbing homopolymer on the interaction between two parallel surfaces is examined in some detail. The results are relevant for the stabilization and flocculation of colloids by adsorbed polymer. The free energy of interaction is derived directly from the partition function using a previously developed lattice model for adsorption of polymers from solution. Comparison with other theories shows partial agreement as well as remarkable discrepancies. Results are presented for a system in full equilibrium with a polymer solution of constant concentration and for a system with a constant amount of polymer between the surfaces. At full equilibrium the force between the surfaces is always attractive due to bridging polymer. With decreasing surface separation a part of the polymer molecules leaves the gap, an increasing fraction of the remaining polymer adsorbs on both surfaces simultaneously, and eventually a monolayer of polymer segments sticks the surfaces together. When the polymer is unable to leave the gap, a strong repulsion between the surfaces appears at small separations and the interaction free energy is mainly determined by the adsorbed amount of polymer, irrespective of chain length. With a large amount of polymer between the surfaces the force is always repulsive, except in a very poor solvent. At smaller surface coverages a minimum in the free energy of interaction develops as a function of surface separation. Recent experimental data confirm our prediction that bridging attraction can also occur in good solvents. As the adsorption of polymer increases with increasing chain length, high molecular weight polymer is a better stabilizer than low molecular weight polymer.

* Submitted for publication in Macromolecules
in coauthorship with G.J. Fleer

5.1 INTRODUCTION

Polymer adsorption is a very effective tool for controlling the stability of colloidal suspensions[1-3]. For instance, high molecular weight flocculants rapidly remove the last submicroscopic particles in one of the last stages of water treatment. In this case uncovered particles are caught by tails and loops extending from covered ones, so that polymer bridges are formed. The same mechanism is operating in particle separation by flotation[4,5]. Bridging can occur only when the adsorbed amount of polymer is below saturation. At high polymer concentrations all particles are fully covered and the dangling tails and loops form a steric barrier against flocculation. Steric stabilisation has important applications in paint industry and food technology. In all these phenomena, steric and/or bridging interactions constitute an important contribution, but in most cases it is not the only one. In addition, Van der Waals forces and electrostatic interactions may play a role.

A variety of polymers, including copolymers, polyelectrolytes, and proteins, are applied to obtain the desired effects. In most instances the compexity of these materials, usually commercial products, is such that even the trends cannot be predicted. For monodisperse homopolymers, however, a detailed picture becomes feasible. The interaction between two polymer layers of this type is the result of a subtle balance between entropic repulsion, free energy of mixing, and bridging attraction. To quantify this interaction the segment density distribution of the polymer between two approaching particles, especially in the overlap region, is required. It can be obtained from a suitable polymer adsorption theory. In such a theory several factors have to be taken into account: the interaction of segments and solvent molecules with the surface, that between segments and solvent in the concentrated surface region, and the loss of configurational entropy of the adsorbed polymer chains.

The first theories that incorporate all these effects to a reasonable approximation divide the adsorbed layer into a train layer in contact with the surface and an adjacent loop layer with a predetermined shape of the segment profile, for instance a step function[6] or an exponential decay[7]. For computational convenience the tail fraction was neglected in these theories.

A complete multilayer theory for adsorption of chain molecules from high solution concentrations was developed by Ash at al.[8] and also used for the

calculation of interaction forces between parallel plates[9]. Unfortunately, the numerical computations were limited to chains of only four segments per chain. Although currently for most computers a chain length of 10 segments seems tractable with this model, it will be long before the polymer range is reached. Therefore some modifications are necessary in order to obtain results for long chains.

A considerably simpler multilayer theory for all chain lengths was developed by Roe[10]. A crucial step in its derivation is the assumption that the ranking number of a segment in the chain is irrelevant for its spatial distribution. This boils down to density distributions for "loops" and "tails" that are of identical shape, which is more or less equivalent to the neglect of end effects. Therefore, a correct predition of the segment density beyond the loop region can not be expected when tails are present.

The self-consistent multilayer theory of Scheutjens and Fleer[11] is more accurate, because this simplifying assumption is avoided. This theory accounts fully for all possible polymer conformations, including those with tails. The generation of the extremely high number of different conformations was possible by adopting the elegant matrix procedure developed by DiMarzio and Rubin[12,13]. Results for almost the whole range of relevant molecular weights can be obtained with this theory. For short molecules the results of Ash et al. are recovered, whereas the densities in the train and loop region agree with the results of Roe. For longer chains, a substantial fraction of the segments are found in tails, which extend far into the solution.

The development of scaling analyses[14,15] might give additional information about adsorbed polymer layers. This technique was first introduced in polymer statistics by De Gennes[16] and employs the analogies between magnetic systems and polymers.

Monte Carlo approaches are still in the state of the single chain problem[17,18]. For a system of many competing polymer molecules, the introduction of a Flory-Huggins type of mixing energy seems promising for more realistic results[19].

The structure of an adsorbed polymer layer at finite solution concentrations is now well established[6,7,10,11,20-24] and quite different from the properties of single chains. Below, we give a summary of the most important results.

In dilute and semidilute solutions, the adsorbed amount depends only

very weakly on the concentration in the bulk solution, i.e., the adsorption isotherms are of the high affinity type with a nearly horizontal pseudoplateau. Adsorption from good solvents is low and hardly dependent on molecular weight. In poor solvents, the adsorbed amount increases with increasing chain length. The extension of the polymer layer depends on such parameters as the segmental adsorption energy, the solvent quality, the solution concentration, and the chain length, but it is found that, for a given adsorption energy and solvent quality, the layer thickness is a function of the adsorbed amount only. In other words, the layer thickness is the same for relatively short chains at high concentrations and for longer chains at (much) lower concentrations, provided the adsorbed amount is the same[22]. Similarly, for a given chain length and solution concentration, the layer thickness is rather insensitive to both adsorption energy and solvent quality. In this case the adsorbed amount increases with increasing adsorption energy or decreasing solvent quality, without affecting the extension of the adsorbed layer, because only the segment densities close to the surface change[22,23].

When the adsorbed amount is below the pseudoplateau value the polymer lies flat on the surface, forming long trains and short loops. Tails are absent in this case and the solution concentration is extremely low (below an experimentally detectable level). In the pseudoplateau region the fraction of occupied surface sites is essentially independent of the solution concentration and the molecular weight; its magnitude is determined by the adsorption energy and solvent quality. Already at semidilute concentrations the tails protude far into the solution[22,25,26], determining completely the layer thickness, whereas the loops remain rather small. The train size and the fraction of segments in trains decrease steadily with increasing bulk solution concentration.

For heterodisperse polymers many of the properties given above are different[27]. The reason is that the chains with the highest affinity for the surface (high molecular weight, high adsorption energy) will ultimately displace all other polymer from the surface. Thus, the composition of the adsorbed layer is a function of the available area and the total amount of polymer in the system. Therefore, in order to check theoretical predictions, it is essential to have experimental data for monodisperse polymers. Unfortunately, the availability of such polymer is very poor, and only very few experimental studies are amenable to comparison with theory.

The statistical mechanical treatment of the interaction between two particles covered with polymer was initially restricted to the case of a single chain between parallel plates[13,28,29]. The neglect of lateral interactions led to results which are of very limited validity for the many chain problem. Mackor and Van der Waals[30] introduced separate surface and bulk phases to overcome this problem. They studied the interaction due to terminally adsorbing rigid rods (dimers and tetramers) in equilibrium with a bulk solution and found a repulsive force. The application of self-consistent field theories has improved the models considerably[9]. Most of the results are obtained for grafted polymer, i.e., chains with one or both ends bound to the surface[31-36]. Unfortunately, in some cases incorrect free energy equations were used, mainly because these theories did not lead to the complete partition function.

Dolan and Edwards[34] obtained the excluded volume parameter which determines the self-consistent field strength, by comparing their free energy equation with the Flory-Huggins equation for the free energy of mixing[37]. They supposed that the free energy is only determined by the change in configurational entropy of the chains. As we will show in the theoretical section, their excluded volume parameter is too small. Apart from that, they neglect higher order terms which become dominant at very high segment densities.

Levine et al.[36] used a similar model as ours to calculate the force between two plates due to grafted polymer. For adsorbing polymer they found qualitatively the same trends as we find. They came to the correct conformational entropy, but missed the accompanying correction to the free energy equation of Dolan and Edwards.

For the important case of (non-anchored) homopolymers we must distinguish between full thermodynamic equilibrium, when the chains can leave the gap, and restricted equilibrium, when for instance during the Brownian collision of two particles the adsorbed polymer is trapped between them. In the latter case the individual segments might still adjust themselves to a local thermodynamic equilibrium, i.e., may adsorb or desorb, whereas the total amount of polymer in the gap remains constant. In such a restricted equilibrium, an exchange between trains, loops, tails, and bridges occurs within the requirement of minimum free energy of the (constant) amount of polymer and the (changing) amount of solvent in the gap, but the chemical potential of the chains in the gap is no longer the same as in the solution.

For adsorbing tetramers in full equilibrium, Ash and Findenegg[9] found attraction between the plates when all segments are of an adsorbing type. If some of the segments are non-adsorbing, repulsion is predicted.

De Gennes[38] elaborated an equation for the surface free energy from Cahn[39] to study the interaction due to adsorbed homopolymer. He arrived at the conclusion that the net force is **always attractive** when the polymer may leave the space between the plates. The chains will escape when the plates are approaching each other, so that the segment density in the gap will never increase. The attractive force originates from the bridging effect. When the polymer is not able to escape, the density between the plates will increase with decreasing plate distance and an extra repulsive force results. Using a mean field approximation De Gennes found a cancellation between volume repulsion and bridging attraction in good solvents. Applying scaling concepts, however, led to the conclusion that the net force is **always repulsive.**

Using the same (mean field) Cahn-De Gennes analysis, Klein and Pincus[40] found the interaction force in poor solvents to be attractive in a distance region comparable with the radius of gyration of the chain in solution, and repulsive at shorter plate separations. The attractive force occurs if the concentration between the plates passes the biphasic region of the bulk phase diagram. Experimental work by Klein[41,42] has shown a similar shape of the interaction curve for polystyrene adsorbed on mica sheets.

In this paper we apply our adsorption model[11,22] to compute the interaction force between parallel plates under different conditions. In the full equilibrium case we find **always attraction,** in agreement with other theories[9,38]. This result differs from that in an earlier paper by us[43], which contains a serious error[44]. At restricted equilibrium a **minimum in the free energy** is found at low solution concentrations in all solvents. This contradicts De Gennes' mean field result and even more his scaling approach for good solvents[38], but it is consistent with recent results of Klein and coworkers[45,46]. The attractive force is attributed to an increase of the entropy by bridging. We feel that the Cahn-De Gennes approach underestimates the restrictions imposed by the walls on the conformational entropy of the chains, at least in the one wall problem. In this analysis, even the sign of the force becomes mainly determined by the solution properties of the polymer.

At high concentrations we find always repulsion in good solvents. We

will also apply the theory of Roe[10] and show interaction curves obtained from this model.

5.2 THEORY

5.2.1 Model

In deriving the relevant equations, we follow roughly refs. (10) and (11). Consider a lattice between two parallel plates, see figure 5.1. Each lattice site has z neighbors, a fraction λ_0 of which is in the same layer and a fraction λ_1 in each of the adjacent layers. In a simple cubic lattice $z = 6$, $\lambda_0 = 4/6$, and $\lambda_1 = 1/6$. The lattice layers, being parallel to the surface, are numbered $i = 1,2,\ldots,M$ and have L lattice sites each. For the sake of generalization, we define a parameter λ_{i-j} such that $z\lambda_{i-j}$ gives the number of immediate neighbors that a site in layer i has in layer j. It is obvious that $\lambda_{i-j} = \lambda_0$ if $i = j$, $\lambda_{i-j} = \lambda_1$ if $i = j \pm 1$, and $\lambda_{i-j} = 0$ otherwise. For a site in layers 1 and M the total number of neighbors is $z\lambda_0 + z\lambda_1 = z(1-\lambda_1)$. More formally, we can write

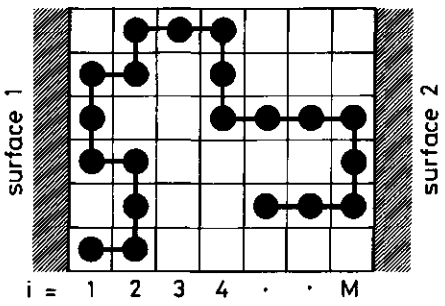

Figure 5.1. A chain of 20 segments in a lattice between two surfaces. This particular conformation has 4 segments adsorbed on surface 1 and 3 on surface 2. According to eqs. (5.12) and (5.17) the total number of chains in this conformation is
$LC\ \lambda_0^{9}\ \lambda_1^{10}\ P_1^{4}\ P_2^{5}\ P_3^{1}\ P_4^{3}\ P_5^{2}\ P_6^{2}\ P_7^{3}$.

$$\sum_{j=1}^{M} \lambda_{i-j} = 1 - \lambda_1\delta_{1,1} - \lambda_1\delta_{i,M} \qquad (1\leq i\leq M) \qquad (5.1)$$

where the Kronecker delta $\delta_{i,j}$ is 1 when $i = j$ and zero otherwise. A lattice site is occupied either by a solvent molecule or a polymer segment. A poly-

mer molecule is represented by a chain of connected segments numbered $s = 1,2,\ldots,r$. Segments and solvent molecules in the layers 1 and M are considered to be adsorbed.

The polymer chains and solvent molecules are distributed over the lattice in such a way that the free energy is at its minimum. Since in equilibrium the various conformations of the chains are not equally probable, we must at least distinguish all conformations which differ in energy. The energy of a particular conformation is determined by the number of its adsorbed segments and the interaction with neighboring segments and solvent molecules, which depends on the local concentration. As yet, it is not possible to account for all local fluctuations which may occur. Obviously, the most important fluctuations are expected in the direction normal to the plates. We neglect the variations within each lattice layer and use an average volume fraction ϕ_i of polymer and a fraction $\phi_i^o = 1 - \phi_i$ of solvent in layer i. Let the total number of segments and solvent molecules in layer i be n_i and n_i^o, respectively, and the total number of chains between the plates n:

$$\phi_i = n_i/L \quad ; \quad \phi_i^o = n_i^o/L \tag{5.2}$$

$$nr + \sum_{i=1}^{M} n_i^o = ML \tag{5.3}$$

Using eq. (5.2) for the local concentration in each layer is equivalent to the well-known mean field or Bragg-Williams approximation, i.e., the distribution within a layer is not affected by mutual interactions. Thus, for the energy of a conformation c it is sufficient to specify the number of segments $r_{i,c}$ that this conformation has in each of the lattice layers. Obviously,

$$\sum_c r_{i,c}\, n_c = n_i \tag{5.4}$$

$$\sum_{i=1}^{M} r_{i,c} = r \tag{5.5}$$

where n_c is the number of chains in conformation c.

5.2.1. Partition function

The grand partition function Ξ of the system in equilibrium with a bulk solution is given by a summation of canonical partition functions Q, weighted with the appropriate Boltzmann factors:

$$\Xi = \sum_{\text{all } n_c\text{'s}} Q(\{n_c\},V,A,T) \exp(\mu^o \Sigma_i n_i^o/kT) \exp(\mu \Sigma_c n_c/kT) \qquad (5.6)$$

where μ^o and μ are the chemical potentials of the solvent molecules and the polymer chains with respect to the reference state, respectively, V is the volume between the plates, A the area per plate, and T the temperature. We replace the sum by the maximum term, which is obtained by differentiating ln Ξ with respect to n_d:

$$\left[\frac{\partial \ln Q}{\partial n_d}\right]_{\{n_{c\neq d}\},V,A,T} + (\mu - r\mu^o)/kT = 0 \qquad (5.7)$$

The second term of eq. (5.7) follows from the substitution of $\Sigma n_i^o = ML - r\Sigma n_c$. The physical process corresponding to the differentiation of ln Ξ is transporting one chain from the bulk solution to the gap between the surfaces, placing $r_{i,d}$ segments in each layer i, while the same number of solvent molecules from each layer i is brought to the bulk solution.

For $Q(\{n_c\},V,A,T)$ we may write

$$Q = Q_+^o Q_+ [\Omega(\{n_c\})/\Omega_+] \exp(\chi_s n_1 + \chi_s n_M) \exp(-\chi \Sigma_i n_i^o \langle\phi_i\rangle) \qquad (5.8)$$

where Q_+ is the partition function of n polymer chains in pure polymer liquid and Q_+^o the same for n^o solvent molecules between two plates of area A each. The first exponential factor accounts for the surface interactions of n_1 and n_M adsorbed segments, displacing n_1 and n_M adsorbed solvent molecules. The adsorption energy of solvent on the plates is included in Q_+^o. The difference in adsorption energy is $-\chi_s$ kT per segment-solvent exchange. The second Boltzmann factor contains the energy of mixing the solvent and polymer chains in accordance with the concentration profile. The total number of segment-solvent contacts is $\Sigma n_i^o \langle\phi_i\rangle z$, where $\langle\phi_i\rangle$ is the fraction of contacts with segments for a solvent molecule in layer i. With the Bragg--Williams approximation within each layer, $\langle\phi_i\rangle$ is given by

$$\langle\phi_i\rangle = \lambda_1\phi_{i-1} + \lambda_0\phi_i + \lambda_1\phi_{i+1} = \sum_{j=1}^{M} \lambda_{i-j}\phi_j \qquad (5.9)$$

The Flory-Huggins parameter χ enters because for each solvent molecule which is transferred from pure solvent to a site surrounded by segments ($\langle\phi_i\rangle = 1$) the energy of mixing is χ kT.

The combinatory factor $\Omega(\{n_c\})$ in eq. (5.8) gives the number of ways of arranging n polymer molecules and n^o solvent molecules in accordance with the conformation profile $\{n_c\}$. It replaces Ω_+, the configurational part of Q_+, representing the number of ways of placing n polymer molecules on rn lattice sites in liquid polymer. Ω_+ has been derived by Flory[37]:

$$\Omega_+ = \left(\frac{z}{rn}\right)^{(r-1)n} \frac{(rn)!}{n!} \qquad (5.10)$$

The factorial (rn)! accounts for the number of ways of placing rn distinguishable monomers; z/(rn) is a correction factor for the r - 1 monomers of a chain that are linked to a previously placed monomer and, hence, have only z instead of rn a priori possible locations. Strictly speaking, z represents the effective number of bond directions for each additional segment and decreases somewhat with the number of bonds per chain if a correction is made for the exclusion of conformations with internal overlapping segments. The factorial n! corrects for the indistinguishability of the n chains. Applying a similar equation for the n^o solvent molecules (r = 1) would give $\Omega_+^o = 1$. Hence, a correction for Ω_+^o in eq. (5.8) is not necessary.

The combinatory factor Ω has been derived before[11]:

$$\Omega(\{n_c\}) = \left(\frac{z}{L}\right)^{(r-1)n} \prod_c \frac{\omega_c^{n_c}}{n_c!} \prod_i \frac{L!}{n_i^o!} \qquad (5.11)$$

There is a close analogy between eqs. (5.10) and (5.11). The M factorials L! give the number of ways of placing $r\Sigma n_c$ distinguishable monomers and Σn_i^o solvent molecules. The correction factor for the (r - 1) linking segments of a chain in conformation c is $\omega_c(z/L)^{r-1}$, where $\omega_c z^{r-1}$ is the number of arrangements within conformation c when the first segment (or the centre of gravity) of the chain is fixed. For instance, when step reversals are allowed, each bond parallel to the surface can point into $\lambda_0 z$ directions and each bond crossing to an adjacent layer has $\lambda_1 z$ choices. Then, if q is the number of bonds in conformation c that are parallel to the surface, we

have $(\lambda_0 z)^q(\lambda_1 z)^{r-1-q}$ arrangements within this conformation and ω_c is given by

$$\omega_c = \lambda_0^{\,q}\lambda_1^{\,r-1-q} \tag{5.12}$$

Note that many arrangements exist with the same segment distribution $\{r_{i,c}\}$, but with a different order of bond directions. According to the current definition, they are grouped into different conformations, because we define a conformation by a specific order of λ_0's and λ_1's.

5.2.3 Conformation probability

The equilibrium distribution of conformations is given by the value of $\{n_c\}$ corresponding to the maximum term in the grand partition function Ξ and is obtained from eq. (5.7) after substitution of eqs. (5.8), (5.10) and (5.11). The logarithm of $\Omega(\{n_c\})/\Omega_+$ can be approximated using Stirling's formula by

$$\ln(\Omega/\Omega_+) = ML \ln L - \sum_c n_c \ln(n_c/\omega_c) - \sum_i n_i^o \ln n_i^o - n \ln r - (r-1)n \ln L \tag{5.13}$$

While performing the diffentiation indicated in eq. (5.7) it must be realized that $n_i^o = L - \sum_c r_{i,c} n_c$ and $\Sigma\, n_i^o \langle\phi_i\rangle = \Sigma\, n_i \langle\phi_i^o\rangle$. The result is

$$\ln(n_d/L) = \ln C + \ln \omega_d + \sum_{i=1}^{M} r_{i,d} \ln P_i \tag{5.14}$$

where

$$\ln C = r - 1 - \ln r + (\mu - r\mu^o)/kT \tag{5.15}$$

and

$$\ln P_i = \chi_s(\delta_{1,i} + \delta_{M,i}) + \chi(\langle\phi_i\rangle - \langle\phi_i^o\rangle) + \ln \phi_i^o \tag{5.16}$$

From eq. (5.14) it follows that the number of chains in conformation c is

given by

$$n_c/L = C\,\omega_c \prod_{i=1}^{M} P_i^{r_{i,c}} \qquad (5.17)$$

Hence, n_c is proportional to a multiple product of weighting factors. According to eq. (5.12), the factor ω_c is a product of r - 1 **bond weighting factors** λ_0 (for each "parallel" bond) or λ_1 (for each "perpendicular" bond) and accounts for the relative number of arrangements in conformation c. Each segment in layer i contributes a **segmental weighting factor** P_i, which is a Boltzmann factor accounting for the free energy change when a solvent molecule in layer i is replaced by a single segment. This Boltzmann factor comprises a contribution for the adsorption energy $-\chi_s$ kT when i = 1 or i = M, a factor for the interaction energy between segments and solvent ($-\chi\langle\phi_i\rangle$ kT for removing the solvent molecule and $\chi\langle\phi_i^o\rangle$ kT for inserting the segment) and a factor for the local entropy - k ln ϕ_i^o of the solvent molecule (see eq. (5.16).

5.2.4 Normalization constant

The value for the normalization constant C is given in eq. (5.15) and can easily be found if μ and μ^o are constant. This is the case when the polymer between the plates is in **full equilibrium** with an infinitely large bulk solution of constant composition. The chemical potentials μ and μ^o have been derived by Flory[37]:

$$\mu/kT = 1 - \phi_* - r\phi_*^o + \ln \phi_* + r\chi\phi_*^o(1-\phi_*) \qquad (5.18)$$

$$\mu^o/kT = 1 - \phi_*^o - \phi_*/r + \ln \phi_*^o + \chi\phi_*(1-\phi_*^o) \qquad (5.19)$$

where ϕ_* and ϕ_*^o are the bulk solution volume fractions of polymer and solvent, respectively. Substitution of eqs. (5.18) and (5.19) into (5.15) gives

$$C = \frac{\phi_*}{rP_*^r} \qquad (5.20)$$

The quantity P_* is the segmental weighting factor in the bulk solution, and is given by $P_* = \phi_*^o \exp\{\chi(\phi_* - \phi_*^o)\}$ (compare eq. 5.16).

In practical situations, it may be impossible for the polymer chains to diffuse out of the gap when the plates are brought closer. It is useful to define a **restricted equilibrium** by the condition that the total amount of polymer between the plates is constant. Then the chemical potential of the polymer changes with varying plate separation. The normalization constant may now be found from the boundary condition $n = \sum_c n_c$. Summation of eq. (5.17) over all conformations gives

$$C = \frac{n}{LP(r)} = \frac{\theta^t}{rP(r)} \tag{5.21}$$

where $\theta^t = \Sigma\phi_i$ is the total amount of polymer between the plates, expressed in equivalent monolayers, and P(r) is the **chain weighting factor** :

$$P(r) = \sum_c \omega_c \prod_{i=1}^{M} P_i^{r_{i,c}} \tag{5.22}$$

In restricted equilibrium, the value for C as calculated from eq. (5.21) may be substituted in eq. (5.20) to obtain an implicit equation for the pseudo-equilibrium concentration ϕ_*, i.e., the bulk solution concentration that would be in full equilibrium with the polymer between the plates. Clearly, this pseudo-equilibrium concentration is now a function of the plate separation M.

5.2.5 Free energy of interaction

In full equilibrium the free energy of interaction between the plates is determined by the change in the surface free energy $\gamma.2A$[30]. From standard thermodynamics we have $2\gamma A = -kT \ln \Xi$. For our system it is more convenient to derive γ from $dF = 2\gamma a\delta L + \mu^o\Sigma\delta n_i^o + \mu\Sigma\delta n_c$, where $a = A/L$ is the area of a surface site, giving $(\delta F/\delta L)_{\{n_c\},M,T} = 2\gamma a + \mu^o M$ because $n_i^o = L - \sum_c r_{i,c} n_c$. Taking the derivative of $F = -kT \ln Q$ with respect to L gives, after substitution of eq. (5.13) into eq. (5.8) and using eq. (5.19) for μ^o:

$$2(\gamma - \gamma^o)a/kT = (1 - \frac{1}{r})\theta^{exc} + \sum_i \ln(\phi_i^o/\phi_*^o) + \chi \sum_i (\phi_i\langle\phi_i\rangle - \phi_*^2) \tag{5.23}$$

Here, γ^o is the surface tension of pure solvent and $\theta^{exc} = \Sigma(\phi_i - \phi_*)$ the

excess amount of polymer between the plates. Eq. (5.23) has been derived before[11] in terms of $\ln(P_i/P_*)$ for adsorption on a single surface, hence, without the factor 2.

The largest term of eq. (5.23) is the second, which is negative if $\phi_i > \phi_*$. Upon expansion of the logarithm, the linear term cancels exactly against the term θ^{exc}. Hence, for $\chi \leq 0$ the right-hand-side of eq. (5.23) is negative, as is to be expected for adsorbing polymer. For $\chi > 0$ the last term of eq. (5.23) gives a positive contribution to the quadratic term of the logarithmic expansion, but the same conclusion as to the sign of $\gamma - \gamma^o$ applies. (Note: for pure bulk polymer, $\phi_i \to 1$ and $\phi_i^o \to 0$, $\Sigma \ln (\phi_i^o/\phi_*^o)$ is **not** zero).

In restricted equilibrium the system is open with respect to solvent but not with respect to polymer. In this case the free energy of interaction is given by $F = -kT \ln \Psi$, where $\Psi(\{n_c\},\mu^o,V,A,T) = Q(\{n_c\},V,A,T) \exp(\mu^o \Sigma n_i^o/kT)$ is the semi-grand partition function.

The characteristic function F at constant amount of polymer Σn_c is found from the characteristic function $2\gamma A$ at constant chemical potential μ (eq. 5.23) via the relation $F = 2\gamma A + \mu\Sigma n_c = 2\gamma A + (\mu - r\mu^o)L\theta^t/r + \mu^o L\theta^t$. From eq. (5.15) we have $(\mu - r\mu^o)/kT = \ln C - (r - 1) + \ln r$, hence, substition of eqs. (5.21) and (5.23) gives

$$(F - F^o)/LkT = \frac{\theta^t}{r} \ln \frac{\theta^t}{P(r)} + \sum_i \ln \phi_i^o + \chi \sum_i \phi_i \langle\phi_i\rangle - \mu^o(M - \theta^t) \qquad (5.24)$$

Here, F^o is the free energy of pure solvent between the plates. The term $-\mu^o(M - \theta^t)$ is a very small **attractive** term accounting for the osmotic pressure of the solution outside the plates and will be neglected in the calculations in order to avoid the parameter ϕ_*. When necessary, it can be evaluated from eq. (5.19).

5.3 COMPARISON WITH OTHER THEORIES

5.3.1 Full equilibrium

Mackor and Van der Waals[30] formulated a theory for stiff rods that may be compared with the present model for dimers. Ash et al.[8,9] developed the

statistics for flexible oligomers (up to r = 4). They excluded conformations with bond angles less than 90°. Both theories account for the fact that one or two of the z contacts per segment are chemical bonds with other segments rather than physical contacts. Their equations reduce to ours for $z \to \infty$. In our model the above mentioned refinements are not taken into account. It has been shown that these extensions hardly affect the adsorbed amount of oligomers[11], whereas the complexity of the equations increases considerably.

The theory of Roe[10] has, in principle, only one more simplification than ours: it assumes that all segments have the same density distribution, independent of their ranking number in the chain. This assumption is valid for monomers, dimers, and two-dimensional chains parallel to the surface. It appears that Roe's equations are identical to ours for r = 1, $\lambda_0 = 1$, or M = 1, but not for r = 2. This discrepancy is due to the lack of inversion symmetry in Roe's model, and has been discussed before[11]. However, his equation for the surface tension (eq. (36) of ref. (10)) for one surface is identical to eq. (5.23) (without the factor 2) after some substitution and rearrangement. For instance, shift all terms of his eq. (29) to the left hand side and call the sum of these terms zero(i), which is zero. Then add $\Sigma\, \phi_i \text{zero}(i)$ to his eq. (36) for the surface tension and after some rearrangement our eq. (5.23) appears. In doing so, one must realize that $\Sigma\, \phi_i \langle\phi_i/\langle\phi_i\rangle\rangle = \Sigma\, \langle\phi_i\rangle\phi_i/\langle\phi_i\rangle = \Sigma\, \phi_i$. The numerical results for the surface tension depend on the segment density profile and are not the same for both theories.

A similar rearrangement is possible for Roe's eq. (36'), representing the surface tension of a multicomponent mixture. For such a system the last two terms of eq. (5.13) are to be replaced by $-\sum_x \{n^x \ln r^x - (r^x - 1)n^x \ln L\}$ and the interaction energy is $-\sum_x \chi_s^x (n_1^x + n_M^x) + \tfrac{1}{2} \sum_x \sum_y \chi^{xy} n_i^x \langle\phi_i^y\rangle$, where x and y are the component indices. The double summation over x and y extends over all components, including solvent. By definition $\chi^{xx} = 0$. Differentiation of $-kT \ln Q$ with respect to L and addition of $\mu^o M$ gives

$$2(\gamma - \gamma^o)a/kT = \sum_x (1 - \frac{1}{r^x})\theta^{x,\text{exc}} + \sum_i \ln (\phi_i^o/\phi_*^o)$$

$$+ \tfrac{1}{2} \sum_x \sum_y (\chi^{xo} + \chi^{yo} - \chi^{xy}) \sum_i (\phi_i^x \langle\phi_i^y\rangle - \phi_*^x \phi_*^y) \qquad (5.25)$$

Eq. (5.25) (without the factor 2) follows from Roe's eq. (36') after addi-

tion of $\sum_i \sum_x \phi_i^x (\Psi_i^o - \Psi_i^x)$ where Ψ_i^x is given by Roe's eq. (41). Hence, Roe's equations for the surface tension in terms of ϕ_i are identical to our equations, although the segment density profiles and, hence, the numerical values are different.

5.3.2 Restricted equilibrium

Many theories have been developed for interactions in restricted equilibrium. For a single chain between two plates (n = 1) eq. (5.24) reduces to $F - F^o + kT \ln (L/r) = - kT \ln P(r)$ which is the free energy equation used by DiMarzio and Rubin[13]. For a single chain ($\phi_i \to 0$ and $\phi_i^o \to 1$) and athermal conditions ($\chi = 0$) our weighting factors P_i are identical to their factors $\exp(\theta_i)$.

Meier[31] and Hesselink et al.[32,33] expressed the free energy of interaction for a system of nonadsorbing, terminally attached chains (or loops, tails) between two surfaces as a sum of a volume restriction term $- kT(n/L) \ln(\Sigma \omega_c)$ and an osmotic term $kT (\frac{1}{2} - \chi)\Sigma \phi_i^2$. We will show that this approximation is consistent with eq. (5.24) when all weighting factors P_i are equal, hence, at low concentrations of nonadsorbing chains ($\chi_s \approx 0$). For that case, we may approximate $(n/L) \ln P(r) \approx (n/L) \ln \Sigma\omega_c + \Sigma \phi_i \ln P_i$, see eq. (5.22).
Substitution into eq. (5.24) gives

$$(F - F^o)/LkT \approx \frac{\theta^t}{r} \ln \left(\frac{\theta^t}{\Sigma\omega_c}\right) - \sum_i \phi_i \ln P_i + \sum_i \ln \phi_i^o + \chi \sum_i \phi_i \langle\phi_i\rangle \qquad (5.26)$$

A Taylor expansion of $- \Sigma\phi_i \ln P_i \approx \chi\theta^t - \Sigma \{2\chi\phi_i^2 + \phi_i \ln(1 - \phi_i)\}$, retaining terms up to order ϕ_i^2, gives $\chi\theta^t + 2(\frac{1}{2} - \chi)\Sigma\phi_i^2$. Similarly, the last two terms of eq. (5.26) can be approximated by $- \theta^t - (\frac{1}{2} - \chi) \Sigma\phi_i^2$ when $\langle\phi_i\rangle$ is replaced by ϕ_i. Since θ^t is constant we may conclude that the sum of the last three terms represents Hesselink's osmotic term and that his approach is correct for low concentrations. A similar conclusion has been drawn by Gaylord[47].

For a comparison with the model of Dolan and Edwards we rewrite the last two terms of eq. (5.26) as $(\frac{1}{2}\chi - 1)\theta^t + \frac{1}{2} \Sigma\phi_i \ln P_i$. Addition of the second term $(- \Sigma\phi_i \ln P_i)$ and combination with the first term gives $(F - F^o)/kT \approx - n \ln(\sum_c \omega_c \prod_i P_i^{\frac{1}{2}r_{i,c}})$ + constants, which is essentially the free energy

function used by these authors[34]. Hence, also their free energy function is correct for low concentrations, but their weighting factor $P_i^{\frac{1}{2}} = \exp\{(\frac{1}{2} - \chi)\phi_i\}$ is just the square root of our weighting factor P_i, i.e., their distribution functions are wrong.

Levine et al.[36] derived nearly the same weighting factor as we found (using ϕ_i for $\langle\phi_i\rangle$, except for i = 1 and i = M). However, they adopted the analogous free energy function - kTn ln P(r), probably taken from DiMarzio and Rubin[13] or Dolan and Edwards[34], and thus missed the middle two terms of eq. (5.24) which are approximately zero in the latter theories. Note that $-\Sigma \ln \phi_i^o$ is infinite for pure polymer between the plates ($\phi_i^o \to 0$), whereas the free energy must remain finite (compare eq. 5.26 for $\phi_i^o \to 0$). In fact, for pure polymer $P_i = 0$ and therefore - n ln P(r) is infinite as well, compensating the sum $\Sigma \ln \phi_i^o$ in eq. (5.24). Since this compensation is absent in Levine's equation, his free energy function is qualitatively wrong.

It is interesting to observe that the term - (n/L) ln P(r) contains twice the osmotic term $(\frac{1}{2} - \chi) \Sigma \phi_i^2$ of Hesselink. The last two terms of eq. (5.24) constitute a correction for one of them. Neglecting this correction (as Levine did) overestimates the osmotic term by a factor of about 2.

In the term -(n/L) ln P(r) as used by Dolan and Edwards, P_i is replaced by $P_i^{\frac{1}{2}}$; hence the osmotic term occurs only once in their expression and correction terms are not necessary in their free energy function.

A detailed comparison with the theory of De Gennes[38] is more difficult because of the differences in the underlying assumptions. In this theory, the free energy is written as a sum of local energies which are a function of the local concentration and concentration gradient only. There are three contributions: i) a term for the adsorption energy, ii) a term for the energy of a homogeneous system of concentration ϕ_i, iii) a positive gradient term $\kappa (\partial\phi_i/\partial i)^2$ which accounts for the spatial variations of the concentration.

A crucial assumption is that κ does not depend on the chain length. It can be shown that the choice $\kappa = (24\ \phi_i)^{-1}$ as used by De Gennes is consistent with the theory of Helfand for infinite chain length, because in this theory each segment of a chain has the same spatial distribution[48]. In our notation this would apply when P(i,s) = P(i,s-1) for most of the segments (see eq. 5.29 below). However, we have shown that end effects are usually not negligible, except in special cases[22]. Clearly, end effects decrease

with decreasing plate distance, so we expect that the gradient method works best when $M < R_g$, where R_g is the radius of gyration of the polymer molecules in solution.

The most important result of De Gennes' method is that in full equilibrium the interaction force $\partial\gamma/\partial M$ follows the free energy of a homogeneous solution of concentration $\phi_{M/2}$ (the concentration midway the plates where the gradient is zero), and is always attractive. In restricted equilibrium, the interaction force follows nearly the osmotic pressure of a solution of concentration $\phi_{M/2}$, and hence, is always repulsive in good solvents. In bad solvents an attractive region occurs when $\phi_{M/2}$ passes the region of biphasic concentrations[40].

In section 5.6.3 we will compare the predictions of several theories mentioned above with the outcome of our model.

5.4. SEGMENT DENSITY DISTRIBUTIONS

The conformation profile $\{n_c\}$ is a function of the weighting factors P_i via eq. (5.14) and the weighting factors are a function of the segment density profile $\{\phi_i\} = \{1-\phi_i^o\}$ via eq. (5.16). In turn, the segment density profile is given by $\phi_i = \sum_c r_{i,c} n_c / L$, see eq. (5.4). Thus, the M weighting factors or volume fractions are implicitly given by M simultaneous equations. In a following section we will discuss these equations in more detail.

Alternatively, one may look for a conformation profile $\{n_c\}$ which gives a segment density profile $\{\phi_i\}$ that is consistent with eq. (5.17) for each conformation. In this way, the number of implicit equations is equal to the number of different conformations and hence, of order $3^{r-1} \approx 10^{r/2}$ per lattice layer. This method has been used by Mackor and Van der Waals[30] and Ash et al.[8], who reduced the number of conformations by forbidding bond angles lower than 90°. It will be clear that this method breaks down for chains longer than a few segments. It is much more economical to have only one equation per lattice layer.

In this section we will show how to compute the segment density profile from a given set of weighting factors via the generation of all conformations, i.e., via eqs. (5.17) and (5.4).

For monomers ($r = 1$) there is only one "conformation" per layer and the

segment density is just $\phi_i = C\ P_i$, where C is given by either eqs. (5.20) or (5.21). From eq. (5.27) it follows that $P(1) = \Sigma\ P_i$ in this case. As the monomer distribution is proportional to $\{P_i\}$ we may call P_i the **free segment probability.**

For symmetric dimers (r = 2) the distribution of the first segment is equal to that of the second, i.e., $\phi_i = 2\ C\ P(i,2)$. We define P(i,r) as the **end segment probability** of an r-mer in layer i. For monomers we have

$$P(i,1) = P_i \tag{5.27}$$

The quantity P(i,r) is a subset of the chain probability P(r), since the number of end segments is equal to the number of chains (for convenience we distinguish the first segment from the last segment of a chain):

$$P(r) = \sum_i P(i,r) \tag{5.28}$$

For dimers there are three different conformations with the second segment in layer i. From eq. (5.17) it follows that their relative probabilities are $P_{i-1}\lambda_1 P_i$, $P_i\lambda_0 P_i$, and $P_{i+1}\lambda_1 P_i$, respectively. Summation gives $P(i,2) = P_i\langle P_i\rangle = P_i\langle P(i,1)\rangle$, where the notation with angular brackets denotes a weighted average over three lattice layers, compare eq. (5.9).

For chains longer than dimers the spatial distribution of the segments is a function of their ranking number in the chain. The distribution of the last segment (and that of the first segment) is given by C P(i,r). To avoid a considerable amount of computing time and complexity, we approximate P(i,r) by assuming that the position of the last segment of a chain is determined by its predecessor and not by the position of other segments, i.e., we generate the chain conformations by a step weighted random walk adding one segment (s) per step. Thus, P(i,s) follows from the end segment probabilities $\{P(i,s-1)\}$ of a chain of s - 1 segments by the recurrent relation

$$P(i,s) = P_i\ \langle P(i,s-1)\rangle \tag{5.29}$$

where P_i accounts for the weighting factor of segment s and the angular brackets for the bond weighting factor of the bond between segement s and s - 1. We note that eq. (5.29) is an alternative representation of the matrix notation developed by DiMarzio and Rubin[13]. Starting from a monomer,

for which $P(i,1) = P_i$, the end segment probabilities of longer chains are calculated by applying eq. (5.29) for each additional segment.

With a step weighted random walk it is easy to compute the distribution of segment s in a chain of r segments, because the conformations of the first subchain of s - 1 segments are independent of the positions of the last r - s segments of the chain. Consequently, the total weight of all conformations with segment s in layer i is given by $\langle P(i,s-1)\rangle P_i \langle P(i,r-s)\rangle = P(i,s)\, P(i,r-s+1)/P_i$. The contribution to the segment density distribution due to all segments s is obtained after normalization:

$$\phi_i(s) = C\, P(i,s)\, P(i,r-s+1)/P_i \tag{5.30}$$

Note that segment s has indeed the same distribution as segment r - s + 1, i.e., $\phi_i(s) = \phi_i(r-s+1)$: the inversion symmetry is obeyed. Summation over all segments gives the overall segment density distribution.

$$\phi_i = C \sum_{s=1}^{r} P(i,s)\, P(i,r-s+1)/P_i \tag{5.31}$$

5.4.1 Adsorbing, bridging, and free polymer

Once the weighting factors $\{P_i\}$ are known for a given system, it is possible to obtain a very detailed picture of the structure of the polymer between the plates, because the number of chains in each conformation is given by eq. (5.17). We will subdivide the amount of polymer θ^t between the plates into five groups of chains: i) nonadsorbed chains, θ^f, ii) chains adsorbed on the first plate only, $\theta^{a'}$, i.e., with segments in layer 1 and none in layer M, iii) chains adsorbed on the second plate only, $\theta^{a''}$, iv) bridging chains with the last chain end leaving from the first plate, $\theta^{b'}$, and v) bridging chains with the last chain end leaving from the second plate, $\theta^{b''}$. Bridging chains have segments in layer 1 as well as in layer M.

If the plates are identical the segment distribution will be symmetric and hence, $\theta^{a'} = \theta^{a''}$ and $\theta^{b'} = \theta^{b''}$. Obviously,

$$\sum_G \theta^G = \theta^t \tag{5.32}$$

where G denotes f, a', a", b', or b". For each group defined above we can define a chain probability $P^G(r)$ which represents the sum of the weights of all conformations belonging to group G, so that

$$\sum_G P^G(r) = P(r) \tag{5.33}$$

Normalization of $P^G(r)$ gives the number of chains in group G. Hence, similar to eq. (5.21) :

$$\theta^G = C\, r\, P^G(r) \tag{5.34}$$

The chain probabilities $P^G(r)$ can be expressed as a sum of end segment probabilities $P^G(i,r)$, compare eq. (5.28):

$$P^G(r) = \sum_i P^G(i,r) \tag{5.35}$$

The generation of end segment probabilities $P^G(i,s)$ of chains of s segments is straightforward. From eq. (5.29) and the condition that $P(i,s) = \sum_G P^G(i,s)$ it follows that

$$\begin{aligned} P(i,s) = {} & P_i\langle P^f(i,s-1)\rangle + P_i\langle P^{a'}(i,s-1)\rangle \\ & + P_i\langle P^{a''}(i,s-1)\rangle + P_i\langle P^{b'}(i,s-1)\rangle + P_i\langle P^{b''}(i,s-1))\rangle \end{aligned} \tag{5.36}$$

The quantity $P^f(i,s)$ is the end segment probability of all chains, s segments long, ending in layer i and never touching one of the surfaces. From this definition it is easy to see that the term $P_i\,\langle P^f(i,s-1)\rangle$ in eq. (5.36) gives $P^f(i,s)$, except for i = 1 and i = M:

$$\begin{aligned} P^f(1,s) &= 0 \\ P^f(i,s) &= P_i\,\langle P^f(i,s-1)\rangle \qquad (1<i<M) \\ P^f(M,s) &= 0 \end{aligned} \tag{5.37}$$

For i = 1 we have $P_1\,\langle P^f(1,s-1)\rangle = P_1\,\lambda_1\,P^f(2,s-1)$ which is the probability of a chain part ending in layer 1 and with the first s - 1 segments in the layers $1 < i < M$, i.e., the chain part is adsorbed, with its last segment only, on plate 1 and belongs to $P^{a'}(1,s)$. Similarly, $P_M\,\langle P^f(M,s-1)\rangle$

contributes to $P^{a''}(M,s)$.

The term $P_i \langle P^{a'}(i,s-1)\rangle$ in eq. (5.36) represents the s-mers of which at least one of the first s - 1 segments is adsorbed on plate 1 and none of them on the second plate. This is only possible when M > 1. The chain belongs to $P^{a'}(i,s)$ when i < M. When i = M, the chain forms a bridge with the last segment of the bridge (segment s) on the second plate, i.e., $P_M \langle P^{a'}(M,s-1)\rangle$ contributes to $P^{b''}(M,s)$. Thus, we can write

$$\begin{aligned} P^{a'}(1,s) &= P_1 \langle P^{a'}(1,s-1) + P^{f}(1,s-1)\rangle && (M>1) \\ P^{a'}(i,s) &= P_i \langle P^{a'}(i,s-1)\rangle && (1<i<M) \\ P^{a'}(M,s) &= 0 \end{aligned} \qquad (5.38)$$

and a similar reasoning applies for the end segment probabilities of s-mers adsorbed on the second plate only:

$$\begin{aligned} P^{a''}(1,s) &= 0 \\ P^{a''}(i,s) &= P_i \langle P^{a''}(i,s-1)\rangle && (1<i<M) \\ P^{a''}(M,s) &= P_M \langle P^{a''}(M,s-1) + P^{f}(M,s-1)\rangle && (M>1) \end{aligned} \qquad (5.39)$$

The last two terms in eq. (5.36) belong to bridging chains. As defined above, such a chain belongs to $P^{b'}(i,s)$ when the last adsorbed segment (i.e., the adsorbed segment with the highest ranking number) is in layer 1 and to $P^{b''}(i,s)$ otherwise. Obviously, $P^{b'}(M,s) = P^{b''}(1,s) = 0$, except when M = 1. When the last segment (s) is in layer 1 the chain contributes to $P^{b'}(1,s)$, when it is in layer M it contributes to $P^{b''}(M,s)$. The result is

$$\begin{aligned} P^{b'}(1,s) &= P_1 \langle P^{b'}(1,s-1) + P^{b''}(1,s-1) + P^{a''}(1,s-1)\rangle && (M>1) \\ P^{b'}(i,s) &= P_i \langle P^{b'}(i,s-1)\rangle && (1<i<M) \\ P^{b'}(M,s) &= 0 && (M>1) \end{aligned} \qquad (5.40)$$

and

$$\begin{aligned} P^{b''}(1,s) &= 0 && (M>1) \\ P^{b''}(i,s) &= P_i \langle P^{b''}(i,s-1)\rangle && (1<i<M) \\ P^{b''}(M,s) &= P_M \langle P^{b''}(M,s-1) + P^{b'}(M,s-1) + P^{a'}(M,s-1)\rangle && (M>1) \end{aligned} \qquad (5.41)$$

For M = 1 all chains belong to either $P^{b'}(1,s)$ or $P^{b''}(1,s)$.

$$P^{b'}(1,s) = P^{b''}(1,s) = P_1 \langle P^{b'}(1,s)\rangle \qquad (M=1) \qquad (5.42)$$

Most of the starting values $P^G(i,1)$ are zero. The nonzero values are

$$\begin{aligned} P^{a'}(1,1) &= P_1 && (M>1) \\ P^{f}(i,1) &= P_i && (1<i<M) \\ P^{a''}(M,1) &= P_M && (M>1) \\ P^{b'}(1,1) &= P^{b''}(1,1) = \tfrac{1}{2}P_1 && (M=1) \end{aligned} \qquad (5.43)$$

since a monomer in layer 1 is adsorbed on plate 1, a monomer in layer M is adsorbed on plate 2, and it forms a bridge when M = 1. A monomer in one of the layers $1 < i < M$ is not adsorbed and hence contributes to $P^f(i,1)$.

The above equations can be used to calculate the end segment probabilities $P^G(i,s)$ of the various types of chains by repeatedly extending the chain with one segment, starting from a monomer. The 5M values of $P^G(i,2)$ are calculated from the various values of $P^G(i,1)$ as given in eq. (5.43) by applying once each of the eqs. (5.37-42). From $P^G(i,2)$ we obtain $P^G(i,3)$, etc. The sum of $P^G(i,r)$ over the 5 values of G equals P(i,r) as defined in eq. (5.28).

5.4.2 Segment distributions of loops, tails and bridges

In the previous section we have subdivided the polymer between the plates in adsorbing, bridging, and free chains. The same subdivision was made for the end segment probabilities P(i,s) of s-mers, giving

$$P(i,s) = P^f(i,s) + P^{a'}(i,s) + P^{a''}(i,s) + P^{b'}(i,s) + P^{b''}(i,s) \qquad (5.44)$$

where f denotes free chains; a' and a" chains adsorbed on plate 1 and plate 2, respectively; and b' and b" bridging chains with the last chain end leaving from plate 1 and plate 2, respectively. Here, we will show a very simple procedure to obtain segment distributions of trains, loops, tails, and bridges from these end segment probabilities.

Substitution of P(i,s) and P(i,r-s+1) from eq. (5.44) into eq. (5.30) and performing the multiplication $\{\sum_G P^G(i,s)\}\{\sum_G P^G(i,r-s+1)\}$ gives 25 terms

which are listed in the second column of table 5.1, where we have dropped the indices i and s. After multiplication by C/P_i, these terms give the distribution of segment s in a free chain, or in a loop, etc. In the third column of table 5.1 we have indicated for each term to which volume fraction segment s contributes, and the corresponding polymer fraction is shown in the fourth column.

For instance, the first line in table 5.1 represents $P^f(i,s)\ P^f(i,r-s+1)$ and gives the distribution of segment s when both of the chain parts meeting at segment s are not adsorbed, i.e., when segment s belongs to a free chain. Summation over all segments and normalization gives ϕ_i^f, the volume fraction of free chains in layer i.

$$\phi_i^f = C \sum_{s=1}^{r} P^f(i,s)\ P^f(i,r-s+1)/P_i \qquad (5.45)$$

Similarly, the second line in table 5.1 refers to conformations in which the first part of s segments of the chain as well as the second part of r - s + 1 segments are adsorbed on plate 1 only, i.e., segment s is part of a loop in a chain adsorbed on plate 1 (when i > 1), or part of a train in such a chain (when i = 1). For i = M both $P^{a'}(i,s)$ and $P^{a'}(i,r-s+1)$ are zero (see eq. 5.38).

The third line in the table corresponds to the distribution of segment s when it belongs to a tail of a chain adsorbed on plate 1, because segment s forms a link between a chain part which is not adsorbed and one which is adsorbed on plate 1. The first term of line 3 accounts for a tail at the beginning of the chain and the second term for a tail at the end.
Lines 4 and 5 account for the chains adsorbed on the second plate and are analogous to lines 2 and 3.

The volume fractions of trains, loops, and tails of chains adsorbed on one surface are found after summation over all segments

$$\phi^{a',tr} = C \sum_{s=1}^{r} P^{a'}(1,s)\ P^{a'}(1,r-s+1)/P_1 \qquad (5.46)$$

$$\phi^{a'',tr} = C \sum_{s=1}^{r} P^{a''}(M,s)\ P^{a''}(M,r-s+1)/P_M \qquad (5.47)$$

$$\phi_i^{a',l} = C \sum_{s=1}^{r} P^{a'}(i,s)\ P^{a'}(i,r-s+1)/P_i \qquad (i>1) \qquad (5.48)$$

Table 5.1. Contribution of segments in trains, loops, tails, bridges, and free chains to the segment density. For explanation see text.

line	term	s contributes to	chain belongs to
1	$P^f P^f$	free chains	θ^f
2	$P^{a'} P^{a'}$	trains (i=1) or loops (i>1)	$\theta^{a'}$
3	$P^f P^{a'} + P^{a'} P^f$	tails	
4	$P^{a''} P^{a''}$	trains (i=M) or loops (i<M)	$\theta^{a''}$
5	$P^f P^{a''} + P^{a''} P^f$	tails	
6	$P^{b'} P^{a'}$	trains (i=1) or loops (i>1)	$\theta^{b'}$
7	$P^{b'} P^f$	tails	
8	$P^{a''} P^{a'} + P^{b''} P^{a'}$	bridges	
9	$P^{b''} P^{a''}$	trains (i=M) or loops (i<M)	$\theta^{b''}$
10	$P^{b''} P^f$	tails	
11	$P^{a'} P^{a''} + P^{b'} P^{a''}$	bridges	
12	$P^{a'} P^{b'} + P^{b'} P^{b'}$	trains (i=1) or loops (i>1)	$\theta^{b'} + \theta^{b''}$
13	$P^{a''} P^{b''} + P^{b''} P^{b''}$	trains (i=M) or loops (i<M)	
14	$P^f P^{b'}$	tails attached to plate 1	
15	$P^f P^{b''}$	tails attached to plate 2	
16	$P^{b'} P^{b''} + P^{b''} P^{b'} + P^{a'} P^{b''} + P^{a''} P^{b'}$	bridges	
+	PP	ϕ	θ^t

$$\phi_i^{a'',l} = C \sum_{s=1}^{r} P^{a''}(i,s)\, P^{a''}(i,r-s+1)/P_i \qquad (i<M) \qquad (5.49)$$

$$\phi_i^{a',t} = 2\, C \sum_{s=1}^{r} P^{a'}(i,s)\, P^{f}(i,r-s+1)/P_i \qquad (i>1) \qquad (5.50)$$

$$\phi_i^{a'',t} = 2\, C \sum_{s=1}^{r} P^{a''}(i,s)\, P^{f}(i,r-s+1)/P_i \qquad (i<M) \qquad (5.51)$$

where the indices tr, l, and t indicate trains, loops, and tails, respectively.

Lines 6-16 in table 5.1 contain 18 terms corresponding to bridging chains. Eight of them (lines 8, 11 and 16) contain two chain probabilities P^a or P^b referring to the two different plates, and give the volume fraction ϕ_i^{br} of bridges. Because of the chain symmetry, these can be combined in four terms:

$$\phi_i^{br} = 2\, C \sum_{s=1}^{r} \{P^{a'}(i,s) + P^{b'}(i,s)\}\{P^{a''}(i,r-s+1) + P^{b''}(i,r-s+1)\}/P_i \qquad (5.52)$$

The sum between the first pair of parentheses in eq. (5.52) represents the first part of the chain connecting segment s with plate 1, the second sum the other chain part which somewhere meets the second plate.

Of the remaining ten terms in table 5.1, six contain a product of P^a and P^b referring to the same plate; they represent trains (for i = 1 or M) or loops (for 1 < i < M) of bridging chains (lines 6, 9, 12, 13). The last four terms (lines 7, 10, 14, 15) are of the type $P^{b}P^{f}$ and correspond to tails belonging to bridging chains. Following a similar reasoning as applied above, the volume fractions of trains, loops, and tails of bridging chains can be written as

$$\phi_i^{b',tr} = C \sum_{s=1}^{r} P^{b'}(1,s)\{2P^{a'}(1,r-s+1) + P^{b'}(1,r-s+1)\}/P_1 \qquad (5.53)$$

$$\phi_i^{b'',tr} = C \sum_{s=1}^{r} P^{b''}(M,s)\{2P^{a''}(M,r-s+1) + P^{b''}(M,r-s+1)\}/P_M \qquad (5.54)$$

$$\phi_i^{b',l} = C \sum_{s=1}^{r} P^{b'}(i,s)\{2P^{a'}(i,r-s+1) + P^{b'}(i,r-s+1)\}/P_i \qquad (i>1) \qquad (5.55)$$

$$\phi_i^{b'',l} = C \sum_{s=1}^{r} P^{b''}(i,s)\{2P^{a''}(i,r-s+1) + P^{b''}(i,r-s+1)\}/P_i \qquad (i<M) \qquad (5.56)$$

$$\phi_i^{b',t} = 2\, C \sum_{s=1}^{r} P^{b'}(i,s)\, P^{f}(i,r-s+1)/P_i \qquad (5.57)$$

$$\phi_i^{b'',t} = 2\, C \sum_{s=1}^{r} P^{b''}(i,s)\, P^{f}(i,r-s+1)/P_i \qquad (5.58)$$

In this way, the segment distributions of trains, loops, tails, and bridges are obtained from the end segment probabilities derived in the previous section.

5.4.3 Train, loop, tail, and bridge size distributions

The end segment probabilities $P^G(i,s)$ contain much more information than we have used above. Of special interest are the numbers and lengths of trains, loops, tails, and bridges in a given system. These quantities can be obtained from $P^G(i,s)$ in different ways, but we will give only the simplest expressions here.

Let us start with the non-bridging chains. Obviously, the expressions for these chains will not differ from those of the one plate model[22]. Hence, the average number of loops, $n^{a',l}$, per chain adsorbed on plate 1, is obtained by following the chain from the first adsorbed segment and counting the number of bonds from layer 2 to layer 1. The total number of such bonds between segment s and segment s + 1 is $C\, P^{a'}(2,s)\, \lambda_1\, P^{a'}(1,r-s)$. Since the number of adsorbed chains on the first plate is $C\, P^{a'}(r)$, we have

$$n^{a',l} = \frac{\lambda_1}{P^{a'}(r)} \sum_{s=2}^{r-1} P^{a'}(2,s)\, P^{a'}(1,r-s) \qquad (5.59)$$

and similarly,

$$n^{a'',l} = \frac{\lambda_1}{P^{a''}(r)} \sum_{s=2}^{r-1} P^{a''}(M-1,s)\, P^{a''}(M,r-s) \qquad (5.60)$$

The summation starts from s = 2, because the smallest possible loop is one segment long, and ends at s = r - 1, since the longest possible loop has r - 2 segments. As each end of a loop is connected to a train, the number of trains, n^{tr} per adsorbed chain is given by

$$n^{a',tr} = n^{a',l} + 1 \; ; \quad n^{a'',tr} = n^{a'',l} + 1 \qquad (5.61)$$

Finally, the number of tails, n^t, equals the number of chain ends (s = r) not ending on the plate.

$$n^{a',t} = 2 - 2P^{a'}(1,r)/P^{a'}(r) \; ; \quad n^{a'',t} = 2 - 2P^{a''}(M,r)/P^{a''}(r) \qquad (5.62)$$

We now examine bridging chains. Their number is $C\{P^{b'}(r) + P^{b''}(r)\}$ and they form not only bridges, but also trains on both of the plates, and, if the chains are long enough, loops and tails as well.

Following the backbone of each chain, we obtain just half the total number of bridges by counting each entry of layer 1 of a chain part that has a previous segment in layer M. That chain part, consisting of s segments, belongs either to the group $P^{a''}$ (no previous segment in layer 1) or $P^{b''}$ (having a previous bridge). The other chain part of r - s segments is either adsorbed on plate 1 only ($P^{a'}$) or forms another bridge ($P^{b'}$). Analogously to eq. (5.59) we obtain the average number n^b of bridges per chain after summation and normalization :

$$n^b = \frac{2\lambda_1}{P^{b'}(r) + P^{b''}(r)} \sum_{s=M-1}^{r-1} \{P^{a''}(2,s) + P^{b''}(2,s)\}\{P^{a'}(1,r-s) + P^{b'}(1,r-s)\} \tag{5.63}$$

The number of loops on the first plate, $n^{b',1}$, of bridging chains consists of three contributions. The first bond in such a loop connects two subchains, each coming from the first plate, of which either i) only the first subchain is a bridging chain, or ii) only the second subchain is a bridging chain, or iii) both subchains are bridging chains. The corresponding number of loops ending at s is $C\,P^{b'}(2,s)\,\lambda_1\,P^{a'}(1,r-s)$, $C\,P^{a'}(2,s)\,\lambda_1\,P^{b'}(1,r-s)$, and $C\,P^{b'}(2,s)\,\lambda_1\,P^{b'}(1,r-s)$, respectively. From symmetry it follows that the sum of contributions i) and ii) are equal. Hence, the result is

$$n^{b',1} = \frac{\lambda_1}{P^{b'}(r) + P^{b''}(r)} \sum_{s=M+1}^{r-1} P^{b'}(2,s)\{2P^{a'}(1,r-s) + P^{b'}(1,r-s)\} \tag{5.64}$$

and equivalently,

$$n^{b'',1} = \frac{\lambda_1}{P^{b'}(r) + P^{b''}(r)} \sum_{s=M+1}^{r-1} P^{b''}(M-1,s)\{2P^{a''}(M,r-s) + P^{b''}(M,r-s)\} \tag{5.65}$$

The number of trains on plate 1, $n^{b',tr}$, per bridging chain is most easily found by counting the number of train ends. This number is determined

by the number of loops (two train ends per loop) and the number of bridges (one train end on each surface per bridge). In addition, each chain end corresponds to one train end. The number of chain ends with the last adsorbed segment on plate 1 and belonging to bridging chains is $2\,C\,P^{b'}(r)$. Since the number of train ends is twice the number of trains, we find for the last number

$$n^{b',tr} = n^{b',1} + \tfrac{1}{2}\, n^{b} + \frac{P^{b'}(r)}{P^{b'}(r) + P^{b''}(r)} \tag{5.66}$$

and

$$n^{b'',tr} = n^{b'',1} + \tfrac{1}{2}\, n^{b} + \frac{P^{b''}(r)}{P^{b'}(r) + P^{b''}(r)} \tag{5.67}$$

The number of tails equals the number of chain ends minus those which are adsorbed (see also eq. 5.62). The number of chain ends on plate 1 of bridging chains is $2\,C\,P^{b'}(r)$, of which $2\,C\,P^{b'}(1,r)$ are adsorbed. Consequently, the number of tails on plate 1, $n^{b',t}$, per bridging chain is

$$n^{b',t} = 2\,\frac{P^{b'}(r) - P^{b'}(1,r)}{P^{b'}(r) + P^{b''}(r)} \tag{5.68}$$

and, similarly,

$$n^{b'',t} = 2\,\frac{P^{b''}(r) - P^{b''}(M,r)}{P^{b'}(r) + P^{b''}(r)} \tag{5.69}$$

The average fraction of segments, ν, in trains, loops, tails, and bridges can be found from

$$\nu^{G,S} = \sum_{i=1}^{M} \phi_i^{G,S} / \Theta^{G} \tag{5.70}$$

where G (= a', a", b) refers to one of the chain fractions: adsorbed on plate 1, adsorbed on plate 2, or bridging chains, and S (= tr, l, t, b) denotes either trains, loops, tails, or bridges. For example, the fraction $\nu^{a',l}$ of segments in loops of chains adsorbed on plate 1 is the ratio between the sum of all volume fractions $\phi_i^{a',l}$ of loops in these chains and the amount of polymer adsorbed on plate 1.

The average length of such a loop, $l^{a',l}$, is the ratio between the number of segments per chain in these loops, $r\,\nu^{a',l}$, and the number of loops

per chain, $n^{a',1}$. Generally, the length $l^{G,S}$ of a chain part S of the chain fraction G is given by

$$l^{G,S} = r\ \nu^{G,S}/n^{G,S} \tag{5.71}$$

It is also possible to obtain the size distributions of trains, loops, tails, and bridges, i.e., the number of chain parts of length s. For example, the number of tails of length s per chain adsorbed on plate 1 is given by[22]

$$n^{a',t}(s) = \frac{2\lambda_1}{P^{a'}(r)} P^{f}(2,s)\ P^{a'}(1,r-s) \tag{5.72}$$

whereas the train size distribution of the same polymer fraction is

$$n^{a',tr}(s) = \frac{\lambda_1^2 \lambda_0^{s-1} P_1^{s}}{P^{a'}(r)} \sum_{t=0}^{r-s} \{P^{a'}(2,t)+P^{f}(2,t)\}\{P^{a'}(2,r-s-t)+P^{f}(2,r-s-t)\} \tag{5.73}$$

For loop and bridge size distributions, the generation of other end segment probabilities are necessary. The procedures are equivalent to those given in ref. (22) and the reader is referred to that paper for more details. An obvious check for the correctness of these equations is the (numerical) check of $n^{G,S} = \sum_s n^{G,S}(s)$.

5.5 METHOD OF COMPUTATION

The M segmental weighting factors $\{P_i\}$ are obtained by solving numerically a set of M simultaneous equations. The values for P_i must be positive. It is therefore convenient to use the unconstrained variables $\{X_i\}$ defined by

$$X_i = \ln P_i \qquad (1 \leq i \leq M) \tag{5.74}$$

Starting with $X_i = 0$ $(1 \leq i \leq M)$ we solve iteratively the following set of equations:

$$P(i,1) = P_i = e^{X_i} \qquad (1\leq i\leq M) \qquad (5.27a)$$

$$P(i,s) = P_i \langle P(i,s-1)\rangle \qquad (1\leq i\leq M;\ 2\leq s\leq r) \qquad (5.29)$$

$$\phi_i = C \sum_{s=1}^{r} P(i,s)\, P(i,r-s+1)/P_i \qquad (1\leq i\leq M) \qquad (5.31)$$

where $C = \phi_*/(r\, P_*^r)$ (full equilibrium) or $C = \Theta^t/\{r \sum_{i=1}^{M} P(i,r)\}$ (restricted equilibrium)

$$\phi_i^o = P_i\, e^{-\chi_s(\delta_{1,i}+\delta_{M,i})-\chi\langle 2\phi_i-1\rangle} \qquad (1\leq i\leq M) \qquad (5.16a)$$

until $\phi_i + \phi_i^o = 1$ (or $\ln(\phi_i + \phi_i^o) = 0$). In principle, several standard routines solving $f(\{X_i\}) = 0$ are available. For example, a Fortran listing of a powerful routine is given in ref. (49).

An important reduction of computer time is possible by further exploiting the symmetry of the equations. For instance, segment s and segment r - s + 1 have the same distribution, so whenever G = G' we may replace $P^G(i,s)\, P^{G'}(i,r-s+1)$ by $P^{G'}(i,s)\, P^G(i,r-s+1)$, or

$$\sum_{s=1}^{r} P^G(i,s)\, P^G(i,r-s+1) = \delta(r) + 2 \sum_{s=1}^{r-s} P^G(i,r-s+1) \qquad (5.75)$$

where $\delta(r) = \{P^G(i,\tfrac{1}{2}+r/2)\}^2$ if r is odd and $\delta(r) = 0$ otherwise. This reduces the number of terms by 50%.

In many cases the two surfaces are of the same type, giving a symmetric segment density profile. Then, many of the variables are mirror images of each other, for example $P^{a'}(i,s) = P^{a''}(M-i+1,s)$, $P^{b'}(i,s) = P^{b''}(M-i+1,s)$, $\phi_i^{a'} = \phi_{M-i+1}^{a''}$, $P_i = P_{M-i+1}$, and $X_i = X_{M-i+1}$. The number of simultaneous equations and the number of variables $\{X_i\}$ is thus reduced to M/2.

Results given in the following section are obtained by a special program written in Simula67 using a DEC10 computer.

5.6 RESULTS AND DISCUSSION

In this section a typical collection of the results for a hexagonal lattice ($\lambda_o = 6/12$) will be shown. Occasionally, data for other lattice

types will be mentioned. The effect of molecular weight, adsorption energy, solvent quality, solution concentration, and adsorbed amount on the interaction free energy will be examined in some detail.

The adsorbed amount of polymer is a function of molecular weight, adsorption energy, solvent quality, and solution concentration. The same adsorbed amount can be obtained for different combinations of these quantities. The properties of adsorbed layers at constant solution concentration are qualitatively different from those at constant amount of adsorbed polymer. For instance, at constant solution concentration the root-mean-square thickness of the adsorbed polymer layer on a single surface is nearly independent of both the adsorption energy and the solvent quality, and proportional to the square root of the molecular weight of the polymer. On the other hand, at constant adsorbed amount the thickness of the polymer layer decreases with increasing adsorption energy and decreasing solvent power, and is independent of the chain length[22].

For the two plate problem, the two cases of constant solution concentration and constant amount of polymer represent important extremes. At full equilibrium, the amount of polymer between the plates adapts itself to a constant solution concentration, whereas at restricted equilibrium the polymer cannot escape from the gap between the plates and the amount of polymer is constant. The former situation is relevant for non-adsorbing polymer or, possibly, when the surfaces are flexible (allowing for lateral compression or diffusion) as is the case for liquid films and liquid-liquid interfaces. A constant amount of polymer is more probable when two polymer covered solid surfaces approach each other. Obviously, in all cases the interaction will be zero at large distances. Also, in restricted equilibrium the free energy of the system will never be lower than that at full equilibrium. Hence, at a given plate separation, the free energy of interaction between two surfaces with a constant amount of polymer between them will be higher than that at full equilibrium, whenever this amount deviates (positively or negatively) from its equilibrium value. However, as we will show below, this deviation is only substantial at small distances. At plate separations corresponding to the minimum in the interaction free energy in restricted equilibrium, the interaction is almost identical with that in full equilibrium. Therefore, we first discuss the equilibrium forces.

5.6.1 Full equilibrium

When the polymer is in equilibrium with a constant bulk solution concentration the interaction between the plates is always found to be attractive. This result supports the analysis of De Gennes[38]. At full equilibrium the interaction free energy is equal to the difference $\Delta\gamma$ between the sum of the two surface free energies $\gamma' + \gamma''$ of the two surfaces at plate separation M and that at infinite separation ($M \to \infty$). In figure 5.2 the total amount of polymer between the plates θ^t (in equivalent monolayers) and $\Delta\gamma$ in units of kT per surface site of one plate) are plotted as a function of the plate separation M (in units of lattice layers) under various conditions. Unless indicated otherwise, the parameters are $\lambda_0 = 0.5$, $\chi = 0.5$, $\chi_s = 1$, $r = 1000$, and $\phi_* = 10^{-6}$.

All interaction curves in figure 5.2 are indeed monotonically decreasing

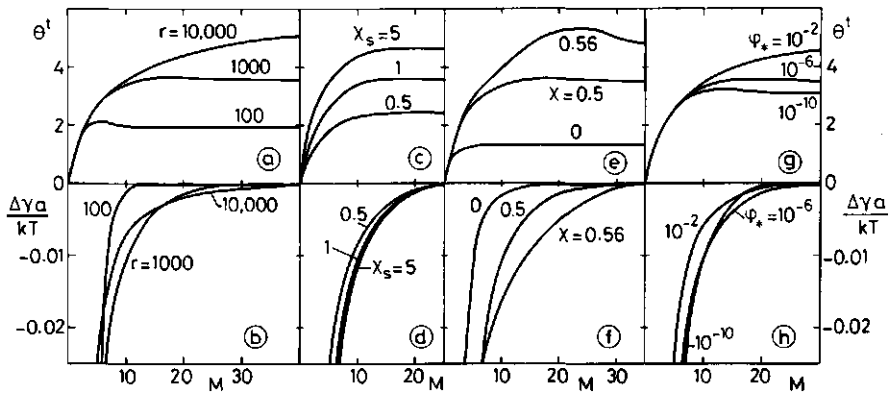

Figure 5.2. Adsorption and interaction curves at full equilibrium. The top figures show the total amount of polymer between the plates (in equivalent monolayers), the bottom figures the free energy of interaction (in units of kT per surface site), both as a function of the plate separation M (in lattice layers). In each graph the curve for $\lambda_0 = 0.5$, $\chi = 0.5$, $\chi_s = 1$, $r = 1000$, and $\phi_* = 10^{-6}$ is given together with two curves for which one parameter has either a lower or a higher value, respectively. The effect of chain length is shown in a and b, that of the adsorption energy in c and d, that of the solvent quality in e and f, and the influence of the solution concentration in g and h.

with decreasing M, whereas the adsorbed amount of polymer in most cases passes through a (sometimes weak) maximum and decreases at smaller M until all the chains are squeezed out. We discuss the origin of the maximum in θ^t in connection with figure 5.4 below. However, the volume fraction of adsorbed segments (trains, not shown in figure 5.2) is nearly constant up to very small M and even increases slightly going from M = 2 to M = 1. Therefore, it is unlikely that the last monolayer of polymer will leave the gap. The ultimate equilibrium situation, having the lowest free energy, will be a sandwich structure of two plates with one layer of polymer segments in between, the concentration of which depends mainly on χ_s and χ.

In figures 5.2a and 5.2b the effect of the chain length r is shown. The onset of interaction occurs at a separation comparable to the diameter of a free coil in solution ($\simeq r^{\frac{1}{2}}$) and is determined by the extension of the tails[22]. Consequently, at large distances the free energy of interaction is more negative for longer chains. When the plates come closer, the tails form bridges and the segment density distribution becomes of the loop-bridge type which is, for small separations, independent of r. The free energy of interaction does not become independent of the chain length, since the free energy of the reference state (γ at $M \to \infty$) depends on chain length. Because $\gamma(\infty)$ decreases with increasing r, $\Delta\gamma$ at small M becomes more negative for short chains.

The adsorption energy χ_s affects the adsorbed amount of polymer (and hence θ^t, see figure 5.2c), without changing the thickness of the adsorbed polymer layer very much[23]. Consequently, the only effect of χ_s on the interaction curves is a small change in magnitude (see figure 5.2d). At $\chi_s = 5$ the surfaces are almost fully covered by polymer segments ($\phi_1 = \phi_M \simeq 0.995$).

In figures 5.2e and 5.2f the effect of the solvent quality is illustrated. In a good solvent (e.g., $\chi = 0$) the adsorption is low, resulting in a relatively short range interaction and the maximum in the adsorbed amount is either weak or absent. In worse than Θ-solvents ($\chi > 0.5$) the adsorption and the range of interaction increase very rapidly with χ and the adsorption maximum is more pronounced. We will return to this point below.

A last parameter which may be important is the solution concentration (figures 5.2g,h). Polymer adsorption isotherms, having a nearly horizontal pseudo- plateau, are of the high affinity type, implying only a weak dependence of the adsorbed amount on the solution concentration. With increasing

ϕ_* the change in the number of train segments is much smaller than that in loops and tails. Hence, at large plate separations the interaction is stronger in more concentrated solutions due to more and longer loops and tails. At smaller plate separations the opposite effect occurs because of a different reference state: $\gamma(\infty)$ is smaller in more concentrated solutions.

The main conclusion from figure 5.2 is that at full equilibrium both the adsorption energy and the solution concentration do not affect the interaction substantially. The range of interaction is mainly determined by the chain length and the solvent quality.

We now examine in more detail the forces in bad solvents. In figure 5.3 binodal curves, giving the boundary between stable and metastable (bulk) solutions are shown for three different chain lengths[37]. The minimum of each curve is the critical point, corresponding to $\chi_{cr} = \frac{1}{2}(1 + 1/\sqrt{r})^2$ and $\phi_{cr} = (1 + \sqrt{r})^{-1}$. At any χ above the critical point, there is an unstable region between the two critical compositions of the solution, given by the spinodal (dotted curve for r = 100), and two metastable regions between the spinodal and the binodal. The chemical potentials of polymer and solvent (eqs. 5.18 and 5.19) at the lower binodal concentration ϕ_α are equal to those at the higher binodal concentration ϕ_β, i.e., $\mu(\phi_\alpha) = \mu(\phi_\beta)$ and $\mu^o(\phi_\alpha^o) = \mu^o(\phi_\beta^o)$. These two equations in two unknowns ($\phi_\alpha = 1 - \phi_\alpha^o$ and $\phi_\beta = 1 - \phi_\beta^o$) are implicit, but can be solved numerically. The spinodal is given by the condition $\delta\mu/\delta\phi = 0$. The free energy of a solution of meta-

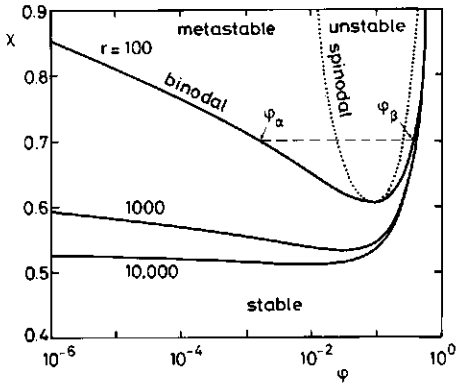

Figure 5.3. Binodals (full curves) for different chain lengths and the spinodal for r = 100 (dotted curve). A binodal gives the boundary between stable and metastable regions, whereas a spinodal indicates the transition between metastable and instable regions. Binodal and spinodals touch at their minimum (critical point). After phase separation, the concentrations of polymer in the two coexisting phases are given by the binodal, e.g. ϕ_α and ϕ_β.

stable composion is lower after phase separation in two phases with concentrations ϕ_α and ϕ_β, respectively.

For solution concentrations corresponding to the lower stable region ($\phi_* < \phi_\alpha$) the adsorbed polymer layers are of finite size, although they become thicker when the solution concentration is increased or the solvent quality is decreased (higher χ). Here, we will examine the region near the binodal by changing ϕ_* at constant χ, since ϕ_* is less critical than χ. We choose r = 100 and χ = 0.7, giving binodal concentrations of ϕ_α = 0.0015014 and ϕ_β = 0.37136, respectively. In figure 5.4 the adsorption and interaction curves are given for several concentrations of polymer in the bulk solution.

At low concentrations the shapes of the curves are as shown before (compare χ = 0.56 in figures 5.2e,f and $\phi_* = 10^{-4}$ in figures 5.4a,b). At $\phi_* = 10^{-4}$ the amount θ^t of polymer between the plates consists almost completely of bridging (θ^b) and adsorbing ($\theta^{a'} + \theta^{a''}$) chains, see the dashed curves in figure 5.4a. The amount of free chains (θ^f) is negligible. The onset of interaction (figure 5.4b) is just at the distance (M = 15) where bridges start to appear. The increase of bridging chains pushes the concentration of segments midway between the plates beyond the critical volume fraction of polymer, but the composition between the plates is not unstable, since the conformational entropy of the chains between the plates is less than that in the bulk solution. The spinodal and binodal curves given in figure 5.3 apply only for solutions which are homogeneous over distances of several molecular diameters. However, the higher concentration midway between the plates in combination with a high χ-value increases the segmental weighting factors P_i (eq. 5.16) in the loop regions of the adsorbed chains, so that the adsorbed amounts $\theta^{a'}$ and $\theta^{a''}$ increase as well. This effect is smaller at lower solution concentrations, where the bridges appear at shorter distances.

In good solvents (χ = 0) $\theta^{a'}$ and $\theta^{a''}$ decrease when bridges appear, but not always enough to compensate the increase in θ^b, e.g., at low concentrations. Hence, also in good solvents a maximum in the adsorption curves due to bridging chains may occur (not shown).

At concentrations close to the binodal, a linear part in the adsorption curve appears with a slope which is equal to the volume fraction $\phi_{M/2}$ midway between the plates. This volume fraction is in the metastable region between the higher spinodal and binodal concentrations, in this case between 0.266 and 0.371. For instance in figure 5.4a, the adsorption for $\phi_* = 10^{-3}$ in-

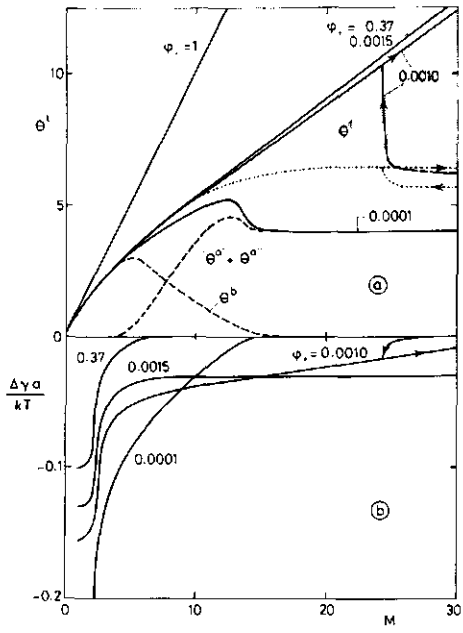

Figure 5.4. Adsorption (a) and interaction (b) curves at full equilibrium in a bad solvent for different volume fractions of polymer in the solution ($\lambda_0 = 0.5$, $\chi = 0.7$, $\chi_s = 1$, $r = 100$). The binodal concentrations are $\phi_\alpha = 0.0015014$ and $\phi_\beta = 0.37136$, respectively. The curves for $\phi_* = \phi_\alpha$ and $\phi_* = \phi_\beta$ are essentially identical. For concentrations slightly below ϕ_α a hysteresis effect occurs. For $\phi_* = 10^{-4}$ the amount of bridging polymer, θ^b, and the rest of adsorbing polymer, $\theta^{a'} + \theta^{a''}$, is indicated (dashed curves). For $\phi_* = 10^{-3}$ the total amount of adsorbed polymer, $\theta^b + \theta^{a'} + \theta^{a''}$, is shown (dotted curve); the hatched area corresponds to the amount of nonadsorbed polymer, θ^f, at $\phi_* = 10^{-3}$.

creases linearly from M = 8 with a slope 0.36. This increase of θ^t is mainly due to the fraction θ^f (indicated by the shaded area in figure 5.4a) of nonadsorbed polymer which fills up the segment density of loops and tails midway the plates to a nearly constant value of 0.36. The interaction curve is also linear beyond M = 8 with a slope that is a measure for the energy of transfer of solvent and polymer from the bulk solution to the space between the surfaces, where the composition is different.

At large plate separations the overlap of adsorbed polymer layers is too small to attract much free polymer and θ^f may suddenly drop to a lower level, so that the concentration $\phi_{M/2}$ becomes equal to ϕ_* and the interaction between the plates jumps to zero. Thus, beyond M = 24, there are two equilibrium states, of which the one with the highest free energy is metastable, and a hysteresis between these states occurs when the interplate distance is successively increased and decreased. This process is very similar to condensation and evaporation in pores.

Very close to the binodal concentration, at $\phi_* = 0.0015$, the linear part of the θ^t curve has a slope of 0.37 ($\phi_{M/2} = 0.37$, the upper binodal concentration) and the interaction curve is nearly horizontal. In this case there is essentially no difference between the two co-existing phases in a biphasic system and the solutions inside and outside the gap, respectively.

Obviously, the distance at which the jump occurs goes to infinity for a concentration on the binodal, because that concentration would be in full equilibrium with the higher concentration (also on the binodal) between the plates. Also, there would be no difference in the chemical potentials and hence, in the segment density between the plates, if also the solution concentration were at the higher binodal concentration. The only difference would be a shift in the free energy reference point, γ at $M \to \infty$. Thus, the adsorption curves for $\phi_* = 0.0015$ and $\phi_* = 0.37$ in figure 5.4a coincide, while the two corresponding interaction curves in figure 5.4b are identical except for a vertical shift. When $\phi_* > 0.37$ and $M \gtrsim 15$ the volume fraction of polymer midway between the plates is close to ϕ_* and the interaction free energy is essentially zero.

5.6.2 Restricted equilibrium

When the polymer is unable to escape from the space between the plates during the approach of the surfaces (θ^t = constant), the chemical potential of the polymer will depend on the interplate distance, i.e., the polymer would be in equilibrium with a bulk solution of continuously changing composition. Hence, the resulting interaction curve is a complicated cross-over between many equilibrium curves which, in addition, are to be shifted to the same reference point. However, it is easy to predict some trends. At large distances the interaction between the surfaces will be zero, whereas at a distance $M = \theta^t$, i.e., no solvent between the plates, the repulsion becomes infinite. As stated before, the free energy of interaction of approaching surfaces will be higher whenever the adsorbed amount deviates from its equilibrium value. This is illustrated in figure 5.5.

In figure 5.5b the interaction curves $\Delta\gamma$ (equilibrium) and ΔF (constant θ^t) are plotted, using the curve for $\phi_* = 10^{-4}$ from figure 5.4 for $\Delta\gamma$. At large separations the equilibrium adsorption is such that $\theta^t \approx 4$ (see figure 5.5a), so we used $\theta^t = 4$ for the restricted equilibrium curve to

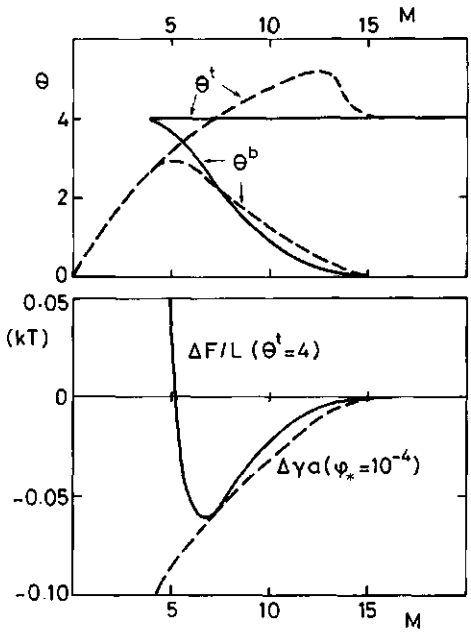

Figure 5.5. Comparison between adsorption and interaction curves at full equilibrium (dashed curves) and those at constant amount of polymer between the surfaces (full curves). The amount of polymer between the plates at large separation is the same in both cases (θ^t = 4 monolayers), corresponding to ϕ_* = 10^{-4}. λ_0 = 0.5, χ = 0.7, χ_s = 1, and r = 100.

obtain the same reference free energy. Since the full equilibrium curve shows a maximum in θ^t, there is another point (at M ≈ 7) where θ^t is the same for full and restricted equilibrium. At that point restricted equilibrium gives necessarily the same results as full equilibrium. In figure 5.5b we see that this point is very close to the position of the free energy minimum at constant θ^t. At all other distances the non-equilibrium curve is above the equilibrium curve.

As we have seen in the discussion of figure 5.4, the adsorption of polymer from a bulk concentration approaching the binodal has essentially no limit, since the surface acts as a nucleus for phase separation. Moreover, under these conditions there is a region of plate separations at which the free energy of interaction is independent of the plate distance, but non-zero. This applies only when full equilibrium with an infinite bulk solution can be maintained. In reality, the bulk concentration will decrease when adsorption sets in, limiting the adsorption at a certain level. The shape of the interaction curves in restricted equilibrium at other levels than θ^t = 4 is shown in figure 5.6. In order to reach high adsorbed amounts, the equilibrium bulk concentration at large distances has to approach the binodal. At a constant amount of polymer between the surfaces, the segment density midway between the plates must necessarily decrease with increasing plate

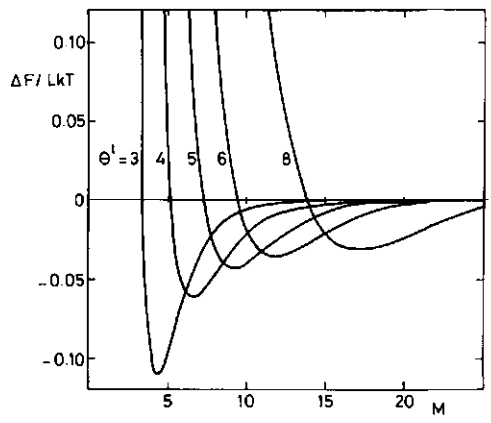

Figure 5.6. Interaction curves at different (constant) amounts of polymer between the surfaces (compare figure 5.5). $\lambda_0 = 0.5$, $\chi = 0.7$, $\chi_s = 1$, and $r = 100$.

separation, because there is no supply of polymer from the bulk solution to keep the volume fraction constant around the higher critical concentration. As a result, with increasing θ^t the minimum free energy shifts to larger separations, closely following the lowest possible equilibrium value from figure 5.4 at each distance, but without the linear regions or jumps in the curves as in full equilibrium.

In practice the conditions which probably apply most often are a full equilibrium adsorption at large plate separation and a constant amount of polymer between the plates during the interaction. In figure 5.7 a series of interaction curves is given for such a case. The equilibrium concentration for each curve is the same as that for the corresponding full equilibrium curve in figure 5.2, i.e., $\phi_* = 10^{-6}$ except for two graphs with $\phi_* = 10^{-10}$ and $\phi_* = 10^{-2}$ in each of the figures 5.7g and 5.7h. As in figure 5.2, the parameters are $\lambda_o = 0.5$, , $\chi = 0.5$, $\chi_s = 1$, and $r = 1000$, unless indicated otherwise.

Nearly all interaction curves in figure 5.7 show a distinct minimum. This minimum is deeper and is situated at a shorter separation if the molecular weight of the polymer is lower (see figure 5.7b), mainly because of the lower adsorbed amount (figure 5.7a). At this concentration (1 ppm) in a Θ-solvent the minimum occurs at $0.27\sqrt{r}$ which is about 60% of the radius of gyration of a free coil in solution.

As discussed in connection with figure 5.2d, a change of the adsorption energy χ_s affects the equilibrium adsorption at large plate separation (compare figures 5.2c and 5.7c) without changing the extension of the adsorbed layer very much. The result is that the interaction curves given in figure 5.7d are nearly independent of χ_s.

In figures 5.7e and 5.7f the effect of the solvent quality is shown. In

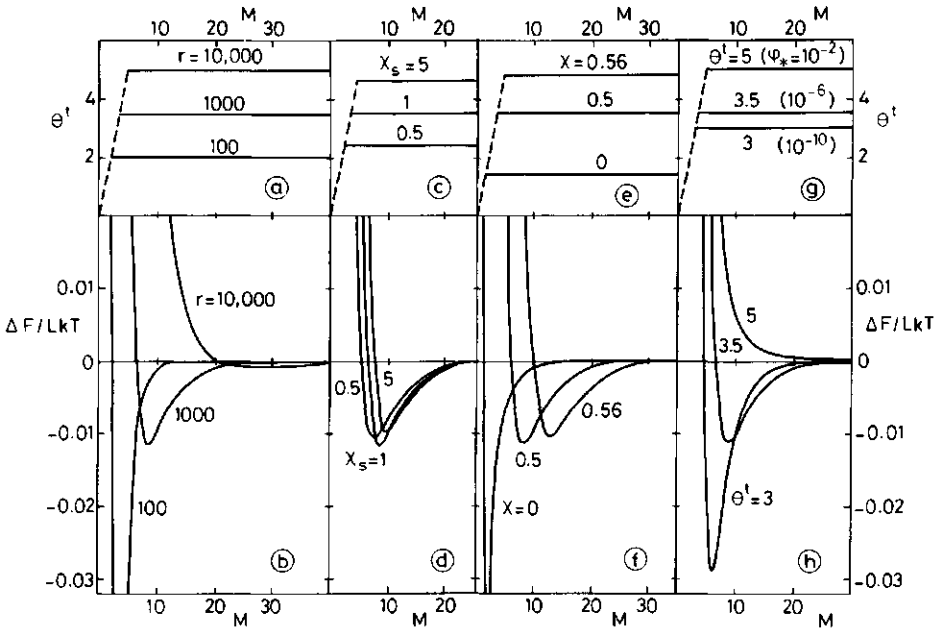

Figure 5.7. "Adsorption" and interaction curves at constant amounts of polymer under various conditions. The top figures show the (constant) amount of polymer between the plates, the bottom figures the free energy of interaction per surface site. In each graph the curve for $\lambda_0 = 0.5$, $\chi = 0.5$, $\chi_s = 1$, $r = 1000$, and $\theta^t = 3.5$ is given. As in figure 5.2, the effect of chain length is shown in a and b, that of the adsorption energy in c and d, and that of the solvent quality in e and f, whereas curves for different amounts of polymer are given in g and h. The amount of polymer between the plates equals the equilibrium adsorption at large surface separation and $\phi_* = 10^{-6}$, except for two curves for $\phi_* = 10^{-10}$ and $\phi_* = 10^{-2}$, respectively, in graphs g and h. The minimum surface separation occurs at $M = \theta^t$, i.e., when the gap is filled with pure polymer.

athermal solvents ($\chi = 0$) the amount of polymer between the plates is low and hence the interaction minimum is deep and occurs at a short separation. With decreasing solvent quality this minimum shifts to larger distances while its magnitude decreases. At phase separation conditions ($\chi \approx 0.59$ at $r = 1000$ and $\phi_* = 10^{-6}$) the equilibrium adsorbed amount can increase without bounds, but the magnitude of the interaction minimum is constant (compare figure 5.6 for high θ^t).

minimum is present up to larger amounts of polymer. When $\chi = 0.6$, very close

The adsorbed amount at large interplate distance (where full equilibrium applies) is a slowly increasing function of the solution concentration.

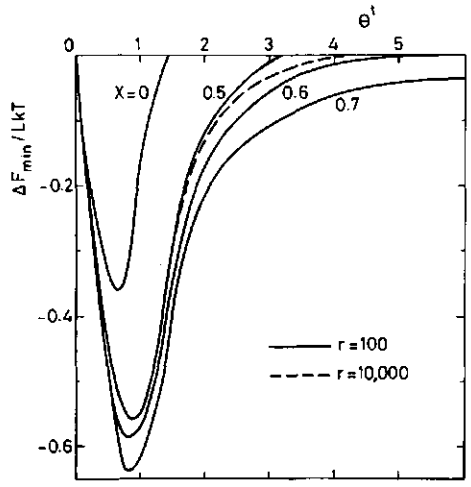

Figure 5.9. Free energy minimum as a function of the total amount of polymer between the surfaces for different solvent qualities. If the minimum is zero (e.g., for $\theta^t > 1.45$ at $\chi = 0$) there is only repulsion between the plates. $\lambda_0 = 0.5$, $\chi_s = 1$, $r = 100$ (full curves, for 4 χ-values), and $r = 10{,}000$ (dashed curves, for $\chi = 0$ and 0.5).

to the critical value $\chi_{cr} = 0.605$ for $r = 100$, ΔF_{min} decreases asymptotically to zero with increasing θ^t. For $\chi = 0.7$ the minimum never disappears, see also figure 5.6. For comparison some curves are given for $r = 10000$. The molecular weight dependence is indeed very low provided that a comparison is made at the same θ^t, hence, at widely different solution concentrations. For athermal solvents, the curves for $r = 100$ and $r = 10000$ virtually coincide. For $\chi = 0.5$ there is some chain length dependence at high adsorbed amounts, mainly because the critical χ value decreases with increasing chain length. For instance, for $r = 10{,}000$ the attraction minimum will not disappear when $\chi > 0.51$.

5.6.3 Comparison with results of other theories

Results for the interaction between two adsorbed layers in full equilibrium with a bulk solution are given by Mackor and Van der Waals[30] and Ash and Findenegg[9]. These authors found repulsion for adsorption of **asymmetric** dimers and tetramers. For oligomers with every segment of the same type, Ash and Findenegg found an attractive force between the plates. A quantitative comparison with this latter result is possible, because their model reduces to ours for $z \to \infty$ and a previous comparison of the adsorption isotherms showed quantitative agreement[23]. We have recalculated figure 2 of ref. (9) using our model and found nearly the same shape of the interaction curves,

both for dimers and tetramers in different solvents, but with the free energy a factor of two lower. We expect a mistake in their free energy axis, because a transition from $z = 12$ to $z \to \infty$ cannot explain such a large difference. Especially for dimers in athermal solvents the same result should have been found.

We concluded already in section 5.6.1 that the prediction of De Gennes that in full equilibrium always attraction occurs agrees with our results.

For restricted equilibrium a quantitative comparison is possible with the free energy equation of Levine et al.[36] and with that of Roe[10]. The latter theory has been developed for adsorption on one plate, but the application to two plates is straightforward. Figure 5.10 shows adsorption (top) and interaction curves (bottom), both for $\chi = 0$ (left) and $\chi = 0.5$ (right). The adsorption curves (figures 5.10a,c) give also the amount of bridging polymer. The interaction curves (figures 5.10b,d) are given according to the theories of Levine et al. (L), Roe (R), and Scheutjens-Fleer (SF).

As discussed in section 5.3.2, Levine et al. used ϕ_i instead of $\langle\phi_i\rangle$ for the fraction of polymer segments around a site in layer i and used a free energy expression in which, implicitly, the osmotic term $-\Sigma(\ln \phi_i^o + \chi\phi_i\langle\phi_i\rangle)$ occurs twice. For $\chi = 0$ the osmotic force is always repulsive (note that $-\Sigma \ln \phi_i^o = \theta^t + \Sigma \tfrac{1}{2} \phi_i^2 + \ldots$. and θ^t is constant). A comparison of the dotted curve and the full curve in figure 5.10b makes it possible to split up the total free energy of interaction in the osmotic term and the free energy due to bridging. The difference between dotted and full curve is just the term $-\Sigma \ln \phi_i^o$ + constants. This difference is much larger than the total interaction energy according to the full curve, which is the sum of the positive osmotic term and the negative bridging term. Hence, the osmotic repulsion and the attraction due to bridging largely compensate each other. In this case the (small) difference results in an interaction curve with a minimum at $M \approx 2$. We have shown in figure 5.8 that this minimum disappears at a higher adsorbed amount. The onset of the osmotic repulsion and the bridging attraction at $M \approx 30$ in figure 5.10b corresponds with the appearance of bridges at that plate separation in figure 5.10a.

The dashed curve in figure 5.10b represents the interaction curve as predicted by the Roe theory. Due to the neglect of tails in this theory, the segment density profile is much steeper. The result is that the onset of bridging occurs at a smaller plate separation than the onset of the osmotic

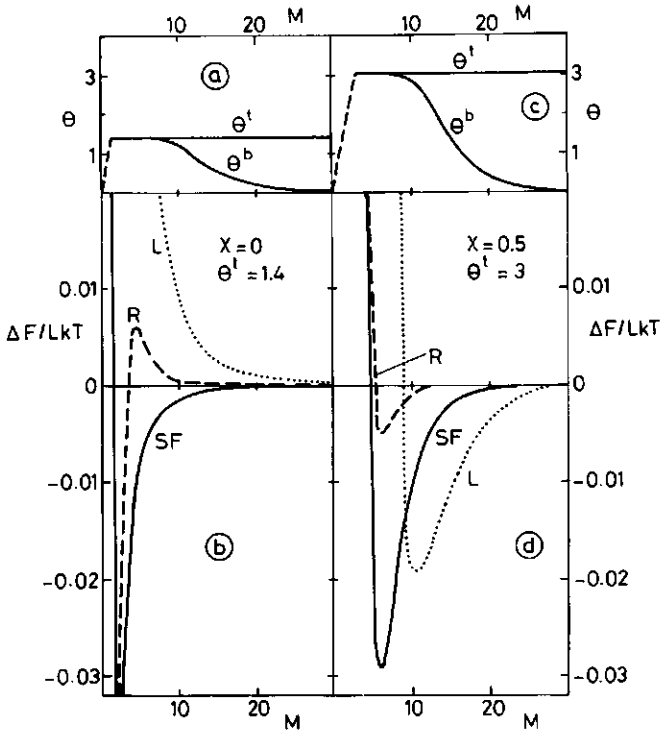

Figure 5.10. Comparison between interaction curves (bottom figures, b and d) according to various theories. Full curves correspond to the present theory (SF), dashed curves to that of Roe (R) and dotted curves to that of Levine (L). The top figures (a and c) give the total amount of polymer θ^t and in addition the contribution of bridging polymer θ^b as derived from the present theory. All curves have been calculated by the present authors. In order to show more clearly the effect of the osmotic term, we have used $\langle\phi_i\rangle$ instead of ϕ_i in Levine's equations where appropriate. Thus, the SF and L curves are based on the same segment density profiles. $\lambda_0 = 0.5$, $\chi_s = 1$, $r = 1000$; a and b: $\chi = 0$, $\theta^t = 1.4$; c and d : $\chi = 0.5$, $\theta^t = 3$.

repulsion between the loop layers, giving rise to a free energy barrier. We have shown in section 5.3.1 that no difference exists between Roe's theory and ours for $M = 1$. In figure 5.10b we see that the curves deviate strongly at $M > 1$. This difference in ΔF arises from the fact that the free energy is very sensitive to small variations in the profile. A consequence is that also the free energy of the reference state (at large plate separations) is different. Despite this problem the existence of a minimum in the interac-

tion free energy in good solvents is fully corroborated, also in Roe's model.

Figures 5.10c and 5.10d give the results for $\chi = 0.5$. The adsorption is much higher and the position of the free energy minimum is shifted to larger plate separations. For the curve form Levine's equations we have used the more correct form $\chi\phi_i\langle\phi_i\rangle$ instead of $\chi\phi_i^2$, i.e., we have used the same segment density profile for the Levine (L) and Scheutjens-Fleer (SF)-curves. The approximate osmotic term $-\Sigma(\ln \phi_i^o + \chi\phi_i^2)$ is always repulsive for $\chi \leq 0.5$, but the more correct form $-\Sigma(\ln \phi_i^o + \chi\phi_i\langle\phi_i\rangle)$, which is the difference between the dotted curve and the full curve in figure 5.10d (apart from a constant), gives a strong attractive contribution in the region between M = 10 and M = 30. However, this contribution is compensated by a bridging term which is in this case **repulsive** unlike at $\chi = 0$. For the region between M = 5 and M = 10 the (correct) osmotic term is repulsive and the bridging term strongly attractive. The dashed curve in figure 5.10d shows that in this case the Roe theory predicts a small minimum without a free energy barrier. The absence of the barrier is probably related to the decreasing steepness of the segment density profile with increasing χ.

A qualitative comparison with results from the Cahn-De Gennes approach shows that there are some discrepancies. At constant amount of polymer, De Gennes[38] found only repulsive forces in good solvents. Klein en Pincus[40], using the same type of analysis, found attraction in bad solvents when the segment density between the surfaces is in the instable region given by the binodal. We find a minimum in the free energy whenever the adsorbed amount is lower than a critical value, and in bad solvents there is always a free energy minimum. As discussed before, the model of De Gennes neglects end effects. However, this cannot be the reason for the discrepancy at low surface coverage, since for a given adsorbed amount we find the attraction to be independent of the chain length, showing that end effects are not dominant in this respect.

5.6.4 Comparison with experimental data

Currently, the only suitable experimental data for testing the theory are those of Klein and coworkers[41,42,45,46,50]. Their results show reversible interaction curves which all exhibit repulsive forces at very

short plate separation. Hence the amount of polymer between the plates does probably not change during compression. We will assume a restricted equilibrium. Qualitatively, all data support the results given in figures 5.7 and 5.8, i.e., there is a minimum in the free energy at a distance comparable to the radius of gyration of a free coil in solution and this minimum is deeper for poorer solvents and lower adsorbed amounts. The minimum disappears for high adsorbed amount in good solvents[45,46]. For a quantitative comparison, the knowledge of the adsorbed amount of polymer would be necessary. However, the reported values are rather uncertain and sometimes contradicting. For instance, in one case the average volume fraction of polystyrene between the mica surfaces was 25% at a distance of 20 nm and 100% at 12 nm[50], i.e., an increase in adsorbed amount of 140% upon compression by less than a factor 2. These uncertainties make a quantitative comparison, as yet, impossible.

In our analysis of the theoretical data, we found, with varying θ^t, a linear relation between ΔF_{min} and M_{min}^{-2}, such that $(\Delta F_{min} - A)M_{min}^{2} = B$, where A is a positive constant for good solvents, zero for θ-solvents and negative for bad solvents. The value of B does not depend on χ and χ_s, varies slightly with r and nearly proportional to the lattice constant λ_1. For $\lambda_1 = 0.25$ ($\lambda_0 = 0.5$) B is around -1.8 kT for r = 100 and B $\approx$ -1.4 kT for r = 1000. The advantage of using B is that it is independent of the scaling of a lattice layer, surface site, or segment lenth. Some experimental data of Klein et al. indicate a B-value between -20 kT and -50 kT, so that posssibly our free energy minima are one order of magnitude too low. The number of available experimental interaction curves for various amounts of polymer is too small for a test on the linearity between ΔF_{min} and M_{min}^{-2}.

5.7 CONCLUSIONS

On the basis of a previously developed lattice model for polymer adsorption, the interaction free energy between two adsorbed polymer layers is derived.

At full equilibrium, when the polymer can freely enter and leave the gap between the surfaces, the interaction is always attractive. The minimum free energy occurs when a monolayer of polymer chains in strictly two-dimensional conformations is sandwiched between the surfaces. A practical consequence might be that stabilization of liquid films by adsorbing homopolymers is

impossible.

If the polymer cannot enter or leave the gap during the time of interaction, the interaction force is attractive at large distances and repulsive at short distances. The attraction is due to bridging of the chains between the opposing walls. In bad solvents an additional osmotic contribution to the attraction exists up to very large distances. The minimum free energy is only slightly above the free energy at full equilibrium at the same plate separation. The attraction is strong for low adsorbances, i.e., for low molecular weight polymer or at low concentrations. This effect explains the bridging flocculation, which is often observed experimentally.

The interaction is determined by the adsorbed amount, rather than by the solution concentration or molecular weight. The range of adsorbed amounts, in which flocculation may occur, decreases with solvent quality. The strongest attraction occurs when the adsorbance on each surface is slightly below 0.5 segments per surface site. However, this strong minimum occurs at a short distance. For a given system, the minimum free energy is nearly inversely proportional to the square of the distance at which it occurs.

At high adsorbed amount the free energy minimum is absent (except in bad solvents) and a strong repulsion occurs. However, in order to obtain a high adsorbed amount, a much higher solution concentration of low molecular weight polymer is required than for longer chains. Hence, at the same solution concentration, high molecular weight polymer is a much better stabilizer.

Comparison with available experimental data of Klein et al. learns that all predictions agree qualitatively, whereas quantitatively the position of the minimum free energy is correct, but its value is possibly one order of magnitude too low. Nevertheless, we have presented the first prediction that both bridging attraction and steric stabilization are possible in good solvents as well.

REFERENCES

1. Vincent, B., Adv. Colloid Interface Sci., 4 (1974) 193.
2. Tadros, T.F., in "The Effect of Polymers on Dispersion Properties", Tadros, T.F., Ed., Academic Press, London, (1982) 1.
3. Yarar, B., in "Solution Behavior of Surfactants", Mittal, K.L.; and

Fendler, E.J., Eds., Plenum Press, New York, **2** (1982) 1333.

4. Kitchener, J.A., Br. Polym. J., **4** (1972) 239.
5. Somasundaran, P., in "Fine Particles Processing", Somasundaran, P., Ed., AIME, New York, Vol. 2 (1980).
6. Silberberg, A., J. Chem. Phys., **48** (1968) 2835.
7. Hoeve, C.A.J., J. Chem. Phys., **44** (1966) 1505.
8. Ash, S.G.; Everett, D.H.; and Findenegg, G.H., Trans. Faraday Soc., **66** (1970) 708.
9. Ash, S.G.; and Findenegg, G.H., Trans. Faraday Soc., **67** (1971) 2122.
10. Roe, R.J., J. Chem. Phys., **60** (1974) 4192.
11. Scheutjens, J.M.H.M.; and Fleer, G.J., J. Phys. Chem., **83** (1979) 1619.
12. DiMarzio, E.A., J. Chem. Phys., **42** (1965) 2101.
13. DiMarzio, E.A.; and Rubin, R.J., J. Chem. Phys., **55** (1971) 4318.
14. De Gennes, P.G., Macromolecules, **13** (1980) 1069.
15. De Gennes, P.G., Macromolecules, **14** (1981) 1637.
16. De Gennes, P.G., Phys, Lett. A, **38** (1972) 339.
17. Clark, A.T.; and Lal, M., J. Chem. Soc., Faraday Trans. 2, **77** (1981) 981.
18. Clark, A.T.; and Lal, M., in "The Effect of Polymers on Dispersion Properties", Tadros, T.F., Ed., Academic Press, London, (1982) 169.
19. Feigin, R.I.; and Napper, D.H., J. Colloid Interface Sci., **75** (1980) 525.
20. Hoeve, C.A.J., J. Polym. Sci. C, **30** (1970) 361.
21. Hoeve, C.A.J., J. Polym. Sci. C, **34** (1971) 1.
22. Scheutjens, J.M.H.M.; and Fleer, G.J., J. Phys. Chem., **84** (1980) 178.
23. Scheutjens, J.M.H.M.; and Fleer, G.J., in "The Effect of Polymers on Dispersion Properties", Tadros, T.F., Ed., Academic Press, London, (1982) 145.
24. Fleer, G.J.; and Scheutjens, J.M.H.M., Adv. Colloid Interface Sci., **16** (1982) 341.
25. Barnett, K.; Cosgrove, T.; Crowley, T.L.; Tadros, T.F.; and Vindent, B., in "the Effect of Polymers on Dispersion Properties", Tadros, T.F., Ed., Academic Press, London, (1982) 183.
26. Cosgrove, T.; Vincent, B.; Crowley, T.L.; and Cohen Stuart, M.A., ACS Symposium Series, **240** (1984) 147.
27. Cohen Stuart, M.A.; Scheutjens, J.M.H.M.; and Fleer, G.J., J. Polym. Sci., Polym. Phys. Ed., **18** (1980) 559.

28. Mackor, E.L., J. Coll. Sci., **6** (1951) 492.
29. Dolan, A.K.; and Edwards, S.F., Proc. Roy. Soc., **A337** (1974) 509.
30. Mackor, E.L.; and van der Waals, J.H., J. Coll. Sci., **7** (1952) 535.
31. Meier, D.J., J. Phys. Chem., **71** (1967) 1861.
32. Hesselink, F.T., J. phys. Chem., **75** (1971) 65.
33. Hesselink, F.T.; Vrij, A.; and Overbeek, J.T.G., J. Phys. Chem., **75** (1971) 2094.
34. Dolan, A.K.; and Edwards, S.F., Proc. Roy. Soc., **A343** (1975) 427.
35. Gerber, P.R.; and Moore, M.A., Macromolecules, **10** (1977) 476.
36. Levine, S.; Thomlinson, M.M.; and Robinson, K., Discuss. Faraday Soc., **65** (1978) 202.
37. Flory, P.J., "Principles of Polymer Chemistry", Cornell University Press, Ithaca, NY, (1953).
38. De Gennes, P.G., Macromolecules, **15** (1982) 492.
39. Cahn, J., J. Chem. Phys., **66** (1977) 3667.
40. Klein, J.; and Pincus, P., Macromolecules, **15** (1982), 1129.
41. Klein, J., Nature, **288** (1980) 248.
42. Klein, J., Adv. Colloid Interface Sci., **16** (1982), 101.
43. Scheutjens, J.M.H.M.; and Fleer, G.J., Adv. Colloid Interface Sci., **16** (1982) 361.
44. Scheutjens, J.M.H.M.; and Fleer, G.J., Adv. Colloid Interface Sci., **18** (1983) 309.
45. Israelachvili, J.N.; Tirrell, M.; Klein, J.; and Almog, Y., Macromolecules, **17** (1984) 204.
46. Klein, J.; and Luckham, P., Nature, **308** (1984) 836.
47. Gaylord, R.J., J. Colloid Interface Sci., **87** (1982) 577.
48. Helfand, E.; and Sapse, A.M., J. Chem. Phys., **62** (1975) 1327.
49. Powell, M.J.D., in "Numerical Methods for Nonlinear Algebraic Equations", Rabinowitz, P., Ed., Gordon and Breach, London, (1970) 87; ibid., 115.
50. Klein, J.; Almog, Y.; and Luckham, P., ACS Symposium Series, **240** (1984) 227.

6 MACROMOLECULES IN VARIOUS INTERFACIAL SYSTEMS

6.1 INTRODUCTION

In the previous chapters the adsorption of homopolymers on a single surface and the interaction between two adsorbed homopolymer layers have been examined in some detail. Although adsorption of homopolymers is already a complex phenomenon, the principles of the theory developed in chapter 2 can be succesfully applied to even more complicated systems. In this chapter the following examples will be discussed. Full account of the details has been or will be given elsewhere.

a. Adsorption of polydisperse polymer. Most polymers used in practice are polydisperse. This fact has been ignored in many polymer adsorption studies. Only recently, the profound effects of the molecular weight distribution on adsorption phenomena have been realized. In (semi-)dilute solutions long chains adsorb preferentially over shorter ones. This leads to apparent irreversibilities, such as adsorption-desorption hysteresis and sol concentration dependence of the adsorbed amount. The adsorption behaviour of polydisperse polymer is quite different from that of homodisperse polymer. Results from the first theory for adsorption of polymer having an arbitrary molecular weight distribution will be given below.

b. Adsorption of star-branched polymer. Branching is an important chain variable influencing the properties of polymers and of polymer solutions. The effect of branches on the adsorption properties of polymers has not been examined before. The capability of the new theory to account for a nonlinear structure of the chains makes it possible to compute the adsorption of branched polymer. As an example, the adsorption of star-branched polymer will be compared with that of linear polymer of the same molecular weight.

c. Adsorption of polyelectrolytes. The adsorption of this important class of polymers is dominated by electrostatic interactions, even at very high salt concentrations. A detailed picture in which the electrostatic interactions and the configurational properties are combined in a proper way

is now emanating.

d. The structure of lipid bilayers. An extension of the theory to account for adsorption of copolymers will be discussed briefly. A special case of a copolymer system is a lipid bilayer. The possibility of examining copolymers under phase separation conditions is exploited to study the association of amphiphatic molecules into bilayer structures. Especially the distribution of polar head groups across the bilayer and the water content of the membrane have been neglected in previous theories for bilayer structures.

e. The amorphous phase of semicrystalline polymer. The mechanical and physical properties of semicrystalline polymer depend largely on the structure of the amorphous polymer regions which interconnect lamellae of crystalline polymer. Segment density profiles as a function of strain have been obtained.

f. Depletion flocculation and restabilization. Non-adsorbing polymer at high concentrations affect the stability of colloidal systems by osmotic forces. Using results from the present theory, a better quantitative prediction of flocculation conditions is gained and a thermodynamic restabilisation mechanism could be proposed.

This list is only a small fraction of the diversity of systems that can be tackled by the present theory. As will be shown below, the incorporation of special properties of the system hardly affect the basic equations. The flexibility and clearness of the model and the detailedness of the results are comparable with those of Monte Carlo studies, whereas the required computing times are very much shorter.

In order to facilitate the explanation of the changes that are to be made in the equations for each of the examples listed above, a summary of the basic equations which have been treated extensively in chapters 2 and 5 will be given first.

The chain conformations are enumerated using a lattice model in which each walk along a series of r lattice sites corresponds to a particular spatial arrangement of the polymer chain. The lattice layers parallel to the surface are numbered $i = 1,2,\ldots,M$. Each step represents a segment-segment bond and has a probability λ_1 for crossing between adjacent lattice layers and λ_0 for moving within the same layer, hence $\lambda_0 + 2\lambda_1 = 1$. In addition, for each visit in a layer i, the walk is weighted by a factor P_i to account for external fields and mutual interactions between polymer segments. Conse-

quently, P_i is a function of the local concentrations. A conformation is defined as the order of lattice layers that are visited during the walk. For a convenient representation of the equations the notation i(s,c) will be used for the layer number where segment s of conformation c finds itself. For each specified conformation i(s,c) is fully known. Then, the probability P_c of conformation c is given by

$$P_c = A \lambda_0^q \lambda_1^{r-1-q} \prod_{s=1}^{r} P_{i(s,c)} \tag{6.1}$$

In this equation, A is a normalization constant that depends on the total number of chains in the system or on the equilibrium concentration of polymer in the bulk solution, q the number of bonds between segments in the same layer, and $P_{i(s,c)}$ the weighting factor of segments being in layer i(s,c).

A conformation c has $r_{i,c}$ segments in layer i, hence he volume fraction of segments in layer i is given by

$$\phi_i = \sum_c r_{i,c} P_c \tag{6.2}$$

In eq. (6.2) a normalization constant is omitted, since it can be included in A. The evaluation of the segment density distribution $\{\phi_i\}$ from the weighting factors $\{P_i\}$ via eqs. (6.1) and (6.2) is most conveniently carried out by using the matrix method (see chapters 2 and 3).

The weighting factor P_i, also called the free segment probability, gives the unnormalized probability of a 'chain' of one segment in layer i. Such a monomer differs from a solvent molecule by its interactions only and hence, the preference factor for a monomer over a solvent molecule for a site in i, P_i/ϕ_i^o, is given by the Boltzmann factor $\exp(-\Delta U_i/kT)$ that accounts for the energy difference ΔU_i when a solvent molecule in i is replaced by a monomer.

$$P_i = \phi_i^o e^{-\Delta U_i/kT} \tag{6.3}$$

Again, any normalization constant is accounted for in A.

The exchange energy comprises contributions from external fields such as the differential adsorption energy $-\chi_s kT$ in layer 1 adjoining the surface or the mutual interactions between segments and solvent. This latter contribution is conveniently expressed in the Flory-Huggins parameter χ. The net interaction energy of a solvent molecule in i surrounded by an average vol-

ume fraction $\langle\phi_i\rangle$ of segments is $\chi\langle\phi_i\rangle$ kT and that of a monomer in a volume fraction $\langle\phi_i^o\rangle$ of solvent equals $\chi\langle\phi_i^o\rangle$ kT. Consequently, in the absence of other interactions,

$$-\Delta U_i/kT = \chi_s \delta_{1,i} + \chi(\langle\phi_i\rangle - \langle\phi_i^o\rangle) \qquad (6.4)$$

Eqs. (6.1-4) form a set of M simultaneous nonlinear equations in M unknowns ϕ_i ($=1-\phi_i^o$) that can be solved numerically. Once the concentration profile is known, the equilibrium probability of each individual conformation is available from eq. (6.1).

6.2 ADSORPTION OF POLYDISPERSE POLYMER

Most polymer samples used in practice comprise a mixture of polymer chains having different chain lengths. In chapter 4 it was pointed out that from (semi-)dilute solutions long chains adsorb preferentially over shorter ones and a simple equation was derived for the relative adsorption from polymer mixtures. In principle, the Roe theory[1] can be used for adsorption of polydisperse polymer. However, the total number of simultaneous equations that are to be solved is proportional with M (the number of lattice layers) and with the number of components present in the polydisperse sample. In this way, the computational effort increases dramatically with increasing number of species. Recently, some calculations have been done for a mixture of eight monodisperse fractions[2].

The present theory is very suitable for adsorption of polydisperse polymer[3]. Eqs. (6.3) and (6.4) remain valid, because they describe the interactions of a free monomer in a concentration profile. The chain length affects only eqs. (6.1) and (6.2). In a polymer sample with chain length distribution $\{\nu(r)\}$ a fraction $\nu(r)$ of the chains are r segments long. For each of these fractions eqs. (6.1) and (6.2) can be applied after a minor modification:

$$P_c(r) = A\ \nu(r)\ \lambda_0^{\,q}\ \lambda_1^{\,r-1-q} \prod_{s=1}^{r} P_{i(s,c)} \qquad (6.1a)$$

$$\phi_i(r) = \sum_c r_{i,c}\ P_c(r)\ ; \qquad \phi_i = \sum_r \phi_i(r) \qquad (6.2a)$$

With the help of the matrix method, the effort for the evaluation of $\{\phi_i\}$ is only slightly larger than that for homodisperse polymer[4]. Hence, a general theory for adsorption of polydisperse polymer is now available.

A few results are collected in figures 6.1-4. The degree of polydispersity is expressed as the ratio r_w/r_n, where r_w is the weight average and r_n the number average chain length. The polydispersity effects on the adsorption isotherms as predicted earlier[5] on the basis of a very simple model are fully corroborated.

Surface fractionation is illustrated in figure 6.1. The chain length distribution of a polymer sample according to a (truncated) Flory distribution before adsorption (full curve, $r_w/r_n = 2.06$) is wider than that of the adsorbate (dashed curve, $r_w/r_n = 1.48$) and of the polymer in the solution (dotted curve, $r_w/r_n = 1.65$). The number average chain length r_n of the adsorbed polymer is five times as high as that of the nonadsorbed fraction. The overlap of solution and adsorbate distributions occurs over only half a decade in chain length. This result agrees with experimental data of Vander Linden and Van Leemput[6].

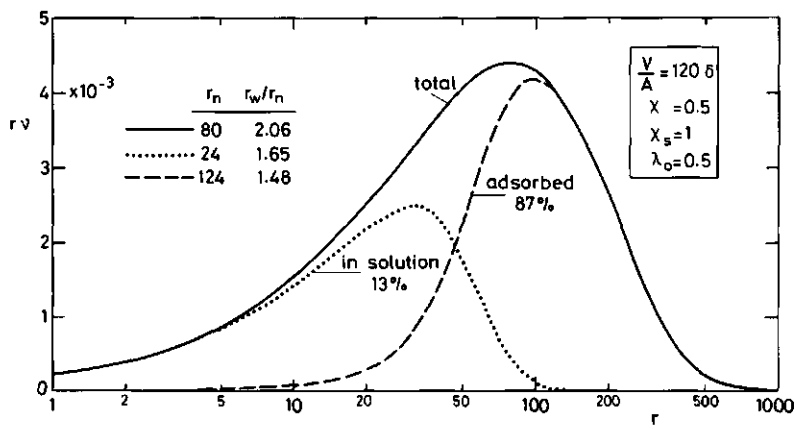

Figure 6.1. Adsorption fractionation for a polydisperse sample with a Flory distribution. The weight distributions, $r\nu(r)$, of the polymer before adsorption (full curve, $M_w/M_n = 2.06$), in the adsorbate (dashed curve, $M_w/M_n = 1.48$), and in the solution (dotted curve, $M_w/M_n = 1.65$) are given. In this case 87% of the total amount of polymer is adsorbed. $\lambda_0 = 0.5$, $\chi = 0.5$, $\chi_s = 1$, V/A = 120 lattice layers.

With increasing total amount of polymer (or with decreasing surface area at constant polymer dosage), a smaller fraction of the total molecular weight distribution can find a place on the surface. Consequently, the average molecular weight on the surface shifts to higher values and since long molecules adsorb with longer loops and tails, the adsorbed amount increases as well. This is shown in figure 6.2 where adsorption isotherms are given for two average chain lengths and different polydispersity ratios of polymer samples having a Schulz-Flory molecular weight distribution. For nearly homodisperse polymer ($r_w/r_n < 1.01$) the adsorbed amount depends only very weakly on the concentration (high affinity isotherms), but the slope of the isotherm increases with increasing polydispersity ratio. Experimental observations confirm this prediction. The adsorption isotherm of a fractionated polymer sample shows a sharp bend between the very steep initial rise and the nearly horizontal plateau, whereas the adsorption of a polydispers sample increases more gradually with increasing solution concentration[7].

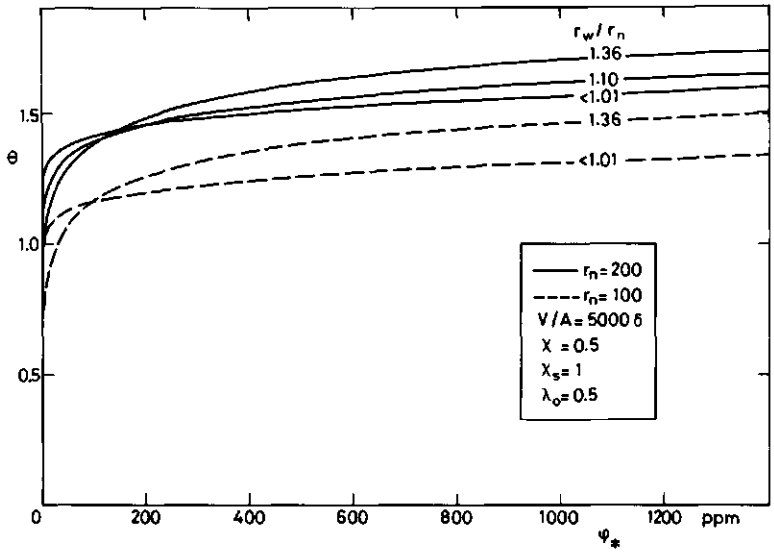

Figure 6.2. Effect of polydispersity on the shape of the adsorption isotherm. Isotherms with $r_n = 100$ (dashed curves) and $r_n = 200$ are given for different degrees of polydispersity, r_w/r_n (Schultz-Flory distributions). A higher degree of polydispersity leads to a more rounded shape of the isotherm and a less horizontal (pseudo-)plateau. $\lambda_0 = 0.5$, $\chi = 0.5$, $\chi_s = 1$, V/A = 5000 lattice layers.

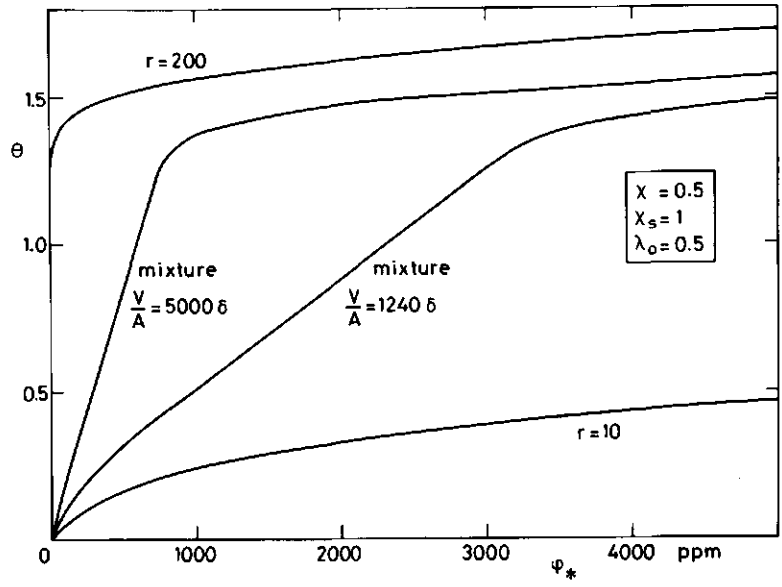

Figure 6.3. Adsorption isotherms for a bimodal mixture of short (r = 10) and long (r = 200) chains, at two V/A ratios. The weight fraction of long chains in the mixture is 0.25. For comparison, the isotherms for the homodisperse samples are also shown. $\lambda_0 = 0.5$, $\chi = 0.5$, $\chi_s = 1$.

In figure 6.3 theoretical isotherms of a bimodal mixture of two homodisperse polymer samples are given and compared with the isotherms of the unmixed samples. From the binary mixture, the long chains (r = 200) adsorb preferentially over the short chains (r = 10). This results in a linearly increasing isotherm section: in this linear region an increasing amount of long chains displaces the short chains from the surface, until virtually the entire adsorbate consists of long molecules and the short ones are all in the solution. A further increase of the concentration does not change the adsorbate composition and, hence, the adsorption levels off. The concentration of the displaced amount of polymer is proportional to the surface area to solution volume ratio A/V. Consequently, the slope of the middle region of the isotherm is proportional to V/A. In this model this ratio is Mδ, the number of lattice layers times the thickness of a lattice layer. The general shape of the curves is the same as found experimentally[5,7,8].

In figure 6.4 adsorption isotherms are compared with a desorption isotherm. The lower adsorption isotherm applies to a V/A of 5000δ, corresponding to a 1% (w/v) solution of an adsorbent of 20 m^2/g if δ = 1 nm, and has a rounded shape: the adsorption increases with increasing amount of polymer. At 1200 ppm the total amount of polymer, θ^t, in the system is 7.7 equivalent monolayers, the adsorbed amount, θ, is 1.6 monolayers. Desorption by dilution is simulated by increasing M (=V/Aδ) while keeping θ^t constant. When $V/A = 5.10^5\delta$ the low molecular weight polymer in the solution is diluted by a factor of 100, but the high molecular weight fraction on the surface is hardly affected. Hence, the desorption isotherm of polydisperse polymer does not coincide with the adsorption isotherm, even if the system is always in

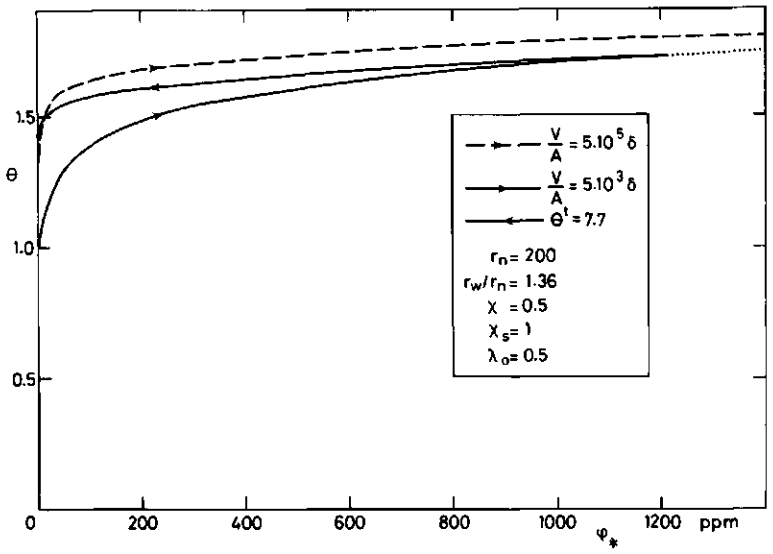

Figure 6.4. Two adsorption isotherms and one desorption isotherm for a polydisperse polymer sample with a Schultz-Flory distribution (M_w/M_n = 1.36). Although for each case the system is in full equilibrium, the isotherms do not coincide because of surface fractionation effects. The adsorption isotherms (arrows pointing to the right) are given for V/A = 5000 lattice layers (full curve) and V/A = 500,000 lattice layers (dashed curve). The desorption isotherm (arrow pointing to the left) simulates desorption by dilution and is given for a constant amount of polymer in the system (7.7 equivalent monolayers) with from right to left increasing V/A. λ_0 = 0.5, χ = 0.5, χ_s = 1.

full equilibrium. The dashed curve shows the increase in adsorption when the amount of polymer is increased again at $V/A = 5.10^5\delta$.

The results show that fractionation effects dominate the adsorption of polydisperse polymer. A detailed examination of these effects has become possible by a simple modification of the present theory. Experimentally observed trends for the adsorption of polydisperse polymer are accurately predicted by this model.

6.3 ADSORPTION OF STAR-BRANCHED POLYMER

Branches in a polymer chain may have various effects on the surface activity of the polymer. For instance, their frequency and length distribution may vary from molecule to molecule so that the branches broaden the molecular weight distribution of the polymer. In addition, the branch points may have a different affinity for the surface than other monomer units. Finally, branch points decrease the local flexibility of the chain.

These effects can be eliminated by choosing an ideally flexible star-branched model chain of which all arms are equal in length and the single branch point has the properties of one segment. A linear chain can be considered as a molecule with two arms. Thus, a first description of the influence of branching on the adsorption behaviour of polymer can be presented by changing the degree of branching of an adsorbing homodisperse polymer sample, while keeping the total number of segments per chain constant.

The basic equations (6.1-4) need no modification for branched polymer, but the set of possible conformations depends on the structure of the chain[9]. Since each arm of a star molecule is identical, the segment distribution of only one arm is to be computed (compare the inversion symmetry for linear chains).

In figure 6.5 the adsorbed amount θ is given as function of the number of arms per molecule. The total number of segments per molecule is kept constant (about 1000 segments). The effect of branching on the surface activity is very low. At $\chi_s = 1$ and $\phi_* = 10^{-6}$, a weak optimum can be observed around 6 arms per molecule. The strongest effect can be expected when the adsorption energy χ_s is just beyond the critical value for adsorption ($\chi_{sc} = 0.29$ if $\lambda_0 = 0.5$). Therefore, two curves are given for $\chi_s = 0.3$ as well. They show a slight increase of θ with increasing degree of branching

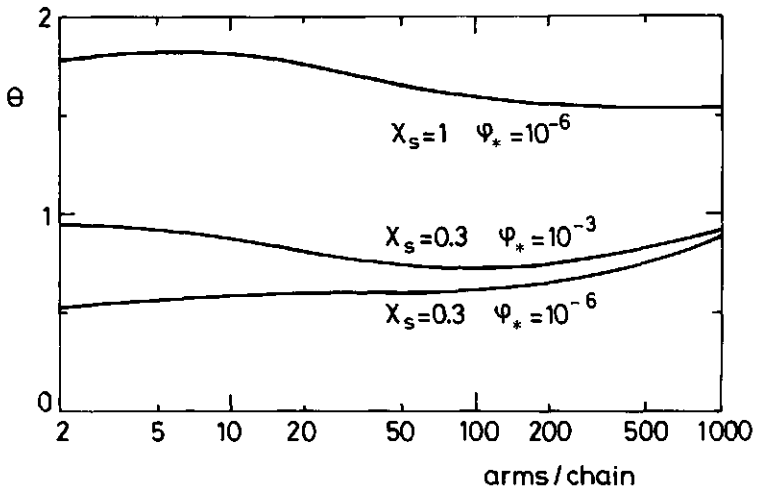

Figure 6.5. The adsorbed amount as a function of the number of arms per chain for a star-branched polymer sample. The total number of segments per molecule is about 1000. The adsorption energy and the concentration in the solution are indicated. λ_0 = 0.5, χ = 0.5.

at low concentrations (ϕ_* = 10^{-6}) and a weak minimum at high concentrations (ϕ_* = 10^{-3}), respectively.

The influence of branching on the structure of the adsorbed polymer layer is illustrated in figure 6.6. The segment density distributions of linear molecules and of chains with 50 arms are plotted on a logarithmic scale. Clearly, branching hardly affects the segment density at very small distances from the surface and decreases the segment density at larger distances, so that the overall shape of the molecules becomes more compact (full curves). This is caused by a decreasing possibility of forming long loops and tails. As the number of chain ends increases with increasing number of arms, the region over which the segment density of tails (dotted curves) dominates is larger for branched molecules than for linear chains. The distribution of loop segments (dashed curves) which is an exponential function for linear chains, is no longer exponential but decreases more strongly for branched molecules.

Density profiles of branch points (or middle segments) for different degrees of branching are shown in figure 6.7. For linear chains the density of middle segments decays gradually with increasing distance from the sur

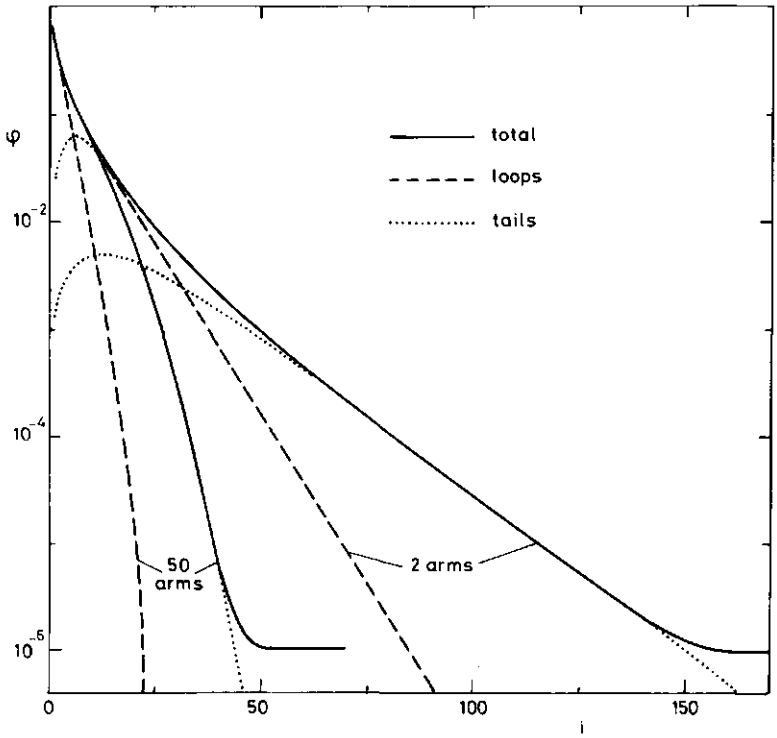

Figure 6.6. Segment density profiles for adsorbed linear (2 arms) and star branched (50 arms) polymer. The total volume fraction (full curves), that due to loops (dashed curves), and that due to tails (dotted curves) are plotted on a logarithmic scale as a function of the distance from the surface. $\lambda_0 = 0.5$, $\chi = 0.5$, $\chi_s = 1$, $r = 10001$, $\phi_* = 10^{-6}$.

face. With increasing number of arms per chain the average position of the branch points shifts towards the surface, until virtually all of them are in the first two lattice layers. A further increase in number of arms causes the branch points to prefer the second layer.

Obviously, a model chain in which one segment forms flexible joints for 10 or even more chain branches is not very realistic. However, from the above results it follows that branching in itself does hardly affect the surface activity of the polymer. Through its influence on, e.g., the degree of polydispersity a much greater effect can be expected. For instance, Kawaguchi and Takahashi[10] found that the amount adsorbed onto metal surfaces

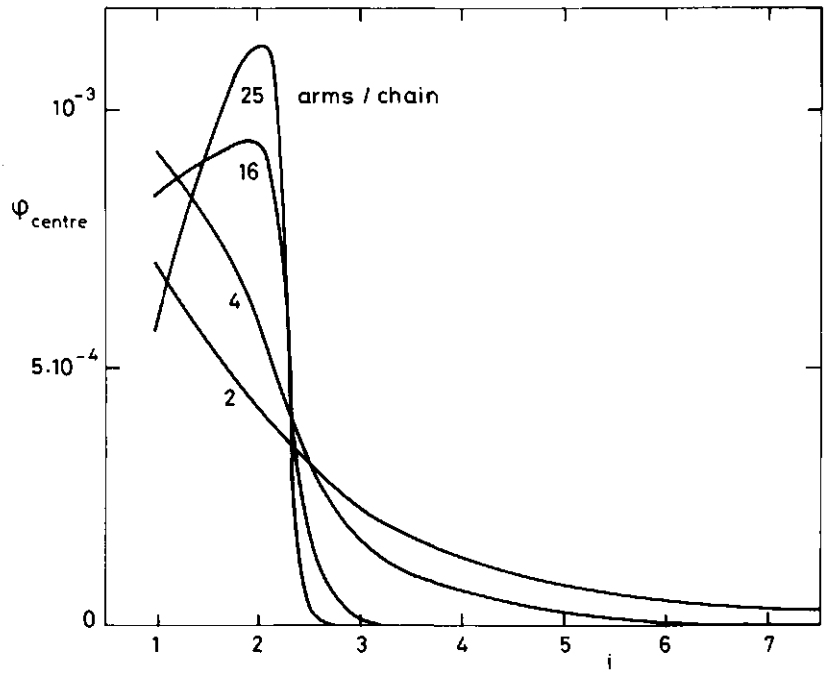

Figure 6.7. Segment density profiles for branch points of adsorbed star molecules of 1001 segments. The number of arms per molecule is indicated. $\lambda_0 = 0.5$, $\chi = 0.5$, $\chi_s = 1$, $\phi_* = 10^{-6}$.

was twice as high when comb-branched polystyrene was used as compared to the adsorbance of linear polystyrene of nearly the same average molecular weight. The establishment of equilibrium was very slow (about two days) and the isotherms show a rounded shape. These observations strongly suggest that, contrary to their conclusion, the increase in adsorption is not due to branching as such, but is caused by surface fractionation.

6.4 ADSORPTION OF POLYELECTROLYTE

Despite the widespread use of polyelectrolytes as adsorbates in many industrial processes, such as in food technology, pharmacy, and paint production, a suitable theory for polyelectrolyte adsorption was lacking until recently. Since electrostatic interactions extend over large distances, it

is not easy to assess the shape of the equilibrium segment density profile of adsorbed polyelectrolyte. Predetermined profiles, such as used by Hesselink[11,12] and Silberberg[13], restrict the validity of a theory severely. In the present theory the segment density profile is found as the result of the minimization of the free energy of the system and can assume any form. Hence, after incorporation of electrostatic interactions, a promising approach for adsorption of polyelectrolytes becomes available. Such an approach has been worked out for strong polyelectrolytes by Van der Schee[2] extending the model described in the previous chapters. He found that a similar extension of the Roe theory gives nearly the same results at low salt concentrations. At higher ionic strength, the predictions of the two theories diverge, due to the neglect of end effects in the Roe theory which become more important when the polyelectrolyte charges are screened by the counterions. A brief description of the theory and some preliminary results will be presented here. The case of weak charged groups on the polyelectrolyte is included[14].

The main difference between polyelectrolytes and non-ionic polymer is the presence of charges on the chains. In principle, the set of conformations is not different, hence eqs. (6.1) and (6.2) are not affected. The only change to be made is in eq. (6.4), containing the energy difference ΔU_i between that of a segment and of a solvent molecule in layer i. For a charged segment with valency z (sign included) and average degree of ionization α_i (that may vary with increasing distance from the surface), and an uncharged solvent molecule, eq. (6.4) becomes a function of the local potential ϕ_i:

$$-\Delta U_i/kT = \chi_s \delta_{1,i} + \chi(\langle\phi_i\rangle - \langle\phi_i^o\rangle) - \alpha_i z e\phi_i/kT \qquad (6.4a)$$

In eq. (6.4a), e is the elementary charge. For strong polyelectrolytes $\alpha_i = 1$, whereas for weak polyelectrolytes the degree of ionization is a function of the local concentration c_i and valency z_c of potential-determining (p.d.) ions and, hence, of the local potential. For example, the dissociation constant K_d for monovalent segments and one type of monovalent p.d. ions (usually H^+ or OH^-) is given by

$$K_d = \frac{\alpha_i}{1-\alpha_i} c_i \qquad (z = z_c = \pm 1) \qquad (6.5)$$

Then,

$$\alpha_i = \frac{1}{1 + c_i/K_d} = \frac{\alpha_*}{\alpha_* + (1-\alpha_*)c_i/c_*} \qquad (z = z_c = \pm 1) \qquad (6.6)$$

where α_* and c_* are the degree of dissociation of segments and the concentration of p.d. ions, respectively, in the bulk solution. For other cases or higher valencies, eqs. (6.5) and (6.6) may be more complex but their derivation is straightforward. The local concentration of p.d. ions of valency z_c is related to the local potential by

$$c_i/c_* = e^{-z_c e(\psi_i - \psi_*)/kT} \qquad (6.7)$$

Thus, the weighting factors $\{P_i\}$ are now a function of both the concentration profile $\{\phi_i\}$ and the potential profile $\{\psi_i\}$, through eqs. (6.3) and (6.4a-7).

Obviously, a relation between $\{\psi_i\}$ and $\{\phi_i\}$ is necessary to obtain a unique relation between $\{P_i\}$ and $\{\phi_i\}$ such as in the case for uncharged polymers. To accomplish this for strong polyelectrolytes, Van der Schee has used a model of parallel charged planes, see figure 6.8. The charges of the segments within each layer are smeared out over a plane through the centres of the lattice sites. All other ions are thought as point charges that are

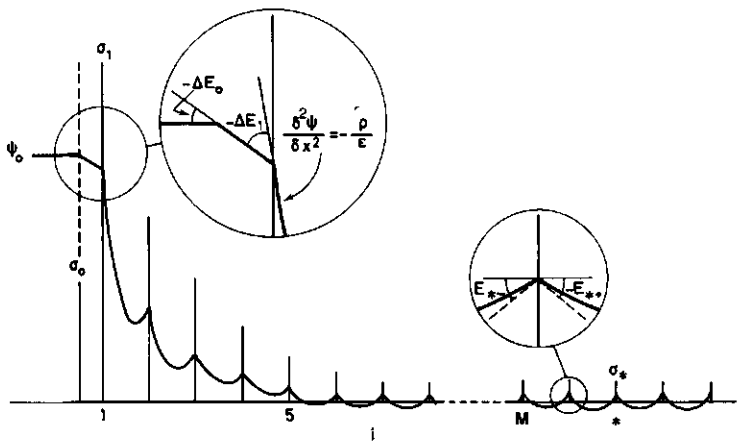

Figure 6.8. Schematic potential profile for a positive surface potential ψ_0 and an adsorbing positively charged polyelectrolyte. At each plate the plane charge causes the field strength to change discontinuously.

distributed between the fixed planes according to the Poisson-Boltzmann (PB) distribution. A few modifications of the model have been tested, in which the plane charges of the segments are replaced by space charges or wherein the small ions are of finite size. These modifications hardly affect the results and complicate the calculations significantly.

If the plane charges are only due to the segmental charges, the plane charge density σ_i of plate i is proportional to the segment concentration ϕ_i, or

$$\sigma_i = \alpha_i \, z \, e \, \phi_i / a_0 \tag{6.8}$$

where a_0 is the cross sectional area of a lattice site. Across plate i the field strength $E(x) = \partial\psi(x)/\partial x$ in the direction x, perpendicular to the surface, changes discontinuously by an amount $-\sigma_i/\varepsilon$:

$$\Delta E_i = E_{i+} - E_{i-} = - \frac{\sigma_i}{\varepsilon} \tag{6.9}$$

where ε is the dielectric permittivity and the notations E_{i+} and E_{i-} stand for $\mathrm{Lim}_{\delta \to 0} \, E_{i+\delta}$ and $\mathrm{Lim}_{\delta \to 0} \, E_{i-\delta}$, respectively.

In the bulk solution the same (artificial) plane charges are used in order to avoid any irregularities between the surface phase and the solution. Across each plate in the bulk solution, the field strength changes sign, hence $E_{*+} = - E_{*-} = \frac{1}{2} \Delta E_*$, or

$$E_{*+} = - E_{*-} = - \frac{\sigma_*}{2\varepsilon} \tag{6.10}$$

The calculation of the potential profile for the layers $i = 1,2,\ldots,M$ involves the following iteration, starting with an initial guess for $\phi_M - \psi_*$. Since $\phi_M - \psi_*$ will be low, the Debije-Hückel (DH) approximation is applicable for the field strength E_{M+} at the solution side of plate M. Obviously, $E_{M+} = E_{*+}$ when $\phi_M = \phi_*$. Hence,

$$E_{M+} = - \kappa(\phi_M - \psi_*) - \frac{\sigma_*}{2\varepsilon} \tag{6.11}$$

The reciprocal Debije length κ is given by the ionic strength in the solution:

$$\kappa^2 = \frac{e^2}{\varepsilon\, kT} \sum_j z_j^2\, n_j(*) \qquad (6.12)$$

where z_j and $n_j(*)$ are the valency and concentration in the bulk solution of ion type j, respectively, and ε is the dielectric constant. The summation includes the p.d. ions, originating from the polymer, but not the polymer segments since their presence is accounted for in $\{\sigma_i\}$.

The field strength E_{M-} follows from eqs. (6.6-9). Starting with $\psi_M - \psi_*$ and E_{M-}, numerical integration of the PB-equation

$$\frac{\partial^2 \psi(x)}{\partial x^2} = -\frac{e\, a_0}{\varepsilon} \sum_j z_j\, n_j(x)\, e^{-z_j e(\psi(x)-\psi_*)/kT} \qquad (6.13)$$

from x = M down to x = M-1 gives $\psi_{M-1} - \psi_*$ and E_{M-1+} at plate M-1. Here, x is the dimensionless distance from the surface, expressed as the number of lattice layers. Repeatedly applying eqs. (6.6-9) and (6.13) gives eventually $\psi_1 - \psi_*$ and E_{1-} in the first layer. This completes one cycle of the iteration.

At the surface a boundary condition applies. For instance $E_{1-} = -\sigma_0/\varepsilon$, if the surface charge density σ_0 is constant. Alternatively, the potential at the surface must be equal to a constant potential ψ_0, see figure 6.8. The iterations are continued with new values for ψ_M until this boundary condition is obeyed. The potential profile $\{\psi_i\}$ found in this way is substituted into eq. (6.4a).

The same procedure may be followed for the incorporation of electrostatic interactions in the Roe theory, since the energy terms in eq. (6.4a) can replace the energy terms in eq. (29) of Ref. (1).

For strong polyelectrolytes (and polyelectrolytes with a constant degree of ionization α, independent of the local potential) a number of results have been given by Van der Schee et al.[2,15-18]. At low salt concentration the adsorbed chains lay essentially flat on the surface. The adsorbed amount increases with increasing salt concentration, up to very high ionic strength. Comparison with experimental data learns that for well-defined systems a semi-quantitiative agreement is found[2,15-19].

The dielectric permittivity ε depends on the local concentration of polymer. As a first approximation we may estimate ε in layer i by

$$\varepsilon_i = \varepsilon^o + (\varepsilon^p - \varepsilon^o)\, \phi_i \qquad (6.14)$$

where ε^p is the permittivity of pure polymer and ε^o that of water. Except

for the first layer (i = 1), it is clear that for strong polyelectrolytes $\varepsilon_i \approx \varepsilon^o$, since ϕ_i is very low. The variation of ε in the first layer can be compensated by a small change in the adsorption energy, which gives also a contribution per adsorbed segment. For weak polyelectrolytes the variation of ε in the first few layers is often significant.

Figures 6.9-11 show some preliminary results[14] for weak polyelectrolytes as predicted by the modified Roe theory. It can be expected that this theory underestimates the adsorbance at high ionic strength, where the adsorbed amount is relatively large. The data are calculated for $\varepsilon^p/\varepsilon^o = 3/80$, so that ε_i is mainly determined by the dielectric permittivity ε^o and volume fraction ϕ_i^o of water.

In figure 6.9 adsorption isotherms are given for polyacids with different intrinsic dissociation constants K of the segments, adsorbing on an uncharged surface. The curves for pK = ∞ and pK = $-\infty$ correspond to adsorption isotherms for non-ionic polymers and strong polyelectrolytes, respectively. No external acid or base is assumed to be present, so that the pH

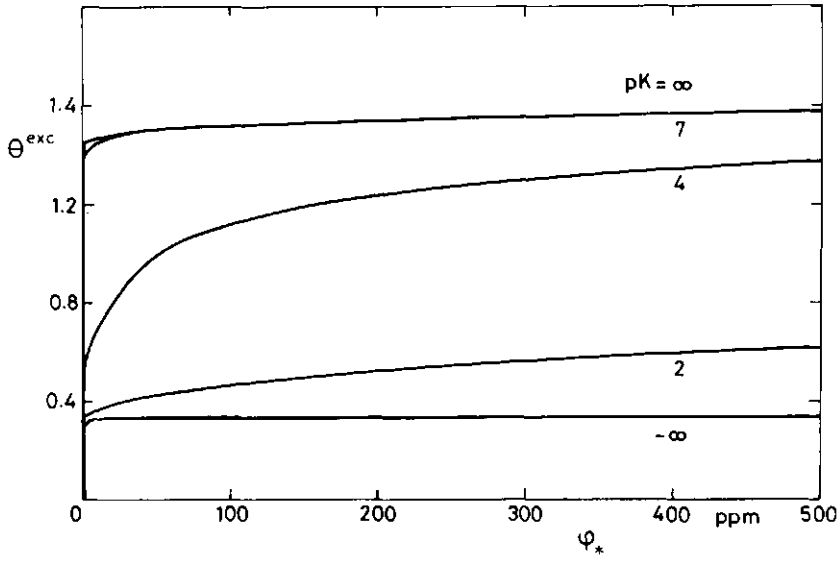

Figure 6.9. Adsorption isotherms of a polyacid adsorbing on an uncharged surface. The pH depends on the concentration of polyacid (no other acid or base is present). The intrinsic pK values of the segments are indicated. $\lambda_0 = 0.5$, $\chi = 0.5$, $\chi_s = 1$, $r = 500$, $z = -1$, $\varepsilon^p/\varepsilon^o = 3/80$, $a_0 = 1\ nm^2$, $\sigma_0 = 0$, salt concentration: 1 M (monovalent).

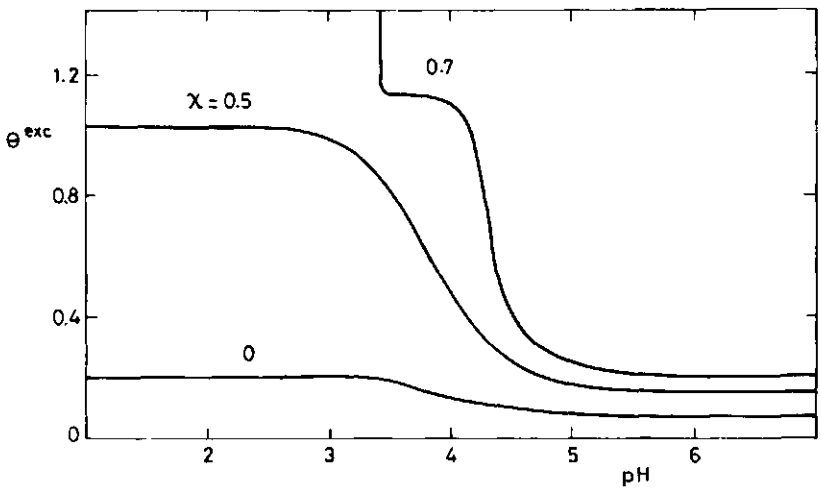

Figure 6.10. Adsorption of polyacid as a function of pH on an uncharged surface for different (nonionic) solvent qualities. $\lambda_0 = 0.5$, χ is indicated, $\chi_s = 0.5$, $r = 500$, $\phi_* = 10^{-4}$, $z = -1$, $pK = 4$, $\varepsilon^p/\varepsilon^o = 3/80$, $a_0 = 1\ nm^2$, $\sigma_0 = 0$, salt concentration: 1 M (monovalent).

depends on the pK and concentration of the polyacid. A fixed pH would give nearly horizontal adsorption plateaus, whereas in figure 6.9 the adsorption increases with increasing concentration due to a decreasing pH and, hence, decreasing dissociation of the polymer. Especially for a pK around 4 the isotherm has a very rounded shape in this concentration region. The pH at equilibrium determines the adsorbed amount at a given pK. Actually, the adsorption is a function of the difference between pH and pK.

The adsorption of a polyacid (pK = 4) from a solution in which the pH is externally controlled is given in figure 6.10 as a function of the pH. Below pH ≃ 3 the polymer is virtually uncharged, whereas beyond pH ≃ 5 the polymer behaves like a strong polyelectrolyte. Since the surface is uncharged, the adsorption at high pH is low due to mutual repulsion between the charged segments. At low pH the adsorption increases strongly with decreasing (nonionic) solvent quality (increasing χ). For uncharged chains of 500 segments phase separation occurs at $\phi_* = 10^{-4}$ when $\chi > 0.545$. Polyelectrolyte solutions are stable in a wider range of χ values, because the charges on the chain lead to an extra repulsion between the segments. From figure 6.10 it follows that for polyelectrolytes under the given conditions at $\chi = 0.7$

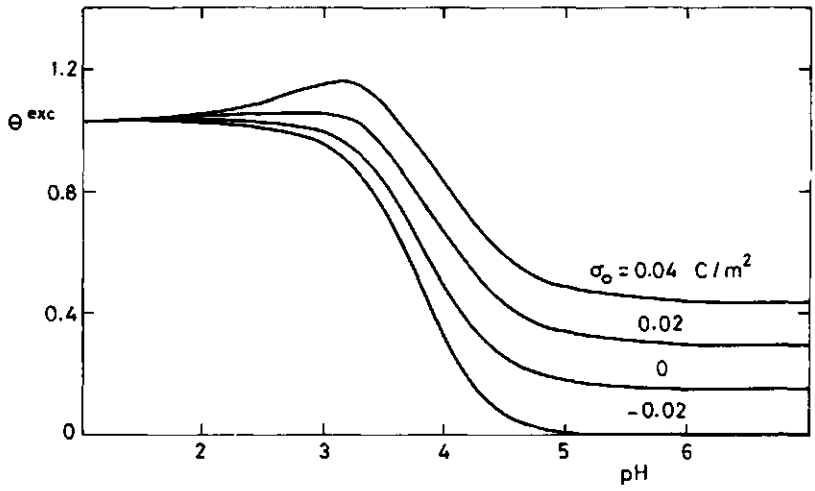

Figure 6.11. Adsorption of polyacid as a function of pH for different values of the surface charge σ_0. $\lambda_0 = 0.5$, $\chi = 0.5$, $\chi_s = 0.5$, $r = 500$, $\phi_* = 10^{-4}$, $z = -1$, pK = 4, $\varepsilon^p/\varepsilon^o = 3/80$, $a_0 = 1$ nm^2, σ_0 is indicated, salt concentration: 1 M (monovalent).

phase separation occurs below pH = 3.4. At pH = 3.4 the degree of ionization α_* is around 0.2.

Figure 6.11 gives the adsorption as a function of pH for different values of the surface charge σ_0. The curve for $\sigma_0 = 0$ is the same as that in figure 6.10. Obviously, the adsorption is only affected at relatively high pH, i.e., when the polymer is charged. When polymer and surface are oppositely charged, adsorption is favoured and may even pass through a maximum. At the pH corresponding to the maximum the electrostatic attraction between surface and polymer is stronger than the mutual repulsion between the polymer charges. For a high degree of ionization (at high pH) the adsorption is proportional to the surface charge.

We conclude that a clear theoretical picture is emerging for the adsorption behaviour of polyelectrolytes. Experimental tests on well-defined systems and new applications of polyelectrolyte adsorption can now be developed more systematically. Unfortunately, so far, experimental work in which all the relevant variables (ionic strength, pH, surface charge, etc.) are completely controlled is very scarce.

6.5 STRUCTURE OF LIPID BILAYERS

The selective permeability of biological membranes for water, ions, proteins, and other molecules is of vital importance for biological organisms, but the underlying mechanisms are not well understood. Much attention has been paid on the capability of membrane proteins to act as carriers or gates across the apolair centre of the lipid bilayer. However, a lipid bilayer is not a semicrystalline phase. Its structure is of a statistical nature, such as that of micels and lipid monolayers. The apolar centre is saturated with water and the distribution of other substances in the bilayer depends on the local interactions between the molecules. On the other hand, the amphiphatic lipid molecules are free to leave and re-enter the bilayer, so that a finite equilibrium concentration of lipid molecules in the water phase is present. For many molecules, the permeability of the membrane depends on the structure of the bilayer. The driving force for the stability of the membrane is the net repulsion between the apolar lipid tails and water. The polar head groups form a boundary between the apolar and hydrophilic phases. In a thin bilayer, the number of amphiphatic molecules, and hence the number of head groups, per unit area is small and a significant fraction of the apolar lipid tails is still in contact with water. With increasing bilayer thickness, the boundaries become saturated with head groups, so that some head groups are forced to enter the apolar phase. The equilibrium thickness of the bilayer is a compromise between these two unfavourable effects.

Since lipid molecules are simple copolymers, only theories that distinguish between individual conformations and between different types of segments are able to predict equilibrium distributions of tail segments and head groups in a membrane. In this case none of the previous theories, not even the Roe theory, is applicable. The theory of Ash et al.[20] would be a candidate if the computational problems for molecules longer than a few segments could be overcome. However, it is straightforward to adapt eqs. (6.1-4) to obtain a theory for copolymers[21].

The set of possible conformations does not depend on the types of the segments within a polymer chain, but the probability P_c that a chain is in a certain conformation c is a function of the local interactions, i.e., of the weighting factor of each segment. The segmental weighting factors depend now on both the layer number (i) and the type of segment (x). Hence, for copoly-

mers eq. (6.1) becomes

$$P_c = A\,\lambda_0^{q}\,\lambda_1^{r-1-q}\prod_{s=1}^{r} P^{x}_{i(s,c)} \qquad (6.1b)$$

and the volume fraction of segments of type x in layer i is

$$\phi_i^x = \sum_c r^x_{i,c}\, P_c \qquad (6.2b)$$

If the matrix method is used for the evaluation of ϕ_i^x there is one matrix for each type of segment and the order in which the different matrix-vector multiplications are to be performed is given by the order in which the types of segments are distributed along the chain.

The weighting factors P_i^x follow from the competition between a monomer of type x and a solvent molecule for a site in layer i:

$$P_i^x = \phi_i^o\; e^{-\Delta U_i^{xo}/kT} \qquad (6.3b)$$

where ΔU_i^{xo} is the exchange energy, depending on the local composition of solvent and segments of any type around a site in layer i. The interaction energy with segments y of a solvent molecule in a layer i surrounded by an average volume fraction $\langle\phi_i^y\rangle$ of these segments y is $\chi^{yo}\langle\phi_i^y\rangle$ kT. Similarly, the interaction energy with other segments y of a segment x in this volume fraction $\langle\phi_i^y\rangle$ equals $\chi^{yx}\langle\phi_i^y\rangle$ kT. In order to cover all types of interaction, we have to sum over y where y stands for segments of any type or solvent. Replacing a solvent molecule in layer i by a monomer x in a mixture of different volume fractions $\sum_y\langle\phi_i^y\rangle$ is accompanied by an energy change ΔU_i^{xo} given by

$$-\Delta U_i^{xo}/kT = \chi_s^{xo}\delta_{1,i} + \sum_y (\chi^{yo}-\chi^{yx})\langle\phi_i^y\rangle \qquad (6.4b)$$

In eq. (6.4b) χ_s^{xo} kT is the adsorption energy difference between a solvent molecule and a monomer x and χ^{yx} kT is the energy change when a monomer x is transferred from pure x towards pure y (or, equivalently, a monomer y from pure y into pure x: $\chi^{xy} = \chi^{yx}$). It is assumed that all monomers are of the same size and occupy one lattice site. The summation over y includes solvent molecules ($y \equiv o$) and monomers of type x ($y \equiv x$), so that for a binary mixture eq. (6.4) is recovered. Obviously, χ^{yy} is zero.

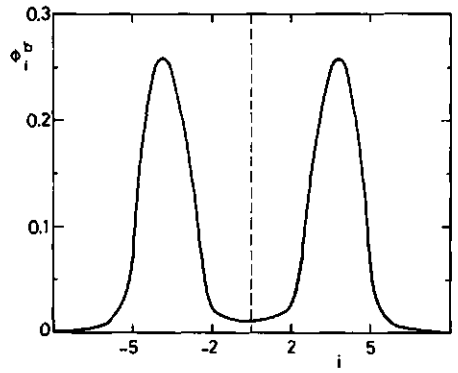

Figure 6.12. Distribution of head groups in a lipid bilayer of a_9b_2 molecules. $\lambda_0 = 0.5$, $\chi^{ao} = \chi^{ab} = 2.5$, $\chi^{bo} = -0.5$, $\phi_* = 10^{-4}$.

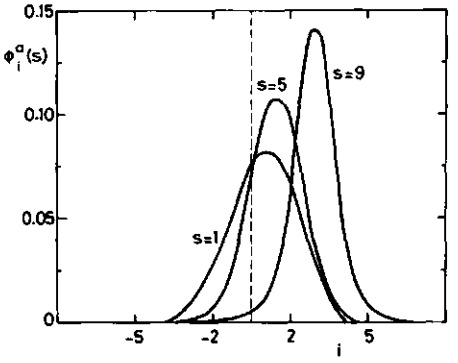

Figure 6.13. Distribution of tail segments of different rank s in a lipid bilayer of a_9b_2 molecules. Only chains with their head group at the right-hand side are counted. The rank s is counted from the tail end. Parameters as in figure 6.12.

The set of simultaneous equations (6.1b-4b) comprises per type of segment M equations and M unknowns ϕ_i^x.

For bilayers, a real surface is absent, hence $\chi_s^{xo} = 0$. Nevertheless it is necessary to fix spatially the position of the membrane, without affecting its composition, in order to allow the computation of a segment density profile. This can be done by locating the lattice on the membrane by placing a reflecting boundary at the centre of the bilayer, i.e., by setting explicitly $P_{-i}^x = P_i^x$, $\phi_{-i}^x = \phi_i^x$, etc., so that i is counted upward or downward from the centre of the membrane. In this way, a shift of the bilayer in a direction perpendicular to the reflecting boundary is transformed into a thinning or thickening of the bilayer and thus the equilibrium thickness is attainable with a fixed position of the membrane.

A typical example of a distribution profile of head groups in a membrane is given in figure 6.12. In this example, the lipid molecules have a tail of 9 segments (a) and a head group (b) of two segments occupying two adjacent lattice sites in the same layer (i.e., for the bond between the two head segments $\lambda_0 = 1$ and $\lambda_1 = 0$). The net interaction between a tail segment with water or head groups is repulsive ($\chi^{ao} = \chi^{ab} = 2.5$), whereas that between

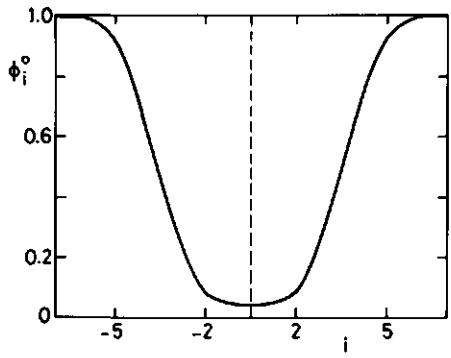

Figure 6.14. Distribution of water in a lipid bilayer of a_9b_2 molecules. Parameters as in figure 6.12.

head groups and water is slightly attractive ($\chi^{bo} = -0.5$). A volume concentration $\phi_* = 10^{-4}$ in the bulk solution and a hexagonal lattice were chosen.

The maximum density of head groups in figure 6.12 is only 25% and their distribution is very broad. A nonzero head group density is found in the apolair region, which points to a high transition (flip-flop) rate of head groups between both sides of the membrane.

Figure 6.13 gives distributions of tail segments of various rank s. With increasing distance from the head group, the distribution of tail segments becomes wider and shifts towards the centre of the bilayer. Also this figure indicates the strongly statistical nature of a membrane: the end segment of the apolar tail (s = 1) shows a very broad spatial distribution.

The distribution of water in the membrane is shown in figure 6.14. The water content of the bilayer is rather high. Therefore, it might be expected that transport of water through a membrane, and also of many other polar molecules, is possible without the need for special gates. This observation is very relevant for the interpretation of biological processes that depend on transport through membranes. Further work on the detailed structure of membranes is in progress.

6.6 AMORPHOUS PHASE OF SEMICRYSTALLINE POLYMER

A melt crystallized, semicrystalline polymer is believed to consist of alternating amorphous regions and lamellar crystalline domains. In the crystalline regions the parallel polymer stretches are oriented perpendicular to the lamellar surfaces. A polymer chain may traverse various crystalline and amorphous zones. Most of the polymer stems that emerge from the crystalline phase fold back into the crystal with a sharp fold or tight loop to give other chain portions in the amorphous region free orientational possibili-

ties. The portions of a chain in the amorphous phase are either loops (subchains grafted with both ends in the same lamella), bridges (subchains grafted in different lamellae), cilia (subchains grafted at one end only), or part of a floating (unattached) chain. Here, the terms 'loops' and 'bridges' have a meaning that is slightly different from that used in the previous chapters, where they represent subchains with **adsorbed** end segments.

The mechanical properties of semicrystalline polymer depend on the molecular structure of the lamellar regions. Most theoretical work has been done on the crystalline lamellae. The structure of the amorphous region has received much theoretical attention in the last few years[22-25]. However, in this work the contributions of cilia and floating chains were neglected. This approximation may be valid when the molecular weight of the polymer is extremely high, but with decreasing chain length end effects become more important.

The use of eqs. (6.1-4) for the amorphous phase provides unprecedented possibilities. Not only the effect of cilia and floating chains, i.e., molecular weight effects, but also the deformation of the amorphous phase can be studied. Although in amorphous polymer the concentration of solvent is usually zero, these equations need no modification since the use of a finite concentration profile of solvent in eqs. (6.3) and (6.4) has no effect on the results when this concentration is very low. Only the shape of the solvent profile is important, as it determines the distribution of weighting factors for the segments. Instead of solvent, it is more appropriate to consider vacant lattice sites ("holes"). A change of volume upon deformation is then accompanied by a change in the number of holes in the amorphous phase. As long as the volume fraction of polymer is nearly 1, the conformations of the chains are completely determined by entropic factors (volume filling). However, a significant fraction of solvent or holes gives more freedom for the segment density distribution, so that the χ-parameter becomes important.

A simple model for the study of deformation is obtained as follows[26]. Consider the polymer just before crystallization and assume that instantaneous crystallization of the melt will take place in the layers $i < 1$ and $i > M$ with no movement of the chains. Since the melt has a constant density, all arrangements of the chains are equally probable (all P_i's are the same, independent of χ) and it is easy to calculate the potential numbers and

length distributions[26] of loops, cilia, bridges, and floating chains in the melt that occupy the layers 1 to M. For simplicity, these numbers are computed by placing reflecting boundaries between layers 0 and 1 as well as between M and M + 1.

Thus, during a walk of r steps, each step into layer 0 terminates either a loop, or a cilium, or a bridge and the walk is continued from layer 1, starting a new loop, cilium, or bridge. Similarly, each step during the walk entering layer M + 1 terminates a subchain and is continued from layer M. In this way, the correct distributions are obtained, since in the melt the number of chains having e.g., segment s in layer 1 and segment s + 1 in layer 0, is equal to that having segment s in layer 0 and segment s + 1 in layer 1.

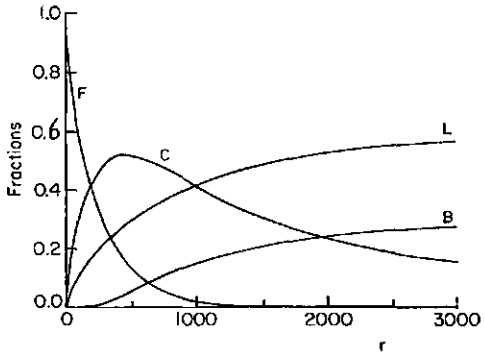

Figure 6.15. Fraction of segments in floating chains (F), cilia (C), loops (L), and bridges (B) in the amorphous phase of a semicrystalline polymer as a function of the chain length in the original melt. The thickness of the amorphous phase is 20 lattice layers. $\lambda_0 = 2/3$ (cubic lattice).

A few results are summarized in figures 6.15 and 6.16. Figure 6.15 gives the fraction of loops, cilia, bridges, and floating chains as a function of the chain length when M = 20. Other values for M give qualitatively the same picture. With increasing chain length the number of floating chains decreases and is essentially zero beyond $r \approx 3M^2$. The amorphous phase can accommodate floating chains with a length proportional to M^2, since their radius of gyration is proportional to $\sqrt{r}$. The fraction of cilia has a maximum at $r \approx M^2$ and decays very slowly for long chains ($\sim M^2/r$). The number of loops and bridges increase to the limiting values predicted by Guttman et al.[23,24].

Figure 6.16 shows the corresponding segment density profiles for r = 400. The bridges and floating chains are concentrated in the middle section of the amorphous phase, the loops are close to the walls and the

cilia are found mainly between each interface and the middle section.

After crystallization, the numbers of loops, cilia, bridges, and floating chains are fixed and given by the distributions obtained by the method described above. Their segment distributions can be calculated by using absorbing instead of reflecting boundaries and normalization with the given number distributions[26]. For instance, for a loop of t segments starting in layer 0, a generation of all walks starting in layer 0 and never visiting layer 0 or M + 1 during the walk, and ending with step t + 1 in layer 0, will give the segment density distribution of these loops after normalization. Obviously, all segment distributions remain the same before and after crystallization, as long as all the segmental weighting factors do not change. However, a deformation will affect all segment distributions and weighting factors in the amorphous phase.

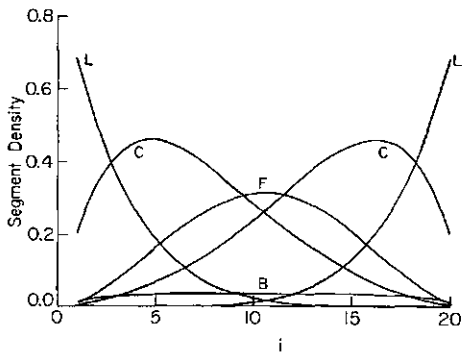

Figure 6.16. Segment density profiles for floating chains (F), cilia (C), loops (L) and bridges (B). $\lambda_0 = 2/3$, r = 400, M = 20.

Deformation is simulated by increasing the separation between the walls while keeping the number distributions constant, except that taut bridges break randomly into cilia or increase their length by pulling segments out of the crystalline regions. The increase in volume is filled up either by floating chains moving from polymer regions under simultaneous compression or by holes. In the latter case, which we will consider here, the fraction of holes will increase substantially and hence, the χ parameter becomes important. In principle, this parameter can be estimated from vapour pressure data of oligomers. Since polymers are not volatile, χ is certainly greater than 0.5.

Segments density distributions at different stages of deformation are given in figure 6.17. The initial value of M is 10 and it is assumed that taut bridges break randomly into cilia. The curves for $\chi = 0$ are relevant when a good solvent may enter the amorphous phase. In this case the segment

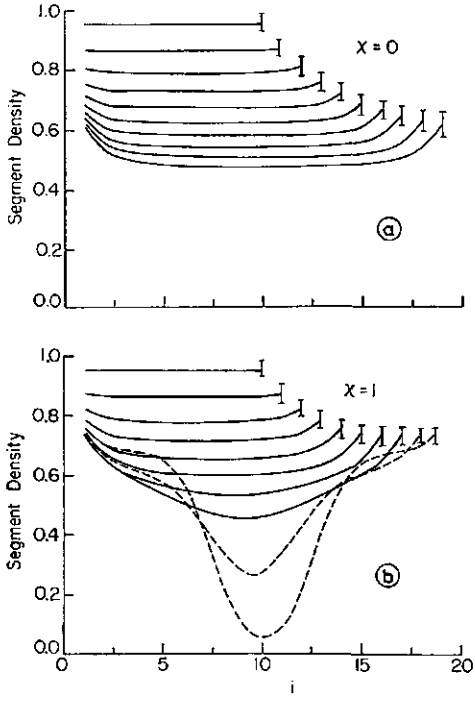

Figure 6.17. Effect of deformation on the segment density profiles of the amorphous phase of a semicrystalline polymer. The initial value of M, the thickness of the amorphous phase, is 10 and the initial volume fraction of polymer is 0.95. The final value of M is indicated by the vertical bars. $\lambda_0 = 2/3$, r = 100. a) $\chi = 0$ (athermal solution); b) $\chi = 1$ (the dashed curves may have an error of a few %).

density decreases homogeneously with increasing M, indicating that the polymer is soft and flexible. The curves for $\chi = 1$ show what happens when no solvent or a very poor solvent is present. At high deformations a 'necking' process takes place so that the segments retract towards the walls: the amorphous phase breaks up. Clearly, the deformation is energetically controlled, rather than entropically: the χ-parameter plays a major role. Hence, an extension of this simple model by incorporation of chain stiffness will give essentially the same deformation results.

The examples given in this section are only illustrations of the capability of the theory when applied to concentrated systems. It is possible to obtain much more detailed information, such as bond directions and distributions of individual segments.

Other systems of bulk polymer with inhomogeneous distributions of segments are block copolymers and blends of immiscible polymers. The absence of solvent in these systems does not prevent the application of the present theory, which was developed for adsorption of macromolecules from solution. In the contrary, the method looks very promising for these systems, since the theory remains valid for any concentration of macromolecules, including bulk polymer.

6.7 DEPLETION FLOCCULATION AND RESTABILIZATION

The presence of nonadsorbing polymer has a destabilizing effect on dispersions. This effect is much weaker than that of adsorbing polymer and has a different origin. In principle, the mechanism is simple[27]. The conformational entropy of a polymer coil in solution decreases as soon as the chain approaches a solid surface. For adsorbing polymer this entropy loss is (over)compensated by the attraction between surface and polymer segments, but for nonadsorbing polymer there is no such compensation. Therefore, the centres of gravity of nonadsorbing molecules will avoid the surface region. Consequently, the chains are depleted from the surface, and we may define a depletion zone where only solvent is present. At low concentrations of polymer the thickness Δ of the depletion layer is approximately equal to the radius of gyration R_g of the polymer coils. A more precise definition of Δ is given by the ratio $-\delta\theta^{exc}/\phi_*$, where δ is the length of a segment, θ^{exc} the (negative) excess adsorbed amount, and ϕ_* the concentration of the polymer in the bulk solution. When two depletion zones overlap each other, the total depletion volume is decreased (see figure 6.18).

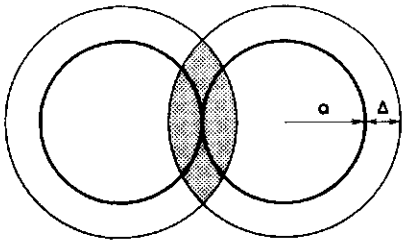

Figure 6.18. Change of depletion volume (hatched region) when two spheres of radius a and depletion thickness Δ come into close contact.

An equivalent description is that an amount of solvent, corresponding to the overlap volume, is transferred from a depletion zone of virtually pure solvent to the bulk solution of concentration ϕ_*^o. Each solvent molecule contributes a free energy which is equal to the chemical potential μ^o of the solvent in the solution with respect to the reference state (pure solvent). This chemical potential is given by[28]

$$\mu^o/kT = \phi_*(1-1/x) + \ln(1-\phi_*) + \chi\phi_*^2 \qquad (6.15)$$

where x is the volume ratio v^p/v^o between polymer chain and solvent molecule. Hence, the osmotic pressure between depletion zone and solution is

$-\mu^o/v^o$. This osmotic pressure is the origin of an attractive force between two overlapping depletion zones. In other words, the osmotic pressure of the homogeneous polymer solution pushes the particles together if these particles are surrounded by a depletion layer where only solvent is present.

The decrease in depletion volume when two particles of radius a come into close contact is $2\pi a\Delta^2(1+2\Delta/3a)$, so that the depletion free energy of interaction Δf_d, due to nonadsorbing polymer, per particle in a floc with co-ordination number z can be written as

$$\Delta f_d = (z\pi a/v^o)\mu^o\Delta^2(1+2\Delta/3a) \qquad (6.16)$$

This expression is valid for $\Delta/a \lesssim 0.5$, which is mostly the case. For higher values of Δ/a, multiple overlap of depletion volumes may occur and a correction is necessary.

With increasing polymer concentration, $-\mu^o$ increases and Δ decreases until in pure bulk polymer $-\mu^o$ is infinite and Δ is zero (since θ^{exc} becomes zero). For a quantitative prediction of Δf_d, the effect of the polymer concentration on the depletion thickness Δ must be known. The new theory, developed in this study, can give this information for all conditions. For nonadsorbing polymer the adsorption energy χ_s is smaller than the critical adsorption energy χ_{sc}. If the number of adsorbed segments is very low, the exact value of χ_s is irrelevant, and may be set equal to zero. The program for adsorption between two plates can be used to obtain θ^{exc}/ϕ_*.

In figure 6.19 the dependence of Δ on the volume fraction ϕ_* for a Θ-solvent is given for different

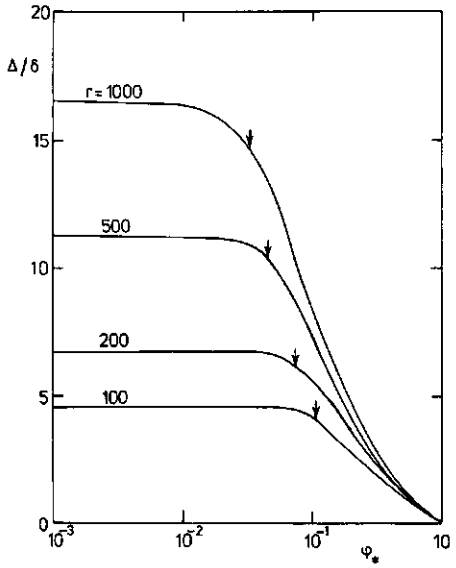

Figure 6.19. Depletion thickness Δ for different chain lengths as a function of polymer concentration. The arrows indicate the concentrations where the polymer coils in solution begin to overlap. $\lambda_0 = 0.5$, $\chi = 0.5$, the chain length r is indicated.

chain lengths r. At low concentrations Δ is independent of ϕ_* and proportional to $\sqrt{r}$, whereas at high concentrations Δ decreases to zero at $\phi_* = 1$. The concentration where Δ starts to decrease is close to the volume fraction where the coils in the solution begin to overlap ($\phi_{ov} \simeq 1/\sqrt{r}$, indicated by the arrows in figure 6.19).

Combining the results from figure 6.19 with eq. (6.16) gives the attraction energy Δf_d as a function of the solution concentration. This is illustrated in figure 6.20 for r = 100 and r = 1000. At low solution concentrations $-\Delta f_d$ increases linearly with ϕ_* and slightly with r. The attraction passes through a maximum at $\phi_* \approx 0.6$ and decreases again at higher concentrations. The reason for the maximum is the fact that the decrease of Δ^2 is stronger than the increase of $-\mu^o$ when ϕ_* approaches unity. The exact value of Δf_d for $\phi_* \to 1$ is not reliable, since at very high concentrations the volume fraction of segments in the depletion zone is not negligible.

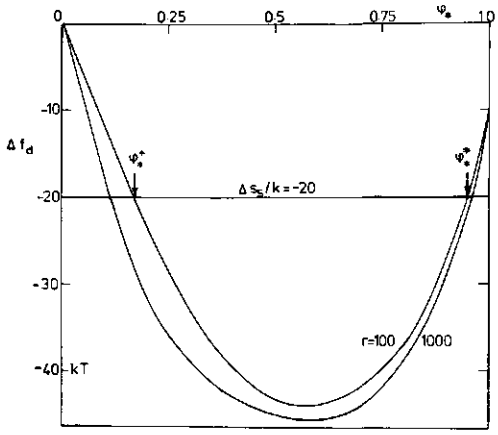

Figure 6.20. Osmotic interaction energy Δf_d per particle and the entropy loss $-\Delta S_s$ per particle, when a particle is transferred from the dispersion towards the floc phase, as a function of the concentration of nonadsorbing polymer. Flocculation occurs when $\phi_*^+ < \phi_* < \phi_*^\pm$. $\lambda_0 = 0.5$, $\chi = 0.5$, r is indicated, $z\pi a/\delta = 500$.

The free energy of attraction due to nonadsorbing polymer must be compared with other interactions between the particles in order to predict the flocculation conditions. One of these is the decrease in entropy ΔS_s of the particles upon flocculation which acts as a repulsion. In the solution the entropy of the particles is linearly increasing with $\ln \phi_d$, where ϕ_d is the volume fraction of particles in the dispersion. In the floc phase the entropy is only a function of the floc structure. In absence of other interactions, such as the Van der Waals forces, flocculation occurs whenever $\Delta S_s T > \Delta f_d$.

The horizontal line in figure 6.20 corresponds to $\Delta S_s/k = -20$ and crosses each attraction curve Δf_d at two concentrations, ϕ_*^+ and $\phi_*^{\ddagger}$, respectively. The dispersion is unstable in the range $\phi_*^+ < \phi_* < \phi_*^{\ddagger}$ and stable for other concentrations. Consequently, not only a critical flocculation concentration ϕ_*^+, but also a critical restabilization concentration $\phi_*^{\ddagger}$ is predicted by this theory. This latter concentration is extremely high, at least for hard spheres. For particles with grafted polymer chains ('soft particles') it has been found experimentally that $\phi_*^{\ddagger}$ exists and is much lower[29,30]. Calculations for soft particles are, in principle, possible with the present theory, since incorporation of grafted chains is straightforward.

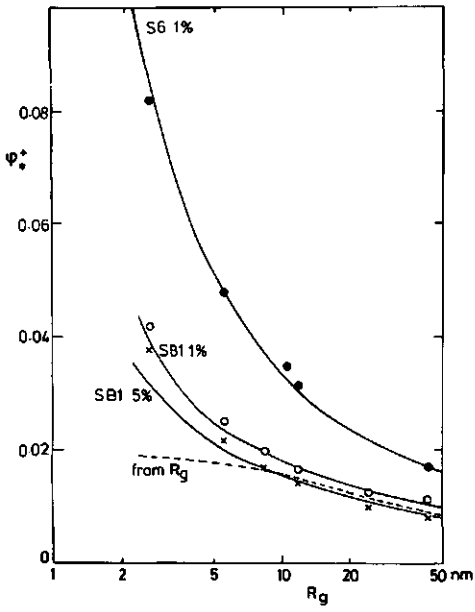

Figure 6.21. Critical flocculation concentrations ϕ_*^+ as a function of the radius of gyration of the polymer. The experimental values (points) are for silicas S6 and SB1 and polystyrene in cyclohexane at 34.5°C (Θ-conditions), taken from ref. (31). The silica concentrations are indicated. The theoretical curves are obtained by adjusting $\Delta S_s T/z$ (≈ -2 kT). The dashed curve gives the theoretical flocculation concentration when Δ is replaced by R_g.

A comparison with experimental values of ϕ_*^+ is possible using data of De Hek and Vrij[31]. In figure 6.21 their results for hard silica spheres and polysterene in cyclohexane under Θ-conditions (34.5°C) are indicated by the points. The theoretical values are shown by full curves. The only adjustable parameter is the entropy of the particles in the floc, for which a constant value has been chosen. The dependence of ϕ_*^+ on the chain length, expressed by R_g, on the particle radius a (21 nm for S6 and 46 nm for SB1), and on the particle concentration (1% or 5%) agrees quantitatively.

De Hek and Vrij used a theoretical model in which Δ was set equal to R_g, independent of the solution concentration. The dashed curve in figure 6.21 shows the prediction for ϕ_*^+ if Δ is assumed to be independent of the polymer concentration: the chain length dependence of ϕ_*^+ becomes qualitatively wrong, especially for low molecular weight polymer. Moreover, when Δ is constant the increase of $-\Delta f_d$ with increasing solution concentration persists at all concentrations. Hence, a restabilization concentration $\phi_*^\ddagger$ is not predicted in this case. For a quantitative prediction of the phase separation conditions, the exact value of Δ under each condition is essential, and the new theory can provide this value.

6.8 CONCLUSIONS

The examples given in this chapter illustrate the flexibility of the new theory of polymers at interfaces. Results are shown for adsorption of polydisperse polymer, star-branched polymer, and polyelectrolytes. The predictions for the structure of lipid bilayers demonstrate the capability of the theory for systems with copolymers or liquid-liquid interfaces. Amorphous bulk polymer can be treated as well as low concentrations of polymer, and adsorption as well as depletion. A particular useful feature of the theory is that it takes into account the chain length (from monomers up to very long chains), the solvent quality (including mixtures), and the polymer concentration over the whole experimental range.

A quantitative comparison between theoretical and experimental results is only possible in a few cases, due to the lack of experimental data on well-defined systems. The examples given in this study, and a few others[2,15-19,32-35] indicate that the agreement is excellent in most cases. A considerable step forward is a new method for the determination of the segmental adsorption energy χ_s[36,37] which allows for more accurate tests of the theory in the near future.

6.9 REFERENCES

1. Roe, R.J., J. Chem. Phys., **60** (1974) 4192.
2. Schee, H.A. van der, Ph.D. Thesis, Agricultural University, Wageningen, (1983).
3. Roefs, S.P.F.M., M.Sci. Thesis, Agricultural University, Wageningen, (1982).
4. Roefs, S.P.F.M.; and Scheutjens, J.M.H.M., Macromolecules, in preparation.
5. Cohen Stuart, M.A.; Scheutjens, J.M.H.M.; and Fleer, G.J., J. Polym. Sci., Polym. Phys. Ed., **18** (1980) 559.
6. Vander Linden, C; and Van Leemput, R., J. Colloid Interface Sci., **67** (1978) 63.
7. Cohen Stuart, M.A., Ph.D. Thesis, Agricultural University, Wageningen, (1980).
8. Hlady, V.; Lyklema, J.; and Fleer, G.J., J. Colloid Interface Sci., **87** (1982) 395.
9. Bouwstra, J.B., M.Sci. Thesis, Agricultural University, Wageningen, (1980).
10. Kawaguchi, M.; and Takahashi, A., J. Polym. Sci., Polym. Phys. Ed., **18** (1980) 943.
11. Hesselink, F.Th., J. Electroanal. Chem., **37** (1972) 317.
12. Hesselink, F.Th., J. Colloid Interface Sci., **60** (1977) 448.
13. Silberberg, A., in: "Ions in Macromolecular and Biological Systems", Everett, D.H.; and Vincent, B., Eds., Scientechnica, Bristol, Colston Papers, **29** (1978) 1.
14. Evers, O.A., M.Sci. Thesis, Agricultural University, Wageningen, (1984).
15. Marra, J.; Schee, H.A. van der; Fleer, G.J.; and Lyklema, J., in: "Adsorption from Solution", Ottewill, R.H.; Rochester, C.H.; and Smith, A.L., Eds., Acad. Press, London, (1983) 245.
16. Bonekamp, B.C.; Schee, H.A. van der; and Lyklema, J., Croat. Chem. Acta, **56** (1983) 695.
17. Schee, H.A. van der; and Lyklema, J., J. Phys. Chem., in press.
18. Papenhuijzen, J.; Schee, H.A. van der; and Fleer, G.J., J. Colloid Interface Sci., in press.

19. Papenhuijzen, J.; Bijsterbosch, B.H.; and Fleer, G.J., J. Colloid Interface Sci., in press.
20. Ash, S.G.; Everett, D.H.; and Findenegg, G.H., Trans. Faraday Soc., **66** (1970) 708.
21. Leermakers, F.A.M.; Scheutjens, J.M.H.M.; and Lyklema, J., Biophys. Chem., **18** (1983) 353.
22. DiMarzio, E.A.; and Guttman, C.M., Polymer, **21** (1981) 733.
23. Guttman, C.M.; DiMarzio, E.A.; and Hoffman, J.D., Polymer, **22** (1981) 1466.
24. Guttman, C.M.; and DiMarzio, E.A., Macromolecules, **15** (1982) 525.
25. Mansfield, M.L., Macromolecules, **16** (1983) 914.
26. Leermakers, F.A.M.; Scheutjens, J.M.H.M.; and Gaylord, R.J., Polymer, in press.
27. Fleer, G.J.; Scheutjens, J.M.H.M.; and Vincent, B., ACS Symposium Series, **240** (1984) 245.
28. Flory, P.J., "Principles of Polymer Chemistry", Cornell University Press, Ithaca, N.Y., (1953).
29. Vincent, B.; Luckham, P.F.; and Waite, F.A., J. Colloid Interface Sci., **73** (1980) 508.
30. Clarke, J.; and Vincent, B., J. Colloid Interface Sci., **82** (1981) 208.
31. De Hek, H.; Vrij, A., J. Colloid Interface Sci., **84** (1981) 409.
32. Cosgrove, T.; Vincent, B.; Crowley, T.L.; and Cohen Stuart, M.A., ACS Symposium Series, **240** (1984) 147.
33. Cohen Stuart, M.A.; Waajen, F.H.W.H.; Cosgrove, T.; Vincent B.; and Crowley, T.L., Macromolecules, in press.
34. Fleer, G.J.; and Lyklema, J., in: "Adsorption from Solution at the Solid/Liquid Interface". Parfitt, G.D.; and Rochester, C.H., Eds., Acad. Press, London, (1983) 153.
35. Fleer, G.J.; and Scheutjens, J.M.H.M., Adv. Colloid Interface Sci., **16** (1982) 341.
36. Cohen Stuart, M.A.; Fleer, G.J.; and Scheutjens, J.M.H.M., J. Colloid Interface Sci., **97** (1984) 515.
37. Cohen Stuart, M.A.; Fleer, G.J.; and Scheutjens, J.M.H.M., J. Colloid Interface Sci., **97** (1984) 526.

SUMMARY

The aim of this study was the development of a theory for a quantitative description of the behaviour of macromolecules at interfaces with special attention to steric stabilization and flocculation of colloids. This has been accomplished by extending the Flory-Huggins theory for homogeneous polymer solutions towards inhomogeneous systems in which also the presence of a surface is accounted for.

In chapter 1 the general background of this study is given. The importance of polymer adsorption for technological applications is shown by several examples and the need for a statistical approach is emphasized. The structure of polymers and their properties, both in solution and at interfaces, are discussed from a theoretical point of view and the limits of applicability of the most important models are pointed out. Thereafter, a short introduction to the basic concepts of the new theory is given and the computational difficulties that may occur are summarized.

Chapter 2 gives a full statistical thermodynamical account of the theory, starting with the derivation of the partition function. A novel feature is that the partition function is expressed as a function of the distribution of molecular conformations. By maximizing this partition function with respect to the numbers of chains in each particular conformation, the equilibrium distribution of conformations is found. In this way a very detailed picture of the system is obtained. The statistical weight of each conformation in a concentration profile comprises a multiple product of segmental weighting factors, one for each segment, accounting for the local interactions of that segment with its surroundings. The actual calculations involve the numerical solution of a set of simultaneous nonlinear equations. Some details of the computational method are described.

A selection of results, including segment density profiles, adsorption isotherms, and bound fractions, is given and compared with results from other theories where appropriate. It turns out that the tails, which are neglected in previous theories, are very important, determining nearly completely the segment density in the outer regions of the adsorbed layer.

In chapter 3 the potentialities of the theory are further elaborated. The average conformation of adsorbed polymer is examined in some detail. In the case of isolated chains, the conformation is nearly flat, with essentially all segments in (long) trains and (short) loops. Interacting adsorbed

polymers occur already in very dilute solutions. In that case a significant fraction of segments form long dangling tails. With increasing solution concentration the length of trains decreases, whereas loops and tails become longer. For surfaces adjoining pure liquid polymer, the tails represent even 2/3 of the adsorbed amount. The density of segments in loops decreases exponentially with increasing distance from the surface, whereas that of tail segments shows a maximum and dominates at larger distances. In all solvents the root-mean-square layer thickness of adsorbed polymer is proportional to the square root of the chain length.

Comparison of theoretical predictions with experimental data is made in chapter 4. In a Θ-solvent, the adsorption increases linearly with the logarithm of the chain length, whereas in better solvents the chain length dependence is weaker. Semiquantitative agreement between theory and experiment is found. Also the fraction of adsorbed segments agrees with theoretical predictions. The correspondence between theoretical data for the r.m.s. layer thickness, in which the contribution of tails dominates, and experimental observations is another indication for the correctness of the analysis.

Simple equations are derived for the relative adsorption from a solution of polydisperse polymer. At low concentrations, long chains adsorb preferentially over shorter ones, in agreement with experimental data. At very high concentrations preferential adsorption of short chains is predicted.

The interaction between two adsorbed polymer layers is examined in chapter 5. As the partition function of the system is known, the calculation of the free energy of interaction is straightforward. Similarities and differences with other theories are discussed. When the polymer is free to leave or enter the gap between the surfaces (full equilibrium) the interaction is always attractive. This attraction is due to polymer chains that adsorb on both surfaces simultaneously (bridging). When the polymer is unable to leave the gap (restricted equilibrium) the force is attractive in (very) dilute solutions and, except in very poor solvents, repulsive in concentrated systems. These predictions are compared with those of other theories and agree with experimental data.

Some applications of the theory for other systems are illustrated in chapter 6.

It is shown that branches in the chain do not drastically affect the surface activity of the molecules, provided that the molecular weight remains the same.

Preferential adsorption from solutions of polydisperse polymer has important practical consequences, since polymer samples are always polydisperse. It is now possible to calculate adsorption properties of polymers having any molecular weight distribution.

By incorporation of electrostatic terms in the segmental weighting factors, a theory for the adsorption of polyelectrolytes becomes available. At low ionic strength the charged molecules adsorb in very flat conformations. Only at very high salt concentrations or when the degree of ionization is low, polyelectrolytes behave more like neutral polymers. Generally, polyelectrolyte adsorption is similar to adsorption of polymers in very good solvents.

As an example of copolymers at liquid-liquid interfaces, the structure of a lipid bilayer is studied. It is shown that a considerable concentration of water is present in the centre of the bilayer and that the fluctuations in the position of, e.g., the head groups are substantial.

Calculations on the structure of the amorphous phase of semicrystalline polymer show that polymer systems without solvent can also be handled by the developed theory. Even some deformation properties of the polymer can be predicted.

Finally, predictions of the theory can be used for studying the stability of colloids in the presence of non-adsorbing polymer (depletion flocculation and restabilization).

Generally, the agreement with experimental observations is very good and it shows that the theory is essentially correct. Due to the lack of reliable experimental data quantitative comparison is possible in only a few cases. However, the capability and flexibility of the theory is clearly demonstrated and it is only a matter of time to elaborate the many applications that are awaiting a closer examination.

MACROMOLECULEN AAN GRENSVLAKKEN

Een soepele theorie voor moeizame systemen

SAMENVATTING

In dit proefschrift wordt een theoretisch onderzoek beschreven naar het gedrag van flexibele macromoleculen aan grensvlakken met bijzondere aandacht voor sterische stabilisatie en vlokking van kolloïden door polymeren. Kolloïden zijn submicroscopische deeltjes die in een vloeistof zweven en (synthetische) polymeren zijn het meest bekend in droge vorm onder de verzamelnamen plastic en kunststof. Het resultaat van dit onderzoek is een theorie voor inhomogene (ongelijkmatige) systemen van polymeren (zoals in de buurt van grensvlakken). Deze theorie vormt een uitbreiding van het roostermodel dat Flory en Huggins in de veertiger jaren hebben ontwikkeld voor homogene polymeeroplossingen.

Hoofdstuk 1 is een inleiding in de achtergronden van dit onderzoek en begint met het noemen van enkele belangrijke toepassingen van macromoleculen (polymeren) aan grensvlakken. Natuurlijke of synthetische polymeren kunnen schifting of uitzakken van kolloïdale systemen tegengaan, zoals in voedingsmiddelen, geneesmiddelen, bestrijdingsmiddelen, cosmetica, verf en inkt, maar ook bevorderen, zoals dat bijvoorbeeld in de mijnbouw en waterzuivering wordt toegepast. Adsorptie (hechting aan grensvlakken) van polymeren komt veelvulding voor in de natuur en is een bekend verschijnsel in de polymeerverwerkende industrie. Verder wordt gebruik gemaakt van polymeeradsorptie bij de fabricage van magneetbanden en autobandenrubber en bij het gummen.

Dertig jaar geleden was er nog nauwelijks iets bekend over het gedrag van polymeren aan grensvlakken: alle toepassingen waren min of meer bij toeval gevonden. Later zijn er theorieën ontwikkeld die verschillende eigenschappen kunnen verklaren, maar om een nauwkeurige voorspelling te kunnen geven moet precies bekend zijn hoe de polymeermoleculen in een grensvlak zitten.

Polymeren zijn in de regel lange draadvormige moleculen die zijn opgebouwd uit een aaneenschakeling van 100 tot 10.000 kleine eenheden (segmenten of monomeren). Er bestaat een groot aantal verschillende soorten. Als de segmenten allemaal gelijk zijn spreken we van homopolymeren. Copolymeren zijn opgebouwd uit een mengsel van verschillende segmenten, in een volgorde

die voor elk molecuul weer anders kan zijn. Verder zijn er vertakte polymeren en soorten die in oplossing electrostatisch geladen zijn (polyelectrolyten). Als alle moleculen even lang zijn spreken we van homodispers polymeer. In de praktijk zijn ze echter meestal van ongelijke lengte: ze zijn polydispers. Een complete theorie moet met al deze variaties rekening kunnen houden.

Een opgelost polymeermolecuul gedraagt zich als een zwevend draadvormig kluwen dat steeds van vorm verandert. Het aantal mogelijke vormen (conformaties) is vrijwel onbeperkt, maar men kan statistisch de gemiddelde grootte van het kluwen uitrekenen. Deze blijkt o.a. af te hangen van het soort oplosmiddel. Hoe slechter het oplosmiddel, des te kleiner is het kluwen. In een z.g. Θ-oplosmiddel lost het polymeer nog juist in elke concentratie op en is de gemiddelde diameter van een kluwen evenredig met de wortel uit het aantal segmenten van het molecuul.

De meeste polymeren hechten erg goed aan oppervlakken, vooral doordat elk molecuul via zijn segmenten vele aanhechtingsplaatsen kan hebben. De polymeerketen krijgt daarbij de vorm van een liggend kluwen, met in de oplossing zwevende lussen en staarten die worden vastgehouden door tegen het oppervlak liggende delen van het molecuul, de zogenaamde treinen. Vergeleken met de situatie voor opgeloste polymeren is het nu veel moeilijker om statistisch de gemiddelde vorm uit te rekenen, want de waarschijnlijkheid van elke conformatie wordt nu mede beïnvloed door de neiging tot hechting aan het oppervlak: er is een voorkeur voor conformaties met veel contacten tussen oppervlak en molecuul. Een kluwen probeert zich zoveel mogelijk over het oppervlak uit te spreiden, met lange treinen en korte lussen en staarten. De geadsorbeerde laag polymeer wordt dan erg dun. Met uitzondering van het, in de praktijk weinig voorkomende, geval van adsorptie uit zeer verdunde oplossingen, wordt het uitspreiden echter tegengewerkt doordat de kluwens elkaar in de weg zitten. Hoe meer kluwens, des te dikker wordt de geadsorbeerde laag. De theorie die in dit onderzoek ontwikkeld is houdt hier rekening mee.

Hoofdstuk 2 geeft de volledige statistisch-thermodynamische afleiding van de theorie, vanaf het opstellen van de toestandssom. Een ongewone stap is dat in de toestandssom alle conformaties van de polymeerketens worden onderscheiden. Daardoor kan de evenwichtstoestand verkregen worden door het aantal moleculen in elke afzonderlijke conformatie zodanig te kiezen dat de toestandssom zo groot mogelijk is. Omdat de evenwichtsverdeling van alle conformaties zodoende bekend is, ontstaat een gedetailleerd beeld van het

systeem. Het blijkt dat het aantal moleculen in een gegeven conformatie evenredig is met een meervoudig produkt van weegfaktoren, één voor elk segment. Zo'n weegfactor brengt de lokale wisselwerkingen van dat segment met zijn omgeving in rekening.

Een reeks resultaten, zoals concentratieprofielen, adsorptie-isothermen en gebonden frakties wordt gegeven en waar mogelijk vergeleken met resultaten van andere theorieën. De staarten, die in voorgaande theorieën niet in rekening gebracht zijn, blijken erg belangrijk te zijn: ze bepalen vrijwel geheel de segmentdichtheid in het buitenste deel van de geadsorbeerde laag.

In hoofdstuk 3 worden de mogelijkheden van de theorie verder uitgewerkt. De gemiddelde conformatie van geadsorbeerde polymeerketens wordt nauwkeurig onderzocht. Geïsoleerde geadsorbeerde ketens hebben een vlakke conformatie met vrijwel alle segmenten in (lange) treinen en (korte) lussen. In verdunde oplossingen zijn de lussen langer, de treinen korter en zit een aanmerkelijk deel van de segmenten in lange staarten. In vloeibaar polymeer vertegenwoordigt de staartfractie zelfs 2/3 van de geadsorbeerde hoeveelheid. De segmentdichtheid van de lussen neemt exponentieel af met toenemende afstand tot het oppervlak, terwijl dat van de staarten een maximum vertoont en op grotere afstand domineert. In alle oplosmiddelen neemt de middelbare laagdikte evenredig toe met de wortel uit de ketenlengte.

In hoofdstuk 4 worden theoretische voorspellingen vergeleken met experimentele resultaten. In een Θ-oplosmiddel neemt de adsorptie evenredig toe met de logaritme van de ketenlengte, terwijl in een beter oplosmiddel de afhankelijkheid van de ketenlengte kleiner is. De overeenstemming tussen theorie en experiment is semi-kwantitatief. Ook de fractie gebonden segmenten komt overeen met theoretische voorspellingen. De goede overeenkomst tussen theoretische gegevens over de middelbare laagdikte, waarin de bijdrage van de staarten domineert, met experimentele waarnemingen is een aanwijzing voor de juistheid van de analyse.

Eenvoudige vergelijkingen worden afgeleid voor de relatieve adsorptie in een oplossing van polydispers polymeer. In verdunde oplossingen adsorberen lange ketens preferent boven korte, in overeenstemming met experimentele gegevens. In zeer hoge concentraties wordt echter voorspeld dat bij voorkeur juist korte moleculen adsorberen.

De wisselwerking tussen twee polymeerlagen wordt onderzocht in hoofdstuk 5. Omdat de toestandssom van het systeem bekend is, is de vrije energie van interactie gemakkelijk uit te rekenen. Overeenkomsten en verschillen met

andere theorieën worden aangegeven. De berekeningen geven informatie over het effect van geadsorbeerd polymeer op de stabiliteit van kolloïden. Als het polymeer de ruimte tussen de beide oppervlakken vrij kan binnenkomen of verlaten (volledig evenwicht) dan trekken de lagen elkaar altijd aan. Deze aantrekking wordt veroorzaakt door polymeerketens die tegelijkertijd op beide oppervlakken adsorberen (brugvorming). Als het polymeer niet weg kan (beperkt evenwicht) is er aantrekking in (zeer) verdunde polymeeroplossingen en, behalve in zeer slechte oplosmiddelen, afstoting in geconcentreerde systemen. Deze voorspellingen worden vergeleken met die van andere theorieën en komen overeen met experimentele waarnemingen.

Enkele toepassingen van de theorie op andere systemen worden geïllustreerd in hoofdstuk 6.

Er wordt gevonden dat vertakkingen in de keten geen grote invloed hebben op de oppervlakteactiviteit van de moleculen, mits het molecuulgewicht gelijk blijft.

Preferente adsorptie in oplossingen van polydispers polymeer heeft belangrijke practische consequenties, want polymeer is altijd polydispers. Het is nu mogelijk de adsorptie-eigenschappen van polymeer met een willekeurige molecuulgewichtsverdeling te berekenen.

Door het inbouwen van electrostatische termen in de weegfactoren van de segmenten ontstaat een adsorptietheorie voor polyelectrolyten. Bij lage ionsterkte adsorberen de geladen moleculen in een erg vlakke conformatie. Alleen bij zeer hoge zoutconcentraties of als de ionisatiegraad laag is gedraagt een polyelectrolyt zich als een neutraal polymeer. In het algemeen lijkt de adsorptie van polyelectrolyt op die van polymeer in goede oplosmiddelen.

Als voorbeeld van copolymeren aan een vloeistof-vloeistof grensvlak wordt de structuur van een vetzuurdubbellaag bestudeerd. Er wordt aangetoond dat een hoge concentratie water in het centrum van de dubbellaag aanwezig is en dat de fluctuaties in de posities van bijvoorbeeld de kopgroepen erg hoog zijn.

Berekeningen aan de structuur van de amorfe fase van half-kristallijn polymeer laten zien dat ook polymeersystemen zonder oplosmiddel met de theorie bestudeerd kunnen worden. Zelfs enkele deformatie-eigenschappen van het polymeer kunnen voorspeld worden.

Tenslotte wordt aangegeven hoe de voorspellingen van de theorie gebruikt kunnen worden voor de stabiliteit van kolloïden in aanwezigheid van niet adsorberend polymeer (depletievlokking en -restabilisatie).

In het algemeen is de overeenstemming met experimentele waarnemingen erg goed. Dit toont aan dat de theorie in wezen correct is. Vanwege het gebrek aan betrouwbare experimentele gegevens is een kwantitatieve vergelijking slechts in enkele gevallen mogelijk. De capaciteit en de flexibiliteit van de theorie zijn echter duidelijk aangetoond en het is slechts een kwestie van tijd om de vele toepassingsmogelijkheden die op een nadere uitwerking liggen te wachten, met de huidige theorie aan te pakken.

ENKELE PERSOONLIJKE GEGEVENS

Op 20 juni 1947 ben ik geboren te Geldrop. Aldaar behaalde ik in 1963 het U.L.O.-diploma, waarna ik werd toegelaten tot de dagopleiding tot electronentechnicus, met specialisatie radiotechniek, aan de onderwijsinstelling van de N.V. Philips te Eindhoven. Na deze opleiding ben ik bij dit bedrijf werkzaam geweest van 1965 tot 1970, met uitzondering van 20 maanden militaire dienst. Intussen volgde ik achtereenvolgens een avondcursus voor electronentechniek aan de H.B.O. te Eindhoven (3 jaar) en voor het diploma H.B.S.-B (2 jaar). Na het staatsexamen in 1970 begon ik aan de studie Moleculaire Wetenschappen aan de Landbouwhogeschool en legde met lof het doctoraalexamen af in januari 1977. De doctoraalstudie omvatte de vakken Kolloidchemie (6 maanden), Plantenphysiologie (6 maanden), Wiskunde (3 maanden), Natuurkunde (3 maanden) en Moleculaire Physica (3 maanden).

Sinds maart 1977 ben ik als wetenschappelijk medewerker verbonden aan de afdeling Fysische en Kolloidchemie van de Landbouwhogeschool.

NAWOORD

Nu U dit proefschrift geheel hebt doorgenomen wilt U natuurlijk graag weten wie tot de totstandkoming ervan hebben bijgedragen. Dit geeft mij tevens de gelegenheid iedereen te bedanken die mij op een of andere manier behulpzaam is geweest. Enkele mensen wil ik persoonlijk noemen.

Mijn promotoren Gerard Fleer en Hans Lyklema hebben mij alle vrijheid en begeleiding gegeven die ik bij het onderzoek nodig dacht te hebben. Aan Hans heb ik o.a. mijn interesse voor de moleculaire thermodynamica te danken. Zijn manier van leiding geven stimuleert een hoge produktie in een ongedwongen sfeer. Gerard heeft mij enthousiast de weg gewezen in het wetenschappelijke wereldje. Zijn kritische instelling, overmoeibare inzet en scherp uitdrukkingsvermogen zijn van onschatbare waarde geweest voor het uiteindelijke resultaat.

Mijn interesse voor het grensgebied tussen theorie en praktijk werd vruchtbaar aangevuld door Martien Cohen Stuart, die door zijn experimenteerkunst en theoretische kennis menig verband wist aan te tonen.

Met Henk van der Schee heb ik vele stimulerende ideeën uitgewisseld. Zijn manier van gebruik en misbruik van programmatuur vormt de strengste test die men zich kan voorstellen. De betrouwbaarheid van mijn computerprogramma's voor (niet-) bedoelde toepassingen is daardoor aanzienlijk verbeterd.

Het merendeel van de resultaten uit hoofdstuk 6 is berekend door Bas Roefs, Jan Bouwstra, Olaf Evers en Frans Leermakers in het kader van hun doctoraalstudie.

Het nauwkeurige tekenwerk is verzorgd door Gert Buurman en de (niet eenvoudige) tekstverwerking was in handen van Clara van Dijk en Yvonne Toussaint.

Dezen en vele anderen van de vakgroep Fysische en Kolloidchemie dank ik voor de plezierige samenwerking en de goede sfeer. Ik verheug me op een prettige voortzetting in de komende jaren.